NUMERICAL ANALYSIS AND MODELLING OF TRANSMISSION SYSTEMS FOR HYBRID ELECTRIC VEHICLES AND ELECTRIC VEHICLES

QINGLIAN REN

A thesis submitted in partial fulfillment of the
requirements of the University of Sunderland
for the degree of Doctor of Philosophy

February 2010

Contents

Index for figures

Index for tables

Index for appendices

Acknowledgement

I would like to express my gratitude to all those who gave me the possibility to complete this thesis. I want to thank the Institute for Automotive and Manufacturing Advanced Practice (AMAP), University of Sunderland for giving me permission to commence this thesis in the first instance. I have furthermore to thank my line manager and director of study, Mr. Adrian Morris, who encouraged me to go ahead with my thesis. Also I would like to thank Professor Wheatley for his assistance over the period of the research study.

I am deeply indebted to my supervisor Prof. Dave Crolla, who gave me huge support and helped me throughout the research project and in writing up of the thesis.

Especially, I would like to give my special thanks to my family whose love enabled me to complete this work.

Abbreviations

A-ECMS	Adaptive equivalent consumption minimisation strategy
AMT	Automated manual transmission
BEC	Battery energy changed
DP	Dynamic programming
DO	Dynamic optimisation
ECMS	Equivalent consumption minimisation strategy
E-CVT	Electronically-controlled continuously variable transmission
EFC	Engine fuel consumpton
EV	Electric vehicle
EVT	Electrically variable transmission
FL	Fuzzy logic
FTP	Federal test procedure
GA	Genetic algorithm
HEV	Hybrid electric vehicle
HE-VESIM	Hybrid electric vehicle simulation tool
HSD	Hybrid synergy drive
ICE	Internal combustion engine
IMA	Integrated motor assist
ISA	Integrated starter alternator
IVT	Infinitely variable transmission
LCV	Low carbon vehicle
MG	Motor generator
NEDC	New european driving cycle
NN	Neural network
OEM	Original equipment manufacturer
OFC	Overall fuel consumption
PHEV	Plug-in hybrid electric vehicle
PI	Proportional-integral
PSAT	Powertrain system analysis toolkit
PSD	Power Split Device

PST	Power splitting transmissions
QSS	Quasistatic simulation
RB	Rule based
SOC	State of charge
SQP	Sequential quadratic programming
SUV	Sport utility vehicles
THS	Toyota hybrid system
TR	Transmission ratio
TSAT	Transmission systems analysis tool
TSB	Technology Strategy board

Annotations

R	Ring gear
S	Sun gear
C	Carrier
CL	Clutch
n	Rotation speed (rpm)
Z	Tooth number
α	Gear ratio
p	The number of connected parts
f	The degree of freedom
q	The number of basic parts
x	The number of gear units
$\vec{n}$	Rotation speed vector
A_n	The speed coefficient matrix
$\vec{T}$	Torque vector
A_T	Te torque coefficient matrix
ρ	Fuel density
η_{eng}	Engine efficiency
D	Driving distance
P_a	Available power
P_n	Required power
F_rr	Rolling resistance force
F_ad	Aerodynamic drag
η_t	Efficiency of the whole powertrain
r	Radius of the tire
V	Vehicle speed
m_e	Equivalent mass of the vehicle
ω	Rotation Speed (rad/s)

Abstract

Interest in hybrid electric vehicles (HEVs) and electric vehicles (EVs) has increased rapidly over recent years from both industrial and academic viewpoints due to increasing concerns about environmental pollution and global oil usage. In the automotive sector, huge efforts have been invested in vehicle technology to improve efficiency and reduce carbon emissions with, for example, hybrid and electric vehicles. This thesis focuses on one design area of these vehicles – the transmission – with the aim of investigating the potential benefits of improved transmissions for HEVs and EVs.

For HEVs, a novel transmission developed by Nexxtdrive based on a twin epicyclic design is analysed using a matrix method and its performance is compared with the more common single epicyclic arrangement used successfully in the Toyota Prius. Simulation models are then used to compare the performance of a typical HEV passenger car fitted with these two transmissions over standard driving cycles. The conclusion is that the twin epicyclic offers substantial improvements of up to 20% reduction in energy consumption, though the benefits are sensitive to the driving cycle used.

For EVs, most designs to date have used a single fixed ratio transmission, and surprisingly little research has explored whether multi-geared transmissions offer any benefits. The research challenge is whether it is possible to optimise the usage of the electric motor in its region of high efficiency by controlling the transmission. Simulation results of two EV examples confirm that energy consumption benefits are indeed achievable – of between 7 and 14% depending on the driving cycle.

Overall, the original aspects of this work – the analysis and modelling the twin epicyclic gearbox; the analysis and modelling the twin epicyclic system in a vehicle and a comparison of the results with single epicyclic system; and the analysis and modelling of EVs with and without a transmission system of varying levels of complexity – have shown that there are worthwhile performance benefits from using improved transmission designs for low carbon vehicles.

1 Introduction

1.1 Energy consumption and emissions

Oil plays a fundamental role in the world economy. Although recent estimates vary, there is absolutely no doubt that global concerns about the finite nature of our oil-based energy reserves are well founded (Hirsch, Bezdek et al. 2005). Global energy demand from all sources is expected to increase by 1.3 percent per year on average from 2005 to 2030 (ExxonMobil 2007).

Apart from the shortage of oil storage, there is equal concern about the growth in emissions – and terms such as 'greenhouse gases' and 'carbon footprint' are in the news every day. Overall, the transportation sector accounts for around 21 percent of current global fossil fuel CO_2 missions to the atmosphere—second only to emissions from power production (IPIECA 2004). According to the Technology Strategy Board (TSB), in the UK it is estimated that transport accounts for 24% of the UK's carbon emissions. Road transport accounts for 80% of this figure (IME 2009). The automotive industry has been very responsive to both legislation and growing consumer demands to reduce emissions.

1.2 Need for research on hybrid electric vehicles

Hybrid electric vehicles (HEVs) are considered to be an intermediate step towards purely electric drive (fuel cells or batteries) (Cole and Amann 2009). Commercial interest in hybrid vehicle technology has grown at a much more dramatic rate than was predicted a decade ago. Around that time, many industry observers were substantially more optimistic about a major leap from current petroleum based technology straight to hydrogen, fuel cells and bio fuel systems. However, it is now widely accepted that hybrid vehicles will have a significant role to play over the next couple of decades as these other technologies continue to be developed.

The development of power splitting transmissions (PST) has been a crucial feature in the technological success of hybrid driveline vehicles. They have played a key role in facilitating the management of the mechanical and electrical power flows, ensuring good driveability, providing improved economy and reducing emissions compared to conventional internal combustion engine vehicles.

Hybrid electric vehicle technology has made a massive impact over the past decade on the automotive engineering industry (Miller 2006, Ehsani et al 2005). The growth in interest has been fuelled by increasing concerns about the environment and fuel efficiency savings. But also, the market uptake of hybrid vehicles – led mainly by the Toyota Prius – has been much greater than most observers originally predicted; this in turn has led most of the other original equipment manufacturers (OEMs) and Tier One suppliers to develop their own systems, often in collaborative partnerships.

Although many versions of hybrid vehicle have been tried, by far the most common layout is the 'series/parallel' hybrid, in which an IC engine and electric motor can either work independently or together. This means that the transmission system must incorporate (a) a power combining device and (b) a regeneration scheme so that the battery can be recharged either by the engine or by the kinetic energy of the vehicle during braking. It is perhaps not widely recognised, but the transmission design has been a crucial issue in the success of hybrid vehicles. These transmissions are also often referred to as power split devices (PSD) – and the control strategy to manage all the engine, motor generator (MG) and transmission elements is also crucial to the goal of achieving improved fuel efficiency from the hybrid vehicle compared with that available from conventional vehicles.

1.3 Need for research on electric vehicles

There has been a massive resurgence of interest in electric vehicles (EVs) over the past decade. Many observers now see them as the long term solution to reducing vehicle emissions and CO_2 usage in comparison to alternative approaches such as hybrid vehicles, fuel cells or biofuels. The public perception of electric vehicles has changed dramatically – and recently announced vehicles such as the Tesla roadster and Chevrolet Volt have reinforced the idea that they are now becoming seriously competitive products. Not long ago, electric vehicles were still seen as niche products – and associated more with 'milk float' technology rather than a viable passenger transport alternative (Chan and Chau 2001; Husain 2003; Larminie and Lowry 2003).

The massive advances have occurred in battery technology – although the progress has been gradual and sustained so that it has not commonly been perceived as a major breakthrough. The vehicle range available with modern battery sets – such as Lithium Ion – is now typically of the order of 200km, which makes electric vehicles acceptable for much urban use. High cost of the batteries is still a problem and despite a relentless downward price trend, the battery sets are often supplied on a leasing arrangement rather than a straightforward purchase.

As the electric vehicles market continues to grow, the vehicle manufacturers will place increasing emphasis on searching for efficiency gains. This process of continual improvement is central to vehicle development and has occurred for example over recent decades with internal combustion engines; the industry has achieved fuel consumption and CO_2 emissions figures that were considered impossible twenty years ago. In all the green solutions, battery electric cars have the best well-to-wheel efficiency of both conventional cars and hydrogen fuel-cell cars. For example, with 1 MWh of electricity, an EV can drive 5525 km; while using the same amount of electricity to generate hydrogen and to drive a fuel cell car, the distance is reduced to 1790 km (Randall 2009).

The electric vehicle part of this research focuses on one particular area in which efficiency gains may be achievable for electric powertrains – the addition of a gearbox. It is commonly argued that one of the distinct advantages of an electric motor as a motive unit is its torque characteristic; it can deliver maximum torque from zero speed and throughout the low speed range – typically up to around 2000 rev/min. Then, the available maximum torque reduces with speed along the motor's maximum power curve. This is a much better characteristic than that associated with internal combustion engines, which cannot deliver useful torque at low speeds and because of their relatively narrow torque and power bands must be used with multispeed transmissions in order to deliver tractive power to the vehicle in a suitable form. Typical electric motors have another desirable feature – their maximum intermittent power is considerably higher than their rated continuous power – for example, 75 kW compared to 45 kW for the example motor used here. The limiting factor is usually related to controlling the amount of heat build-up. Consequently, good acceleration times can be achieved providing they

are only used for relatively short periods – a situation which fortunately is typical of normal driving.

1.4 Aim and objectives

The proposed research is focused on transmissions for hybrid and electric vehicles.

In the HEV part, the research is focused on the NexxtDrive system (Moeller 2006) which is marketed as 'DualDrive' for automotive and off-highway applications. The transmission provides a continuously variable gearbox based on two epicyclic gear sets plus two electric motor/generator units. This unique, patented scheme offers potential efficiency benefits over its competitors. It has a crucial benefit of providing two ratios at which the electrical path transmits no power (and therefore no losses). A key design issue is to design the transmission to match the vehicle application such that these two points occur at common operating speeds. The DualDrive system is covered by patent protection and potentially has applications in other industrial drive situations, bicycle drive units, engine ancillary units etc. It is similar in principle to the successful Toyota Prius unit, but differs in particular in that the Toyota scheme only has one epicyclic gear set.

In the EV part, the research is focused on the effect of transmissions on performance of electric vehicles. The efficiency curves for a typical electric motor are highly dependent on both speed and torque – and the motor efficiency tails off rapidly at low speeds and torques where its efficiency might drop to say 50%, whereas in its mid speed and torque range it can be as high as 93%. Consequently, it is of interest to the energy efficient vehicle community to try and quantify any potential gains from utilising a gearbox in order to operate the motor for longer periods in its high efficiency region.

The overall aim of the proposed research is to study the new type of transmission for hybrid electric vehicles and to investigate the effect of transmissions on electric vehicles. This can be broken down into the following objectives:

1. Analyze the behavior of the twin epicyclic gearbox and the single epicyclic gearbox;

2. Compare the twin and single epicyclic gear box and investigate the potential benefits of the twin epicyclic gearbox.
3. Build up Matlab/Simulink models of hybrid electric vehicles equipped with the single and twin epicyclic gearboxes.
4. Compare the overall performance of HEVs fitted with the single and the twin epicyclic transmission.
5. Model the powertrain of a generic electric vehicle and investigate whether the addition of a gearbox results in significant values of predicted efficiency gains.

The original aspects of this work are:

1. The analysis and modelling the twin epicyclic gearbox.

2. The analysis and modelling the twin epicyclic system in a vehicle and a comparison of the results with single epicyclic system.

3. Modelling and analyzing EVs with and without a transmission system of varying levels of complexity.

2 Review of previous work

2.1 Introduction

In this chapter, previous work on hybrid electric vehicles (HEVs), electric vehicles (EVs), transmissions for HEVs and EVs, and control strategies for HEVs are reviewed. The definitions and classifications for HEVs are summarised and the main tools for HEV analysis are introduced. For EVs, the current situation and the future trends are analyzed. Transmissions for HEVs have received a substantial amount of attention and several different designs have been proposed over the past decade. And finally, the control strategies for hybrid vehicles, a crucial feature in optimizing performance and overall efficiency are reviewed.

2.2 Hybrid electric vehicles

2.2.1 Definition and classification

According to Ehsani (Ehsani, Gao et al. 2004), “A hybrid electric vehicle (HEV) is a vehicle with two or more energy sources and energy converters, one of which is electrical”. There are at least two power sources – a primary power source and a secondary power source. The primary power source is normally a thermal energy source, for example, petrol or diesel for an internal combustion engine, or hydrogen for a fuel cell stack. The secondary energy source is normally electricity in a battery or supercapacitors.

There are several ways to classify HEVs. From the different powertrain structure, or the different energy flow routes, HEVs can be classified into three kinds: series hybrid, parallel hybrid, and series-parallel hybrid (Vaughan 2008). Some other authors separate the fourth kind of hybrid – complex hybrid (Ehsani, Gao et al. 2004; Chan 2007). But the definitions are not universally agreed and complications can arise in the literature. The structure of each kind of HEV is shown in Fig 2.1.

In series hybrid vehicles, the engine drives the generator to generate electricity, which either is stored in the battery, or is supplied to the motor to drive the car. There is no mechanical connection from the engine to the drive wheels (Fig 2.1 a). By decoupling the engine from the driving wheels, the engine can always work at

its highest efficiency point. But, the energy is converted twice, namely mechanical to electrical in the generator and electrical to mechanical in the motor. So the efficiency of these two processes is a major issue for series hybrid vehicles.

In parallel hybrid vehicles, both the engine and motor/generator are mechanically connected to the drive wheels via two clutches. The propulsion power may be supplied by the engine, the motor, or by both (Fig 2.1 b). Compared to the series hybrid, the parallel hybrid needs two propulsion devices – the ICE and the electric motor. But both engine and motor can be downsized to get the same performance.

In series-parallel hybrid vehicles, there is an additional mechanical link between the engine and the motor, via a generator. Hence, depending on the conditions, part of the power from the engine can be converted into electricity to either charge the battery or drive the electric motor (Fig 2.1 c). Obviously, the series-parallel is more complicated and more expensive than the previous two kinds of hybrids. But it possesses the advantages of both series and parallel hybrid.

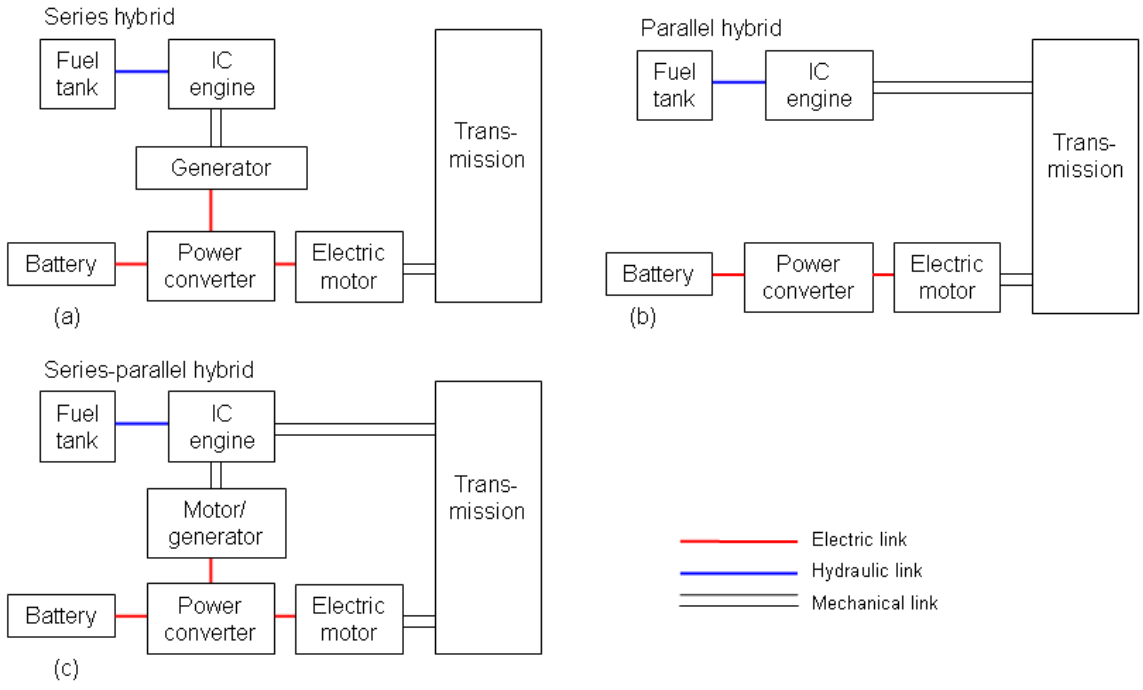

Fig 2.1 Classification of hybrid electric vehicles

According to the hybridization ratio, namely the level of electric power and the function of the electric motor, HEVs can be classified as: micro hybrid, mild hybrid and full hybrid (Chan 2007). For a micro hybrid, the main function of the electric

motor, which usually is about 2.5 kW, is for start and stop, and the energy saving may reach about 5% to 10%. In a mild hybrid, the motor is about 10-20 kW. The motor can replace the original flywheel of the engine, and add to the propulsion as in the parallel hybrid system. A mild hybrid can achieve energy saving of amount 20% - 30%. For a full hybrid, which can save energy about 30%-50%, the motor power is about 50 kW. In this design, the motor alone mode is used for start up and mid-range speed driving.

A summary of classification of HEVs is shown in Table 2.1.

Table 2.1 Classification of HEVs

	Classification	Examples
Drivetrain structure	Series hybrid	Toyota Coaster Hybrid bus, Chevy Volt
	Parallel hybrid	Honda Insight
	Series-parallel hybrid	Ford Escape, Toyota Prius, Ferrari hybrid
Hybridisation ratio	Micro hybrid	Citoren C3, Chevrolet Silverado, GM Saturn VUE Green line, new BMW X1 & Smart MHD
	Mild hybrid	Honda IMA (Integrated Motor Assist) system (Civic, Insight), Toyota Crown, Chevy Malibu, BMW ED
	Full hybrid	Nissan Tino, Toyota Estima, Toyota Prius & Ford Escape, Lexus RX
Position of the motor and the transmission	Pre-transmission hybrid	In mild hybrid HEVs
	Post-transmission hybrid	GM Autonomy(in-wheel motor)
The method of refuelling the energy	Petrol station refuelling	Most of current HEVs
	Plug-In hybrid (PHEV)	BYD F3DM, Renault Kangoo

According to the position of transmission and motor, the hybrid can be classed as pre-transmission (the motor is ahead of the transmission) and post-transmission (the motor is behind the transmission) (Miller 2004; Ehsani, Gao et al. 2007).

According to the method of the refueling the energy, HEVs can be classified as gas station refueling and plug in hybrid (PHEV)(Chan 2007). PHEV is becoming a popular topic in recent years and most of the global OEMs have development programmes. In December 2008 in China, BYD Auto started selling the world's first mass-produced plug-in hybrid vehicle, the BYD F3DM, produced for the domestic Chinese market. A Toyota plug-in hybrid is planned to be available commercially in 2009.

(Friedman 2003) summarised a checklist to check whether a vehicle is a hybrid or not, which is shown in Table 2.2. The vehicle that has two checkmarks is described as a muscle-hybrid, which is an American term, and is similar in definition to a micro-hybrid. Generally speaking, hybrids with more checkmarks obtain higher fuel saving rates and less emissions. But the best way to judge a vehicle is the practical performance on normal road conditions.

Table 2.2 Hybrid checklist: is this vehicle a hybrid?(Friedman 2003)

Does this vehicle...	Conventional Vehicle	Muscle Hybrid	Mild Hybrid	Full Hybrid	Plug-in Hybrid
Shut off the engine at stop-lights and in stop-and-go traffic	✓	✓	✓	✓	✓
Use regenerative braking and operate above 60 volts		✓	✓	✓	✓
Use a smaller engine than a conventional version with the same performance			✓	✓	✓
Drive using only electric power				✓	✓
Recharge batteries from the wall plug and have a range of at least 20 miles on electricity alone					✓

2.2.2 Hybrid vehicle development

Hybrid vehicle technology is a relatively new aspect of automotive engineering; most of the developments have occurred over the past 2 decades. The landmark date was probably 1997 when Toyota introduced the first commercial hybrid, the Prius.

Despite its relative newness in automotive technology, interest has grown at a staggering rate. This is reflected in the fact that there are several excellent textbooks on hybrids (Husain 2003; Ehsani, Gao et al. 2004; Miller 2004; Guzzella

and Sciarretta 2007) and the underpinning electric vehicle technology (Chan and Chau 2001; Larminie and Lowry 2003).

Hybrid vehicle technology inevitably involves a systems-design approach, based on a collection of components such as:

i) Petrol, diesel engines
ii) Electric motor/generator units
iii) Batteries
iv) Supercapacitors, ultracapacitors
v) Fuel cells
vi) Electrical components, e.g. inverters

Needless to say, there remains a vast range of viewpoints about the relative merits of competing schemes. There have been several excellent review papers published recently (Chau and Wong 2002; Friedman 2003; Miller 2006; Van, Maggetto et al. 2006; Chan 2007; Ehsani, Gao et al. 2007) . Key topical questions include:

i) Will fuel cells have a future given the hydrogen storage/infrastructure problems?
ii) Can telematics-enabled conventional powertrains compete with hybrids (Manzie, Watson et al. 2007)?
iii) Are mild hybrids (highly efficient diesels, integrated starter alternator(ISA), regeneration) more cost-effective than full hybrids (Cho and Vaughan 2006b; Chau and Chan 2007)?
iv) Are plug-in hybrids becoming commercially attractive (Gonder, Markel et al. 2007; Shabashevich, Saucedo et al. 2007)?

2.2.3 Hybrid vehicle analysis

The worldwide debate about hybrid powertrains has led to a proliferation of research in analysing and predicting vehicle performance. This in turn has led to the development of several software packages specifically aimed at modelling the energy management in hybrid drivelines (Gao, Mi et al. 2007). The best known of these is probably ADVISOR (Wipke, Cuddy et al. 1999; Markel, Brooker et al. 2002), developed in 1999 by the US NREL and based on Matlab/Simulink blocks.

Other well-known codes include the QSS-Toolbox (QuasiStatic Simulation Toolbox) (Rizzoni, Guzzella et al. 1999) and PSAT(Powertrain system analysis toolkit) sponsored by the US Department of Energy (Argonne 2007), both of which also use Matlab/Simulink. Further codes include PSIM, Simplorer and V-ELPH (Gao, Mi et al. 2007).

2.3 Electric vehicles

The current level of interest in Electric Vehicles (EVs) could hardly be overstated as manufacturers and governments around the world appear to have increased interest at a substantial rate. The historical perspective of EVs is a fascinating engineering story; few people realise that they pre-dated Internal Combustion (IC) engine powered vehicles and were commercially available at the end of the 19th century. An electric car even held the world land speed record in 1899 and was the first car to exceed one mile per minute! At this time, for a given power output, one only had to compare the size and complexities of three competing devices – electric motor, IC engine and steam engine – to realise that the electric motor was a clear winner. Nevertheless, its downfall when deployed in a vehicle was the energy storage using rechargeable batteries; the specific energy (Wh/kg) of gasoline is around 300 times higher than that of the original lead acid batteries. There are several excellent references (Chan and Chau 2001; Westbrook 2001; Husain 2003; Larminie and Lowry 2003) recounting the story of electric vehicle development up to the present day.

The resurgence of current interest in the early part of the 21st century has been driven by both political and technological developments, namely a requirement to control global emissions and the emergence of new battery designs with improved specific energy, energy density and rechargability properties.

One of the great advantages of the electric motor is its torque characteristic; it provides maximum torque from zero up to low speeds, and then it is governed by the maximum power available as motor speed increases. This has two significant advantages over the typical torque-speed properties of the competing IC engine:

i) It provides fundamentally a more desirable characteristic spread of torque over the speed range in contrast to the peakiness of an IC engine.

ii) It removes the need for any additional transmission – clutch or gears.

Consequently, the vast majority of current EV designs to date have exploited this advantage and the motor is usually connected to the drive wheels via a single reduction ratio – often incorporated in the differential unit. This advantage of the electric motor is further helped by the fact that most motors have two ratings – an intermittent high power curve and a lower continuous power curve, normally constrained by heat dissipation. So, high torques are always available for good acceleration, particularly from low speeds, and the vehicle top speed is controlled by the torque on the continuous power curve, so the fixed reduction gear is normally selected to control this.

However, one of the main conclusions to emerge from the plethora of research work into energy efficient vehicles is that it is necessary to pursue every possible avenue for minor efficiency gains. The point is then that only when all these gains are added together does the vehicle begin to show worthwhile advantages. A classic case study to underline this conclusion is to compare two contrasting approaches to energy efficient vehicles (i) a full hybrid, e.g. Toyota Prius and (ii) a conventional state of the art diesel vehicle, e.g. BMW118d. The Toyota Prius is a highly sophisticated hybrid design using a combination of an IC engine based on the Atkinson cycle, coupled with two electric motors and a unique epicyclic gearbox. The BMW118d is a conventional vehicle with a diesel engine modified for high efficiencies particularly at part load, a conventional transmission, stop-start arrangement and some regeneration capability. For both these vehicles all the input energy derives from the fuel input – although they have very different ways of managing the efficient usage of it – but crucially they both support the key issue that research into energy efficient vehicles depends on the pursuit of all avenues of efficiency gains together.

Returning to the case of EVs, it is therefore of interest to investigate whether it is possible to manage the efficiency of the electric motor, so that by using an intermediate gearbox the motor is operated more often in its higher efficiency region.

In similar fashion to HEVs, plug-in EVs have also become a very topical subject. For example, the ‘i MiEV’ from Mitsubishi Motors has been commercially produced

and 200 of these vehicles have been put into the UK for test driving. Using the on-board charger, the vehicle can be charged with a 100 V or 200 V power source in the home. The range over one of the driving cycles, Japan 10-15, for one charge is 160 km, which is enough for most commuting applications. For example, in the United States, half of U.S. households have a daily mileage of under 30 miles per day; 78 percent of daily work commuters travel 40 miles or less (Babik 2006).

2.4 Transmission designs

Continuously Variable Transmissions (CVTs) have been around for many years – some authors claim that Leonardo da Vinci sketched a design concept over 500 years ago. However, although the first patent was filed in 1886, CVTs did not have any commercial impact until DAF produced a CVT car based on a pulley and rubber belt principle in 1958. Interest in the US followed much later – in 1989 when the Subaru Justy offered a CVT – because US vehicles had been dominated by conventional automatic transmission systems for many decades.

The cost-benefit issues relating to CVTs are well understood. The potential advantages are improved performance, economy and emissions or more importantly an improved compromise between them. Their disadvantages have been cost, complexity, noise and driving refinement. Only over the past five years or so has the development of CVTs reached a stage at which they are beginning to be genuinely competitive with the alternatives, e.g. conventional, torque converter automatics and automated manual gearboxes, such as the twin clutch VW DSG system.

There are several generic approaches to CVT technology:

i) Variable pulleys using rubber or steel belts (e.g. DAF, Audi, GM, Honda, Nissan)
ii) Toroidal schemes using the friction between discs and rollers (e.g. Torotrak, Nissan Extroid)
iii) Hydrostatic using variable displacement pump and motors (Torvec IVT)
iv) Hydromechanical using a controlled power split between mechanical and hydrostatic components (e.g. agricultural, all-terrain vehicles)

v) Electromechanical using epicyclic gears plus electric motor/generator systems (e.g. Toyota Prius, NexxtDrive)

2.4.1 Transmissions for HEVs

The first successful electromechanical PSD transmission is generally credited to TRW (Gelb, Richardson et al. 1971). The key feature is to use an epicyclic gear to combine the power from the engine and two MG (motor/generator) units. Note that two MG units are required in order to exercise sufficient control of both speeds and torques in the system. The transmission effectively has two functions – it provides a continuously variable gear ratio over a certain range and it selects the balance of torques, and hence powers, applied to and from the drive wheels by the engine and MG units. The Toyota Prius, introduced in Japan in 1997, used this transmission design, with an IC engine of 52 kW and MG units of 33 and 10 kW, and is now widely recognised as making it commercially successful (Inoue, Kusada et al. 2000; Miller and Miller 2005).

Further developments have occurred since the Prius was introduced, and there are now two generic types of power splitting transmissions used in hybrid vehicles – the single and dual mode designs. Examples of these, including the latest developments are discussed here.

- Toyota Prius, THS design – single mode

Because of the commercial success of the Toyota Prius, this transmission arrangement is the most common layout used in the industry; it has already been used by several other manufacturers in their hybrid vehicle designs. The layout is shown diagrammatically in Fig 2.2. In this research, R, C, S represent the ring gear, the carrier and the sun gear respectively.

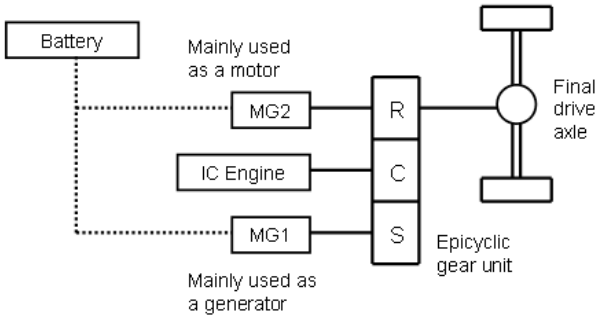

Fig 2.2 Toyota Prius, THS arrangement

The clever feature of this relatively simple looking arrangement is that (a) it controls the split of power between the mechanical and electrical paths and (b) it offers an infinitely variable transmission ratio by controlling the relative speed of the sun, carrier and ring gears of the epicyclic. A lot of the other challenging design aspects which are not shown in Fig 2.2 relate to the control of the different elements and the inevitable compromise between achieving good driveability together with high levels of efficiency. Basically, this system can be characterized by five main modes of operation.

i) Electric drive – the IC engine is off and the battery powers MG2 and hence the vehicle.

ii) Normal drive, cruising – the IC engine is on; the tractive power is a summation of the mechanical path directly from the engine plus the electrical path from the MG2 motor. The engine also supplies power to drive MG1 which acts as a generator to supply MG2.

iii) Power boost, acceleration – this is similar to mode 2 except that torque delivery to the drive wheels is given priority, so for example, the battery will be used to supply the MG units for these periods.

iv) Battery charge, idle – the IC engine simply drives MG1 as a generator to supply current to charge the battery, depending on its state of charge (SOC).

v) Negative split – in this case, both MG1 and MG2 can act as motors, which results in a lower IC engine speed, or engine lugging, as a means of optimizing fuel economy.

An example of the speed ratios for this system is shown in Fig 2.3. The Transmission Ratio (TR) is defined as (input speed/output speed) for the gearbox. Normally, the input is connected directly to the engine and the output is connected to a final drive, differential unit. There is one point on these curves which is of particular interest, because at this point all the power is transmitted by the mechanical path. It occurs for the example shown in Fig 2.3 at a TR of 0.72, at which point the speed of MG1 is zero, and although MG2 is still turning, it can be controlled to spin freely. As a rough guide, the mechanical efficiency of a typical gear set is around 98%, compared to an overall efficiency of around 80% for the

electrical path. Hence, the design choice of this ratio is extremely important; it is usually chosen to optimise economy on one of the established industry-standard drive cycles.

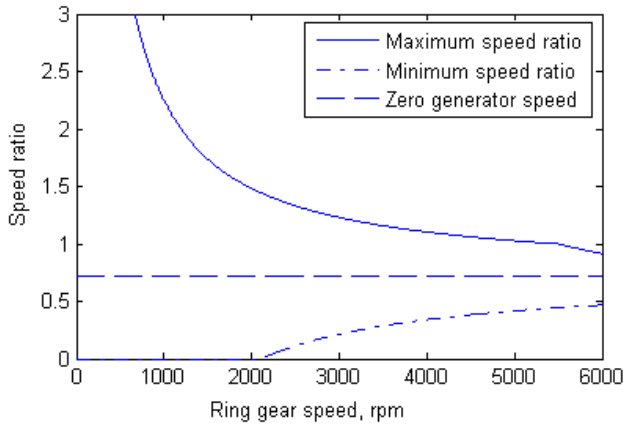

Fig 2.3 Transmission speed ratio limits of the THS system (Cho, Ahn et al. 2006a)

- **GM Allison, AHS system – dual mode**

The addition of clutches to a transmission based on two epicyclic gear units opens up an opportunity to fundamentally change the power flow through the system (Miller and Miller 2005). An example is shown in Fig 2.4.

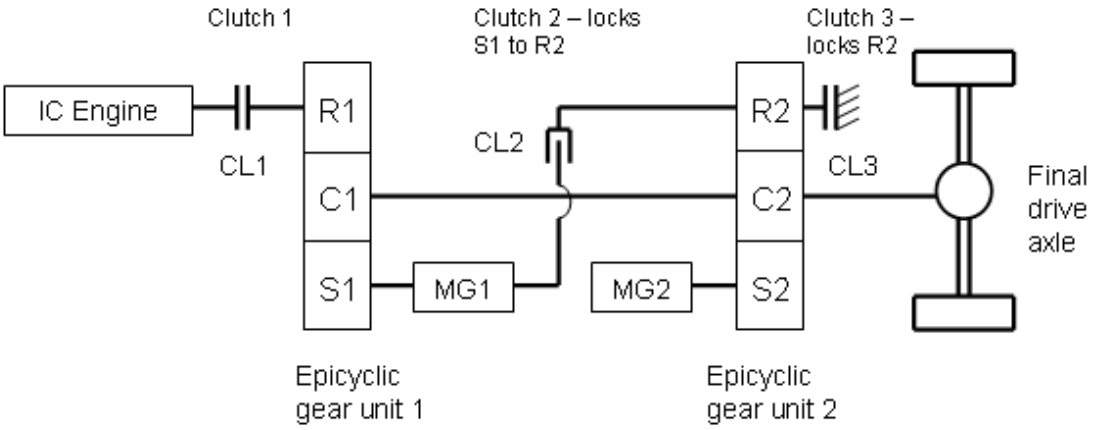

Fig 2.4 GM Allison AHS arrangement

Basically, the two modes of operation are usually referred to as:

i) Low range – input power split

ii) High range – compound power split

In the first of these – input power split, the transmission behaves in exactly the same way as the single mode system. In the second – compound split – mode the sun gear 1 (S1) is connected via MG1 to ring gear 2 (R2). The ability to switch

between these two modes smoothly is a crucial aspect of this design, and this is usually referred to as synchronous shifting. In other words, the clutches are shifted when the MG speeds are zero, such that torque transfers can take place without involving sudden speed changes.

The benefits of this system are.

i) A low and high range is available without the need for a gear shift. The low range is used for starting, low speeds and reverse, whereas the high range is used for highway operation, grades and towing.

ii) The required speed ranges of the MG units are reduced.

iii) The MG units can be induction type machines.

iv) In the compound split arrangement, less power is transmitted via the electrical path, so the motor size can be reduced and overall electrical losses reduced.

- **Generic dual mode + 4 fixed ratios systems**

An interesting software package for generating novel transmission designs has been developed by GM Research and Development Laboratories (Raghavan, Bucknor et al. 2006; Raghavan, Bucknor et al. 2007). One of the examples described in these papers is a dual mode system which also offers four fixed gear ratios. The design is shown in Fig 2.5, and it emphasises the potential benefits of the software, because (a) this arrangement is rather complicated, (b) it is not intuitively obvious to understand exactly how it will meet the performance specifications and (c) it is not a design that would naturally be proposed using traditional design methods.

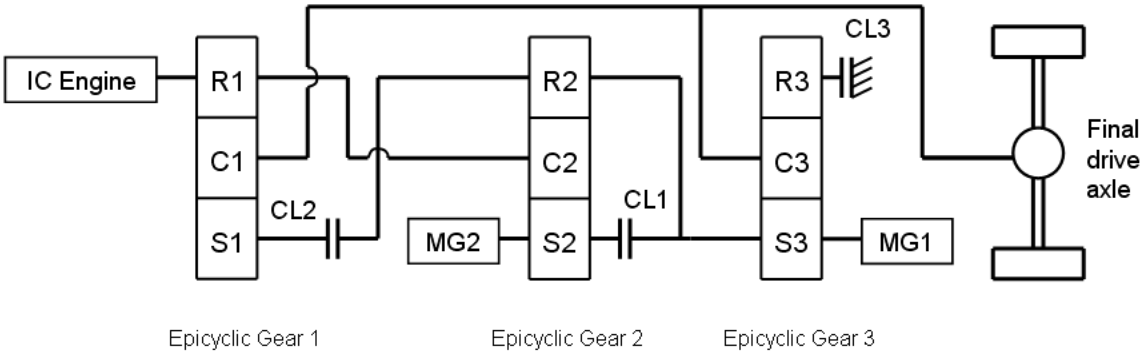

Fig 2.5 Generic dual mode + 4 fixed ratios arrangement

- **GM/DC/BMW system - dual mode**

One of the latest development of a dual mode system was announced in 2006 (Nitz 2006a; Nitz, Truckenbrodt et al. 2006b), as the result of a consortium agreement between these three major vehicle manufacturers. It involves the addition of a third epicyclic gear unit and a total of four clutches. The benefits of this additional complexity are related to the addition of four fixed gear operating modes as well as the retention of two ranges of continuously variable transmission capability.

Overall, therefore this system offers six methods of operation.

i) Input-split eCVT mode, or continuously variable mode 1, operates from vehicle launch through the second fixed gear ratio.
ii) Compound-split eCVT mode, or continuously variable mode 2, operates after the second fixed gear ratio.
iii) First fixed-gear ratio with both electric motors available to boost the internal combustion engine or capture and store energy from regenerative braking, deceleration and coasting.
iv) Second fixed-gear ratio with one electric motor available for boost/braking.
v) Third fixed-gear ratio with two electric motors available for boost/braking.
vi) Fourth fixed-gear ratio with one electric motor available for boost/braking.

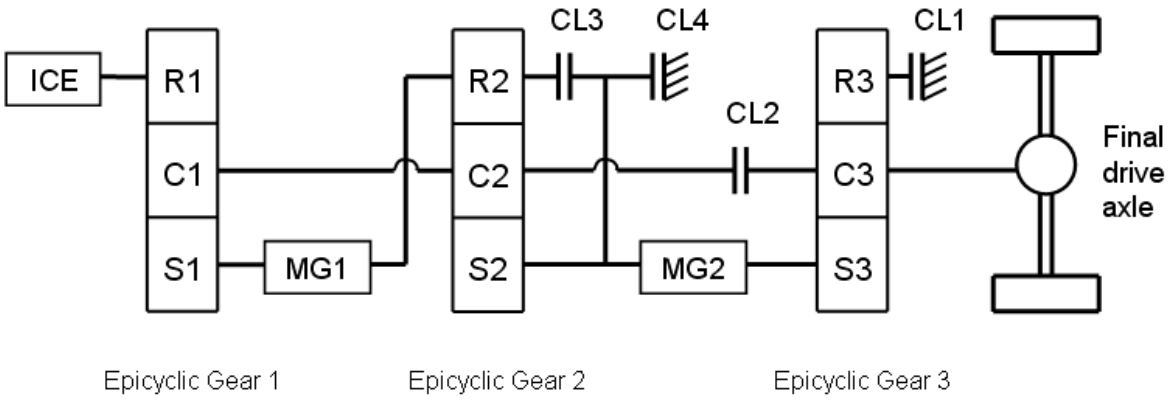

Fig 2.6 GM two mode hybrid transmission with 4 fixed gear ratios

Full details of this transmission building upon substantial experience with one and two mode transmissions were recently released by GM (Grewe, Conlon et al. 2007). It is particularly suited to larger vehicles, such as full size SUVs (sport utility

vehicles) and personal trucks, where towing and high continuous engine power conditions are important aspects of the vehicle capabilities. The range of fixed gear ratio options means that more reliance can be placed on the mechanical power transmission path, thus reducing the extreme, continuous duty motor requirements of other systems without sacrificing fuel economy. These claims are supported (Grewe et al 2007) by power and economy calculations for a large GM SUV over the EPA Urban, EPA Highway and US06 schedules. In the longer term, the consortium believes that this arrangement will set a new industry standard for hybrid vehicle transmissions.

- **Bosch Dual-E transmission**

Bosch have recently announced a new prototype transmission system called Dual-E, which is described in a paper by Schultz (Schulz 2004; Schultz 2006). In Schultz's work, two separate epicyclic gear units are connected with a 5 speed automated manual transmission (AMT). This differs from the NexxtDrive system studied here in which two epicyclic gear units are directly connected together and not connected to an AMT. The Dual-E system is shown in Fig 2.7. Each motor generator unit plus epicyclic gear unit controls one of the main gearbox shafts. Hence, overall it offers a total of five fixed gear ranges plus an infinitely variable capability within each range. For a mid size saloon, the motor generator units are rated at 8 kW each. The benefits of this system are high efficiency because the power used in the electrical path can be minimised and a wide range of transmission ratios. Gear changes in the AMT when necessary are performed automatically without traction interruption.

2.4.2 Transmissions for EVs

The possible configurations of EVs are shown in Fig 2.8 (Ehsani, Gao et al. 2004), from which it can be seen that mainly two types of transmissions are used on EVs: multi-gear transmission and single-gear transmission. Currently, single gear transmissions are used on most EVs. For example, on the Gulliver U500 design from Tecnobus, the transmission is a single gear with a fixed ratio of 1:4.37. For configurations like Fig 2.8 (a) and (b), an electric propulsion motor replaces the IC engine of a conventional vehicle drive train. The multi-gear transmissions here were originally designed for an engine, not especially for electric motors. It is

perhaps surprising, but there is very little published research on the potential benefits from fitting transmissions into the drivelines of electric vehicles.

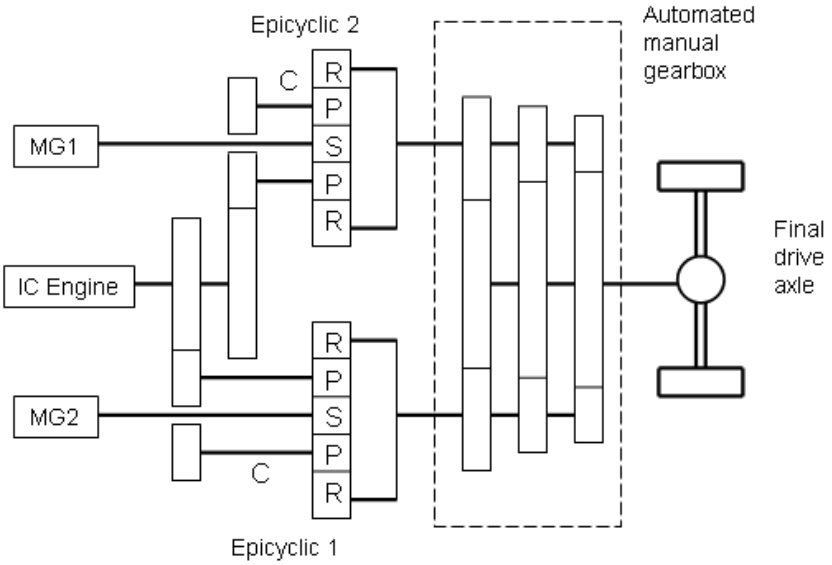

Fig 2.7 Bosch Dual-E transmission (Schultz 2006)

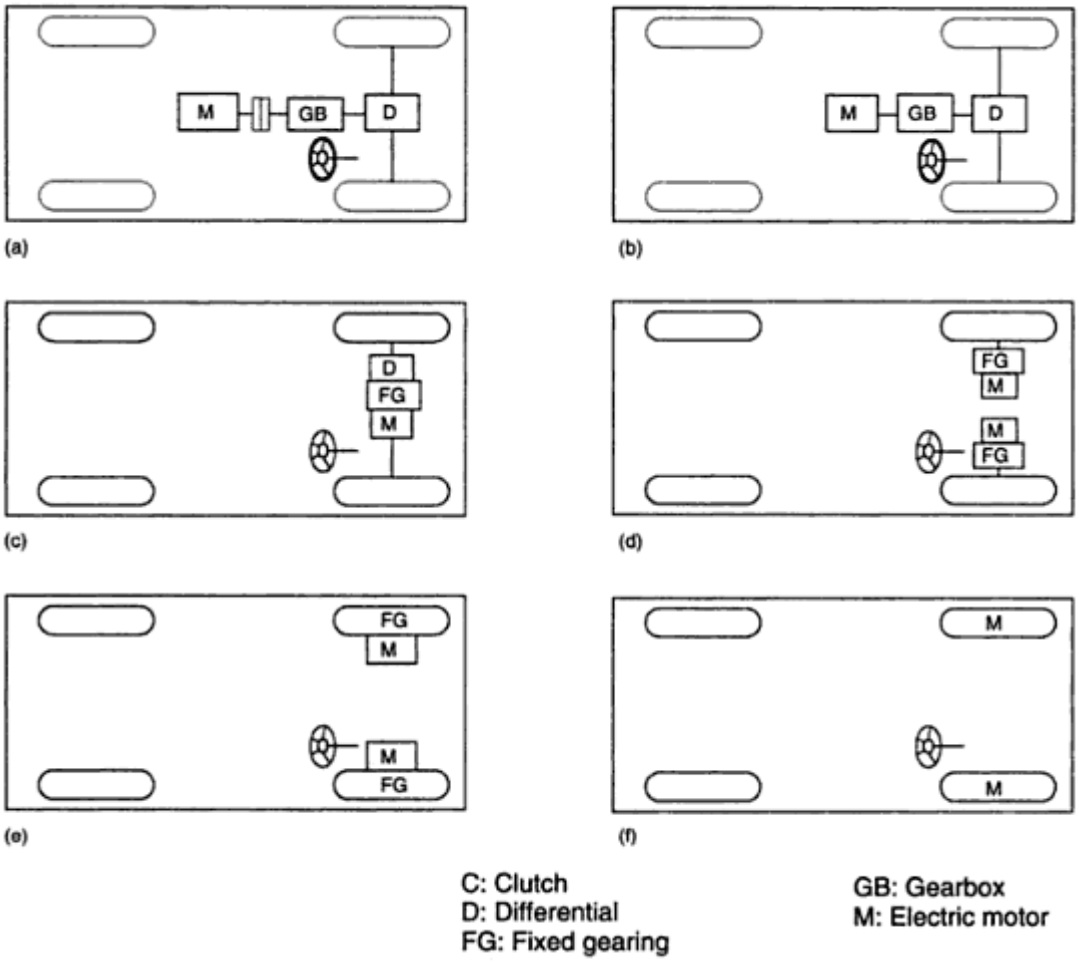

Fig 2.8 Possible EV configurations (Ehsani, Gao et al. 2004)

One of the few published reports of work in this area was recently published in June 2009 (Honeywill 2009). It describes work by a UK company, Vocis, on the development of a two speed gearbox suitable for a 70kW delivery van application. It highlights one of the important problems of the actuator required to switch between gear ratios, assuming that this would be automated rather than under manual control. The authors refer to simulations indicating a claimed 5 to 10% reduction in energy consumption over the NEDC cycle. No details are given, but these figures appear to be in line with the results reported later in this thesis.

2.5 Control strategies

2.5.1 Importance of control strategy

Implicit in the design of hybrid vehicles is the fact that there are no 'magic' energy sources! Hence, the design philosophy is based on managing the energy – from gasoline engines, electrical storage, fuel cells – more effectively somehow. This overall effectiveness is usually judged against one of the so-called standard drive cycles in the EU, USA or Japan to enable fair comparisons to be made.

Hence, the controller design is absolutely central to the overall effectiveness of a hybrid powertrain. The aim of this section is to review recent contributions (since 2000) and summarise the current state of the art in controller strategy and design.

The review focuses on control techniques and their usefulness both for analytical and practical situations. In the main text of this section, little reference is made to authors' claims about the performance improvements of their systems. This is because they can be misleading; in order to make informed judgments about improvements it is necessary to know all the details of the modeling, assumptions and driving cycles used. However, some overall comments about relative performance are included in section 2.5.3.

2.5.2 Controller design

The generic structure of a hybrid vehicle control system (Paganelli, Ercole et al. 2001; Koot, Kessels et al. 2005; Pisu and Rizzoni 2007) is shown in Fig 2.9.

The first, and by far the most common hybrid vehicle control system, is a rule-based approach largely based on engineering intuition. The potential problem with

this approach is that it is difficult to fine-tune the rules without any further help from more rigorous mathematical approaches. There have also been several attempts to enhance this rule-based strategy by using more formal techniques such as Fuzzy Logic (FL), or Neural Networks (NN).

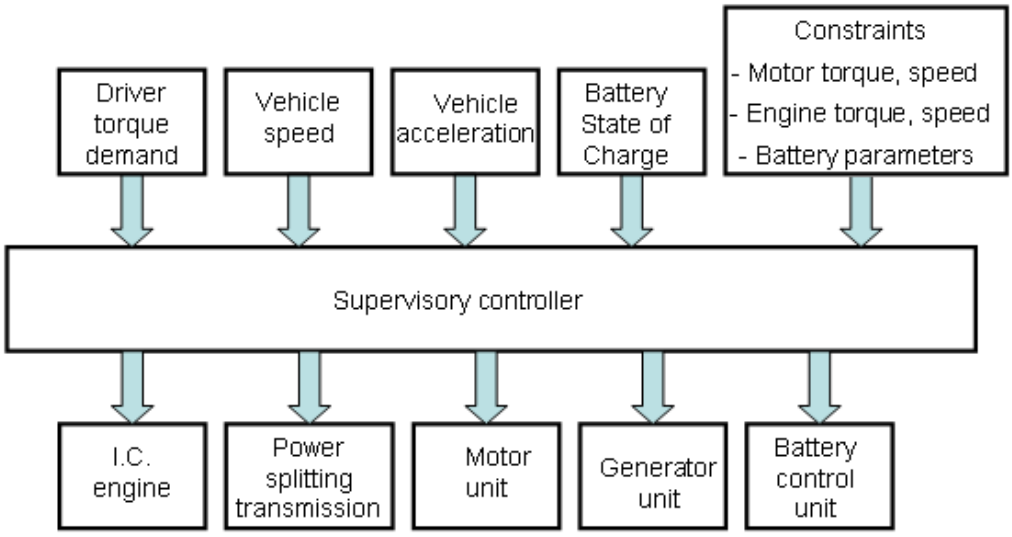

Fig 2.9 The generic structure of a hybrid vehicle control system

The second approach is usually referred to generally as Static Optimisation. This uses quasi steady conditions and obtains points which are optimum in some sense. This may, for example, be optimum fuel economy with details of energy usage between the electrical and mechanical paths. However, because it is a relatively simple point-wise approach, it is possible to extend the optimisation to incorporate both economy and emissions for example. This is also often referred to as Sequential Quadratic Programming (SQP) and has the potential disadvantage that it is not robust against disturbances.

The third, and most sophisticated approach, is Dynamic Optimisation. This deals with transient conditions typically over a specified time frame; in the case of vehicle studies this usually involves one of the well known industry standard drive cycles. There are a range of detailed approaches to this particular problem under the general heading of Dynamic Programming (DP). Most recent contributions agree that this approach is computationally intensive and that although it results in a global optimisation of the control problem, it is not possible to directly implement it as a real time controller. Some observers argue therefore, that it is not a

practical approach, because it requires a priori knowledge of the input profile – speeds, accelerations, grades etc in this case. However, others argue that it is valuable for two reasons. First, it provides a benchmark of the best performance that is achievable; hence other control schemes can be assessed against this yardstick. Second, it can lead to suggestions for improvements in the rule-based strategies that may not have been apparent from engineering intuition. Indeed, there have been several recent research projects which attempt to exploit a combined SQP and DP analysis to develop a practical rule-based plus fuzzy logic controller.

- **Rule–based (RB) control**

The rule based approach is often described as a heuristic control strategy. It has been described in many recent papers (Lin, Filipi et al. 2001a; Lin, Filipi et al. 2004; Zhang, Lin et al. 2006; Zhu, Chen et al. 2006; Ahn, Cha et al. 2007; Hofman, Steinbuch et al. 2007a; Hofman, Steinbuch et al. 2007b), although most of these papers also contain comparisons with other control techniques. In the development of practical prototype vehicle systems, the majority have used rule-base controllers, although details are rarely published because of commercial aspects. Hence, it is currently by far the most commonly implemented on-line approach.

It is based on a set of rules, usually implemented as nests of ‘if-then-else’ statements. The system components can be described by parametric or empirically derived maps, and the controller largely controls the switching between different modes, e.g. engine power, motor power, battery charging or energy regeneration. Because the rules are specific to a particular application they require considerable calibration and are not usually transferable.

The work reported in (Zhang, Lin et al. 2006) is interesting in that it applies an RB scheme to a hybrid vehicle fitted with a novel transmission based on a single epicyclic gear, single motor/generator unit and 4 fixed gears. Predictions using ADVISOR compare the results of this drivetrain with that of the standard Prius and show that over 6 typical driving cycles, fuel economy improvements of around 12 - 15% are available.

- **Rule-based plus Fuzzy Logic**

The use of a fuzzy logic controller enables the rule-based approach to be improved since it removes the restriction for ‘hard’ on/off type rules. It is well known for its robustness and ability to deal with non-linear systems and time-varying components – and hence, it appears well suited to the hybrid powertrain problem.

Several recent papers have used fuzzy logic control (Baumann, Washington et al. 2000; Won and Langari 2002) with a variety of views of how to set the membership functions to trade off acceleration, power split, energy/fuel usage, emissions and battery state-of-charge. References (Salman, Schouten et al. 2000; Kheir, Salam et al. 2004) used a set of 44 rules in an attempt to balance fuel usage and emissions as a performance index, and also used the Matlab PSAT (Power System Analysis Toolbox) rule-based controller for comparison. In (Rajagopalan, G. et al. 2003), the fuzzy logic controller was derived as an NREL(National Renewable Energy Laboratory, USA) project for use in the ADVISOR package.

- **Rule-based plus Neural Network (NN)**

The Neural Network approach has been used together with both rule-based and DP systems. In (Suzuki, Yamaguchi et al. 2007), the NN was trained on the hardware fitted to a light duty hybrid truck, in particular to model the fuel usage and electric current. This was then used to assist a conventional rule-based controller in driving conditions away from the normal regions represented in the standard driving cycles.

In (Hung, Tsai et al. 2007), the NN was tuned using the results from a DP controller over the 5 driving cycles used in ADVISOR. The inputs were 4 indices – velocity average and standard deviation, acceleration standard deviation and standstill time – and the outputs were 3 polynomial coefficients. A very different approach was used in (Arsie, Graziosi et al. 2004) where a Recurrent NN was used to continuously predict the vehicle load. It was argued that this information could then effectively be fed to a DP control algorithm, which could then be implementable as an on-line controller.

- **Equivalent Consumption Minimisation Strategy (ECMS)**

This technique is based on the concept of combining the energies from the IC engine and electrical machines on the same scale, by defining equivalent fuel consumption. In this way, a single cost function can be formulated in order to apply conventional optimisation techniques (Delprat, Guerra et al. 2001; Sciarretta, Back et al. 2004). The principle behind this approach is shown in Fig 2.10 for the case of battery discharge and Fig 2.11 for the case of battery recharge (Musardo, Rizzoni et al. 2005). The path on the left side of each figure shows the equivalent route by which energy is stored and restored to the system. Of course, there are losses involved in all the conversion processes, and these losses are different in the charging and recharging directions; consequently there are some approximations that need to be made in this equivalence approach. The results for the HEV over 6 standard driving cycles are shown in Table 2.3.

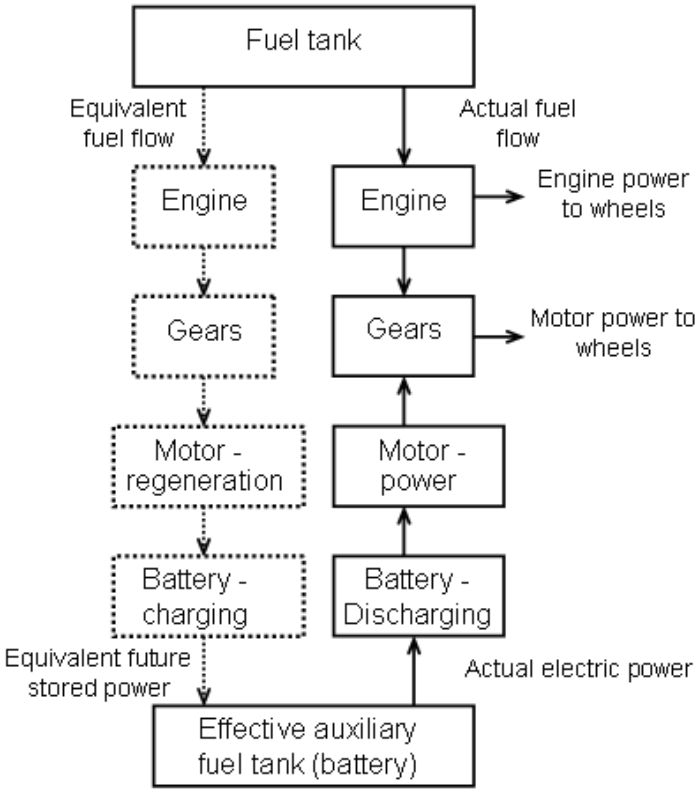

Fig 2.10 Energy paths for equivalent fuel consumption calculation during battery discharge

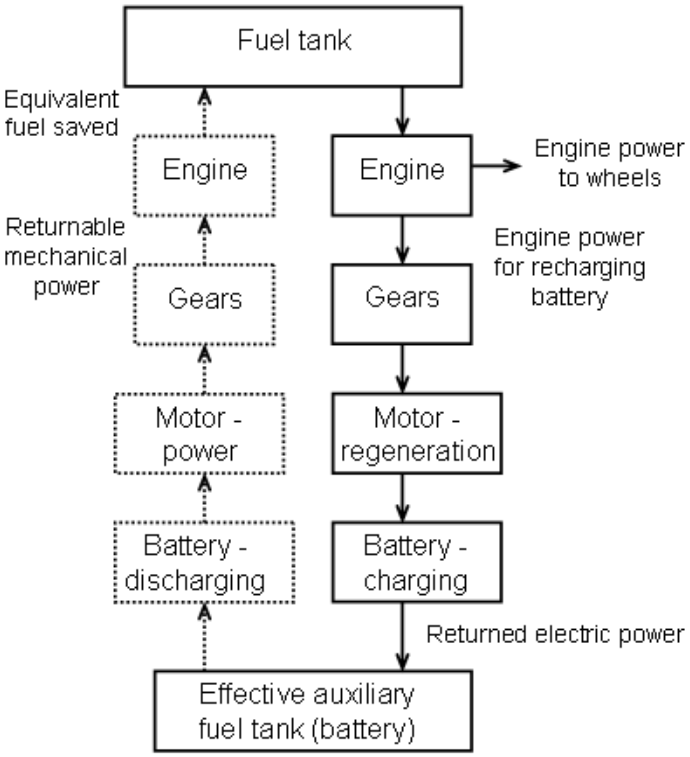

Fig 2.11 Energy paths for equivalent fuel consumption calculation during battery charge

One of the potential difficulties is in dealing with the battery state of charge (SOC), which effectively provides constraints since it should remain within a fixed range. Also, it is important in calculating comparative results that the final and initial battery states are the same, in order that there are no hidden energy losses or gains. In Paganelli's research (Paganelli, Guerra et al. 2000b), the predicted results from an ECMS controller are compared favourably with results derived from an optimum controller (Delprat, Lauber et al. 2004). In Paganelli's research (Paganelli, Guerra et al. 2000b), an adaptive term is added to provide an A-ECMS control scheme which deals with the battery state of charge by varying a control parameter based on a function of the road load. Again, the results are compared with those from an optimal DP solution, but the authors make the interesting point that although they use a sophisticated vehicle model, based on the VP-SIM code (Rizzoni 2000) for the A-ECMS calculations, the DP code must use a much simpler vehicle model in order to restrict the computing times; hence, the two solutions are not exactly comparable.

In Hofman's research (Hofman, Steinbuch et al. 2007a; Hofman, Steinbuch et al. 2007b), a novel controller (RB-ECMS) based on a combination of rule–based and

ECMS systems is introduced. This overcomes the difficulties of each individual approach in that they are sensitive to the input topology. Effectively, the RB-ECMS provides a collection of driving modes selected through various states and conditions. It is based on one decision variable – the maximum propulsion of power of the secondary power source, i.e. motor/battery during pure electric driving. The proposed controller then requires no tuning of the threshold values and variables and is implementable in real time. Simulation results predicted using ADVISOR for the Japanese cycle show that it achieves a 12% improvement over the RB scheme and achieves the same (within 1% accuracy) of the performance of the optimum DP controller.

- **Dynamic Programming (DP)**

The overall energy management of a hybrid electric vehicle can be viewed as a global optimisation problem. The performance index is linked to minimising the fuel consumption and emissions outputs. The controller specifies the commands and settings, e.g. power split between IC engine and electric motor, which achieves this goal, within certain constraints, e.g. battery state of charge. Since a typical driving cycle lasts several minutes, it is necessary to repeat this calculation many thousands of times. The DP technique is well suited to this problem. Also, the DP algorithm is based on a global solution which requires a specific time frame over which the problem is known. Thus, it appears highly appropriate for a specific driving cycle where the complete input profile is defined.

However, as mentioned previously, this comes with two main drawbacks; (i) it is extremely computationally intensive and (ii) it cannot be implemented in real time since it requires a priori knowledge of the input.

Applications of the Dynamic Programming approach have been reported many times in the literature over recent years (Lin, Filipi et al. 2001a; Lin, Filipi et al. 2004; Scordia, Besbois-Renaudin et al. 2005; Zhu, Chen et al. 2006; Perez, Bossio et al. 2006a; Perez, Bossio et al. 2006b; Pu and Yin 2007). Often the results from the DP solution have been used as the benchmark against which to compare other implementable, but sub-optimal, controllers. For example, at the University of Michigan (Lin, Kang et al. 2001b; Lin, Kang et al. 2003), the DP generated results have been cleverly used to inform the development of near-

optimum rules which are then implementable in a real time controller, using their own software package, HE-VESIM, a hybrid electric vehicle simulation tool.

Because of the argument that the DP approach is not implementable since its optimality is linked to a specific driving cycle, further recent work at University of Michigan (Lin, Filipi et al. 2004) has expanded it to treat it as an infinite horizon stochastic optimisation problem. The power demand from the driver is treated as a random Markov process. It is shown how the optimal control solution can de derived from this Stochastic DP technique, leading to a full state feedback scheme which in principle could be implemented as a real time controller. Predicted results are generated both for a hybrid diesel truck (Lin, Filipi et al. 2004) and a fuel cell powered, medium size SUV (Lin, Kim et al. 2006).

- **Others**

The Genetic Algorithm (GA) approach which is a probabilistic global search and optimisation technique, based on natural biological evolution, has been applied to the HEV driveline management problem. However, because it is not suitable for constrained optimisation, the constraints in the HEV model have, for example (Montazeri-Gh, Poursamad et al. 2006) been dealt with as penalty functions. In another study (Ippolito, Loia et al. 2003), a so called fuzzy clustering criterion was used with GA to develop a knowledge based control strategy. Finally, in yet another version (Wang 2005), a Pareto dominance concept was combined with GA to result in a multi objective optimisation problem formulation. However, on balance the consensus is that GA techniques are not well suited to the HEV control case.

Other variations on the various detailed approaches to optimal controller design have been tried, e.g. Sequential Quadratic Programming (Oh, Min et al. 2007), simulated annealing (Paganelli, Guerra et al. 2000b), Pareto optimality (Ahn, Cha et al. 2007), Pontryagin's minimum principle (Wei, Guzzella et al. 2007) and direct transcription approach (Perez and Pilotta 2007)

2.5.3 Discussion

The recent work on HEV control reviewed here is dominated by theoretical studies aimed at improving controller design over the early rule-based systems. It

is clear that there are two distinctly different types of modeling simulation – commonly referred to as backwards and forwards facing. In the backwards approach, the vehicle speed is known and the required powers throughout the system are calculated. This technique clearly suits the HEV problem where comparisons are most commonly made using one of the standard driving cycles. In the forwards approach, the input is a driver command which then results in the vehicle performance as an output. This is clearly more representative of the normal driving situation and is useful for predicting the performance of real time controllers. If this technique is used over a driving cycle, then a driver model is needed – often a simple PI (proportional-integral) controller is used.

One of the important issues which is not well covered in the literature is drivability. Of course, it is a difficult subject since it relies heavily on driver subjective judgements, but it is crucial in the commercial acceptance of any controller which has primarily been optimized around energy management and emissions targets. A useful research goal would be to specify some objective targets which correlated well with driver subjective assessments and which could then be used to quantitatively assess controller designs. Some work has been done in this area in relation to Infinitely Variable Transmissions (IVT) (Cacciatori, Bonnet et al. 2005a; Cacciatori, Bonnet et al. 2005b) and objective assessments based on driver step inputs of various levels of throttle demand at (a) rest, (b) slow speed and (c) deceleration have been suggested.

Such assessments would require a forwards facing simulation approach. A related potential problem of the much used backwards simulations is that it is possible for the ‘optimum’ solution at each increment to jump between solution points. In practice, this would imply non-smooth transitions during normal driving. In fact, this is recognized in (Sciarretta, Back et al. 2004) and an additional penalty is included for the IC engine stopping and starting.

Another important issue which is not well covered is braking behaviour. It is rather straightforward to aim for maximum energy recovery in any control scheme. However, in normal driving this must be blended smoothly with the conventional brakes. It is another key aspect of overall drivability. Also, there will inevitably be occasions when regeneration is not possible because of the battery SOC or temperature. This issue is discussed in (Kim, Kim et al. 2007) who also raise the

potential problem of interaction between the regeneration algorithm and the yaw stability controller.

Table 2.3 Predicted results using VP-SIM for a 103 kW hybrid SUV over 6 standard driving cycles (Musardo, Rizzoni et al. 2005)

Percentage improvement in fuel economy over the pure thermal (engine) mode			
Driving cycle	DP	Tuned ECMS (single parameter)	Adaptive ECMS
FUDS	16.4	16.3	15.5
FHDS	4.9	4.1	3.9
ECE	18.2	18.0	17.9
EUDC	6.3	6.2	6.1
NEDC	10.7	10.7	10.1
JP1015	20.1	19.8	18.2

2.6 Methods to analyse gearbox used on HEVs

2.6.1 Description of epicyclic gear set

Epicyclic gearing, also called planetary gearing, is widely used in vehicle transmission systems. For example, most conventional automatic gearboxes utilise epicyclic gear sets. A planetary gear train is defined as any gear train containing at least one gear that orbits by rotating about its own axis and also about the axis of an arm, or carrier (Corey 2003). Examples of simple and complex epicyclic gear sets are shown in Fig 2.12.

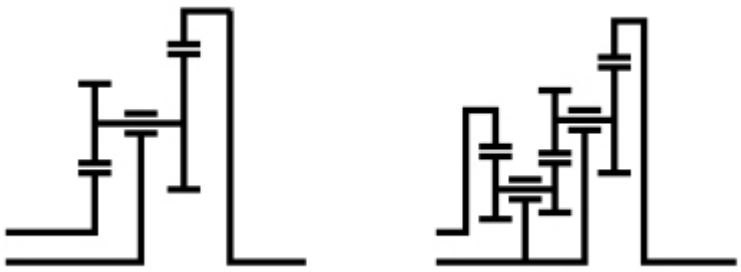

Fig 2.12 A simple and a complex epicyclic gear set (Corey 2003)

There are three kinds of components in an epicyclic gear train:

i) The sun gear

ii) Planet gears and the planet carrier, or the arm

iii) The ring gear, or the annulus

Each of the three kinds of component can be used as the input, output, or kept stationary. Different gear ratios can be achieved by choosing each component to play a different role. In an automatic transmission, clutches and brake are used to hold different components stationary and change the input and output, thus changing the transmission ratio.

Compared to the conventional gearbox arrangement, the epicyclic gear set has many advantages, such as high speed reduction, gear shifting while the vehicle is in motion, and structural compactness (Tian and Lu 1997). The epicyclic gearing is also used in the Power Split Device (PSD) in hybrid vehicles. Toyota used the PSD in the hybrid model Prius, which was launched in 1997. A dual mode PSD similar to the Toyota Prius has also been studied (Mashadi and Emadi 2009). General Motors have also designed several new transmissions based on the epicyclic gear set (Raghavan, Bucknor et al. 2006).

2.6.2 Lever analogy

A method to analyze transmissions called the 'lever analogy' was introduced in 1981 (Benford and Leising 1981). In this method, 'an entire transmission can usually be represented by a single vertical lever. The input, output and reaction torques are represented by horizontal forces on the lever, and the lever motion, relative to the reaction point, represents rotational velocities.'

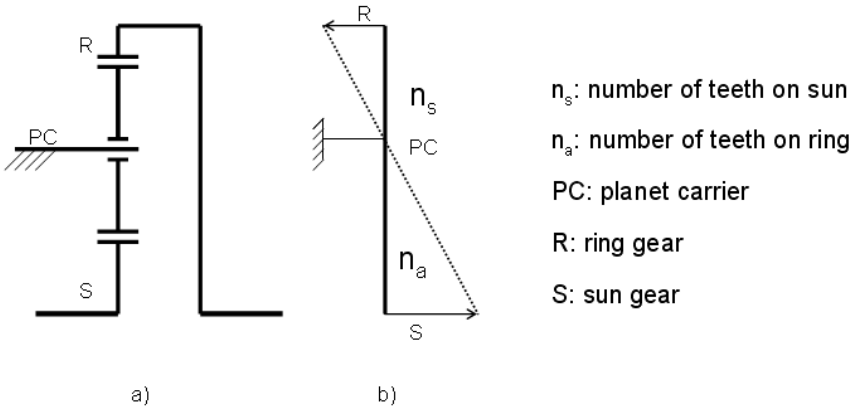

Fig 2.13 Simple epicyclic gearset and analogous lever diagram

The procedure for setting up a lever to a transmission is: replace each gearset by a vertical lever, then rescale and connect levers according to the gearsets'

interconnections. The horizontal force and the velocity relationships of the lever are identical to the torque and rotational velocity relationships of the gearset.

For example, for a simple planetary gearset shown in Fig 2.13a; if the carrier is grounded, the lever diagram is shown in Fig 2.13b.

Because the lever diagram provides an intuitive way of analyzing planetary gear sets, it is widely used to analyze transmissions on vehicles, including hybrid electric vehicles. The advantage of this method is that it is simple, and easy to understand. The disadvantage of it is that for different transmissions or the same transmission but with different modes, different lever diagrams have to be created. In addition, if use this method to analyze transmissions which contain 3 or more planetary gear sets, the lever diagram becomes very complex and not easy to read.

2.6.3 Algebraic design technologies

Researchers from General Motors Research and Development Center developed a method of creation of novel transmission mechanisms, both conventional as well as hybrid, using algebraic design techniques (Raghavan, Bucknor et al. 2006). To use the method, an upfront decision regarding the number of planetary gear sets and clutches to be used in the proposed transmission is made. (Raghavan, Bucknor et al. 2006) observed that: “The design process uses graph theory to handle issues related to mechanism planarity and isomorphism. Following the identification of attractive transmission candidates at the lever diagram level, we prepare layouts and detailed stick diagrams, taking into account the packaging of bearings, hydraulic circuitry, supporting shafts and structures”. The steps of the synthesis strategy are outlined in Fig 2.14. A detailed explanation of the methodology can be found in the paper by (Raghavan, Bucknor et al. 2006).

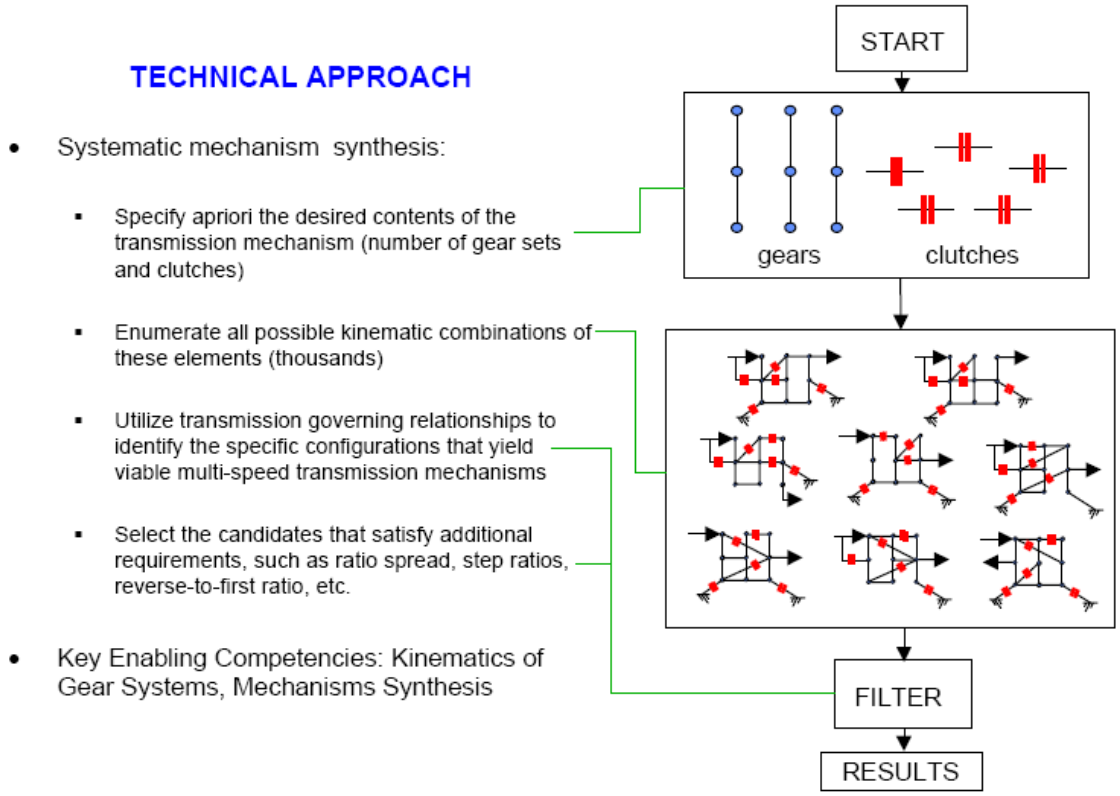

Fig 2.14 Methodology of the Algebraic design method (Raghavan, Bucknor et al. 2006)

The advantage of the method is that it allows the designer to generate and assess novel designs without relying on intuition and prior experience. Because the computer will consider all possible connections of the proposed transmission, the method may create some unusual arrangements which even experienced designers might overlook. Furthermore, because of the ever-increasing requirements on fuel economy and performance, the transmissions for both conventional vehicles and HEVs are becoming more and more complicated. This method is very useful for creating this sort of transmission in this complex environment.

The disadvantage is that the method itself is very complex, using graph theory, lever diagram method, and stick diagrams. Besides, the detailed procedure and computing program have not been made publicly available yet.

2.6.4 Matrix method

A matrix method for the analysis of planetary transmissions was proposed in (Tian and Lu 1997). The method analyzes both kinematics and dynamics of a whole planetary transmission system with a general program. First, the

transmission is broken into finite function units and each basic part, such as a gear, a carrier, a clutch drum, or a brake disk, is enumerated. The basic parts that are always connected together are defined as connected parts. The basic parts from one connected part turn at same speed. Then, a representing matrix is created, including a speed matrix and a torque matrix, according to both the configuration relationships between those units and the transmission manipulating characteristics. Once these matrixes are generated, the kinematic and dynamic problems of the transmission can be solved by means of standard matrix operations. An example of an encoded planetary transmission is shown in Fig 2.15.

The advantage of this method is that it is described clearly the paper (Tian and Lu 1997), so that the readers can follow and understand the method. Also, the whole process of analysis is standardized to become very straightforward, making it especially good for the development of a general-purpose planetary transmission computer-aided-design package. Once the package is built up, it is very easy to analyse any given planetary transmission.

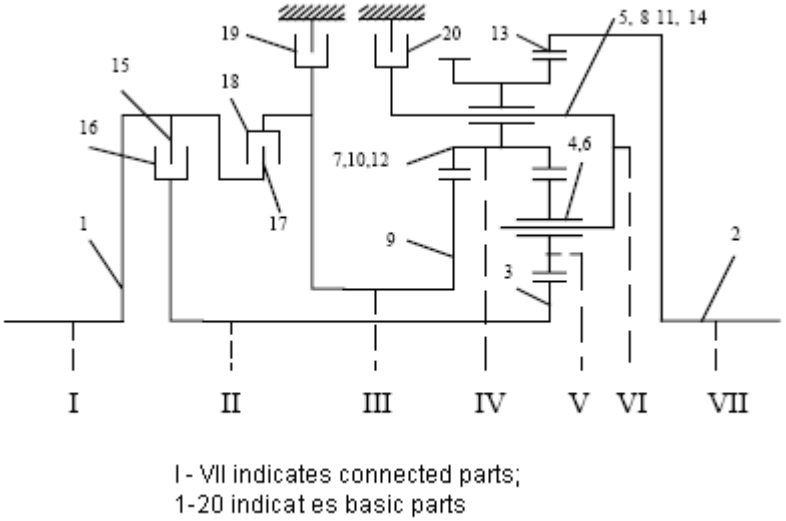

Fig 2.15 An example of an encoded transmission (Tian and Lu 1997)

In this research, the matrix method is used to analyse two transmissions for an HEV: a single epicyclic transmission and a dual epicyclic transmission. Also, a universal software package to analyze different types of PSD for HEVs is developed.

2.7 Concluding remarks

- HEVs and EVs

Interest in HEVs and EVs has increased rapidly recent years, from both industry and academic viewpoints. Research and development efforts have been focused on developing new concepts and low cost systems, but this has proved difficult primarily because of high battery costs. However, hybrid vehicles have been successfully mass produced, e.g. Toyota Prius, and at present many manufacturers are trying to put plug-in electric vehicles, often with some form of range-extender technology into the market.

- Transmission designs

Current design trends in power splitting transmissions have been summarised. Historically, the role of the power splitting transmissions in the overall development of hybrid vehicle technology has commonly been underestimated. But PSTs have actually played a crucial role in managing the electrical and mechanical power flows and ensuring good driveability and efficiency. It is concluded that it has been an area of rapidly changing technology over the past decade. But perhaps more importantly, this is certain to continue over the next decade. The overall conclusion about the current picture is that whilst the first generation, single mode units have proved to be adequate in the small/mid size passenger car sector, dual mode systems are set to become dominant in the large car, SUV and commercial vehicle sectors.

For EVs, the effect of transmissions on the vehicle performance and energy consumption has not yet received much attention in the current research.

- Control strategies

Although it is clear that many different control techniques have been applied to the HEV problem, the overall conclusion is that only three generic types are likely to have a future in the short to medium term:

i) Rule-based – still at the heart of most practical and prototype systems
ii) Equivalent energy methods – an elegant simplification which enables near-optimal performance to be obtained
iii) Dynamic programming – crucial in defining the optimum performance and useful in informing rule-based system design.

Almost all this recent work reviewed here has used standard driving cycles as a basis for comparisons. Whilst there are good reasons to justify this, it nevertheless raises a fundamental global concern of whether the industry is designing cars around arbitrarily selected driving cycles – rather than around practical, consumer-driven demands.

There remains further scope for research into drivability issues – in the acceleration and braking manoeuvres associated with normal driving. A significant goal of benefit to the industry would be a better understanding of the subjective/objective correlation of drivability.

- Methods to analyse the epicyclic gear box

There are three approaches used to analyse the epicyclic gear box: the lever method, the algebraic design method, and the matrix method. In this research, the matrix method is chosen mainly because it is straightforward and easy to program.

3 Analysis of epicyclic transmissions

3.1 Introduction

In this chapter, the single and twin epicyclic transmissions are analyzed in detail and the relationships of speed and torque of the engine, the motor and the generator are generated. Computer programmes for the analysis of epicyclic transmission based on a matrix method are developed and examples of using the programmes are given.

3.2 Analysis of a single epicyclic transmission

A typical and successful example of a single epicyclic power split device (PSD) is the Toyota Prius, as shown in Fig 3.1. In the device, the internal combustion engine (ICE) is connected to the planet carrier. When the ICE rotates, the planets mesh with and tend to push both the sun gear and the ring gear in the same direction as the carrier. So the torque from the engine is split into two directions.

The ring gear is connected the reduction gear unit, which is connected to the differential, then to the wheel. So the torque from the ring gear actually drives the car. The sun gear is connected to one of the motor generators (MG1), which largely acts as a generator. The planetary PSD is designed so that the ring gets larger part of the engine torque, and the sun gear gets smaller part of the engine torque.

The PSD is called E-CVT (Electronically-Controlled Continuously Variable Transmission). It combines the characteristics of an electric drive and a continuously variable transmission, using motor generator units in addition to toothed gears. In the PSD, MG2 is mounted on the driveshaft, and thus couples torque into or out of the driveshaft. So MG2 is sometimes called “MG-T” for “Torque”. MG1 is connected with the sun gear and is used to change the sun gear speed. So MG1 is sometimes called “MG-S” for “Speed”. Because MG2 is connected with the driveshaft, it cannot change speed and torque freely. Hence there are three power input/output branches in the system: the engine, MG1, the output (MG2). Because the speed of the output shaft is decided by the speed of the vehicle, there is some limitation on the control strategy to achieve optimum performance.

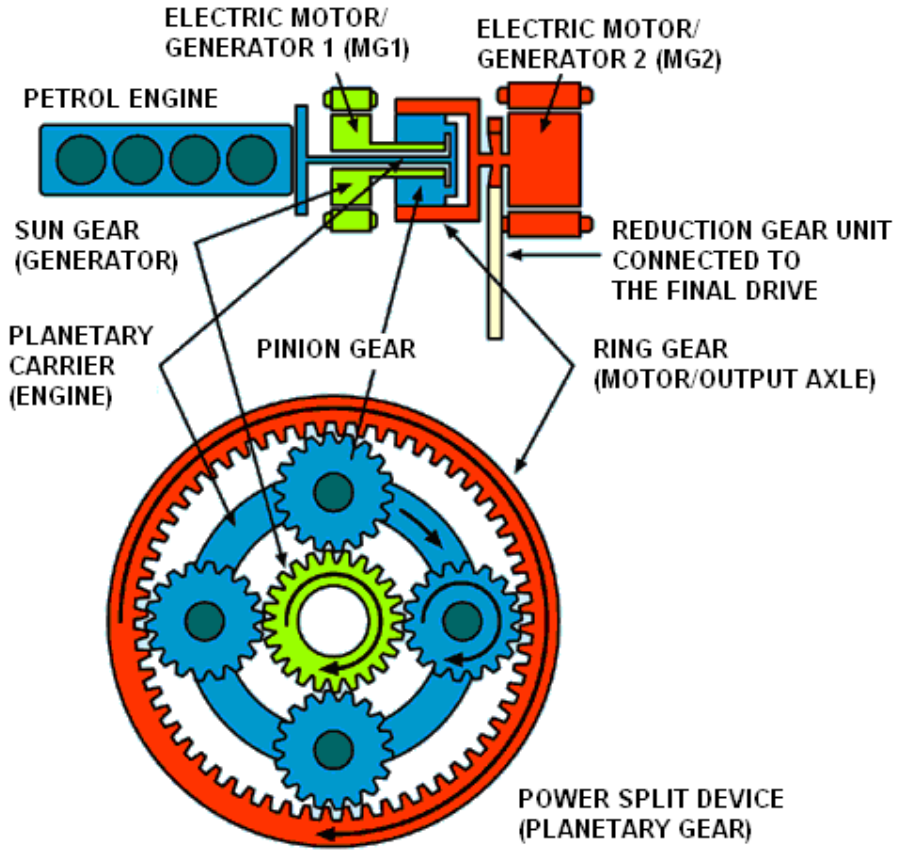

Fig 3.1 Toyota Prius PSD (Ayers, Hsu et al. 2004)

The first generation of the Toyota Hybrid System (THS) is used in the 1997-2003 Toyota Prius. After that, the second generation, THS II, is called as Hybrid Synergy Drive (HSD). The HSD is used in Prius, Highlander Hybrid, Camry Hybrid, and Lexus RX 450h automotives. The name was changed from THS to HSD, because some other car makers may use the power split technology. For example, Ford Escape Hybrid uses the hybrid synergy drive technology, and it claims to be the most fuel-efficient SUV on the planet. Usually, a vehicle with a HSD is a full hybrid, because it can drive using only electric power.

Because the Toyota Prius PSD has only one set of epicyclic gears, it is called the single epicyclic transmission in this research. The single epicyclic system has three branches of power input/output:

i) Branch 1: the engine input;

ii) Branch 2: the MG1 input/output, depending on whether MG1 is acting as a motor or a generator;

iii) Branch 3: the driveline output, and also the MG2 input/output, depending on whether MG2 is acting as a motor or a generator.

Hence, it is also called a three branch system. The simplified diagram of the single epicyclic system is shown in Fig 3.2. The terms of a single epicyclic transmission and a three branch system are distinguished from a twin epicyclic transmission and a four branch system, which will be introduced later.

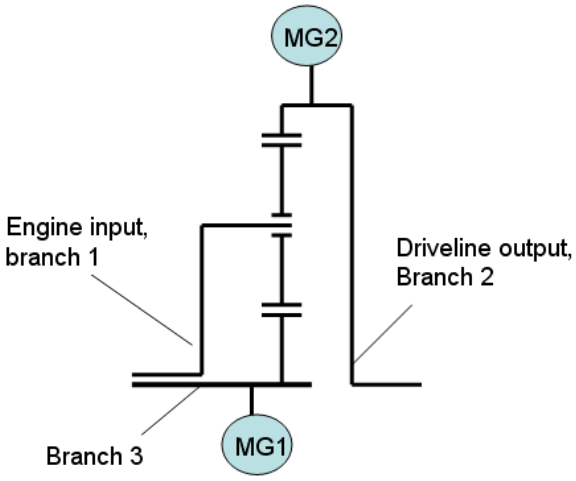

Fig 3.2 Single epicyclic gearbox, three branch system

To use the matrix method to analyse the transmission, each basic part is numbered, from 1 to 10. There are 4 connected parts: I to IV. The connected part I includes basic part 1, 5 and 8; the connected part II include basic part 2, 7 and 9; the connected part III includes basic part 4 and 6; the connected part IV includes basic parts 3 and 10. There are two gear units X1 and X2

The basic parts, the connected parts and the gear units are as shown in Fig 3.3.

In the matrix method, all the basic parts are numbered as 1, 2, 3, etc and nearly all the basic parts are repeatedly named. For example, numbers 1, 5 and 8 point to the same part: 1 stands for input shaft, 5 stands for the carrier of the gear mesh X1 and 8 stands for the carrier of the gear mesh X2.

The whole system has q basic parts:

$$q = 2 + 3 * 2 + 2 = 10 \qquad (3.1)$$

in which the last 2 parts are the rotor of MG1 and the rotor of MG2.

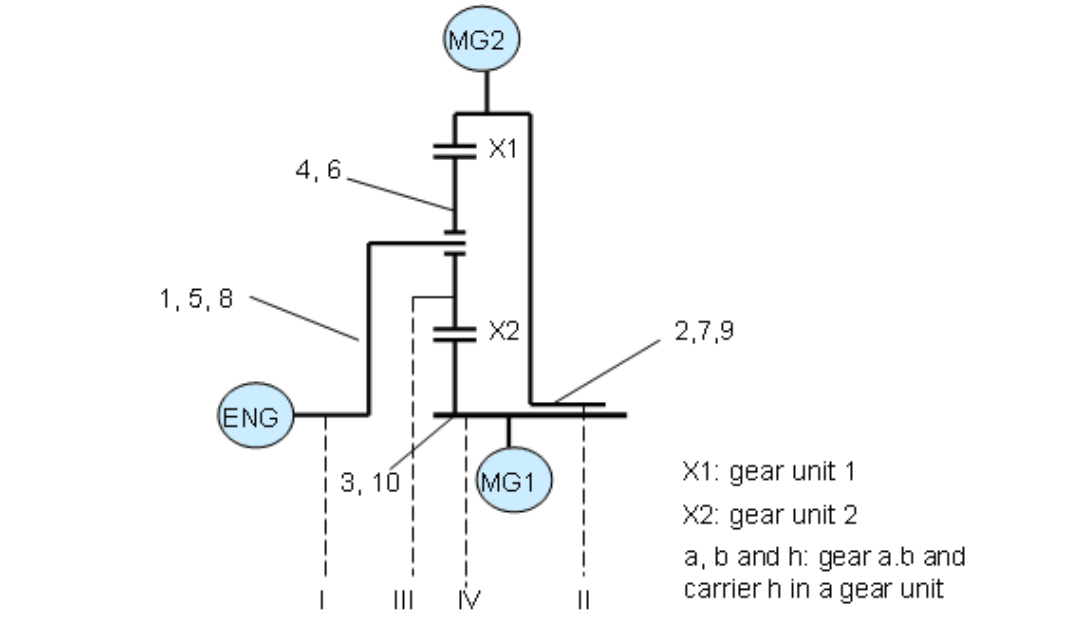

1 – input shaft; 2 – output shaft; 3, 4 & 5 – a, b & h of unit X1 ; 6, 7 & 8 – a, b & h of unit X2; 9 – rotor of MG2; 10 – rotor of MG1

Fig 3.3 Encode of basic parts and connected parts

The number of connected parts p is:

$$p = 4 \tag{3.2}$$

The number of degrees of freedom f is:

$$f = p - x = 4 - 2 = 2 \tag{3.3}$$

where x is the number of gear units.

The gears turn in a ratio determined by the number of teeth in each gear, where α is the gear ratio and Z is the number of teeth. $\alpha = Z_b / Z_a$ (inside engaged) and $\alpha = -Z_b / Z_a$ (outside engaged). Let α_1 to α_3 represent the gear ratios of units X1 and X2 respectively. The tooth number for the sun gear, the pinion gear and the ring gear is 30, 24, and 78 respectively. So the gear ratios for X1 and X2 are

$$\alpha_1 = -\frac{Z_4}{Z_3} = -24/30 = -0.8 \tag{3.4}$$

$$\alpha_2 = \frac{Z_7}{Z_6} = \frac{Z_7}{Z_4} = \frac{Z_3 + 2Z_4}{Z_3} = 2 - \frac{1}{\alpha_1} = 3.25 \tag{3.5}$$

where Z_n represents the tooth number for gear defined by n in Fig 3.3. In Equation (3.5), α_2 is expressed in α_1, so there is actually only one parameter for the single epicyclic gearbox - α_1.

3.2.1 Speed and ratio analysis

The following describes the rotation equation group (3.6) for the single epicyclic transmission:

Connected part 1: $n_1 - n_5 = 0$

$$n_1 - n_8 = 0$$

Connected part 2: $n_2 - n_7 = 0$

$$n_2 - n_9 = 0$$

Connected part 3: $n_3 - n_{10} = 0$

Connected part 4: $n_4 - n_6 = 0$

Gear system unit X1: $n_3 - \alpha_1 n_4 + (\alpha_1 - 1) n_5 = 0$

Gear system unit X2: $n_6 - \alpha_2 n_7 + (\alpha_2 - 1) n_8 = 0$ (3.6)

The above linear equation group can be written in the following vector form:

$$A_n \vec{n} = \vec{0} \quad (3.7)$$

where:

$\vec{n}$ equals $[n_1\ n_2 \ldots n_{10}]^{\mathsf{T}}$;

A_n is the speed coefficient matrix for the single epicyclic gearbox.

Equation (3.8) is the Integration of Equations (3.6) and (3.7) .

Equation (3.8) can be solved using a standard method, for example, the Gauss-Jordan elimination method. The computer programme (gjelim.m, Appendix 1) of the Gauss-Jordan elimination method used in this research is from (Williams 2007).

$$\begin{bmatrix} 1 & 0 & 0 & 0 & 0 & -1 & 0 & 0 & 0 & 0 \\ 1 & 0 & 0 & 0 & 0 & 0 & 0 & -1 & 0 & 0 \\ 0 & 1 & 0 & 0 & 0 & 0 & -1 & 0 & 0 & 0 \\ 0 & 1 & 0 & 0 & 0 & 0 & 0 & 0 & -1 & 0 \\ 0 & 0 & 1 & 0 & 0 & 0 & 0 & 0 & 0 & -1 \\ 0 & 0 & 0 & 1 & 0 & -1 & 0 & 0 & 0 & 0 \\ 0 & 0 & 1 & -\alpha_1 & \alpha_1 - 1 & 0 & 0 & 0 & 0 & 0 \\ 0 & 0 & 0 & 0 & 0 & 1 & -\alpha_2 & \alpha_2 - 1 & 0 & 0 \end{bmatrix} \begin{bmatrix} n_1 \\ n_2 \\ n_3 \\ n_4 \\ n_5 \\ n_6 \\ n_7 \\ n_8 \\ n_9 \\ n_{10} \end{bmatrix} = \begin{bmatrix} 0 \\ 0 \\ 0 \\ 0 \\ 0 \\ 0 \\ 0 \\ 0 \\ 0 \end{bmatrix} \quad (3.8)$$

The Matlab program to obtain the speed coefficient matrix A_n and to derive the relationship of rotation speeds for each component is shown in Appendix 2. From running the program, the speed coefficient matrix A_n is shown in Appendix 3, and the relationship of rotation speeds for the single epicyclic gearbox is shown in Appendix 4.

The result shown in matrix format is:

$$\begin{bmatrix} 1 & 0 & 0 & 0 & 0 & 0 & 0 & 0 & -18/5 & 13/5 \\ 0 & 1 & 0 & 0 & 0 & 0 & 0 & 0 & 45/20 & -65/20 \\ 0 & 0 & 1 & 0 & 0 & 0 & 0 & 0 & -1 & 0 \\ 0 & 0 & 0 & 1 & 0 & 0 & 0 & 0 & 45/20 & -65/10 \\ 0 & 0 & 0 & 0 & 1 & 0 & 0 & 0 & 0 & -1 \\ 0 & 0 & 0 & 0 & 0 & 1 & 0 & 0 & -1 & 0 \\ 0 & 0 & 0 & 0 & 0 & 0 & 1 & 0 & 0 & -1 \\ 0 & 0 & 0 & 0 & 0 & 0 & 0 & 1 & -18/5 & 13/5 \end{bmatrix} \begin{bmatrix} n_3 \\ n_4 \\ n_5 \\ n_6 \\ n_7 \\ n_8 \\ n_9 \\ n_{10} \\ n_1 \\ n_2 \end{bmatrix} = \begin{bmatrix} 0 \\ 0 \\ 0 \\ 0 \\ 0 \\ 0 \\ 0 \\ 0 \end{bmatrix} \quad (3.9)$$

The speed relationships for MG1 and MG2 with the engine and the driveline are:

$$n_3 - \frac{18}{5} n_1 + \frac{13}{5} n_2 = 0 \quad (3.10)$$

$$n_9 - n_2 = 0 \quad (3.11)$$

This agrees with the equation in Miller's presentation (Miller and Miller 2005), in slide 30:

$$n_s + k \cdot n_r - (k+1)n_c = 0 \qquad (3.12)$$

where $k = 2.6$. Hence, this confirms the accuracy of the matrix method and the whole calculation process.

The engine speed is set to be 1 as a reference point so that the speed of part 1, namely $n_1 = 1$. The speed of each other part is actually the speed of that part relative to the speed of the engine. The transmission ratio of the system is defined as

$$i = \frac{engine\_speed}{output\_speed} = \frac{n_1}{n_2} = \frac{1}{n_2} \qquad (3.13)$$

The Matlab program to plot MG1 and MG2 speed vs. transmission ratio for the single epicyclic gearbox is shown in Appendix 5. From running the program, the result is shown in Fig 3.4. When the transmission ratio is 0.72, the speed of MG1 is 0. This means that at this point, if MG2 does not add torque to the wheels, zero power is transmitted via the electrical path. The point is called a node point. At the node point, the transmission efficiency is higher. The design of the powertrain should therefore make use of this node point. For example, this node point could be arranged to coincide with a vehicle speed around 70 mile/h, which is a typical cruising speed on the highway, with a transmission ratio of 0.72.

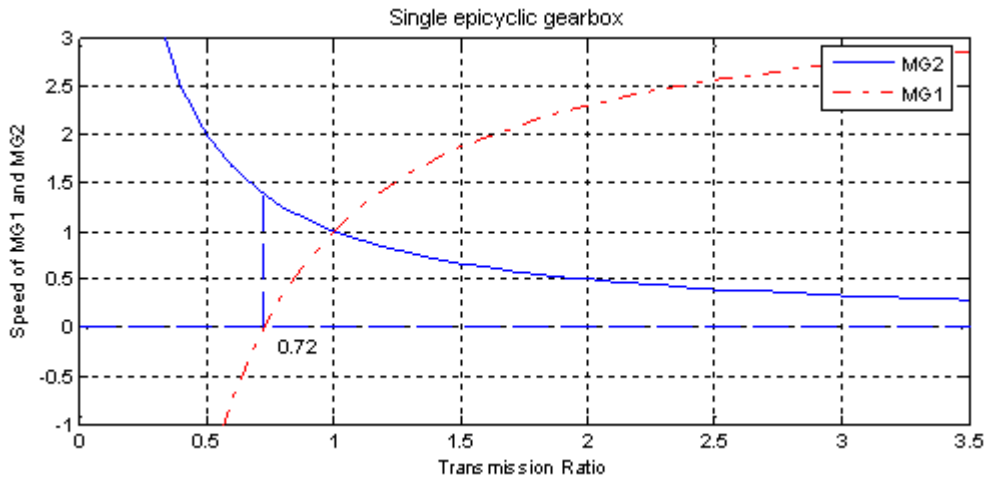

Fig 3.4 Relationship of transmission ratio and motor generator speeds for the single epicyclic gearbox

To study the effect of the parameter α_1 on the speeds of MG1 and MG2, two gear ratios are chosen: 0.8 and 1.2. The curves of speed of MG1 and MG2 versus transmission ratio are shown in Fig 3.5.

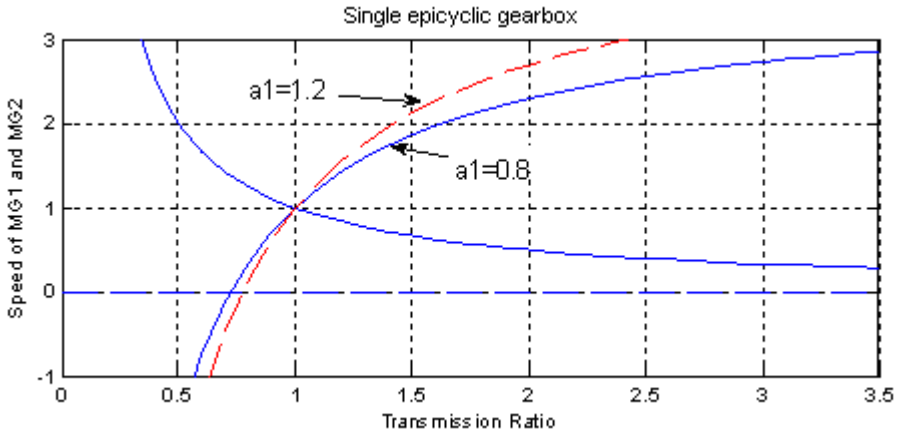

Fig 3.5 Effects of two values of α_1 on the single epicyclic gearbox

With the increase of the gear ratio α_1, the speed of MG1 vs. speed of engine also increases. The speed of MG2 does change with different α_1. This is because MG2 is fixed with the output shaft, namely $n_9 = n_2$. From Equation (3.13), the speed of MG1 can be obtained:

$$n_9 = \frac{1}{i} \qquad (3.14)$$

Hence, the speed of MG1 does not change when gear ratio α_1 changes.

3.2.2 Torque analysis

While the system is running steadily, the sum of all the torques applied to a connected part should be zero. For example, connected part II in Fig 3.3 has a torque equation like $T_3 + T_6 + T_9 = 0$, and so on.

For a gear system unit, the torque equation would be:

$$\alpha_1 \eta^t T_a + T_b = 0 \qquad (3.15)$$

$$T_a + T_b + T_c = 0 \qquad (3.16)$$

where T_a, T_b and T_c are the torques applied to the connected part by the gear a, b, and the carrier h. η^t is the transmission efficiency of the gear unit. If a is the driving part, $t = 1$; if a is the driven part, $t = -1$.

The torque equation group (3.17) for the simple epicyclic gearbox is written below:

Connected part 1: $T_1 + T_5 + T_8 = 0$

Connected part 2: $T_2 + T_7 + T_9 = 0$

Connected part 3: $T_3 + T_{10} = 0$

Connected part 4: $T_4 + T_6 = 0$

Gear unit X1: $\alpha_1 \eta^t T_3 + T_4 = 0$

$T_3 + T_4 + T_5 = 0$

Gear unit X2: $\alpha_2 \eta^t T_6 + T_7 = 0$

$T_6 + T_7 + T_8 = 0$ (3.17)

At the moment, it has not been decided which gear is the driving part and which gear is the driven part. It is assumed at this stage that there is no loss in the transmission.

In the later part of the simulation studies, the efficiency of the transmission is taken into consideration. In this case, the input speed and torque are known for each individual driving condition, so the directions of the power transmission are known, thus the efficiency can be incorporated.

The above linear equation group can be written in the following vector form:

$$A_T \vec{T} = \vec{0} \qquad (3.18)$$

where:

$\vec{T}$ equals $[T_1\ T_2 \ldots T_{10}]^T$

A_T is the torque coefficient matrix.

Integrating Equations (3.17) and (3.18) gives,

$$\begin{bmatrix} 1 & 0 & 0 & 0 & 1 & 0 & 0 & 1 & 0 & 0 \\ 0 & 1 & 0 & 0 & 0 & 0 & 1 & 0 & 1 & 0 \\ 0 & 0 & 1 & 0 & 0 & 0 & 0 & 0 & 0 & 1 \\ 0 & 0 & 0 & 1 & 0 & 1 & 0 & 0 & 0 & 0 \\ 0 & 0 & 0 & \alpha_1\eta^t & 1 & 0 & 0 & 0 & 0 & 0 \\ 0 & 0 & 1 & 1 & 1 & 0 & 0 & 0 & 0 & 0 \\ 0 & 0 & 0 & 0 & 0 & \alpha_2\eta^t & 1 & 0 & 0 & 0 \\ 0 & 0 & 0 & 0 & 0 & 1 & 1 & 1 & 0 & 0 \end{bmatrix} \begin{bmatrix} T_1 \\ T_2 \\ T_3 \\ T_4 \\ T_5 \\ T_6 \\ T_7 \\ T_8 \\ T_9 \\ T_{10} \end{bmatrix} = \begin{bmatrix} 0 \\ 0 \\ 0 \\ 0 \\ 0 \\ 0 \\ 0 \\ 0 \end{bmatrix} \quad (3.19)$$

The Matlab program to get the torque coefficient matrix A_T and to get the relationship of torque for each component is shown in Appendix 6. From running the program, the torque coefficient matrix A_T is shown in Appendix 7, and the relationship of torque for the single epicyclic gearbox is shown in Appendix 8.

The result shown in matrix format is:

$$\begin{bmatrix} 1 & 0 & 0 & 0 & 0 & 0 & 0 & 0 & 0 & -5/18 \\ 0 & 1 & 0 & 0 & 0 & 0 & 0 & 0 & 0 & -2/9 \\ 0 & 0 & 1 & 0 & 0 & 0 & 0 & 0 & 0 & 1/2 \\ 0 & 0 & 0 & 1 & 0 & 1 & 0 & 0 & 0 & 2/9 \\ 0 & 0 & 0 & 0 & 1 & 0 & 0 & 0 & 0 & -13/18 \\ 0 & 0 & 0 & 0 & 0 & 1 & 0 & 0 & 0 & 1/2 \\ 0 & 0 & 0 & 0 & 0 & 0 & 1 & 0 & 1 & 13/18 \\ 0 & 0 & 0 & 0 & 0 & 0 & 0 & 1 & 0 & 5/18 \end{bmatrix} \begin{bmatrix} T_3 \\ T_4 \\ T_5 \\ T_6 \\ T_7 \\ T_8 \\ T_9 \\ T_{10} \\ T_1 \\ T_2 \end{bmatrix} = \begin{bmatrix} 0 \\ 0 \\ 0 \\ 0 \\ 0 \\ 0 \\ 0 \\ 0 \end{bmatrix} \quad (3.20)$$

The torque relationships for MG1 and MG2 with the engine and the driveline are:

$$T_9 + \frac{13}{18}T_1 + T_2 = 0 \quad (3.21)$$

$$T_{10} + \frac{5}{18}T_1 = 0 \quad (3.22)$$

3.3 Analysis of a twin epicyclic transmission

In a twin epicyclic transmission system, which is presented in this paper, there are two sets of epicyclic gear units. The engine output shaft is connected to the carrier of the first epicyclic set. The carrier of the second epicyclic set is connected to the ring gear of the first epicyclic set. The driveline output is connected to the carrier of the second epicyclic set. Neither of the motor generator units is mounted on the driveshaft or on the engine input shaft, which gives more freedom and benefits to the system which is shown in Fig 3.6.

One motor/generator (MG1) is connected to the sun gear, and the other motor/generator (MG2) is connected with a ring gear. So there are four branches of power input/output:

i) Branch 1: the engine input;
ii) Branch 2: the driveline output;
iii) Branch 3: the MG1 input/output, depending on whether MG1 is acting as a motor or a generator;
iv) Branch 3: the MG2 input/output, depending on whether MG2 is acting as a motor or a generator.

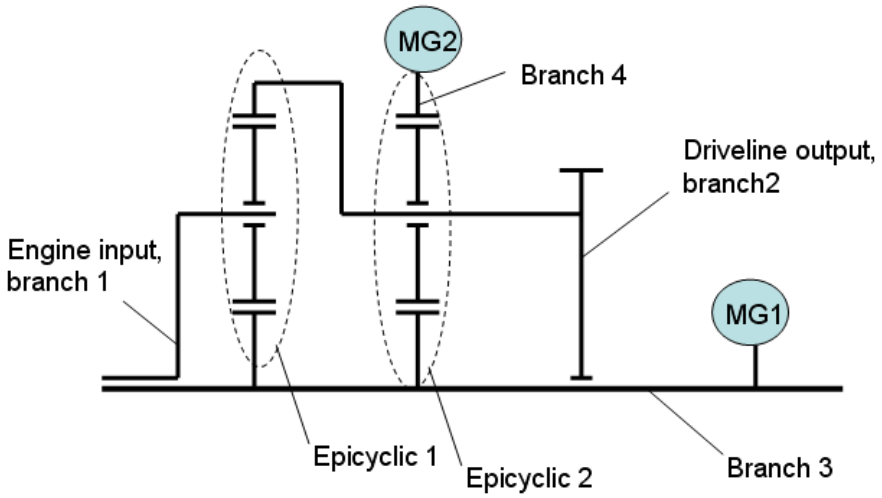

Fig 3.6 Twin epicyclic transmission

This type of four branch transmission system has been described recently by Moeller (Moeller 2006) who proposed that it offers advantages in many automotive applications, including hybrid and non-hybrid vehicles, such as light electric

vehicles or off-road vehicles. However, its usage in a hybrid electric vehicle driveline will be analysed here for the first time.

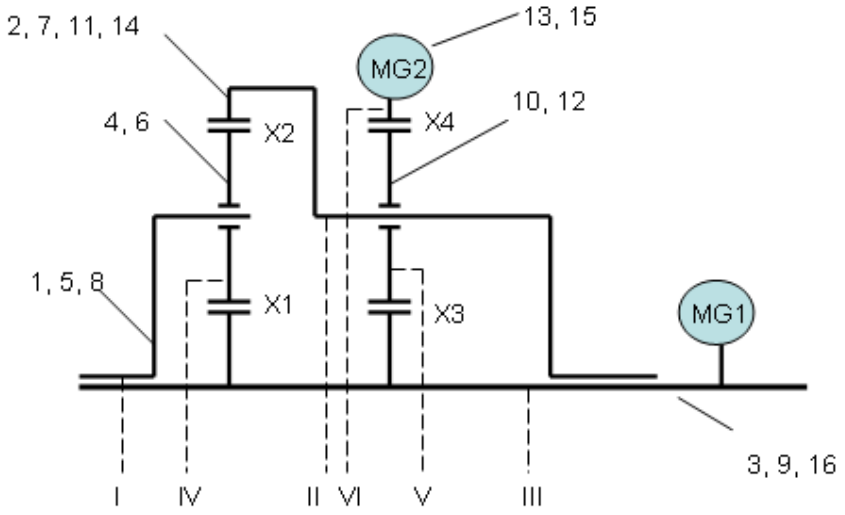

1 – input shaft; 2 – output shaft; 3, 4 & 5 – a, b & h of unit X_1 ; 6, 7 & 8 – a, b & h of unit X_2; 9, 10 & 11 – a, b & h of unit X_3 ; 12, 13 & 14 – a, b & h of unit X_4 ; 15 – rotor of Motor/Genetor1; 16 – rotor of Motor/Genetor2

Fig 3.7 Encode of basic parts and connected part of the twin epicyclic transmission

The simplified structure and the encode of the 4 branch system is shown in Fig 3.7. There are 16 basic parts which are numbered from 1 to 16 respectively. There are 6 connected parts which are numbered from I to VI respectively. There are 4 gear units which are numbered from X1 to X4 respectively.

The number of basic parts q for the whole system:

$$q = 2 + 3 * 4 + 2 = 16 \tag{3.23}$$

in which the last 2 parts are the rotor of MG1 and the rotor of MG2.

The number of connected parts is:

$$p = 6 \tag{3.24}$$

The degree of freedom

$$f = p - x = 6 - 4 = 2 \tag{3.25}$$

where x is the number of gear units.

Let α_1 to α_4 represent the gear ratios of units X1 to X4 respectively. Hence,

$$\alpha_1 = -Z_4 / Z_3 \tag{3.26}$$

$$\alpha_2 = Z_7 / Z_6 = Z_7 / Z_4 = (Z_3 + 2Z_4) / Z_3 = 2 - 1/\alpha_1 \quad (3.27)$$

$$\alpha_3 = -Z_{10} / z_9 \quad (3.28)$$

$$\alpha_4 = Z_{13} / Z_{12} = Z_7 / Z_{10} = (Z_9 + 2Z_{10}) / z_{10} = 2 - 1/\alpha_3 \quad (3.29)$$

So actually there are 2 variables, α_1 and α_3 in the system. The values of α_1 and α_3 are both set to be 0.8.

3.3.1 The rotation speed equation group

The speed equation group for the twin epicyclic gearbox is written below:

Connected part 1: $n_1 - n_5 = 0$

$n_1 - n_8 = 0$

Connected part 2: $n_2 - n_7 = 0$

$n_2 - n_{11} = 0$

$n_2 - n_{14} = 0$

Connected part 3: $n_3 - n_{10} = 0$

$n_3 - n_{16} = 0$

Connected part 4: $n_4 - n_6 = 0$

Connected part 5: $n_{10} - n_{12} = 0$

Connected part 6: $n_{13} - n_{15} = 0$

Gear system unit X1: $n_3 - \alpha_1 n_4 + (\alpha_1 - 1) n_5 = 0$

Gear system unit X2: $n_6 - \alpha_2 n_7 + (\alpha_2 - 1) n_8 = 0$

Gear system unit X3: $n_9 - \alpha_3 n_{10} + (\alpha_3 - 1) n_{11} = 0$

Gear system unit X4: $n_{12} - \alpha_4 n_{13} + (\alpha_4 - 1) n_{14} = 0$ (3.30)

In similar fashion to the analysis for the single epicyclic gearbox, the above linear equation group can be written in the following vector form:

$$A_n \vec{n} = \vec{0} \quad (3.31)$$

where:

$\vec{n}$ equals $[n_1\ n_2 \ldots n_{16}]^T$

A_n is the speed coefficient matrix for the twin epicyclic.

Integrate Equations (3.30) and (3.31) :

$$\begin{bmatrix} 1 & 0 & 0 & 0 & -1 & 0 & 0 & 0 & 0 & 0 & 0 & 0 & 0 & 0 & 0 & 0 \\ 1 & 0 & 0 & 0 & 0 & 0 & 0 & -1 & 0 & 0 & 0 & 0 & 0 & 0 & 0 & 0 \\ 0 & 1 & 0 & 0 & 0 & 0 & -1 & 0 & 0 & 0 & 0 & 0 & 0 & 0 & 0 & 0 \\ 0 & 1 & 0 & 0 & 0 & 0 & 0 & 0 & 0 & 0 & -1 & 0 & 0 & 0 & 0 & 0 \\ 0 & 1 & 0 & 0 & 0 & 0 & 0 & 0 & 0 & 0 & 0 & 0 & 0 & -1 & 0 & 0 \\ 0 & 0 & 1 & 0 & 0 & 0 & 0 & 0 & 0 & -1 & 0 & 0 & 0 & 0 & 0 & 0 \\ 0 & 0 & 1 & 0 & 0 & 0 & 0 & 0 & 0 & 0 & 0 & 0 & 0 & 0 & 0 & -1 \\ 0 & 0 & 0 & 1 & 0 & -1 & 0 & 0 & 0 & 0 & 0 & 0 & 0 & 0 & 0 & 0 \\ 0 & 0 & 0 & 0 & 0 & 0 & 0 & 0 & 0 & 1 & 0 & -1 & 0 & 0 & 0 & 0 \\ 0 & 0 & 0 & 0 & 0 & 0 & 0 & 0 & 0 & 0 & 0 & 0 & 1 & 0 & -1 & 0 \\ 0 & 0 & 1 & -\alpha_1 & \alpha_1 - 1 & 0 & 0 & 0 & 0 & 0 & 0 & 0 & 0 & 0 & 0 & 0 \\ 0 & 0 & 0 & 0 & 0 & 1 & -\alpha_2 & \alpha_2 - 1 & 0 & 0 & 0 & 0 & 0 & 0 & 0 & 0 \\ 0 & 0 & 0 & 0 & 0 & 0 & 0 & 0 & 1 & \alpha_3 & \alpha_3 - 1 & 0 & 0 & 0 & 0 & 0 \\ 0 & 0 & 0 & 0 & 0 & 0 & 0 & 0 & 0 & 0 & 0 & 1 & \alpha_4 - 1 & 0 & 0 & 0 \end{bmatrix} \begin{bmatrix} n_1 \\ n_2 \\ n_3 \\ n_4 \\ n_5 \\ n_6 \\ n_7 \\ n_8 \\ n_9 \\ n_{10} \\ n_{11} \\ n_{12} \\ n_{13} \\ n_{14} \\ n_{15} \\ n_{16} \end{bmatrix} = \begin{bmatrix} 0 \\ 0 \\ 0 \\ 0 \\ 0 \\ 0 \\ 0 \\ 0 \\ 0 \\ 0 \\ 0 \\ 0 \\ 0 \\ 0 \\ 0 \\ 0 \end{bmatrix}$$

(3.32)

The Matlab program to obtain the speed coefficient matrix A_n and to derive the relationship of rotation speeds for each component for the twin epicyclic gearbox is shown in Appendix 9. From running the program, the speed coefficient matrix A_n is shown in Appendix 10, and the relationship of rotation speeds for the single epicyclic gearbox is shown in Appendix 11.

The relationships MG1 and MG2 with the engine and the output shaft are:

$$n_{15} + \frac{18}{13} n_1 - \frac{31}{13} n_2 = 0 \qquad (3.33)$$

$$n_{16} - \frac{18}{5} n_1 + \frac{13}{5} n_2 = 0 \qquad (3.34)$$

The Matlab program to plot the speeds of MG1 and MG2 relative to the transmission ratio are shown in Appendix 12. From running the program, the result is shown is Fig 3.8. There are two node points for the twin epicyclic gearbox, when the transmission ratios are 0.72 and 1.72 respectively. In contrast, for a single epicyclic gearbox, there is only one node point, when the transmission ratio is 0.72 (Fig 3.4).

$$\begin{bmatrix} 1 & 0 & 0 & 0 & 0 & 0 & 0 & 0 & 0 & 0 & 0 & 0 & 0 & 0 & -18/5 & 13/5 \\ 0 & 1 & 0 & 0 & 0 & 0 & 0 & 0 & 0 & 0 & 0 & 0 & 0 & 0 & 9/4 & -13/4 \\ 0 & 0 & 1 & 0 & 0 & 0 & 0 & 0 & 0 & 0 & 0 & 0 & 0 & 0 & -1 & 0 \\ 0 & 0 & 0 & 1 & 0 & 0 & 0 & 0 & 0 & 0 & 0 & 0 & 0 & 0 & 9/4 & -13/4 \\ 0 & 0 & 0 & 0 & 1 & 0 & 0 & 0 & 0 & 0 & 0 & 0 & 0 & 0 & 0 & -1 \\ 0 & 0 & 0 & 0 & 0 & 1 & 0 & 0 & 0 & 0 & 0 & 0 & 0 & 0 & -1 & 0 \\ 0 & 0 & 0 & 0 & 0 & 0 & 1 & 0 & 0 & 0 & 0 & 0 & 0 & 0 & -18/5 & 13/5 \\ 0 & 0 & 0 & 0 & 0 & 0 & 0 & 1 & 0 & 0 & 0 & 0 & 0 & 0 & 3 & -4 \\ 0 & 0 & 0 & 0 & 0 & 0 & 0 & 0 & 1 & 0 & 0 & 0 & 0 & 0 & 0 & -1 \\ 0 & 0 & 0 & 0 & 0 & 0 & 0 & 0 & 0 & 1 & 0 & 0 & 0 & 0 & 9/2 & -11/2 \\ 0 & 0 & 0 & 0 & 0 & 0 & 0 & 0 & 0 & 0 & 1 & 0 & 0 & 0 & 18/13 & -31/13 \\ 0 & 0 & 0 & 0 & 0 & 0 & 0 & 0 & 0 & 0 & 0 & 1 & 0 & 0 & 0 & -1 \\ 0 & 0 & 0 & 0 & 0 & 0 & 0 & 0 & 0 & 0 & 0 & 0 & 1 & 0 & 18/13 & -31/13 \\ 0 & 0 & 0 & 0 & 0 & 0 & 0 & 0 & 0 & 0 & 0 & 0 & 0 & 1 & -18/5 & 13/5 \end{bmatrix} \begin{bmatrix} n_3 \\ n_4 \\ n_5 \\ n_6 \\ n_7 \\ n_8 \\ n_9 \\ n_{10} \\ n_{11} \\ n_{12} \\ n_{13} \\ n_{14} \\ n_{15} \\ n_{16} \\ n_1 \\ n_2 \end{bmatrix} = \begin{bmatrix} 0 \\ 0 \\ 0 \\ 0 \\ 0 \\ 0 \\ 0 \\ 0 \\ 0 \\ 0 \\ 0 \\ 0 \\ 0 \\ 0 \\ 0 \\ 0 \end{bmatrix} \quad (3.35)$$

Fig 3.8 Relationship of transmission ratio and motor generator speeds for the 4 branch systems

To study the effect of α_1, two different values for α_1 are chosen, keeping a constant value of $\alpha_3 = 0.8$. Fig 3.9 shows the effect of α_1 on the speeds of MG1 and MG2. For the blue lines, α_1 and α_3 are both 0.8. For the red lines, $\alpha_3 = 1.2$

and $\alpha_3 = 0.8$. The results show that for an increase of α_1, the speeds of both MG1 and MG2 increase.

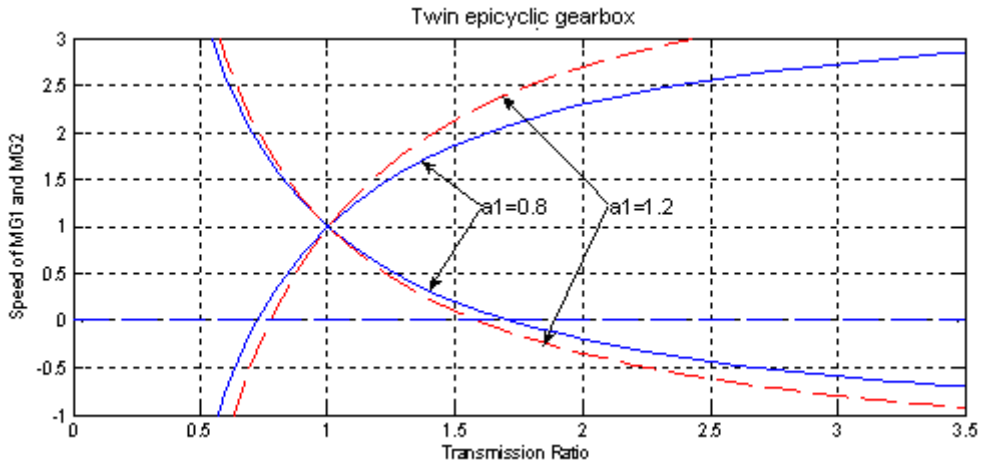

Fig 3.9 Effects of two values of α_1 on the twin epicyclic gearbox

To study the effect of α_3, two different values for α_1, 0.8 and 1.2, are chosen, keeping a constant value of $\alpha_1 = 0.8$. The result is shown in Fig 3.10.

Fig 3.10 shows changing α_3 only affects the speed of MG2 while the speed of MG1 keeps unchanged. The reason is that the speed of MG1 is decided by the first epicyclic gear unit and the speed of MG2 is decided by the two epicyclic units (Fig 3.6). Because α_1 is kept unchanged, so the curve of the speed of MG1 does not change.

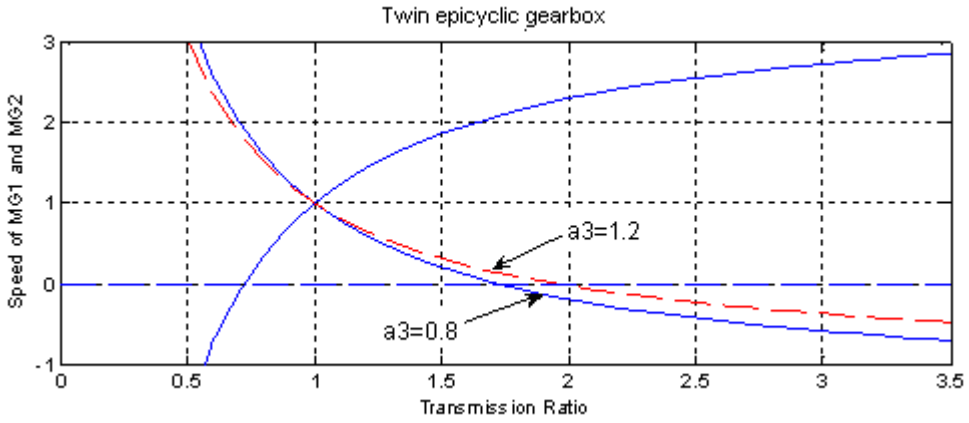

Fig 3.10 Effects of two values of α_3 on the twin epicyclic gearbox

3.3.2 Torque and efficiency analysis

The torque equation group (3.36) for the twin epicyclic gearbox is written below:

Connected part 1: $T_1 + T_5 + T_8 = 0$

Connected part 2: $T_2 + T_7 + T_{11} + T_{14} = 0$

Connected part 3: $T_3 + T_9 + T_{16} = 0$

Connected part 4: $T_4 + T_6 = 0$

Connected part 5: $T_{10} + T_{12} = 0$

Connected part 6: $T_{13} + T_{15} = 0$

Gear unit X1: $\alpha_1 \eta^t T_3 + T_4 = 0$

$$T_3 + T_4 + T_5 = 0$$

Gear unit X2: $\alpha_2 \eta^t T_6 + T_7 = 0$

$$T_6 + T_7 + T_8 = 0$$

Gear unit X3: $\alpha_3 \eta^t T_9 + T_{10} = 0$

$$T_9 + T_{10} + T_{11} = 0$$

Gear unit X4: $\alpha_4 \eta^t T_{12} + T_{13} = 0$

$$T_{12} + T_{13} + T_{14} = 0 \qquad (3.36)$$

Again at the moment, it has not been decided which gear is the driving part and which gear is the driven part. Hence, it is assumed that there is no loss in the transmission, so the analysis can be completed.

The efficiency of the transmission is taken into consideration in the later part of simulation and calculation when the input speed and torque are known.

The above linear equation group can be written in the following vector form:

$$A_T \vec{T} = \vec{0} \qquad (3.37)$$

where:

$\vec{T}$ equals $[T_1\ T_2 \ldots T_{16}]^{\mathrm{T}}$

A_T is the torque coefficient matrix.

Integrating Equations (3.36) and (3.37) gives,

$$\begin{bmatrix} 1 & 0 & 0 & 0 & 1 & 0 & 0 & 1 & 0 & 0 & 0 & 0 & 0 & 0 & 0 & 0 \\ 0 & 1 & 0 & 0 & 0 & 0 & 1 & 0 & 0 & 0 & 1 & 0 & 0 & 1 & 0 & 0 \\ 0 & 0 & 1 & 0 & 0 & 0 & 0 & 0 & 1 & 0 & 0 & 0 & 0 & 0 & 0 & 1 \\ 0 & 0 & 0 & 1 & 0 & 1 & 0 & 0 & 0 & 0 & 0 & 0 & 0 & 0 & 0 & 0 \\ 0 & 0 & 0 & 0 & 0 & 0 & 0 & 0 & 0 & 1 & 0 & 1 & 0 & 0 & 0 & 0 \\ 0 & 0 & 0 & 0 & 0 & 0 & 0 & 0 & 0 & 0 & 0 & 0 & 1 & 0 & 1 & 0 \\ 0 & 0 & \alpha_1\eta^t & 1 & 0 & 0 & 0 & 0 & 0 & 0 & 0 & 0 & 0 & 0 & 0 & 0 \\ 0 & 0 & 1 & 1 & 1 & 0 & 0 & 0 & 0 & 0 & 0 & 0 & 0 & 0 & 0 & 0 \\ 0 & 0 & 0 & 0 & 0 & \alpha_2\eta^t & 1 & 0 & 0 & 0 & 0 & 0 & 0 & 0 & 0 & 0 \\ 0 & 0 & 0 & 0 & 0 & 1 & 1 & 1 & 0 & 0 & 0 & 0 & 0 & 0 & 0 & 0 \\ 0 & 0 & 0 & 0 & 0 & 0 & 0 & 0 & \alpha_3\eta^t & 1 & 0 & 0 & 0 & 0 & 0 & 0 \\ 0 & 0 & 0 & 0 & 0 & 0 & 0 & 0 & 1 & 1 & 1 & 0 & 0 & 0 & 0 & 0 \\ 0 & 0 & 0 & 0 & 0 & 0 & 0 & 0 & 0 & 0 & 0 & \alpha_4\eta^t & 1 & 0 & 0 & 0 \\ 0 & 0 & 0 & 0 & 0 & 0 & 0 & 0 & 0 & 0 & 0 & 1 & 1 & 1 & 0 & 0 \end{bmatrix} \begin{bmatrix} T_1 \\ T_2 \\ T_3 \\ T_4 \\ T_5 \\ T_6 \\ T_7 \\ T_8 \\ T_9 \\ T_{10} \\ T_{11} \\ T_{12} \\ T_{13} \\ T_{14} \\ T_{15} \\ T_{16} \end{bmatrix} = \begin{bmatrix} 0 \\ 0 \\ 0 \\ 0 \\ 0 \\ 0 \\ 0 \\ 0 \\ 0 \\ 0 \\ 0 \\ 0 \\ 0 \\ 0 \\ 0 \\ 0 \end{bmatrix}$$

(3.38)

The Matlab program to obtain the torque coefficient matrix A_T and to obtain the relationship of torque for each component is shown in Appendix 13. From running the program, the torque coefficient matrix A_T is shown in Appendix 14, and the relationship of torque for the single epicyclic gearbox is shown in Appendix 15.

From Equation (3.38), the relations of the torque of the electrical machines with the torque of the engine and the torque of the output shaft are obtained as the following equations.

$$T_{15} + \frac{169}{324}T_1 + \frac{13}{18}T_2 = 0 \qquad (3.39)$$

$$T_{16} + \frac{155}{324}T_1 + \frac{5}{18}T_2 = 0 \qquad (3.40)$$

$$\begin{bmatrix} 1 & 0 & 0 & 0 & 0 & 0 & 0 & 0 & 0 & 0 & 0 & 0 & 0 & 0 & -5/18 & 0 \\ 0 & 1 & 0 & 0 & 0 & 0 & 0 & 0 & 0 & 0 & 0 & 0 & 0 & 0 & -2/9 & 0 \\ 0 & 0 & 1 & 0 & 0 & 0 & 0 & 0 & 0 & 0 & 0 & 0 & 0 & 0 & 1/2 & 0 \\ 0 & 0 & 0 & 1 & 0 & 0 & 0 & 0 & 0 & 0 & 0 & 0 & 0 & 0 & 2/9 & 0 \\ 0 & 0 & 0 & 0 & 1 & 0 & 0 & 0 & 0 & 0 & 0 & 0 & 0 & 0 & -13/18 & 0 \\ 0 & 0 & 0 & 0 & 0 & 1 & 0 & 0 & 0 & 0 & 0 & 0 & 0 & 0 & 1/2 & 0 \\ 0 & 0 & 0 & 0 & 0 & 0 & 1 & 0 & 0 & 0 & 0 & 0 & 0 & 0 & -65/324 & -5/18 \\ 0 & 0 & 0 & 0 & 0 & 0 & 0 & 1 & 0 & 0 & 0 & 0 & 0 & 0 & -13/81 & 2/9 \\ 0 & 0 & 0 & 0 & 0 & 0 & 0 & 0 & 1 & 0 & 0 & 0 & 0 & 0 & 13/36 & 1/2 \\ 0 & 0 & 0 & 0 & 0 & 0 & 0 & 0 & 0 & 1 & 0 & 0 & 0 & 0 & 13/81 & 2/9 \\ 0 & 0 & 0 & 0 & 0 & 0 & 0 & 0 & 0 & 0 & 1 & 0 & 0 & 0 & -169/324 & -13/18 \\ 0 & 0 & 0 & 0 & 0 & 0 & 0 & 0 & 0 & 0 & 0 & 1 & 0 & 0 & 13/36 & 1/2 \\ 0 & 0 & 0 & 0 & 0 & 0 & 0 & 0 & 0 & 0 & 0 & 0 & 1 & 0 & 169/324 & 13/18 \\ 0 & 0 & 0 & 0 & 0 & 0 & 0 & 0 & 0 & 0 & 0 & 0 & 0 & 1 & 155/324 & 5/18 \end{bmatrix} \begin{bmatrix} T_3 \\ T_4 \\ T_5 \\ T_6 \\ T_7 \\ T_8 \\ T_9 \\ T_{10} \\ T_{11} \\ T_{12} \\ T_{13} \\ T_{14} \\ T_{15} \\ T_{16} \\ T_1 \\ T_2 \end{bmatrix} = \begin{bmatrix} 0 \\ 0 \\ 0 \\ 0 \\ 0 \\ 0 \\ 0 \\ 0 \\ 0 \\ 0 \\ 0 \\ 0 \\ 0 \\ 0 \\ 0 \\ 0 \end{bmatrix} \quad (3.41)$$

3.4 Computer program for the analysis of epicyclic transmissions

3.4.1 Transmission systems analysis tool (TSAT)

The common features of the many designs proposed for power splitting transmissions to date is that they all contain epicyclic gear units, clutches, brakes and motor generator units, which are often interconnected in quite complicated ways. In this research, a software tool has therefore been developed to allow a speedy analysis of the wide variety of candidate designs. The user interface requires the designer to input the data for all the components and connections in a straightforward structured fashion. The mathematical calculations are based on the matrix analysis approach which is coded in a MATLAB environment. Typical outputs include the speeds and torques of all components from which the power flow details through the transmission elements can be calculated. The software is currently upgraded to incorporate transmission efficiencies.

The procedure to obtain the relationships of speed of a transmission using TSAT is shown in Fig 3.11.

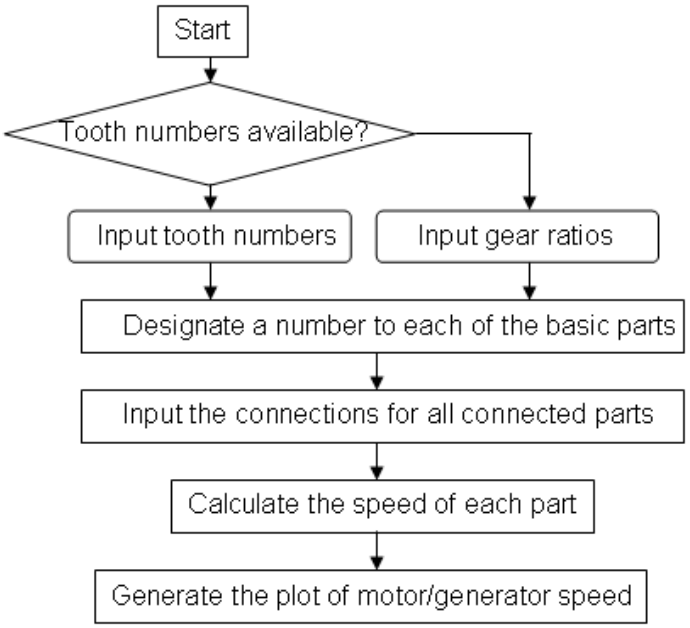

Fig 3.11 Flowchart for the TSAT program

There are mainly 6 steps in the calculation:

1. Ask the user to input the configuration of the transmission, namely the number of epicyclic gear units, clutches, brakes, and motor/generators (Fig 3.12);

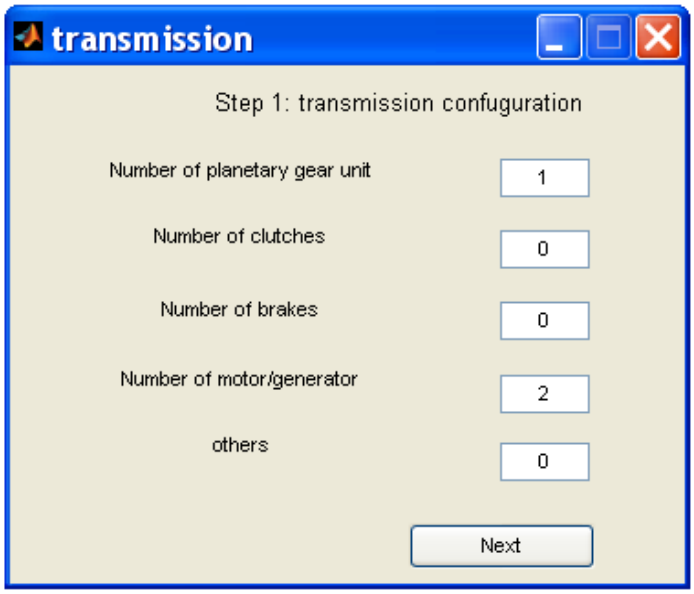

Fig 3.12 Step 1: transmission configuration

2. Ask the user to input the tooth number of each gear. If the tooth numbers are not available, you can also input the gear ratios for each gear unit (Fig 3.13);

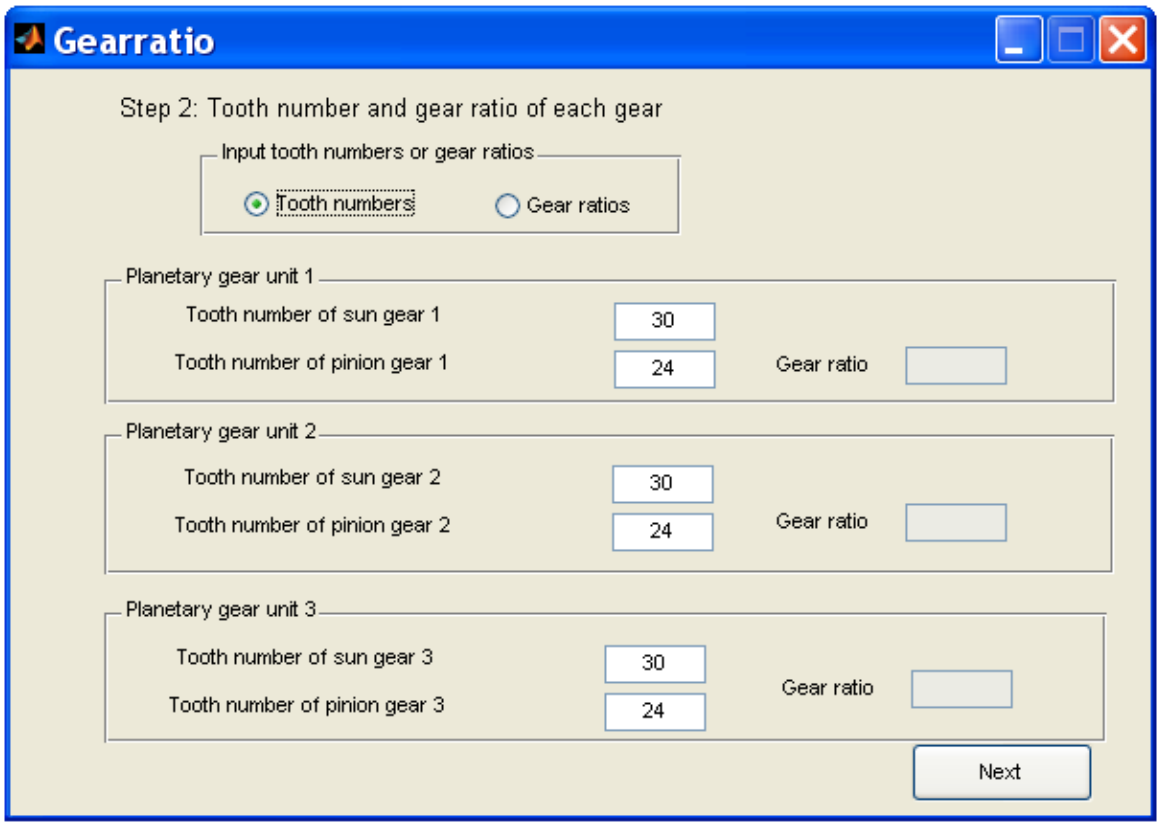

Fig 3.13 Step 2: tooth number of each gear

3. Designate a number to each of the basic parts. The sequence is: the input axle, the output axle, the gears, the clutch drums, the brake disks. Every planetary gear unit has three basic parts. A clutch has two basic parts. A brake has only one basic part. The whole system has q basic parts:

$$q = 2 + 3x + 2y + z \qquad (3.42)$$

where :

x is the number of gear units,

y is the number of clutches,

z is the number of brakes.

4. Ask the user to input the connections for all connected parts (Fig 3.14).

The programme will list out all the basic parts, according to the input from step 1. Then the user selects which part is connected to which.

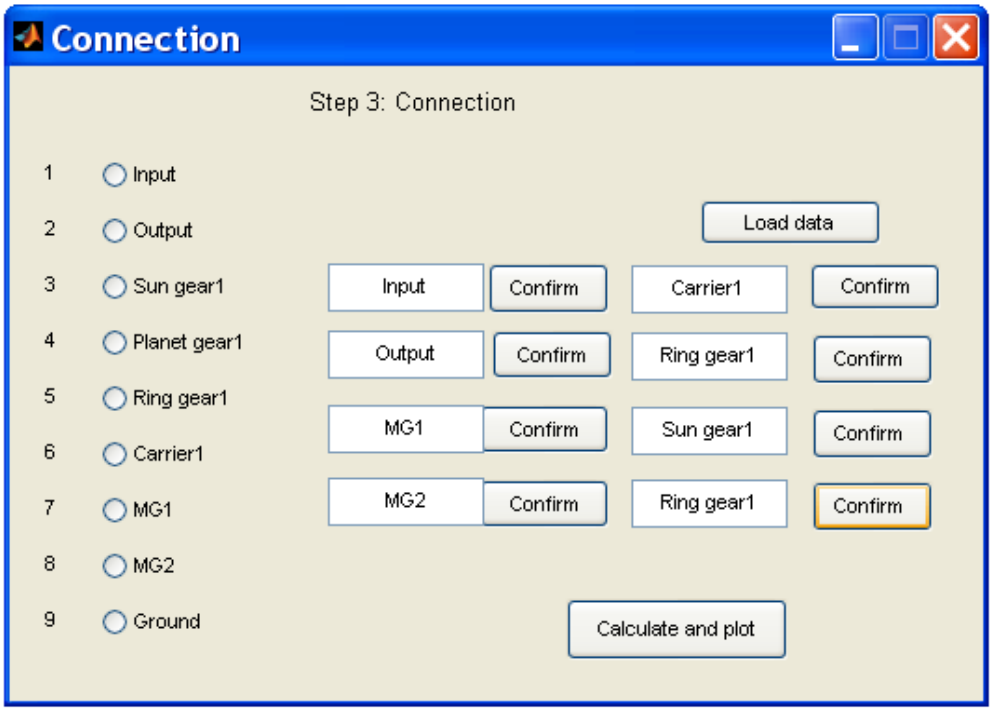

Fig 3.14 Step 3: Connection

5. Calculate the speed of each part, assuming that the engine speed is 1, and the output speed equals the engine speed divided by the transmission ratio.

For all the basic parts in a connected part, the speeds of all basic parts are the same.

For a gear unit, the kinematic relationship between gears a, b and the carrier h are:

$$n_a - \alpha n_b + (\alpha - 1) n_h = 0 \tag{3.43}$$

where n_a, n_b and n_h are the speeds of rotation of geasr a, b and the carrier h respectively. α is the gear ratio.

All the linear equation group can be written in the following vector form:

$$A_n \vec{n} = \vec{0} \tag{3.44}$$

where:

$\vec{n}$ is the speed vector;

A_n is the speed coefficient matrix.

6. Generate the plot of motor/generator speed vs. transmission ratio.

The engine speed is set to be 1. So for any transmission ratio i_T ,

$$i_T = \frac{n_{engine}}{n_{output}} \tag{3.45}$$

The speed of motor/generator is calculated when the transmission ratio changes.

3.4.2 Use of TSAT to analyze some complex PSDs

- **GM Allison, AHS-2 system**

The arrangement of the GM Allison, AHS-2 system is shown in Fig 3.15. The addition of clutches to a transmission based on two epicyclic gear units opens up an opportunity to fundamentally change the power flow through the system.

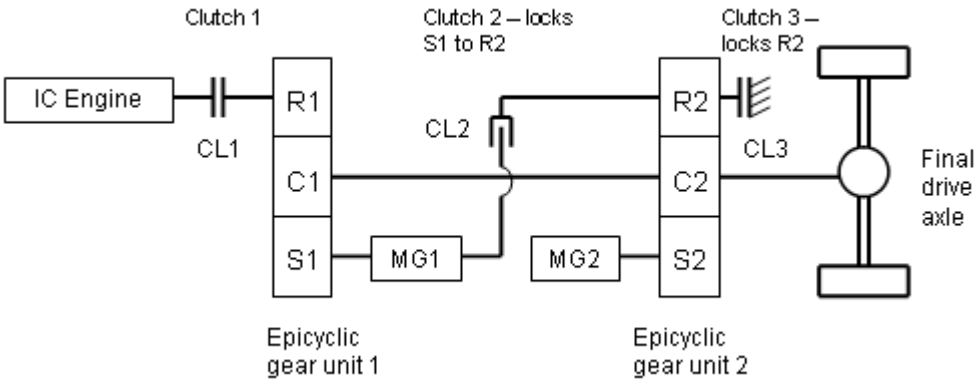

Fig 3.15 GM Allison AHS arrangement

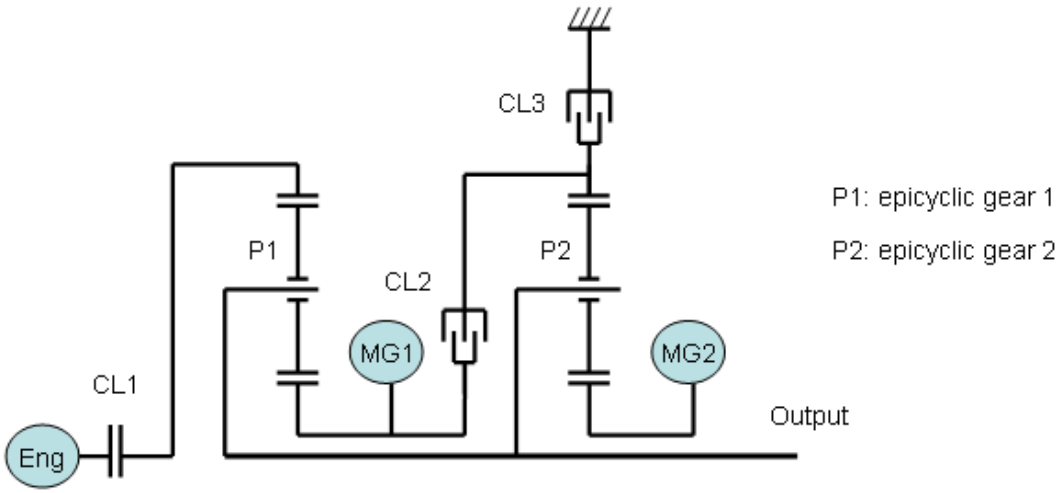

Fig 3.16 Simplified drawing of GM Allison AHS arrangement

Basically, the two modes of operation are usually referred to as:

Low range – input power split

High range– compound power split

In the first of these – input power split - the clutches are set as:

CL1 locked

CL2 unlocked

CL3 locked

The transmission behaves in exactly the same way as the single mode system.

In the second – compound split – mode, the clutches are set as:

CL1 locked

CL2 locked

CL3 unlocked

Thus, the sun gear 1 (S1) is connected via MG1 to ring gear 2 (R2). The ability to switch between these two modes smoothly is a crucial aspect of this design, and this is usually referred to as synchronous shifting. As mentioned in Chapter 2, there is no sudden speed changes during torque transfer because the clutches are shifted when the MG speeds are zero.

The speed results for this system are shown in Fig 3.17. In this example, the shift point is arranged at a transmission ratio of 1.3.

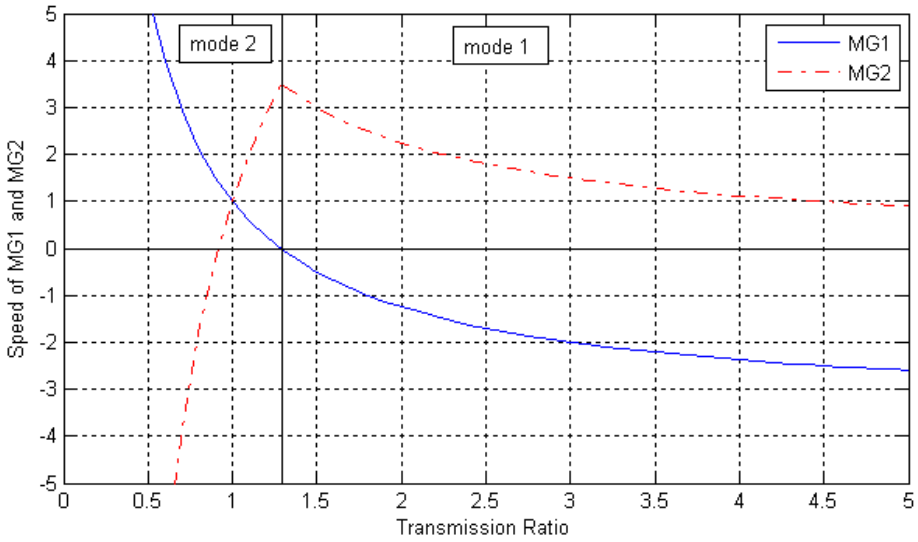

Fig 3.17 GM Allison AHS mode 1 and mode 2

- **Generic dual mode + 4 fixed ratios systems**

As mentioned already in the introduction, an interesting software package for generating novel transmission designs has been developed by GM Research and Development Laboratories (Raghavan, Bucknor et al. 2007). One of the examples described in this paper is a dual mode system which also offers four fixed gear ratios. This transmission is a full-function EVT (electrically variable transmission) comprised of 3 simple planetary gear sets, 2 rotating clutches, 1 stationary clutch, and 2 motor-generators, labelled MG1 and MG2. It operates in Battery Reverse, EVT Reverse and Forward, Battery-charging Reverse and Forward, and has 4 fixed (i.e., all mechanical) speed-ratios.

The design is shown in Fig 3.18, and it emphasises the potential benefits of the software, because (a) this arrangement is rather complicated, (b) it is not intuitively obvious to understand exactly how it will meet the performance specifications and (c) it is not a design that would naturally be proposed using traditional design methods.

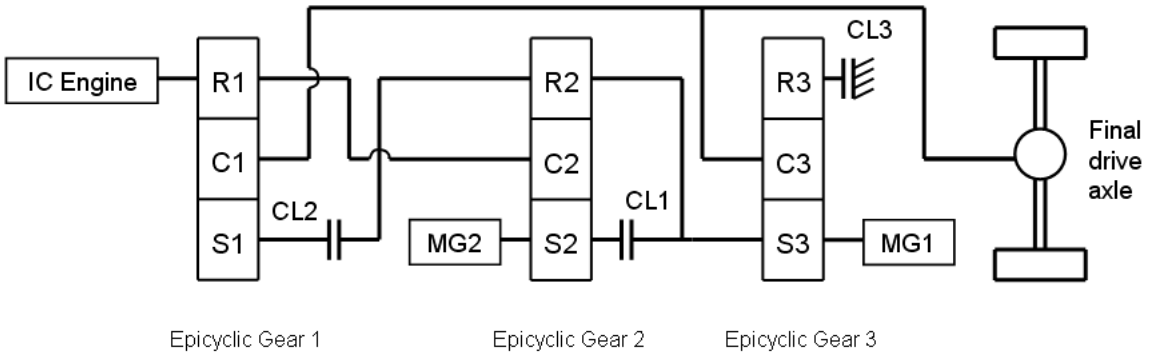

Fig 3.18 Generic dual mode + 4 fixed ratios arrangement

A simplified diagram of the design is shown in Fig 3.19

In mode 1, the clutches are set as:

CL1 unlocked

CL2 unlocked

CL3 locked

In mode 2, the clutches are set as:

CL1 unlocked

CL2 locked

CL3 unlocked

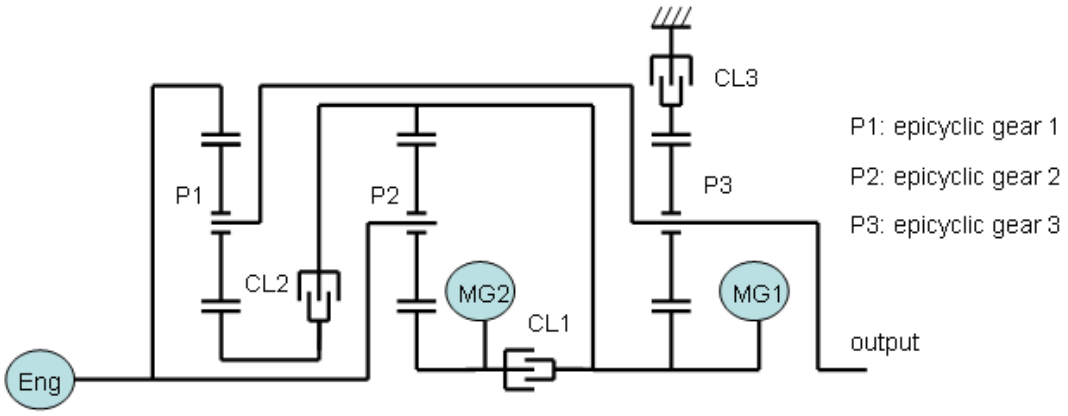

Fig 3.19 Simplified drawing of Generic dual mode + 4 fixed ratios arrangement

The speeds and torques of this design have been analysed using the TSAT software, and the speed results for the eCVT modes 1 and 2 are shown in Fig 3.20.

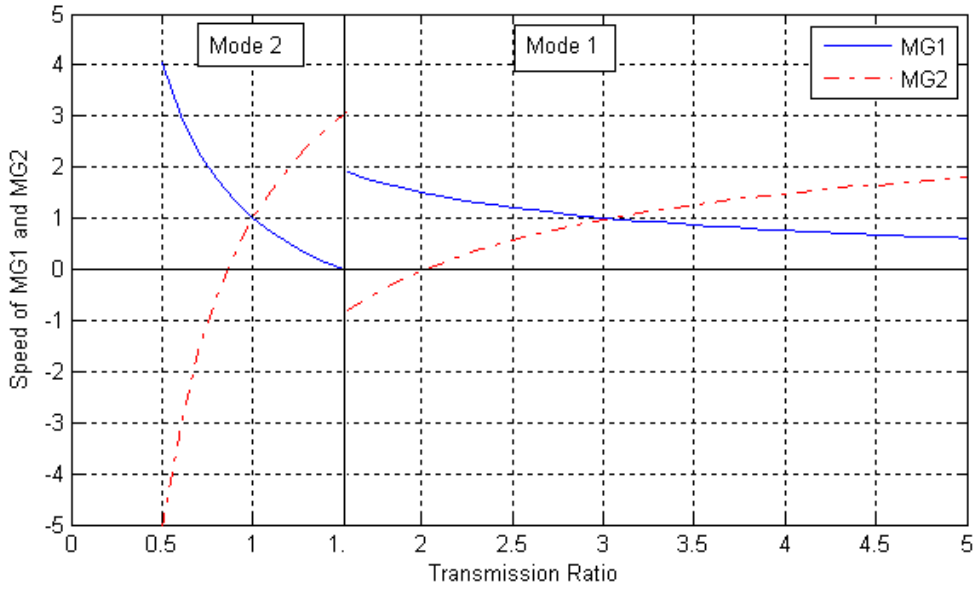

Fig 3.20 Generic dual mode + 4 fixed ratios

3.5 Concluding remarks

- The speeds and the torques for each component in the single epicyclic gearbox are analyzed and the relationships of MG1 and MG2 with the engine and the output shaft are given.

- The speeds and torques for each component in the twin epicyclic gearbox are analyzed and the relationships of MG1 and MG2 with the engine and the output shaft are given.
- A software package to analyse epicyclic transmissions, especially transmissions for hybrid vehicles is developed and examples of using the software have been described.

4 Comparison of a single and twin epicyclic gearbox

4.1 Introduction

The aim of this chapter is to compare the behaviors of the single and twin epicyclic transmissions. In order to do this, the analysis described in Chapter 3 is combined with a simple vehicle model. This enables typical torque, speed and power results to be generated, assuming these two gearboxes are fitted to a typical, medium sized passenger car.

Two driving conditions are examined: constant speed running and accelerating at a constant value of 0.8 m/s^2. This enables comparisons to be drawn about the potential benefits of the twin epicyclic transmission.

4.2 Mathematical model

The behaviors of the single and twin epicyclic systems are now compared, by assuming they are fitted to a typical vehicle, which is about the same size, for example, as Toyota Prius (see Table 4.1); the engine data is a simple look up table based on the idea of trying to use the maximum fuel economy line. Two conditions are analyzed:

i) constant speed, steady running

ii) acceleration of 0.8 m/s^2

Table 4.1 Typical vehicle parameters ((Miller 2004)

Vehicle curb weight	1313 kg
Drag coefficient, Cd	0.26
Frontal Area	2.29 m^2
Tire radius	0.3425 m
Final drive	4.0:1

The mathematical model is built following the 6 steps below:

1. Calculate the road load for the stated condition;
2. Reflect the road load to the driveline –speed and torque;

3. Assign the engine speed;
4. Use the planetary gear speed equation to determine the motor/generator speed and torque;
5. Calculate the engine mechanical path torque per the planetary gear torque expression;
6. Calculate all power flows for motor/generators.

The calculation procedure is summarized in Fig 4.1.

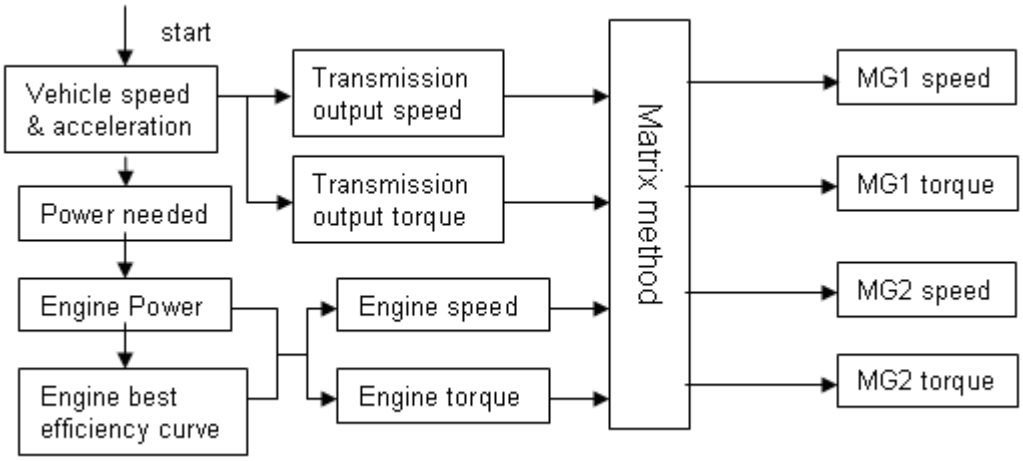

Fig 4.1 Calculation process

A similar calculation strategy is used for both the single and twin epicyclic transmissions. For the two systems, the value of the degrees of freedom is 2. These calculations are repeated over the speed range from 10 m/s to 35 m/s (22 mile/h to 77 mile/h). The power for MG1 and MG2 are calculated. Also the torque split, namely how much percent of the engine torque is directed towards the wheels is derived. The Matlab program to perform the calculations is shown in Appendix 16.

4.3 Results and comparison

4.3.1 Torque and power split

For the single epicyclic transmission, the torque of engine is split between the wheels, via the ring gear, and MG1, via the sun gear. Due to its structure, the ratio of the torque to the wheels and the MG1 torque is fixed as 2.6:1, which means that 1/3.6 (28%) of the engine torque is sent to the sun gear (MG1), and 2.6/3.6 (72%) of the engine torque is sent to the ring gear (the driving wheels). But this does

mean that the power of engine is transmitted to the wheels and to the MG1 at a fixed rate, because the power is the product of torque and rotation speed. For the single epicyclic transmission, the torque split and the percentage of the power through the electrical route are shown in Fig 4.2.

The percentage of the power through electrical route is defined as the power of MG1 relative to the power of the engine. The values are negative because, when the power is input to the system, it is defined as positive; whereas when the power is drawn from the system, it is defined as negative. In this simulation, the power of MG1 is always negative, meaning that it acts as a generator over the speed range from 10 m/s to 35 m/s (22 mile/h to 77 mile/h).

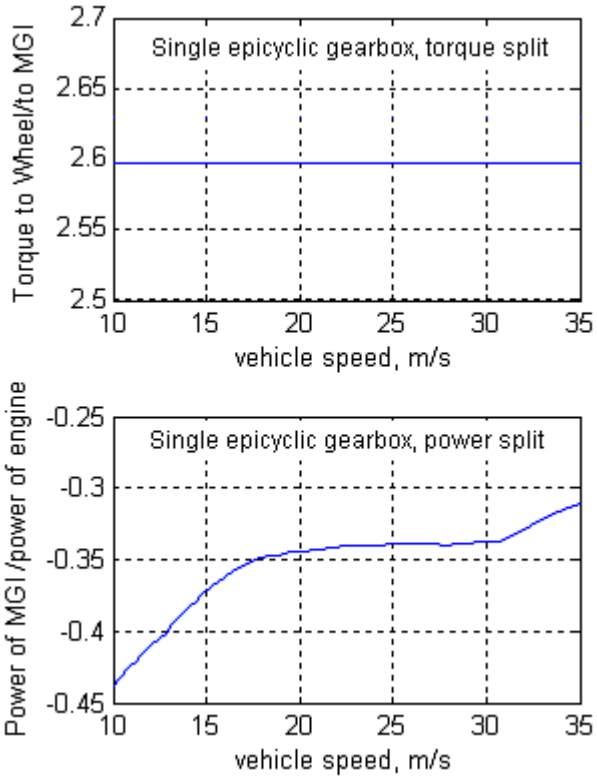

Fig 4.2 Single epicyclic transmission, torque and power split

For the twin epicyclic transmission, the torque split and the percentage of the power through the electrical route are shown in Fig 4.3, from which it can be seen that the ratio of the torque to the wheels and the torque to the MG1 is not fixed. It varies when the transmission ratio changes. Most of the torque split ratio for the twin epicyclic transmission is bigger than 2.6:1. Comparing the two lower curves in Fig 4.2 and Fig 4.3, it can be seen that the absolute values of the power of MG1 vs. the power of the engine for the twin epicyclic transmission are much lower than

for the single epicyclic arrangement, which means for the twin epicyclic transmission, less percentage of engine power is transmitted by the electrical path.

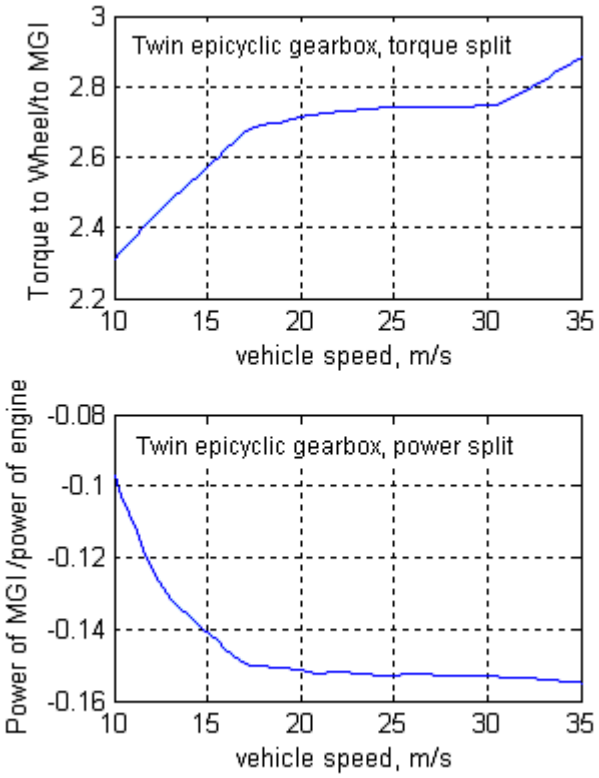

Fig 4.3 Twin epicyclic transmission, torque and power split

4.3.2 Power of MG1 and MG2

The results for the power in MG1 and MG2, for constant speed running, i.e. no acceleration are shown in Fig 4.4 and Fig 4.5 for the single and twin epicyclic transmission respectively. For the single epicyclic transmission (Fig 4.4), MG2 is acting as a motor. The power demanded from MG1 increases as the vehicle speed increases, whereas the power used to drive MG2 stays fairly constant up until the higher speed.

For the twin epicyclic transmission (Fig 4.5), the situation is very similar: MG2 acts as a generator and MG1 acts as a motor. Also, their characteristics as the forward speed changes are rather similar to each other.

The MG1 and MG2 power results when the vehicle is accelerating at 0.8 m/s^2 are shown in Fig 4.6 and Fig 4.7 for the single and twin epicyclic transmissions. The power splits are now very different from the zero acceleration case. For the single epicyclic transmission, MG2 acts as a motor, delivering from around 8 to 30

kW as forward speed increases. At the same time, MG1 acts as a generator with a power demand from around -5 to -17 kW. Thus considerable power is transmitted through the electrical route.

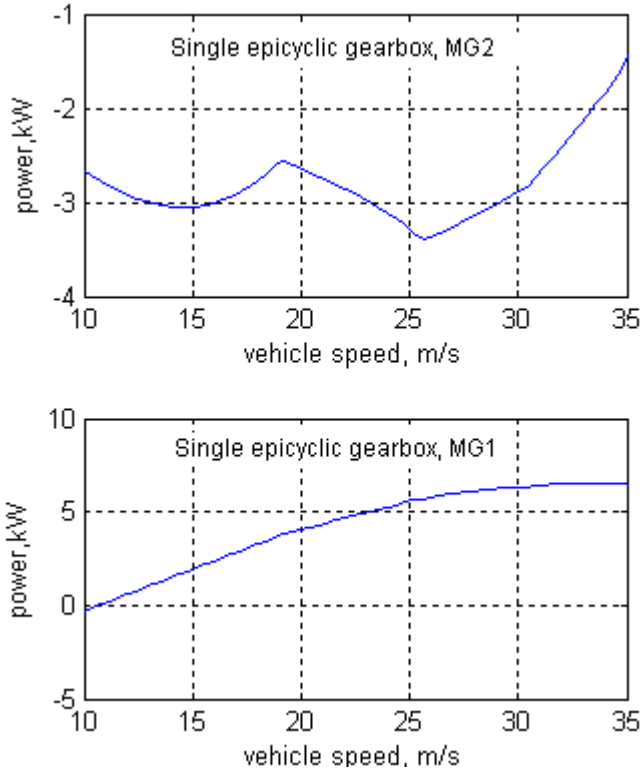

Fig 4.4 Single epicyclic transmission, power of MG1 & MG2, no acceleration

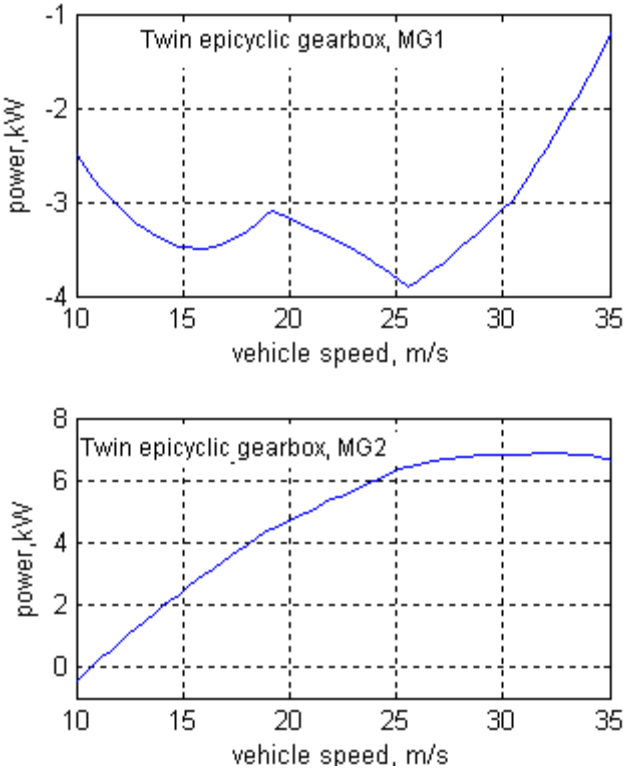

Fig 4.5 Twin epicyclic transmission, power of MG1 and MG2, no acceleration

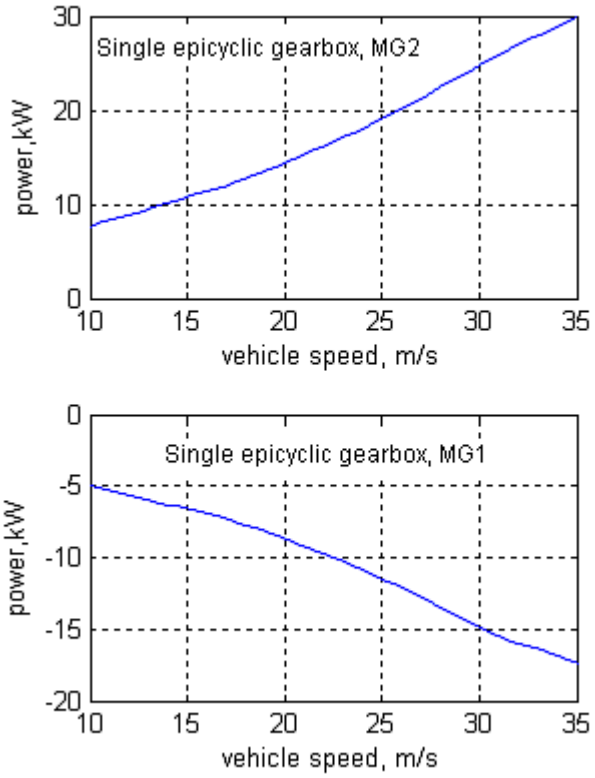

Fig 4.6 Single epicyclic transmission, power of MG1 and MG2, with acceleration

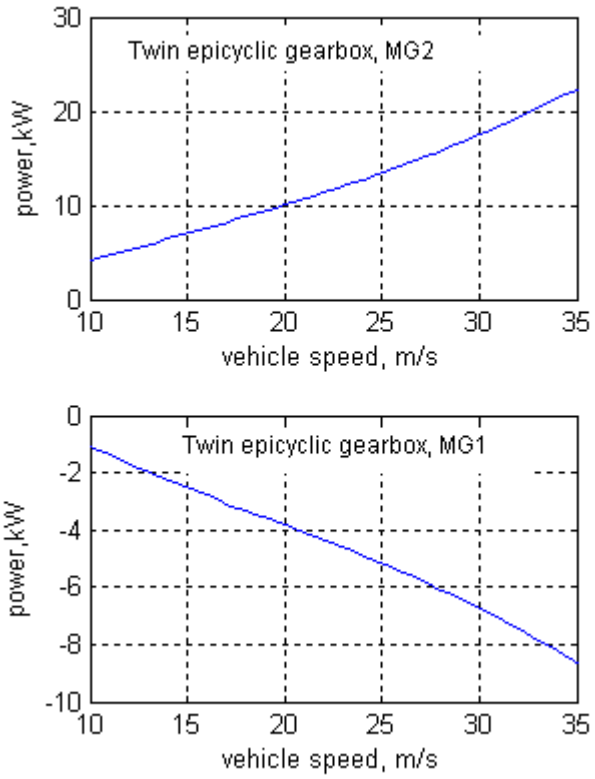

Fig 4.7 Twin epicyclic transmission, power of MG1 and MG2, with acceleration

For the twin epicyclic transmission, the overall situation is rather similar; MG2 acts as a motor and MG1 as a generator. However, the absolute power values are considerably lower. Thus, the twin epicyclic transmission demonstrates clearly its potential advantage, namely that less power is transmitted via the electrical routes and consequently, the overall transmission efficiency will be higher.

4.4 Potential benefits of the twin epicyclic gearbox

- **More flexibility for control**

For a single epicyclic transmission, MG2 is connected to the output shaft. So its speed is decided by the vehicle. In contrast, for a twin epicyclic transmission, neither of the electric machines is connected to the input or output shaft, which gives an opportunity to choose the electric machine to work in its highest efficiency area.

- **One more node where one of the electric machines is at standstill**

In a three branch system, there is only one node point. In the four branch system, two node points occur over the entire speed range (Fig 4.8).

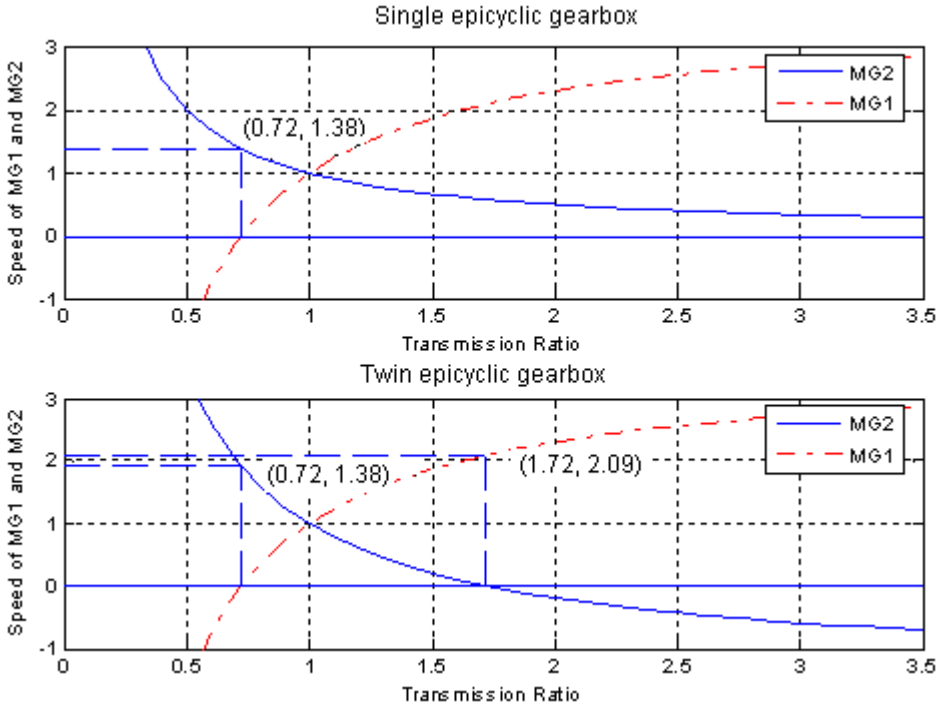

Fig 4.8 Transmission ratios and speeds of MG1 and MG2

In the four branch transmission, at the node 1, MG1 is at a standstill; at node 2, MG2 is at standstill. So at node points the power via the electrical path goes to

zero, and the system works at its highest efficiency. By comparison, in a single epicyclic transmission, there is only one node point. There is potential to improve efficiency by designing the controller to make the transmission work at the two node points. In this study, the two node points occur when the transmission ratios are 0.72 and 1.72 respectively.

To show that it is possible to use the 2 node points to reduce the overall power, an example calculation is done:

The engine speed is set to be 300 rad/s and torque is set to be 100 Nm. The transmission ratio is set to be 1.72. The powers of the electric machines are shown in Table 4.2.

Table 4.2 Electric power for two transmission at the node point 2

Power of MG1, single epicyclic transmission	P_mg1_3branch	-17.4 kW
Power of MG2, single epicyclic transmission	P_mg2_3branch	22.2 kW
Power of MG1, twin epicyclic transmission	P_mg1_4branch	4.8 kW
Power of MG2, twin epicyclic transmission	P_mg2_4branch	0

Note: Postive power means input power into the system, like a motor;
Negative power means power out of the system, like a generator.

Suppose the efficiency of a motor taking power from the battery and the efficiency of generator saving the energy into the battery are both 0.8, then the difference between a twin epicyclic transmission and a single epicyclic transmission is:

$$P\_3branch = P\_mg2\_3branch / 0.8 + P\_mg1\_3branch * 0.8 = 13.9kW$$

$$P\_4branch = P\_mg2\_4branch / 0.8 + P\_mg1\_4branch * 0.8 = 3.9kW$$

Hence, the difference between the two systems is 13.9-3.9 = 10 kW.

For a vehicle operating in the UK, it is likely that the two most typical speeds are 30 mile/h, in a city driving, and 70 mile/h, when high speed cruising. To make full use of the two node points, the design of the powertrain should be arranged so that the two node points coincide with the speeds 30 mile/h and 70 mile/h

respectively. With the vehicle parameters given in Table 4.1, the wheel speeds and engine speeds at the vehicle speed of 30 mile/h and 70 mile/h are given in Table 4.3. So when selecting the engine, the best efficiency area should be around 280 rad/s.

Table 4.3 The wheel and engine speeds at the two typical vehicle speeds

Vehicle speed (mile/h)	Transmission ratio	Wheel speed (rad/s)	Engine speed (rad/s)
30	1.72	41.3	284.3
70	0.72	96.4	277.7

- **Smaller size of electric machines**

Integrating Fig 4.6 and Fig 4.7, when accelerating the typical car with 0.8 m/s^2 from 10 to 35 m/s, the powers of MG1 and MG2 for the two systems are shown in Fig 4.9.

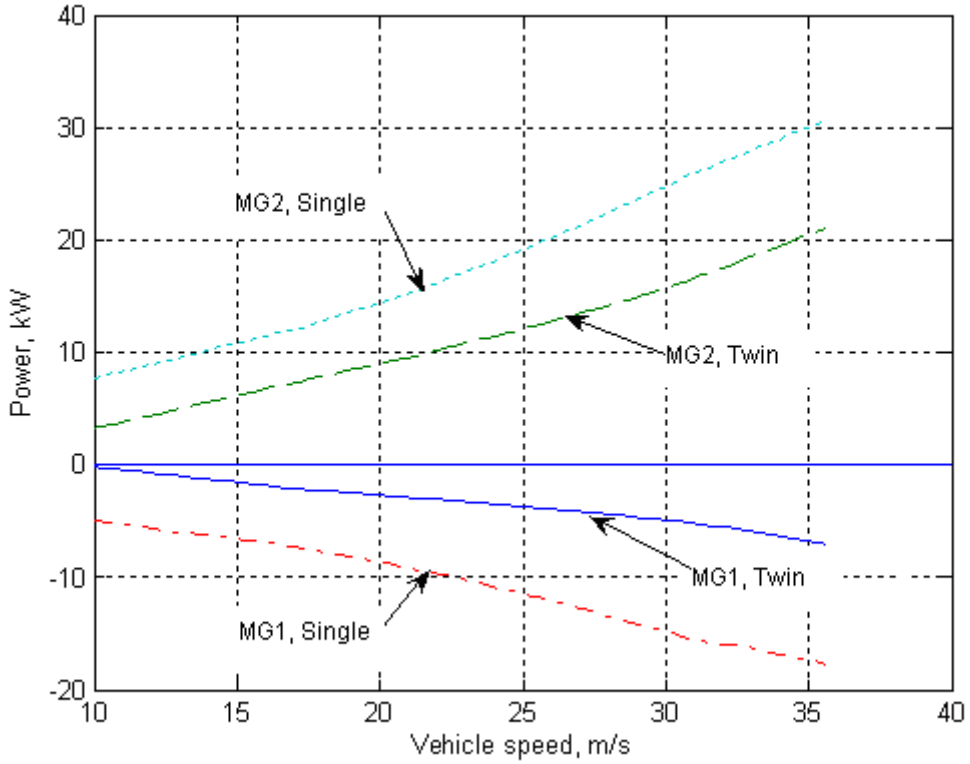

Fig 4.9 Power of MG1 and GM2

From Fig 4.9, it can be seen that the power of MG1 and MG2 for a twin epicyclic transmission is smaller than a single epicyclic transmission. For example, when the vehicle speed is 30 m/s, the power of each machine is shown in Table 4.4.

Table 4.4 Power of MG1 and MG2 at 30m/s

Twin epicyclic transmission	Power of MG1	-4.96 kW
	Power of MG2	15.67 kW
Single epicyclic transmission	Power of MG1	-14.88 kW
	Power of MG2	24.70 kW

4.5 Concluding remarks

- The single epicyclic gearbox although used successfully on, for example, the Toyota Prius has the limitation that one of the MG units is connected directly to the fixed drive, the twin epicyclic gearbox does not have this restriction, and so it offers the opportunity of more freedom to control the speeds of MG1 and MG2.
- For the twin epicyclic gearbox, it has been shown over a limited range of operating conditions that it is possible to direct less power via the electrical route, thus offering potential efficiency gains.
- Also, the twin epicyclic gearbox has tow node points, whereas the single epicyclic only has one. Again, this offers potential if these two mode points are arranged to coincide with common operating speeds, say 30 and 70 mile/h.
- The final potential benefit of the twin epicyclic gearbox is that it should be possible to downsize the electric machines. However, this benefit must be weighed against the slight disadvantage of increased complexity of the gear system.

5 Modeling hybrid electric vehicle (HEV) performance

5.1 Introduction

In this chapter, the modelling is further developed to investigate in more detail the effect of the single and twin epicyclic gearbox when fitted to a typical HEV. The modelling is therefore extended to include all the subsystems and the controller design of a typical HEV, and the vehicle is simulated over more typical driving cycles.

Three vehicle models are built up: a traditional ICE vehicle, a HEV with single epicyclic gearbox, and a HEV with twin epicyclic gearbox. Firstly, the subsystem models, such as the engine, transmission, and motor/generator are introduced. Then, the control strategy for an HEV is studied and controllers for 3 branch and the single and dual epicyclic systems are described in detail.

The vehicle models are built based on the quasistatic approach (Guzzella, 2007). This approach allows the fuel consumptions of each vehicle under different driving cycles to be calculated. The QSS toolbox (Guzzella and Amstutz 2005) is used for some of the system elements such as driving cycles, engine, and battery model.

5.2 Overview of Vehicle Models

The modelling of the hybrid electric vehicle performance is done using the QSS Toolkit (Guzzella and Amstutz 2005). This is a quasistatic simulation package based on a collection of Simulink blocks and the appropriate parameter files that can be run in any Matlab/Simulink environment. The traditional ICE vehicle model itself is straightforward and is shown in Fig 5.1. There are 5 sub-systems: the driving cycle subsystem, vehicle subsystem, the gearbox subsystem, the combustion engine subsystem, and the fuel tank subsystem. The data for the engine and gearbox are taken from generic data in the QSS package. The function of the engine subsystem is to compute the fuel consumption from a consumption map, according to the torque and the rotational speed demand. The gearbox has 5 gears ranging from 3.84 to 0.63. the differential gear ratio is 3.95. The other vehicle data are shown in Table 5.1. It is not intended to represent any specific

vehicle – but rather to act as a generic vehicle platform to focus attention on the differences obtainable from the three vehicle models.

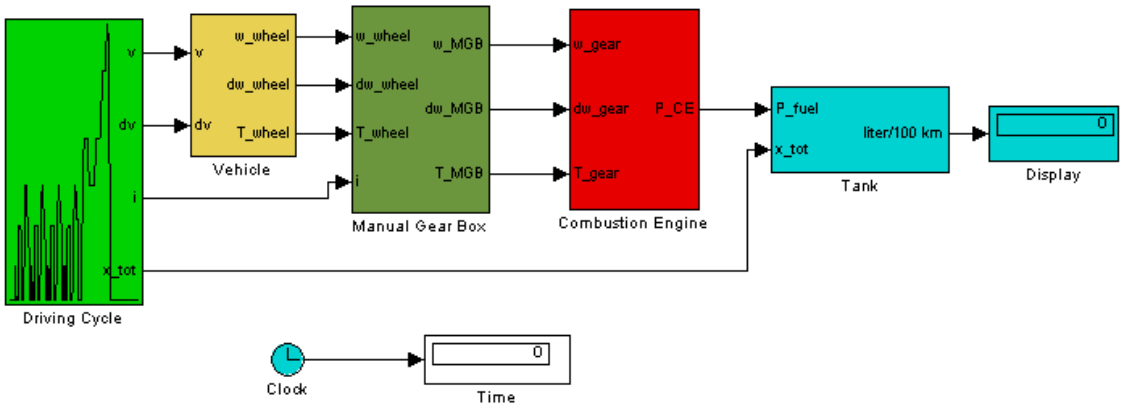

Fig 5.1 Overview of the conventional ICE vehicle model

Table 5.1 Vehicle parameters (Miller 2004)

Vehicle curb weight	1257 kg
Drag coefficient, Cd	0.29
Frontal Area	2.23 m^2
Tire radius	0.292 m
Final drive	3.95:1

The models for the 2 HEV vehicles are built based on the same baseline vehicle, with the same vehicle parameters, but different transmissions, as shown in Fig 5.2.

The input to the model is one of the standard driving cycles – the NEDC and USA FTP-75 cycles are used extensively in this work – and the solution procedure is based on stepping through the driving cycle at typically one second steps, calculating the equilibrium condition and then collecting all the data for plotting at the end of the cycle. Thus, the focus of attention is on the overall efficiency of the engine and motor generator units and the major issue of whether it is possible to improve overall energy usage by operating the whole system at or near to the best efficiency points.

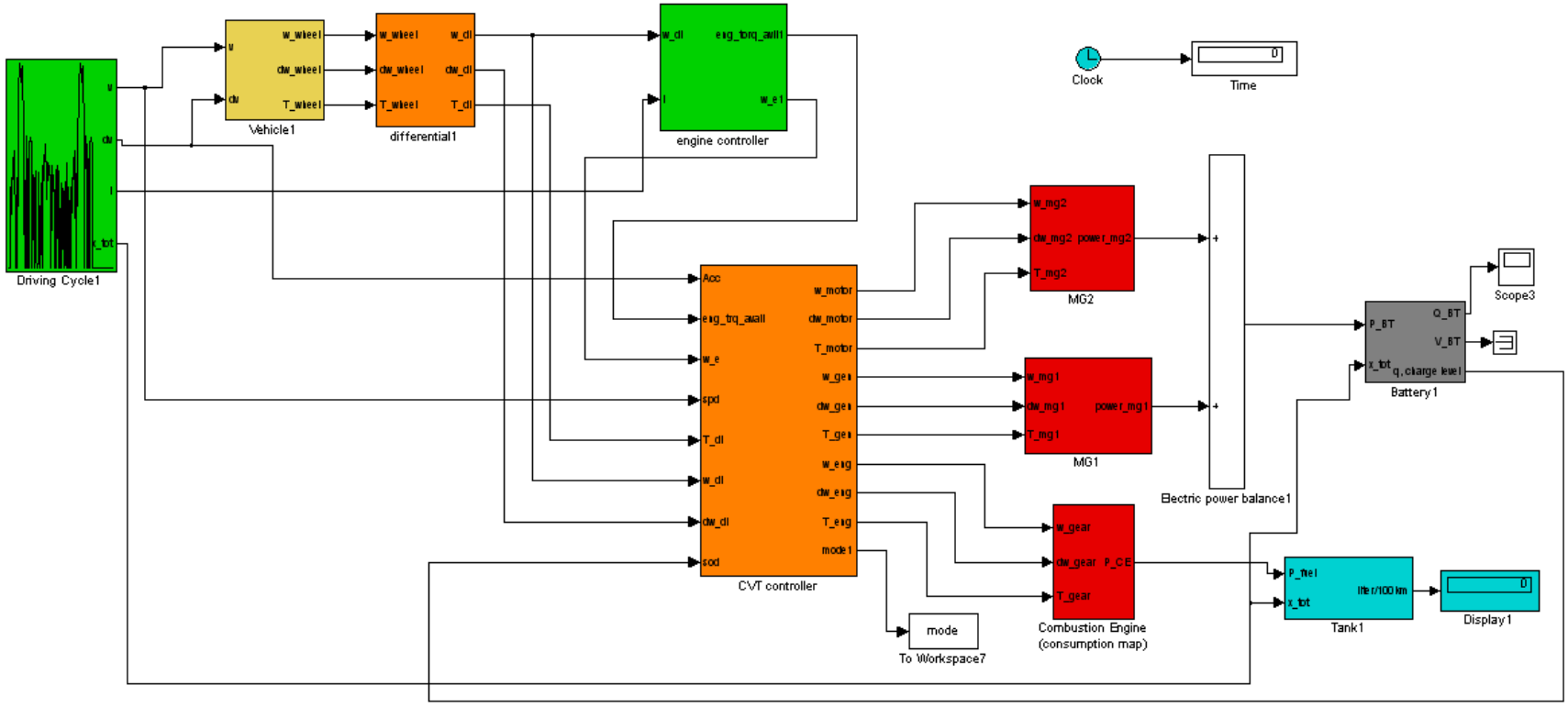

Fig 5.2 Overview of the hybrid vehicle model

5.3 Engine model

The engine model from QSS Toolbox was used in this research. The function of the engine model is to compute the fuel consumption from a consumption map. Inputs for the model include engine speed, engine acceleration and engine torque. The output of the model is the fuel consumption of the engine at each sampling point.

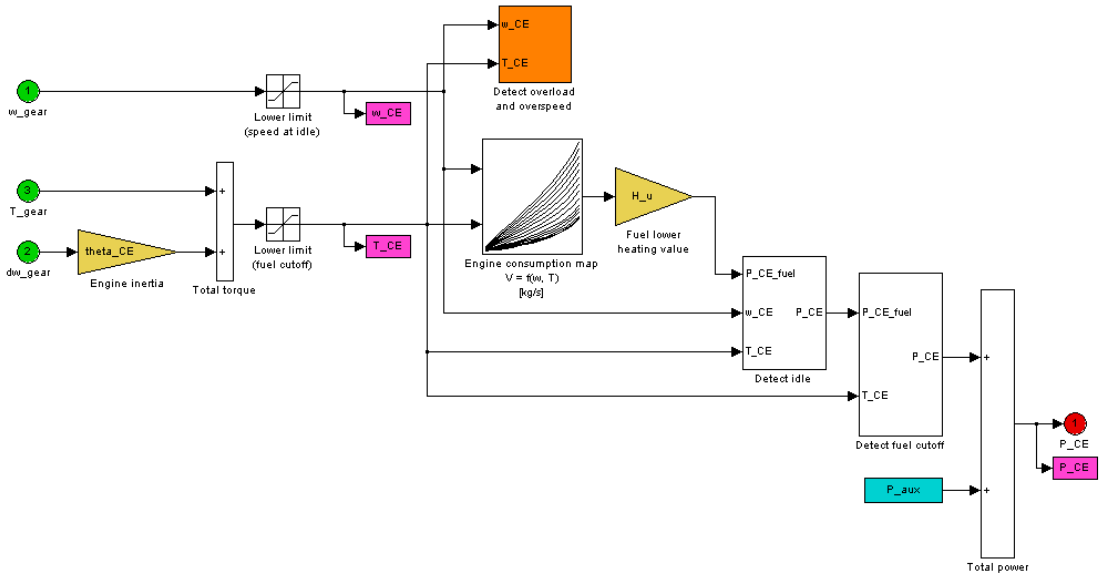

Fig 5.3 Top view of the engine model based on a consumption map

The function of overload and overspeed detection was built in the engine model. As soon as the engine torque or speed is over the limit, the simulation is stopped. The similar detection function is built in the motor/generator models. To finish the simulation with the whole driving cycle, once any overload or overspeed is detected, the controller will reselect the related speed and/or torque, to make sure every component, including the engine and the motors, work within these the speed-torque limit.

The data for the fuel consumption map represents a small engine with maximum speed 500 rad/s and maximum torque 118 Nm. There are 3 parameters for the map: a vector ($1\times n$) containing the rotational speed, a vector ($m\times 1$) containing the torque and an efficiency map ($n\times m$) containing the fuel efficiency point (kg/s) at each combination of speed and torque. Fig 5.4 shows the engine efficiency map used in the simulation.

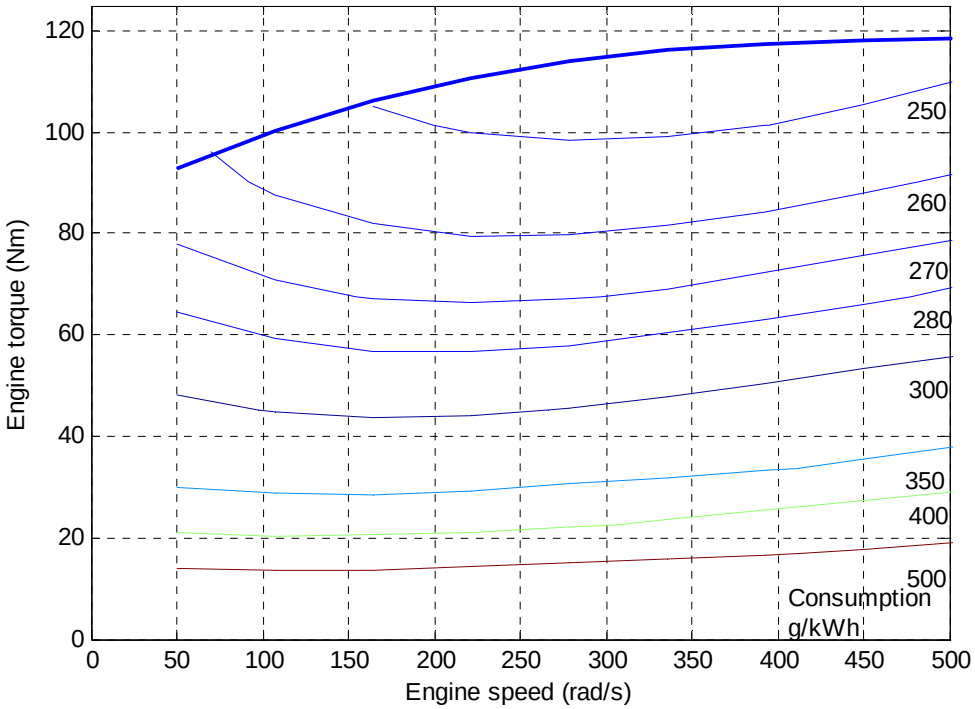

Fig 5.4 Engine efficiency map

5.4 Transmission models

5.4.1 Conventional manual gearbox

The model of a 5-gear shift manual gearbox was taken from one of the standard blocks in the QSS toolbox, the top level of which is shown in Fig 5.5. The gear ratios from the first gear to the fifth gear are 3.84, 2.11, 1.36, 0.86 and 0.63 respectively. The differential gear ratio is 3.95. The efficiency of the whole gearbox is set to be 0.9. The inputs of the block are wheel speed, wheel acceleration, wheel torque, forward speed, and gear number. The gear number specifies which gear to use and it is generated from the driving cycles. The outputs of the block are speed of the fly wheel, acceleration of the flywheel and torque on the flywheel.

The function of the gearbox model is to reflect the road load to the output shaft of the engine, then to calculate the engine fuel consumption according to the rotation speed and the torque demand.

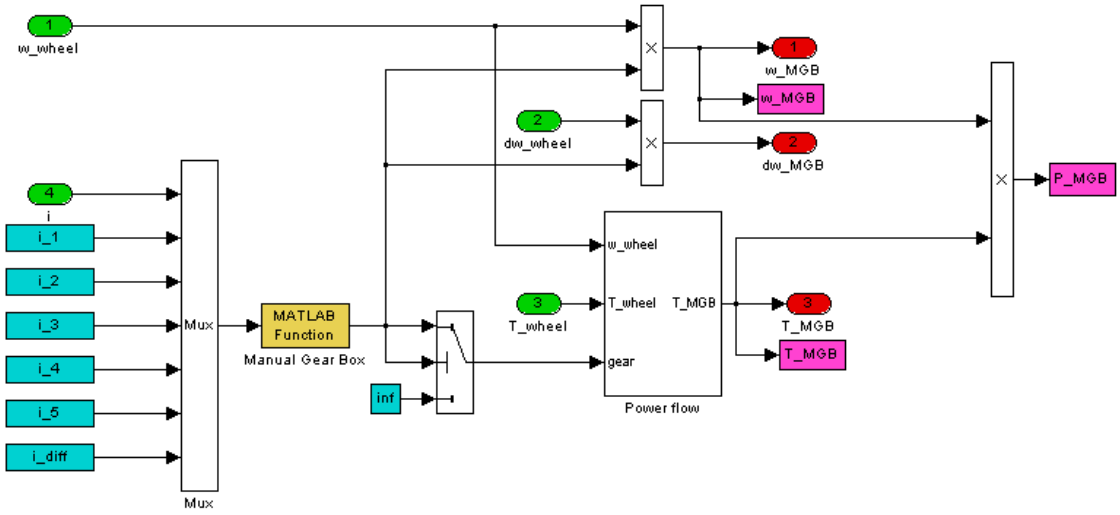

Fig 5.5 Top level of the block "Manual Gear Box"

5.4.2 Single epicyclic gearbox model

The layout of a single epicyclic gearbox is shown in Fig 5.6.

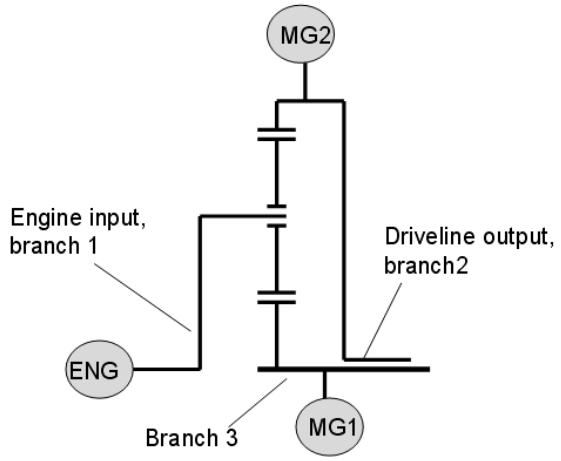

Fig 5.6 Single epicyclic gearbox as used in the Toyota Prius – also referred to as a 3 branch system

The power flow of the single epicyclic gearbox is shown is Fig 5.7. MG1, which is mainly used as a generator and MG2, which is mainly used as a motor, are connected to the battery, taking or saving electricity from or to the battery. The power of the engine is split into two ways: to the wheel via the ring gear, and to the MG1. The vehicle can be driven on engine alone, the MG2 alone, or both, depending on the power required and state of charge (SOC) of the battery.

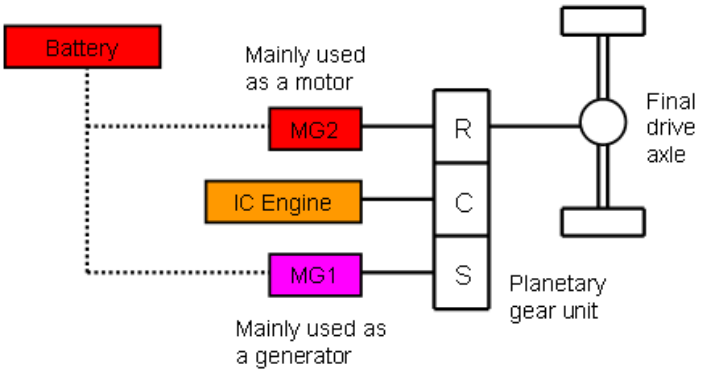

Fig 5.7 Power flow of the single epicyclic system

As described previously in Chapter 3, the speed and torque relations of the 3 branch system are:

Speed relationships:

$$n_{mg1} = 3.6n_e - 2.6n_{dl} \tag{5.1}$$

$$n_{mg2} = n_{dl} \tag{5.2}$$

Torque relationships:

$$T_{mg1} = -(5/18)T_e \tag{5.3}$$

$$T_{mg2} = -(13/18)T_e - T_{dl} \tag{5.4}$$

The speed and torque for each element under different operation modes are calculated based on the above equations. The equations for torques do not take losses into consideration at the moment. In the whole simulation model, the transmission loss is taken into consideration for each specific input speed and torque. The efficiency for each gear pair is set to be 98.5%. The accelerations of each element, represented as dn_e , dn_{mg1} and dn_{mg2} , are also taken into consideration. The relations of acceleration are simply derived from the relations of the rotation speed.

- **Mode 1: Motor alone mode (silent operation, battery-EV)**

When the vehicle speed is low and there is enough electricity is the battery, the engine can be shut off and the vehicle driven purely by electric motor. In Miller's analysis (Miller and Miller 2005), the engine-off-speed is 30 mph; in Mi's study (Mi,

Zhang et al. 2003), the speed is 35 mph. In this research, the engine-cut-off speed is set to be 35mph. In this mode, electricity is supplied to MG2, and MG1 is locked. Because the engine is off, the car runs quietly. So this mode is often also referred to as ‘silent mode’. Of course, this situation would also occur if the car runs out of fuel, and the energy in the battery is used as an emergency to get to a gas station.

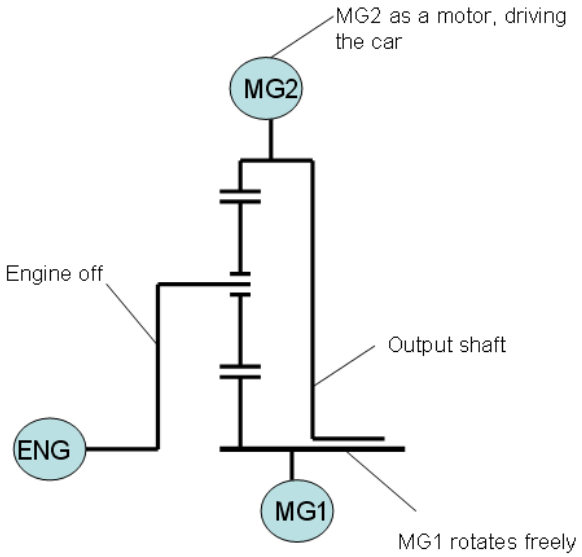

Fig 5.8 Mode 1: Motor alone

Output speed and torque for all elements are shown in equation group (5.5) :

$$
\begin{aligned}
&n_e = 0 \\
&dn_e = 0 \\
&T_e = 0 \\
\\
&n_{mg2} = n_{dl} \\
&dn_{mg2} = dn_{dl} \\
&T_{mg2} = T_{dl} \\
\\
&n_{mg1} = 0 \\
&dn_{mg1} = 0 \\
&T_{mg1} = 0
\end{aligned}
\qquad (5.5)
$$

- **Mode 2: Combined power (electric boost)**

When accelerating at low speeds in normal operation, the engine turns more rapidly than the wheels but does not develop sufficient torque. The extra engine

speed is fed to MG1 acting as a generator. The electricity from MG1 is fed to MG2, which acts as a motor and adds torque at the driveshaft.

When hard acceleration is needed or on an uphill road, if engine has insufficient power to meet the road load, extra power from the battery will be added via MG2. In this case, there are two sources of electricity for MG2: from MG1 and from the battery.

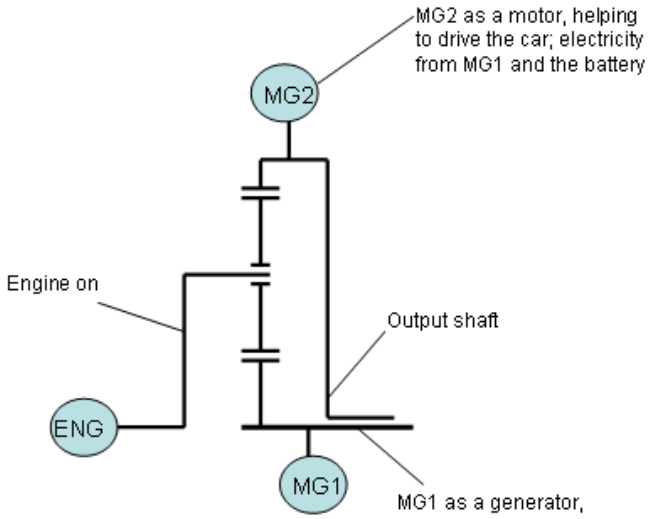

Fig 5.9 Mode 2: Combined power

Output speed and torque for all elements are shown in equation group (5.6):

$$
\begin{aligned}
&n_e = n_{e1} \\
&dn_e = (n_e / n_{dl}) dn_{dl} \\
&T_e = T_{e1} \\
\\
&n_{mg2} = n_{dl} \\
&dn_{mg2} = dn_{dl} \\
&T_{mg2} = T_{dl} - (13/18) T_{e1} \\
\\
&n_{mg1} = 3.6 * n_e - 2.6 * n_{dl} \\
&dn_{mg1} = 3.6 * dn_e - 2.6 * dn_{dl} \\
&T_{mg1} = (1/3.6) T_e
\end{aligned}
\qquad (5.6)
$$

- **Mode 3: Cruise mode (normal driving)**

Cruise mode is used when the vehicle is cruising at high speed. At this time the engine turns more slowly than the wheels but develops more torque than needed.

MG2 then runs as a generator to direct the excess engine torque, producing power that is fed to MG1 acting as a motor to increase the wheel speed.

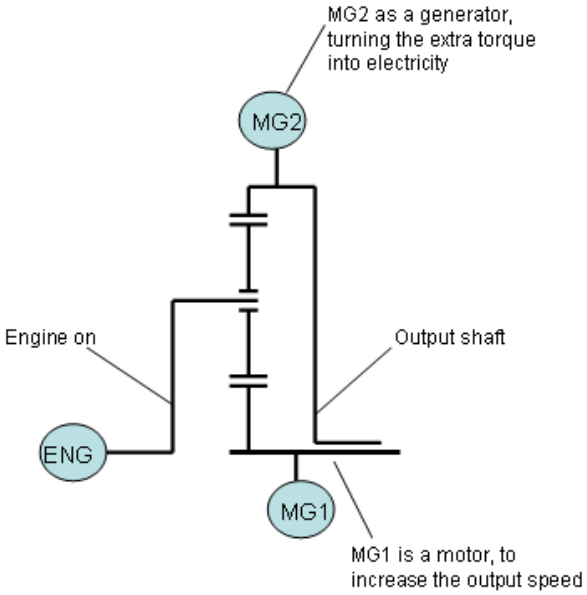

Fig 5.10 Mode 3: Cruise mode

Output speed and torque for all elements are shown in equation group (5.7):

$$
\begin{aligned}
&n_e = n_{e1} \\
&dn_e = (n_e / n_{dl})dn_{dl} \\
&T_e = T_{e1} \\
\\
&n_{mg2} = n_{dl} \\
&dn_{mg2} = dn_{dl} \\
&T_{mg2} = (2.6/3.6)T_{e1} - T_{dl} \\
\\
&n_{mg1} = 3.6 * n_e - 2.6 * n_{dl} \\
&dn_{mg1} = 3.6 * dn_e - 2.6 * dn_{dl} \\
&T_{mg1} = (1/3.6)T_e
\end{aligned}
\tag{5.7}
$$

- **Mode 4: Engine alone mode**

In this mode, MG2 rotates freely, and MG1 is locked. All the power of the engine is transmitted to the driveline. The HEV operates in this mode when the SOC of the battery is too low, so no electric machine should be used, or SOC is too high, so there is no need to charge the battery.

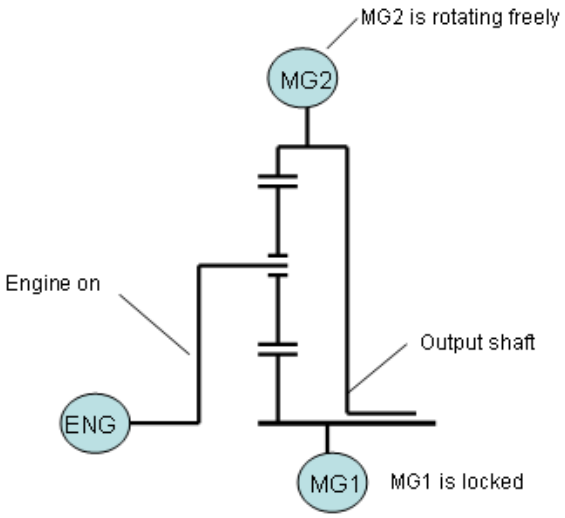

Fig 5.11 Mode 4: Engine alone

Output speed and torque for all elements are shown in equation group (5.8):

$$
\begin{aligned}
n_e &= (13/18) n_{dl} \\
dn_e &= (n_e / n_{dl}) dn_{dl} \\
T_e &= (18/13) T_{dl} \\
\\
n_{mg2} &= 0 \\
dn_{mg2} &= 0 \\
T_{mg2} &= 0 \\
\\
n_{mg1} &= 0 \\
dn_{mg1} &= 0 \\
T_{mg1} &= 0
\end{aligned}
\qquad (5.8)
$$

- **Mode 5: Regenerative braking**

When the vehicle is braking, if the battery is not fully charged, MG2, as a generator, will absorb the energy and use it to charge the battery. The practical difficulty is in blending the braking torque obtained via regenerative braking with the braking demanded by the driver through the brake pedal. The driver would prefer to have a seamless transmission between regenerative braking and application of the normal vehicle brakes for more severe stops. In this case, MG1 rotates freely.

Brake blending for HEVs and EVs is an important feature of driveability and is a topic for further research work in future.

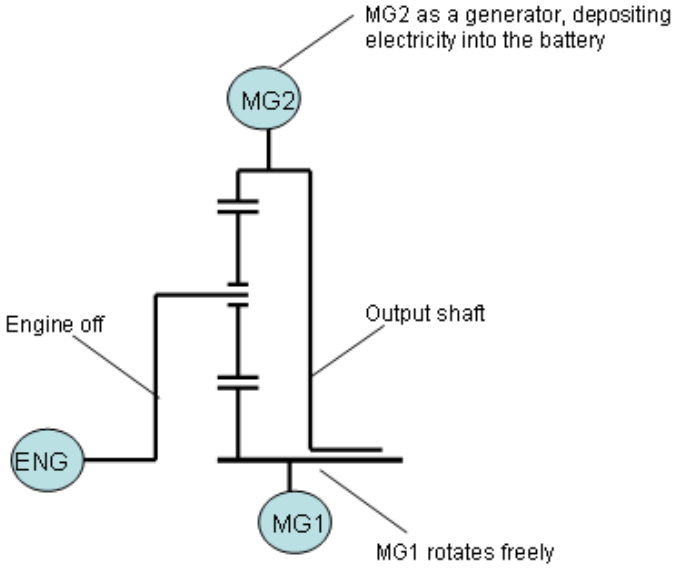

Fig 5.12 Mode 5: Regenerative braking

Output speed and torque for all elements are shown in equation group (5.9):

$$
\begin{aligned}
&n_e = 0 \\
&dn_e = 0 \\
&T_e = 0 \\
\\
&n_{mg2} = n_{dl} \\
&dn_{mg2} = dn_{dl} \\
&T_{mg2} = Min(T_{dl}, \text{interp1}(\omega_{mg2\_row}, T_{mg2\_\max}, \omega_{mg2})) \\
\\
&n_{mg1} = 0 \\
&dn_{mg1} = 0 \\
&T_{mg1} = 0
\end{aligned}
\qquad (5.9)
$$

where ω_{mg2_row} is the speed of MG2 and $T_{mg2\_\max}$ is the maximum torque of MG2.

- **Mode 6: Mechanical braking**

If the battery is fully changed then acts MG2 as a generator, absorbs the energy, generating electricity and shunt it to MG1. MG1 acts as a motor driving the engine rapidly forward. The purpose of using MG2 to draw power to MG1 is to reduce the

load for the normal compression braking. So the size of the brake can be downsized and brake linings last longer than for most cars of similar mass.

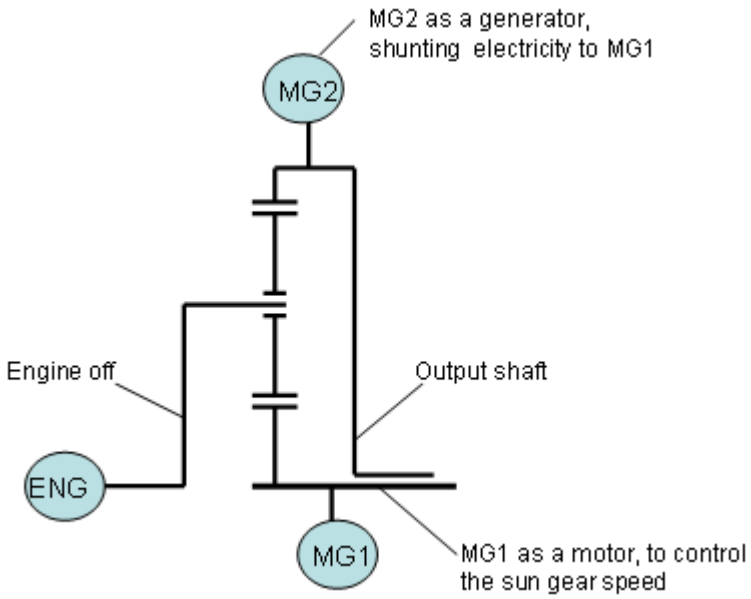

Fig 5.13 Mode 6: Mechanical braking

Output speed and torque for all elements are shown in equation group (5.10). The speeds and the torques of MG1 and MG2 are all set to be zero, because no electricity is saving or taking from the battery.

$$
\begin{aligned}
&n_e = 0 \\
&dn_e = 0 \\
&T_e = 0 \\
\\
&n_{mg2} = 0 \\
&dn_{mg2} = 0 \\
&T_{mg2} = 0 \\
\\
&n_{mg1} = 0 \\
&dn_{mg1} = 0 \\
&T_{mg1} = 0
\end{aligned}
\qquad (5.10)
$$

- **Mode 7: Standstill charge mode**

The single epicyclic gearbox can be designed to charge the battery when the vehicle is stationary, by running the engine and generating electricity from MG1.

The engine operation point will be arranged according to the efficiency of both MG1 and the engine itself. In this study, the engine speed and torque are set to be 1000 rpm and 90 Nm.

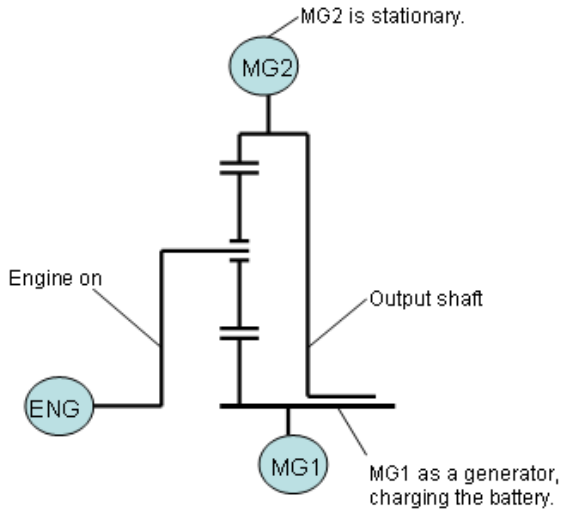

Fig 5.14 Mode 7: Standstill charge

Output speed and torque for all elements are shown in equation group (5.11):

$$
\begin{aligned}
&n_e = 200 \\
&dn_e = 0 \\
&T_e = 90 \\
\\
&n_{mg2} = 0 \\
&dn_{mg2} = 0 \\
&T_{mg2} = 0 \\
\\
&n_{mg1} = 3.6 * n_e \\
&dn_{mg1} = 0 \\
&T_{mg1} = (1/3.6) T_e
\end{aligned}
\qquad (5.11)
$$

- **Mode 8: Driving charge**

When driving at high speed, if the battery state of charge is lower than certain level, say, 50%, the engine will operate at the maximum power area. Both MG2 and MG1 act as generators, turning the extra power into electricity to charge the

battery. In this case the engine does not necessarily work in the highest efficiency area.

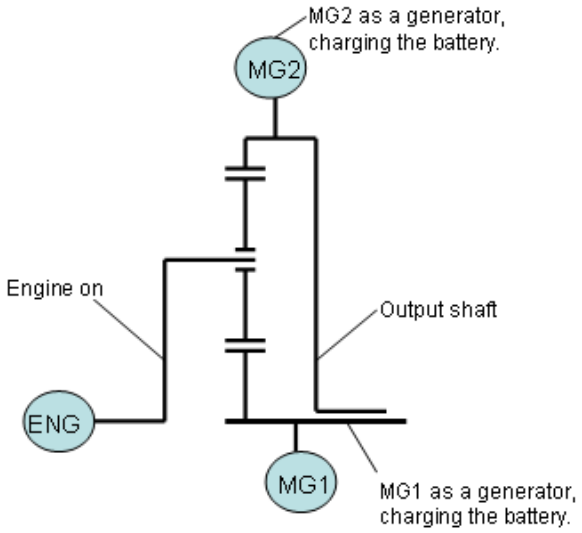

Fig 5.15 Mode 8: Driving charge

The output speed and torque for all elements are shown in equation group (5.12):

$$
\begin{aligned}
n_e &= n_{e1} \\
dn_e &= (n_e / n_{dl}) dn_{dl} \\
T_e &= \text{interp1}(w_{eng\_\max}, T_{eng\_\max}, w_e)
\end{aligned}
$$

where $w_{eng\_\max}$ is engine maximum rotation speed and $T_{eng\_\max}$ is the engine maximum torque.

$$
\begin{aligned}
n_{mg2} &= n_{dl} \\
dn_{mg2} &= dn_{dl} \\
T_{mg2} &= -(T_e * 0.72 + T_{dl}) \\
\\
n_{mg1} &= 3.6 * n_e - 2.6 * n_{dl} \\
dn_{mg1} &= 3.6 * dn_e - 2.6 * dn_{dl} \\
T_{mg1} &= -(1/3.6) T_e
\end{aligned}
\qquad (5.12)
$$

5.4.3 Twin epicyclic gearbox model

The layout of the twin epicyclic gearbox is shown in Fig 5.16. The structure is taken from one of patented designs from (Moeller 2005). Compared to the single epicyclic gearbox, the twin epicyclic gearbox has two epicyclic gearsets. The carrier of the first epicyclic gearset is connected to the engine input and the carrier

of the second epicyclic gearset is connected to the driveline output. The purpose of adding one more epicyclic gearset is to give the system more flexibility of controlling the speeds and torques of MG1 and MG2.

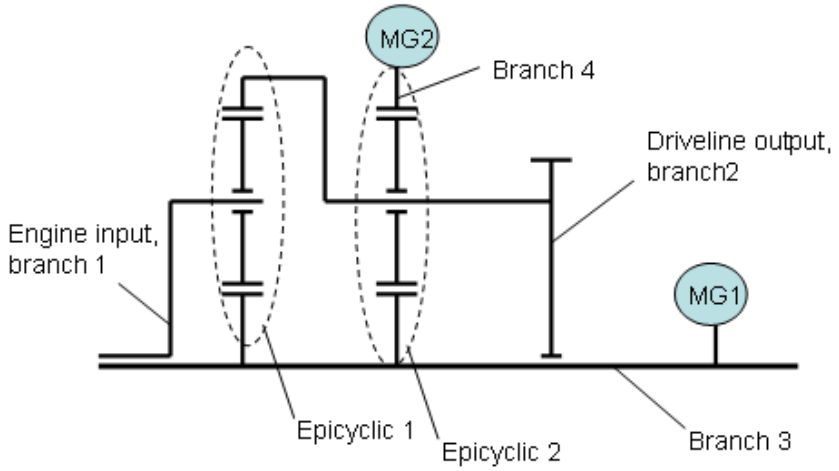

Fig 5.16 Twin epicyclic gearbox as proposed by NexxtDrive - also referred to as a four branch system

The power flow of the twin epicyclic gearbox is shown in Fig 5.17. As before, MG1 is mainly used as a generator and MG2 is mainly used as a motor; both are connected to the battery, taking or saving electricity from or to the battery. The power of the engine is split into two ways: to the wheel via the ring gear, and to the MG1. The vehicle can be driven on engine alone, the MG2 alone, or combined power, depending on the power required and state of charge (SOC) of the battery.

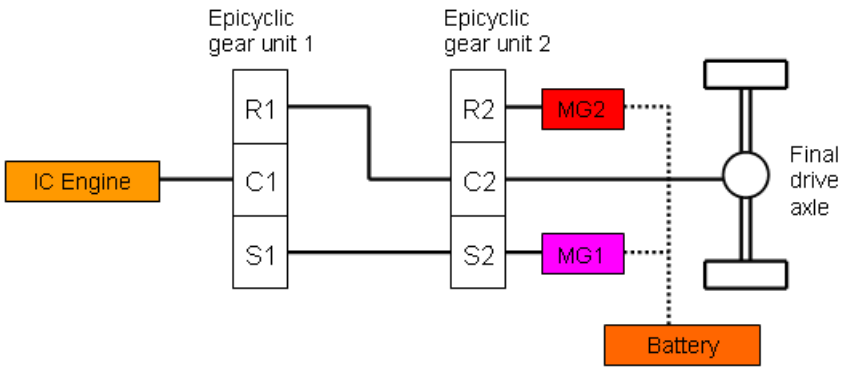

Fig 5.17 Power flow of the dual epicyclic system

Following on from the results in Chapter 3, the speed and torque equations of the dual epicyclic gearbox are:

Speed equations:

$$n_{mg1} + (18/13) * n_e - (31/13) * n_{dl} = 0 \quad (5.13)$$

$$n_{mg2} - (18/5) * n_e - (13/5) * n_{dl} = 0 \quad (5.14)$$

Torque equations:

$$T_{mg1} + (169/324) * T_e + (13/18) * T_{dl} = 0 \quad (5.15)$$

$$T_{mg2} + (155/324) * T_e + (5/18) * T_{dl} = 0 \quad (5.16)$$

The speed and torque for each element of the 4 branch system under different operation mode are calculated based on the above equations. Again, the equations for torques do not take individual losses into consideration at the moment. In the whole simulation model, the transmission loss is taken into consideration for each specific input speed and torque. The efficiency for each gear pair is set to be 98.5%. By doing this, any additional losses of the twin epicyclic gearbox due to the increased number of gear pairs compared to the single epicyclic gearbox are taken in to consideration. Again, the accelerations of each element are represented as $d\omega_e$, $d\omega_{mg1}$ and $d\omega_{mg2}$.

The detailed description of each operation mode for the 4 branch system, some aspects of which are similar to the 3 branch system, will not be repeated again in the following text. Only the differences will be mentioned.

- **Mode 1: Motor alone mode (silent operation, Battery-EV)**

This mode is used when the vehicle starts from stationary and the speed is lower than 35 mph. The engine is shut down, and MG1 is locked. Electricity is supplied to MG2 to drive the car. In this mode, the vehicle is running purely on electricity, so it also called the battery EV mode, or silent mode operation.

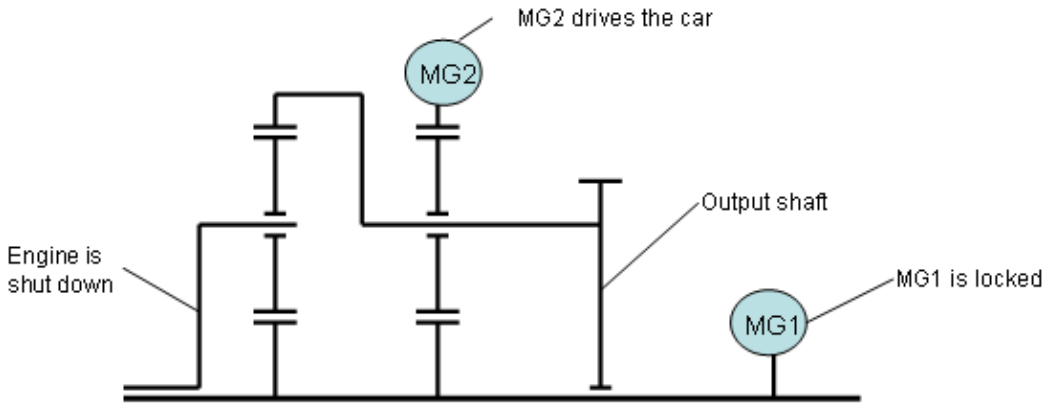

Fig 5.18 Mode 1: Motor alone

The output speed and torque for all elements are shown in equation group (5.17):

$$
\begin{aligned}
&n_e = 0 \\
&dn_e = 0 \\
&T_e = 0 \\
\\
&n_{mg2} = (18/13)n_{dl} \\
&dn_{mg2} = (18/13)dn_{dl} \\
&T_{mg2} = (13/18)T_{dl} \\
\\
&n_{mg1} = 0 \\
&dn_{mg1} = 0 \\
&T_{mg1} = 0
\end{aligned}
\tag{5.17}
$$

- **Mode 2: Combined power (electric boost)**

When accelerating or driving on the uphill road, both the engine and MG2 are driving the vehicle. MG1 is a generator, supplying electricity to MG2. If more power is needed, the battery will supply electricity to MG2 as well.

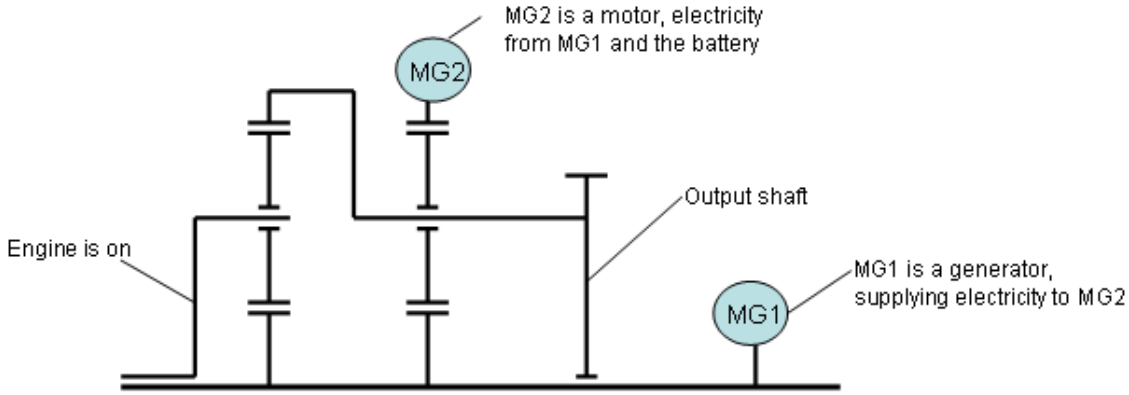

Fig 5.19 Mode 2: Combined power

The output speed and torque for all elements are shown in equation group (5.18):

$$
\begin{aligned}
&n_e = n_{e1} \\
&dn_e = (n_e / n_{dl})dn_{dl} \\
&T_e = T_{e1}
\end{aligned}
$$

$$
\begin{aligned}
&n_{mg2} = -(18/13)n_e + (31/13)n_{dl} \\
&dn_{mg2} = -(18/13)dn_e + (31/13)dn_{dl} \\
&T_{mg2} = -(169/324)T_e - (31/13)T_{dl}
\end{aligned}
$$

$$
\begin{aligned}
&n_{mg1} = 3.6 * n_e - 2.6 * n_{dl} \\
&dn_{mg1} = 3.6 * dn_e - 2.6 * dn_{dl} \\
&T_{mg1} = -(155/324)T_e - (5/18)T_{dl}
\end{aligned}
\qquad (5.18)
$$

- **Mode 3: Cruise mode (Normal driving)**

When the vehicle is cruising at high speed, the engine is controlled to run at a lower speed and higher torque than would be the case for a conventional geared car. In this case, MG1 is controlled as a motor to change the gear ratio and increase the output speed. MG2 acts a generator to absorb the extra torque and supply electricity to the battery and MG1.

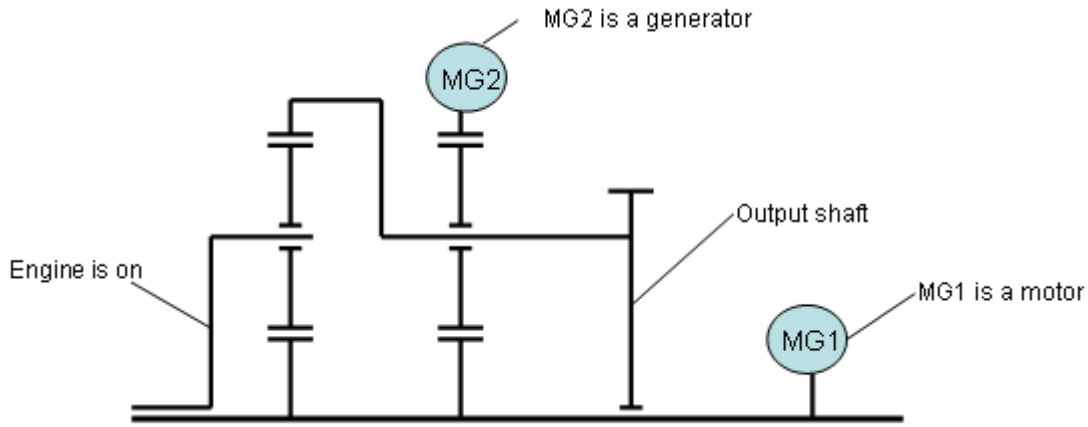

Fig 5.20 Mode 3: Cruise mode

The output speed and torque for all elements are shown in equation group (5.19):

$$
\begin{aligned}
&n_e = n_{e1} \\
&dn_e = (n_e / n_{dl}) dn_{dl} \\
&T_e = T_{e1} \\
\\
&n_{mg2} = -(18/13) n_e + (31/13) n_{dl} \\
&dn_{mg2} = -(18/13) dn_e + (31/13) dn_{dl} \\
&T_{mg2} = -(169/324) T_e - (31/13) T_{dl} \\
\\
&n_{mg1} = 3.6 * n_e - 2.6 * n_{dl} \\
&dn_{mg1} = 3.6 * dn_e - 2.6 * dn_{dl} \\
&T_{mg1} = -(155/324) T_e - (5/18) T_{dl}
\end{aligned}
\qquad (5.19)
$$

- **Mode 4: Engine alone mode**

When the battery SOC is too low or too high, the vehicle will drive only on engine. In this mode, MG1 is locked and MG2 rotates freely. The dual epicyclic system actually turns into a single epicyclic system.

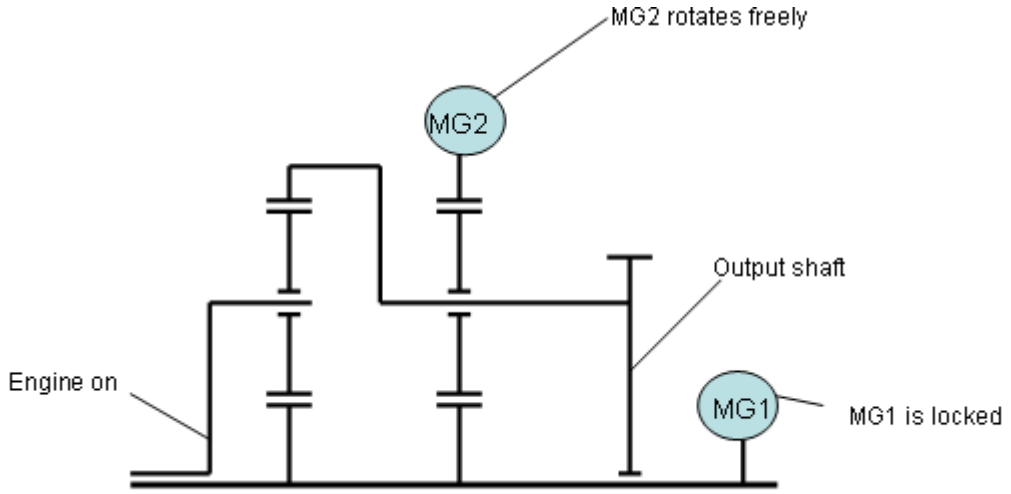

Fig 5.21 Mode 4: Engine alone

Output speed and torque for all elements are shown in equation group (5.20):

$$
\begin{aligned}
n_e &= (13/18)n_{e1} \\
dn_e &= (n_e / n_{dl})dn_{dl} \\
T_e &= (18/13)T_{e1} \\
\\
n_{mg2} &= 0 \\
dn_{mg2} &= 0 \\
T_{mg2} &= 0 \\
\\
n_{mg1} &= 0 \\
dn_{mg1} &= 0 \\
T_{mg1} &= 0
\end{aligned}
\qquad (5.20)
$$

- **Mode 5: Regenerative braking**

In this mode, the system acts in similar manner to the single epicyclic system, with MG1 locked and MG2 supplying power to the battery.

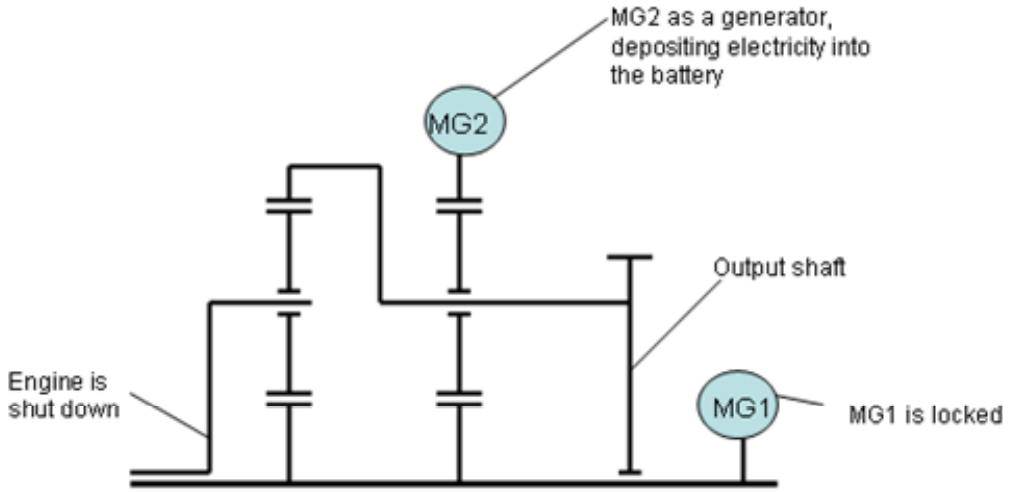

Fig 5.22 Mode 5: Regenerative braking

The output speed and torque for all elements are shown in equation group (5.21):

$$
\begin{aligned}
&n_e = 0 \\
&dn_e = 0 \\
&T_e = 0 \\
\\
&n_{mg2} = n_{dl} \\
&dn_{mg2} = dn_{dl} \\
&T_{mg2} = -Min(T_{dl}, \text{int}erp1(\omega_{mg2\_row}, T_{mg2\_\max}, \omega_{mg2})) \\
&n_{mg1} = 0 \\
&dn_{mg1} = 0 \\
&T_{mg1} = 0
\end{aligned}
\tag{5.21}
$$

where ω_{mg2_row} is the speed of MG2 and $T_{mg2\_\max}$ is the maximum torque of MG2.

- **Mode 6: Mechanical brake**

If the battery is full, no electricity is needed to be saved to the battery. But the MG2 will still act as a generator to absorb the energy from the rotating wheel. The electricity will be shunt to MG1, which dissipating the electricity by turning the engine. When the maximum torque MG2 can provide less than the needed brake torque, the convention bake on the car will provide the rest of it. The purpose of this is to absorb the braking energy as much as possible, thus to reduce the size or the normal brake and to prolong the life of the normal brake.

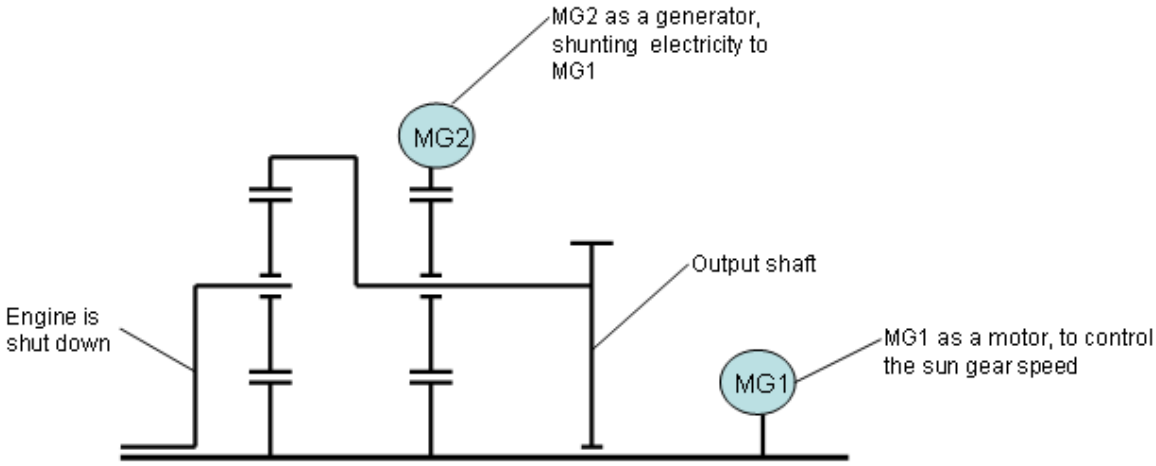

Fig 5.23 Mode 6: Mechanical brake

The output speed and torque for all elements are shown in equation group (5.22). The speeds and the torques of MG1 and MG2 are all set to be zero, because no electricity is saving or taking from the battery.

$$
\begin{aligned}
&n_e = 0 \\
&dn_e = 0 \\
&T_e = 0 \\
&n_{mg2} = 0 \\
&dn_{mg2} = 0 \\
&T_{mg2} = 0 \\
&n_{mg1} = 0 \\
&dn_{mg1} = 0 \\
&T_{mg1} = 0
\end{aligned}
\tag{5.22}
$$

- **Mode 7: Standstill charge mode**

For a 3 branch system, MG2 is connected to the output shaft, which means it can not move when the vehicle is stationary. So in the standstill mode, only MG1 can be used as a generator. This limitation does not exist for a 4 branch system. Both the two electric machines can be used as generators, charging the battery more quickly.

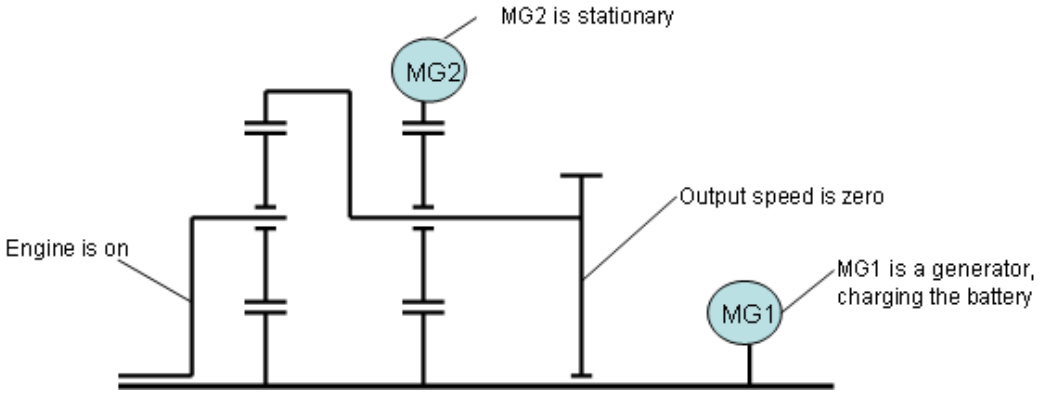

Fig 5.24 Mode 7: Standstill charge

Output speed and torque for all elements are shown in equation group (5.23):

$$
\begin{aligned}
&n_e = 200 \\
&dn_e = 0 \\
&T_e = 90 \\
&n_{mg2} = -(18/13)n_e \\
&dn_{mg2} = -(18/13)dn_e \\
&T_{mg2} = 0.78 * T_e \\
&n_{mg1} = 3.6 * n_e \\
&dn_{mg1} = 0 \\
&T_{mg1} = (1/3.6)T_e
\end{aligned}
\tag{5.23}
$$

- **Mode 8: Driving charge**

For most normal driving, the control strategy for the HEV system attempts to operate the ICE in an optimum efficiency area and it manages MG1 and MG2 within the battery SOC constraints to achieve this – often this means operating the ICE at a higher torque and lower speed than for conventional geared vehicles. However, if the battery SOC becomes too low, the engine power will be increased such that both MG1 and MG2 might generate electrical power to charge the battery.

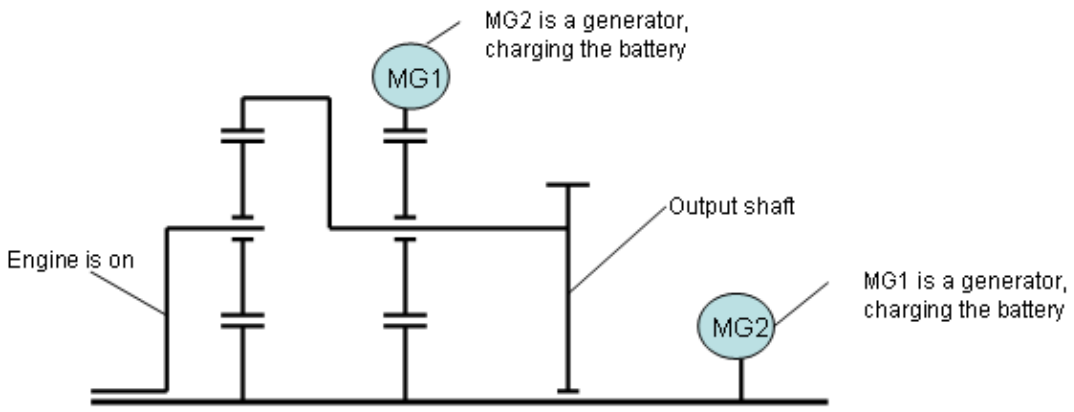

Fig 5.25 Mode 8: Driving charge

Output speed and torque for all elements are shown in equation group (5.24):

$$
\begin{aligned}
n_e &= n_{e1} \\
dn_e &= (n_e / n_{dl}) dn_{dl} \\
T_e &= \text{interp1}(w_{eng\_\max}, T_{eng\_\max}, w_e)
\end{aligned}
$$

where $w_{eng\_\max}$ is engine maximum rotation speed and $T_{eng\_\max}$ is the engine maximum torque.

$$
\begin{aligned}
n_{mg2} &= -(18/13) n_e + (31/13) n_{dl} \\
dn_{mg2} &= -(18/13) dn_e + (31/13) dn_{dl} \\
T_{mg2} &= -(169/324) T_e - (31/13) T_{dl}
\end{aligned}
$$

$$
\begin{aligned}
n_{mg1} &= 3.6 * n_e - 2.6 * n_{dl} \\
dn_{mg1} &= 3.6 * dn_e - 2.6 * dn_{dl} \\
T_{mg1} &= -(155/324) T_e - (5/18) T_{dl}
\end{aligned}
\qquad (5.24)
$$

- **Mode 9: High efficiency mode**

This is a mode that a single epicyclic system does not have. As shown in Fig 3.8, the twin epicyclic system has one more node point when the transmission ration is 1.72. When the vehicle is cruising at high speed, with the speeds of MG1 and MG2 controlled in the reasonable range, the transmission ratio is set to be 1.72 to get higher transmission efficiency. In this mode, MG1 is a motor and MG2 is a generator, which are the same as in mode 3.

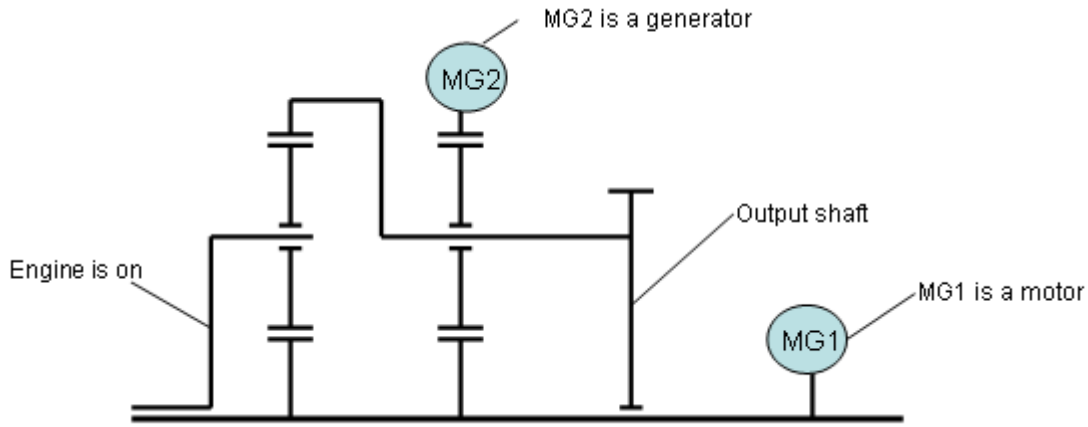

Fig 5.26 Mode 9: High efficiency mode

Output speed and torque for all elements are shown in equation group (5.25):

$$n_e = 200$$
$$dn_e = 0$$
$$T_e = \text{interp1}(\omega_{eng\_best}, T_{eng\_best}, w_{eng})$$

where ω_{eng_best} is the engine's rotation speed and T_{eng_best} is the engine's best efficiency torque.

$$n_{mg2} = 0$$
$$dn_{mg2} = 0$$
$$T_{mg2} = 0$$

$$n_{mg1} = 2.09 * n_e$$
$$dn_{mg1} = 0$$
$$T_{mg1} = -(155/324)T_e - (5/18)T_{dl} \quad (5.25)$$

5.5 Motor and generator model

In this study, both MG1 and MG2 can be used in 4 quadrants; this means they can act either as a motor or generator in both the positive and negative rotation directions. Within the motor quadrants, the electric power required can be expressed as:

$$P_{EM} = \omega_{EM} \cdot T_{EM} \cdot \frac{1}{\eta_{EM}(\omega_{EM}, T_{EM})} \quad (5.26)$$

While in the generator quadrants, the power generated can be expressed as:

$$P_{EM} = \omega_{EM} \cdot T_{EM} \cdot \eta_{EM}(\omega_{EM}, T_{EM}) \tag{5.27}$$

In QSS, it combines the two cases into a single efficiency map to avoid having to keeping distinguishing between the two cases. This causes a fundamental flaw which may make the simulation results not precise enough. When calculating the interpolation to get the motor efficiency, it is possible to obtain unrealistically high efficiency points around the zero torque area, which is obviously not correct, as shown in Fig 5.27.

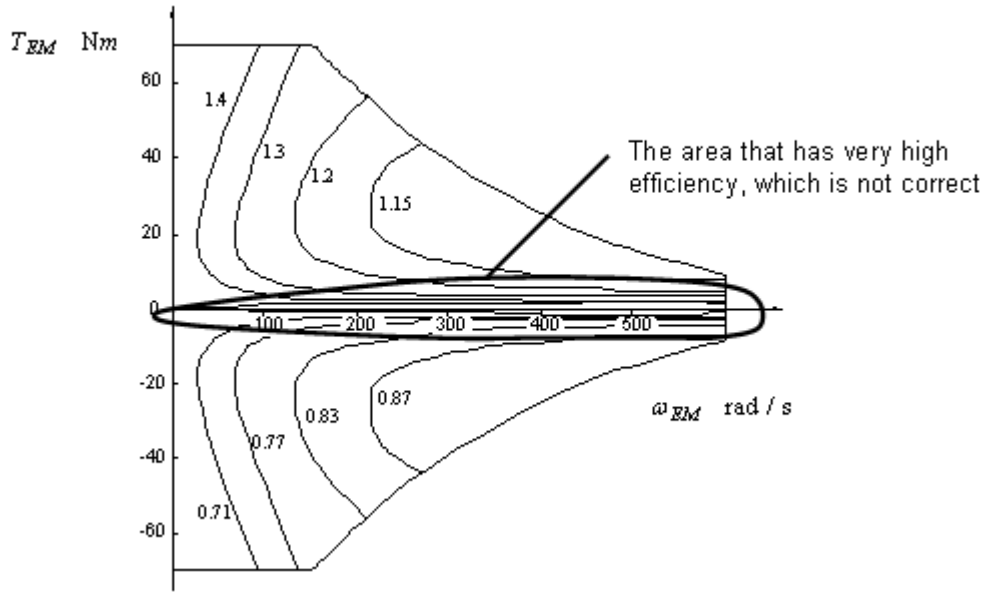

Fig 5.27 A flaw in QSS motor/generator model

In this study, models for MG1 and MG2 with separate motor and generator quadrants were built, using S-function blocks. The top view of the MG2 model is shown in Fig 5.28. The MG1 and MG2 efficiency maps are shown in Fig 5.29 and Fig 5.30.

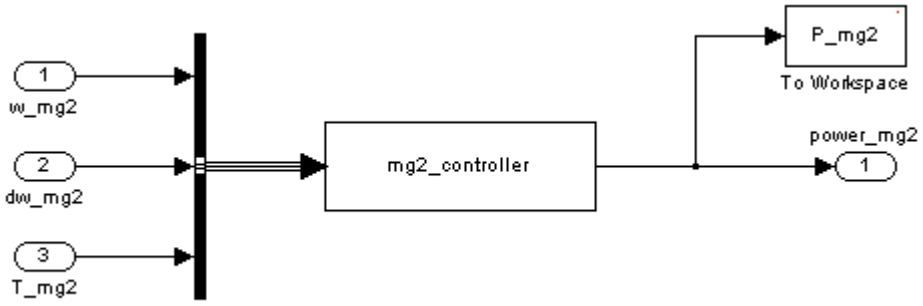

Fig 5.28 Top view of MG2 model

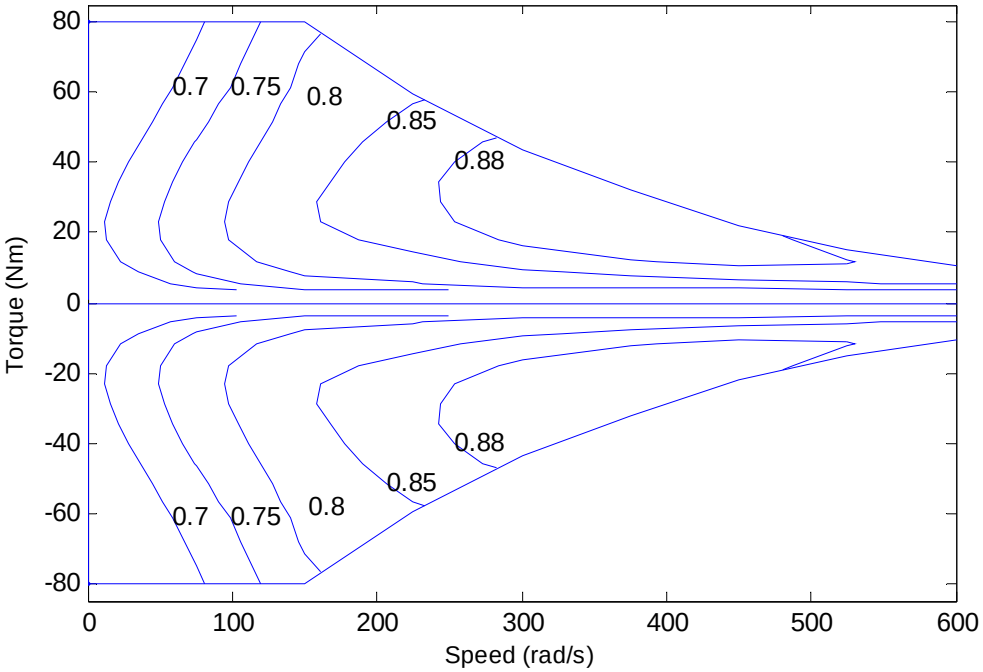

Fig 5.29 MG1 efficiency map

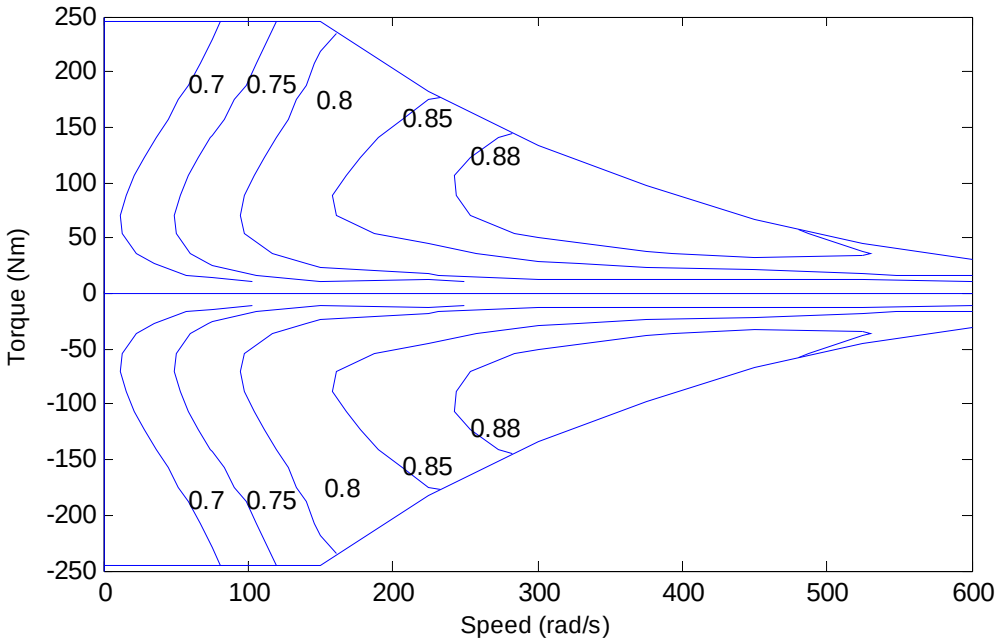

Fig 5.30 MG2 efficiency map

5.6 Control strategy

The advantages and disadvantages of different control strategies for hybrid vehicle have been discussed in Chapter 2. In this research, the rule based control strategy will be used in the modeling and simulation.

The data flow for the 2 HEV models is shown in Fig 5.31. During the whole driving cycle, for each sampling time, the driveline speed and torque (w_dl and T_dl respectively) can be calculated from the current vehicle speed and acceleration. The pre-selected engine speed and engine torque (w_e1 and T_e1 respectively) are decided from the combined consideration of power required and engine best efficiency curve. According to the current vehicle speed, acc, engine speed and torque, driveline speed and torque, and the battery State of Change (SOC), the CVT controller will decide the driving mode, and speed and torque for each element, include MG1, MG2 and the engine. Then, the results for current fuel consumption and updated battery SOC can be obtained. In the model, the acceleration of MG1, MG2 and engine are also taken into consideration, because they are related to the energy consumption or energy generation.

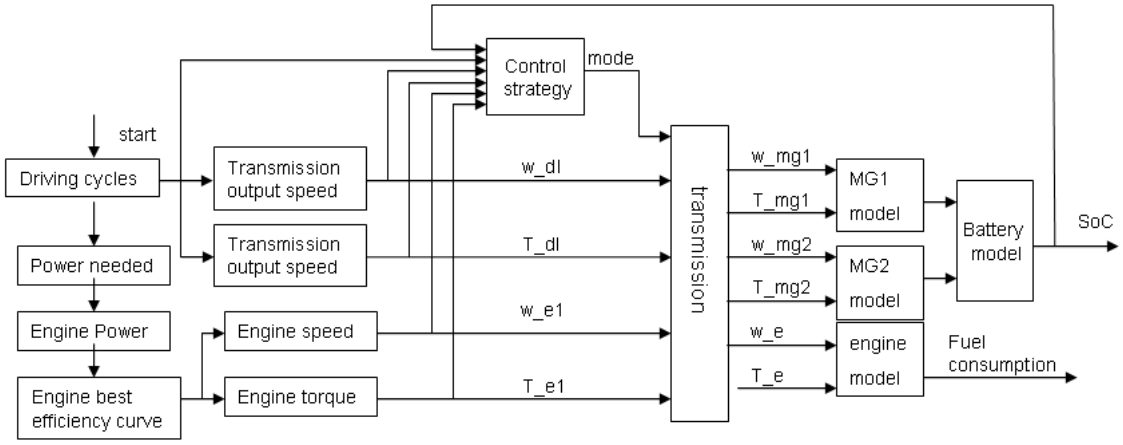

Fig 5.31 Data flow for HEV models

In this study, there are 8 driving modes which are used during the simulation for the HEV with the single epicyclic system:

1. Mode 1 : Motor alone mode
2. Mode 2: Combined power
3. Mode 3: Ccruise mode
4. Mode 4: Engine alone mode
5. Mode 5: Regeneration braking
6. Mode 6: Mechanical braking
7. Mode 7: Standstill charge
8. Mode 8: Driving charge

In the simulation, the SOC is controlled to remain within a reasonable range: for example, 0.6-0.75 as selected by (Mashadi and Emadi 2009). Because the engine is kept working in the most efficient area, then, if the required power is low, the extra energy will be used to charge the battery. So the final SOC maybe higher or lower than the initial SOC, depending on the demand of the driving cycles. This important factor is allowed for later in the overall energy or fuel consumption results.

The control strategy to decide the driving mode for the HEV with single epicyclic system is shown in Fig 5.33.

For the HEV with the twin epicyclic system, one more mode is added: high efficiency mode. This is because for a twin epicyclic system, there is one more point that the speed of one of the motor/generator is zero (Fig 5.32). This means that at this point, less power is transmitted via the electrical route. To make full use of this, when the transmission ratio fall within the range 1.5 to 2, MG2 is locked, and the speed of the engine and MG1 are adjusted to make the transmission ratio to be 1.72. In this mode, less power is converted into electricity and the whole efficiency of the powertrain is higher.

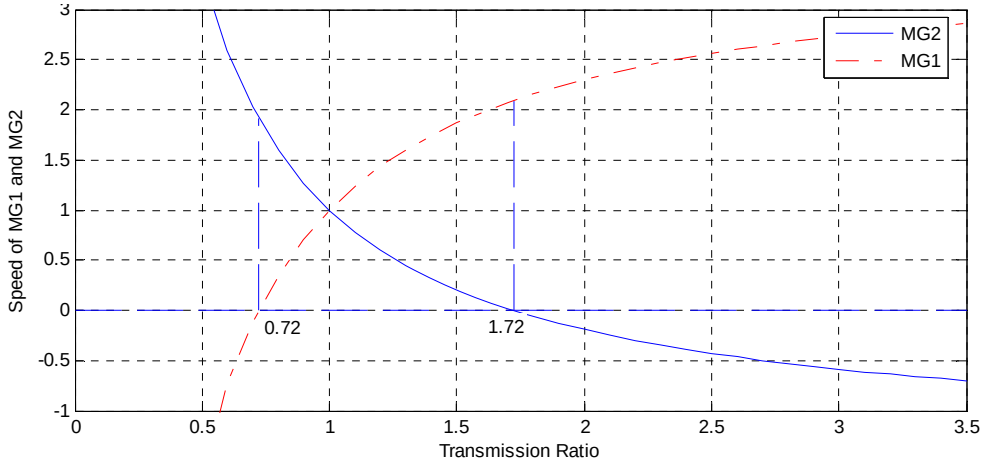

Fig 5.32 Relationship of transmission ratio and motor generator speeds for the twin epicyclic system

The condition for the high efficiency mode to be used is $58 < n_{dl} < 166.8$. T is the procedure to describe this condition is as follows:

For MG1, best speed range is 150 to 600 rad/s

$$150 < n_{mg1} < 600 \tag{5.28}$$

$$\frac{n_{mg1}}{n_e} = 2.09 \tag{5.29}$$

$$71.77 < n_e < 287.08 \tag{5.30}$$

To ensure the engine always works around the optimum efficiency area:

$$100 < n_e < 287.08 \tag{5.31}$$

$$\frac{n_{dl}}{n_e} = 1.72 \tag{5.32}$$

$$58 < n_{dl} < 166.8 \tag{5.33}$$

Hence, there are 9 driving modes used during the simulation for the HEV with the twin epicyclic system:

1. Mode 1 : Motor alone mode
2. Mode 2: Combined power
3. Mode 3: Cruise mode
4. Mode 4: Engine alone mode
5. Mode 5: Regeneration braking
6. Mode 6: Mechanical braking
7. Mode 7: Standstill charge
8. Mode 8: Driving charge
9. Mode 9: High efficiency mode

The control strategy to decide the driving mode for the HEV with twin epicyclic system is shown in Fig 5.34.

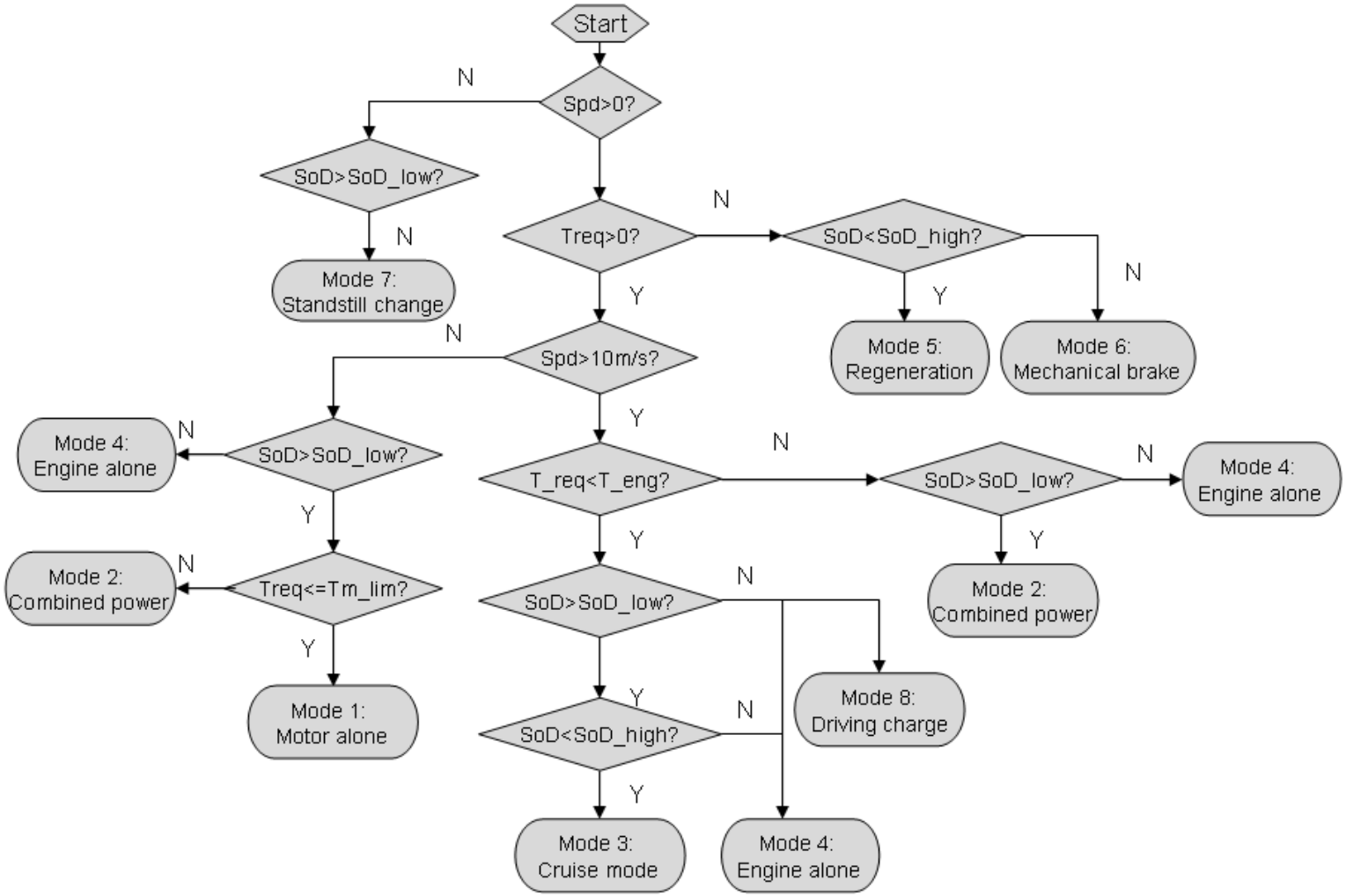

Fig 5.33 Rule based control strategy for HEV with a single epicyclic transmission

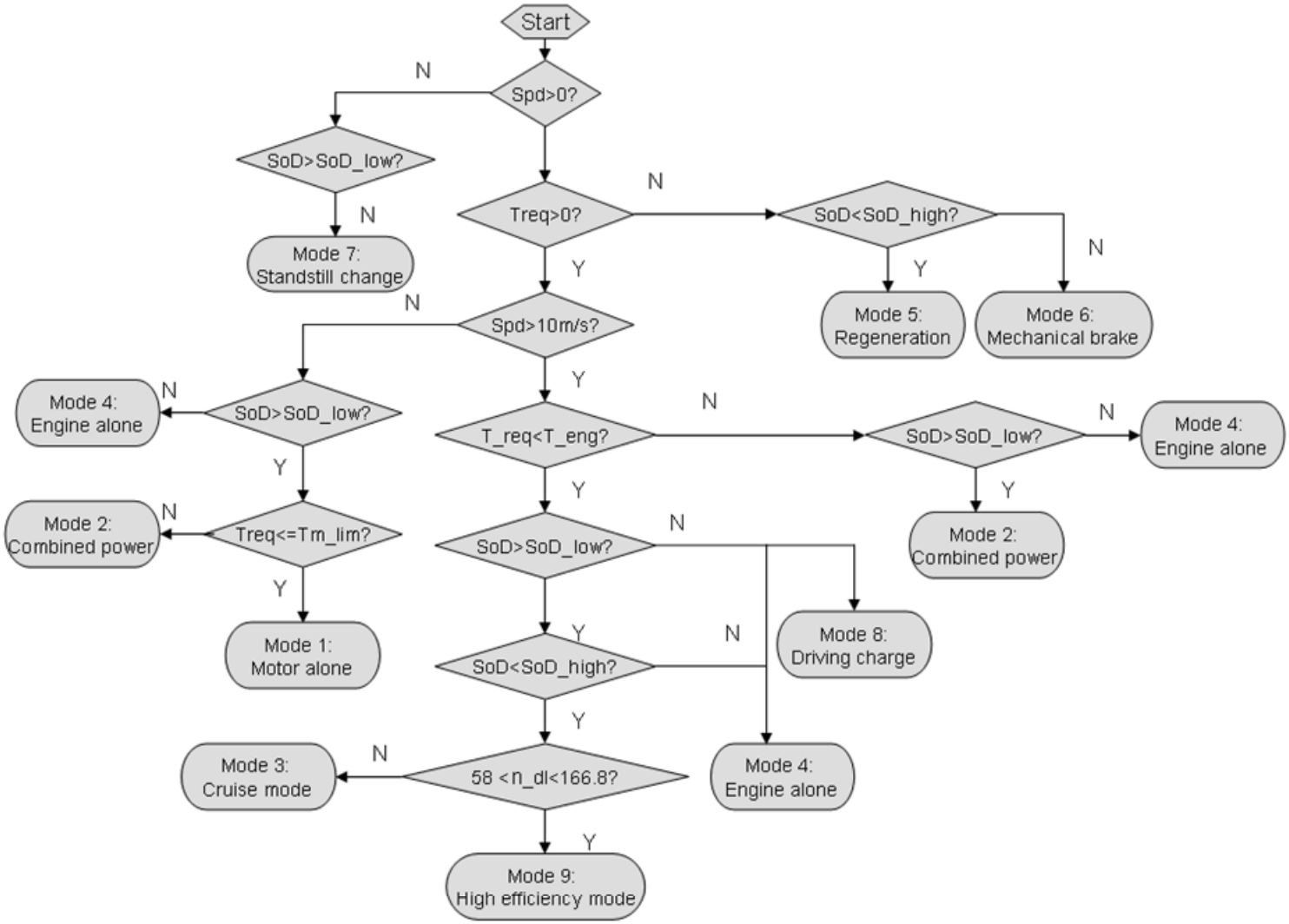

Fig 5.34 Rule based control strategy for HEV with a twin epicyclic transmission

5.7 Concluding remarks

- Three vehicle models have been developed; a conventional IC engine vehicle with a manual gear box, an HEV with a single epicyclic gearbox, and an HEV with a twin epicyclic gearbox.
- The models were derived using a combination of the QSS toolbox together with additional Matlab/Simulation blocks. For example, it was convenient to use the QSS software for some of the straightforward subsystems such as the IC engine and battery, whereas new Simulink blocks were written for more specialized subsystems such as the epicyclic gearboxes.
- For the hybrid electric vehicle with the single epicyclic gearbox model, a total of eight driving modes were identified. While for the HEV model with the twin epicyclic gearbox, one more mode was added to make a good use of the node point. Rule based control strategies were derived for both the single and dual epicyclic gearbox cases.
- For the modelling of the motor generator units, it was found that the QSS software experienced difficulties at very low torques, so a new Simulink S function approach was proposed to overcome this problem.

6 Comparison of HEVs fitted with single and dual epicyclic transmissions

6.1 Introduction

In previous chapters, the single and twin epicyclic gearbox arrangements have been analyzed and modeled. Then these gearbox models were combined with a hybrid electric vehicle model in Chapter 5.

Results are now generated to investigate the performance of these two gearboxes in a hybrid electric vehicle (HEV). The results are calculated using two of the commonly used driving cycles – the European NEDC and USA FTP-75cylces. The HEV results are also compared against a conventional IC engine plus manual gearbox vehicle.

The results focus on fuel consumption comparisons, but it is also shown how the single and twin epicyclic gearboxes use the engine and motor generator units differently.

Finally, some observations about drivability of the HEVs are made.

6.2 Driving cycles

Driving cycles, which are produced by different countries and organizations, are standardized driving patterns described by means of a velocity-time table. One use of driving cycles is to assess the performance of vehicles, such as fuel consumption and emission. In this case, the tests are usually performed on chassis dynamometers. Another use of driving cycles is in vehicle simulations, especially used in propulsion system simulations, as used in this research. In the simulation, the drive system is modeled to predict performance of internal combustion engines, transmissions, electric drive systems, batteries, fuel cell systems, etc.

There are two types of driving cycle: modal driving cycles and transient driving cycles. Modal driving cycles involve protracted periods at constant speeds, while transient driving cycles involves many changes, representing the constant speed changes while driving.

There are 3 groups of driving cycles used around the world:

1. European driving cycles, including ECE 15, EUDC, EUDCL, NEDC, HYZEM, etc. - these belong to the modal cycle category.
2. US driving cycles, including FTP 72, SFUDS, FTP 75, HFEDS, IM240, LA 92, NYCC, US 06, etc. - these are transient cycles.
3. Japanese driving cycles, including 10 Mode, 15 Mode, 10-15 Mode, etc. - these are modal cycles.

The choice of driving cycles influences HEV design decisions. Nearly all standard driving cycles are suggested to be less aggressive than real-world driving conditions. (Stobart and Chen 2009) who also claim that designing new driving cycles that are more representative of real world driving patterns is a emerging research direction for HEV research. In this research, European NEDC and the American FTP-75 will be used because they are relatively more representative of real world driving condition than other cycles, and they are probably the most commonly used driving cycles

6.3 Simulation results

6.3.1 Fuel consumption

For HEVs, the difference between the initial and final battery SOC can significantly affect the measurement of fuel economy. To eliminate this effect, the concept of 'overall fuel consumption (OFC)' was introduced. The total additional energy stored or drawn from the battery (kWh) is claculated and then converted into how much fuel (liter) would be used for the engine to produced this amount of energy.

i) Engine fuel consumpton (EFC, liter/100km): actual fuel burned by the engine devided by the driving distance;
ii) Overall fuel consumption (OFC, liter/100km): the fuel consumtion after taking the battery energy changed (BEC) into considion.

$$OFC = EFC + \frac{100 \times BEC \times \eta_{eng}}{\rho} / D \qquad (6.1)$$

in which ρ is the fuel density (g/ml), η_{eng} is the engine efficeency(g/kWh) and D is the driving distance (m) . The values for ρ and η are 0.76 g/ml and 240 g/kWh resepctively.

In the simulation, BEC is positive if energy is drawn from the battery and negative if the energy is stored into the battery. So at the end of each driving cycle, if final SOC is smaller than the initial SOC, namely the energy is drawn from the battery, overall fuel consumption is greater than the engine fuel consumption, and vice versa.

It is very improtant to take account of the battery SOC in the calculations, because if it is different at the end of the driving cycle from its value at the start then some net energy has effectively been lost or gained in the vehicle calculations. In several examples of results in the literature, it is not clear whether this effect has been accounted for. Also, some researches acutally use the control system to ensure that the battery start and finish conditions are exactly the same. However, this can cause difficulties because the control system is not necessaryly representative of what it would be doing during normal practical driving.

The first set of results was used to compare the two PST arrangements with a baseline, conventional vehicle equipped with a five speed gearbox (3.84, 2.11, 1.36, 0.86 and 0.63 with the same final dive ratio). The control strategies for the two PST arrangements were based on a rule-based approach to compromise between overall energy efficiency and maintaining the battery state of charge (SOC) under control. The vehicle models were run over several different driving cycles, including the standard NEDC and USA FTP-75 driving cycles, and the overall fuel consumption results are shown in Table 6.1.

Table 6.1 Comparisons of fuel consumption for the hybrid vehicle fitted with the 3 and 4 branch systems compared with a conventional, manual gearbox vehicle over different driving cycles

Driving cycle	Fuel consumption over driving cycle, l/100km				
	Traditional	Single epicyclic system		Dual epicyclic system	
		Engine FC	Overall FC	Engine FC	Overall FC
Europe NEDC	3.8	4.0	2.7	3.9	2.5
USA FTP-75	3.6	3.8	3.0	3.7	2.4

Europe EUDC	3.2	4.6	2.4	4.8	2.1
USA City I	3.5	4.3	2.9	4.3	2.4
Japan 15	3.5	3.9	1.9	4.0	1.7
Japan 11	3.9	3.1	2.1	3.3	1.7

As expected, both hybrid vehicles show economy advantages over the conventional, manual gearbox vehicle. However, the improvements are not as great as published in some other studies, but this is understandable because the systems used here – and in particular their controllers – have not yet been optimised. The main aim of this work was rather to compare the 3 and 4 branch drivelines under exactly comparable conditions; this comparison is shown in Table 6.2 and it shows that the 4 branch system offers around significant improvements over all the driving cycles. The improvements vary substentially with the different cycles, varying from 7.4% for the NEDC to 20% over the USA FTP-75 cycle. The reson for these substantial differences is the suage of the mode 9 for the twin epucyclic gearbox. This is the high efficiency mode which is one of the potential benefits of the twin epicyclic arrangement and as shown later in Figs 6.13 to 6.16 it is used more in the USA-FTP-75 driving cycle. Once again, these results highlight the sensitively of efficiency predictions to the assumption about which driving cycle to use in the calculations

Table 6.2 Percentage improvement of the 4 branch over the 3 branch driveline over different driving cycles

Driving cycle	Percentage improvement of 4 branch over the 3 branch driveline (%)
Europe NEDC	7.4
USA FTP-75	20.0
Europe City	12.5
USA City I	17.2
Japan 10	10.5
Japan 11	19.0

6.3.2 Engine operation points, power flow and battery SOC

The associated engine utilisation maps are shown in Fig 6.1 to Fig 6.6 for the baseline gearbox, the single epicyclic gearbox and the twin epicyclic gearbox vehicles respectively. Each point on the map of engine torque vs speed is the solution at a single point during the NEDC cycle; the cycle defines input from t = 0s to t = 1220s. However, the NEDC cycle contains a percentage of constant speed running conditions, so that several points will sit on top of each other.

First, these results highlight in Fig 6.1 and Fig 6.4 the shortcoming associated with conventional IC engine cars – namely that they inevitably spend considerable time at part load conditions well away from the areas of maximum efficiency. In contrast, it can be seen in Fig 6.2 and Fig 6.5 for the single epicyclic gearbox, that it manages the IC engine rather well through the combination of effectively its continuously variable gear ratio plus its ability to manage the electrical power flows in and out of the battery. This results in the usage points being constrained around the area of maximum specific fuel consumption of the engine. Finally, in Fig 6.3 and Fig 6.6 it can be see that the dual epicyclic gearbox actually manages some further improvement and also reduces the use of the higher engine speeds.

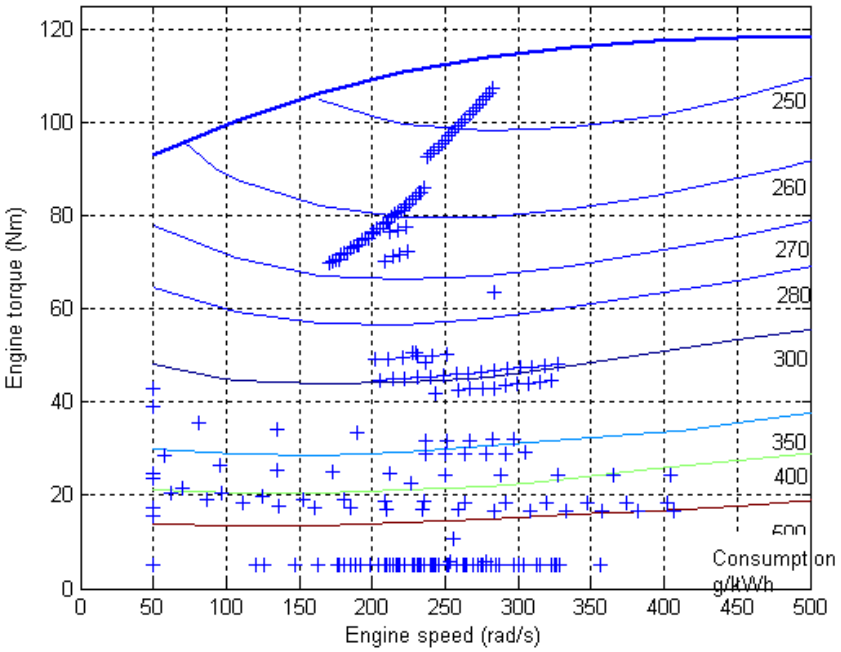

Fig 6.1 Engine operation points, NEDC cycle, traditional ICE vehicle

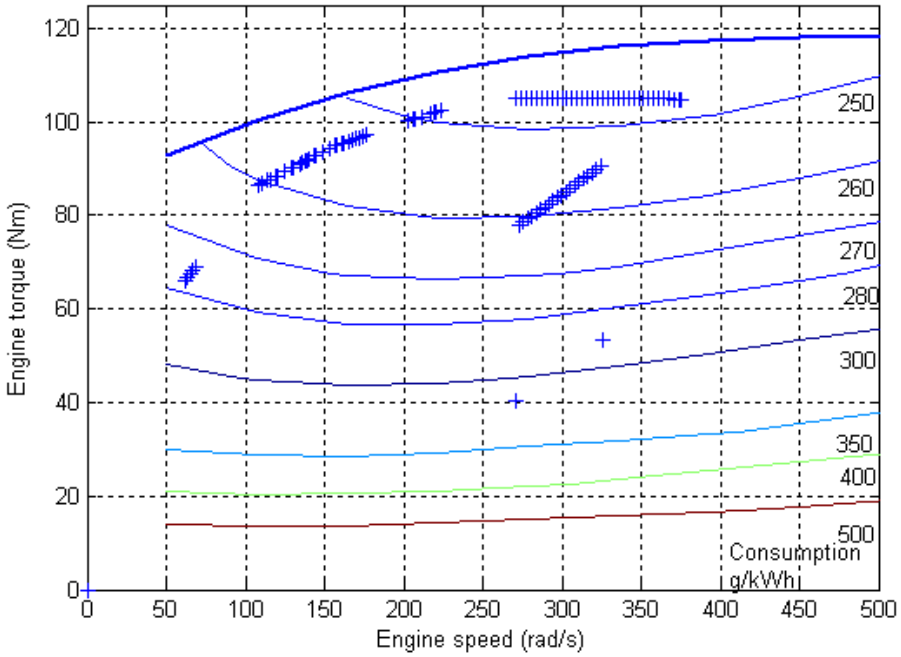

Fig 6.2 Engine operation points, NEDC cycle, single epicyclic system

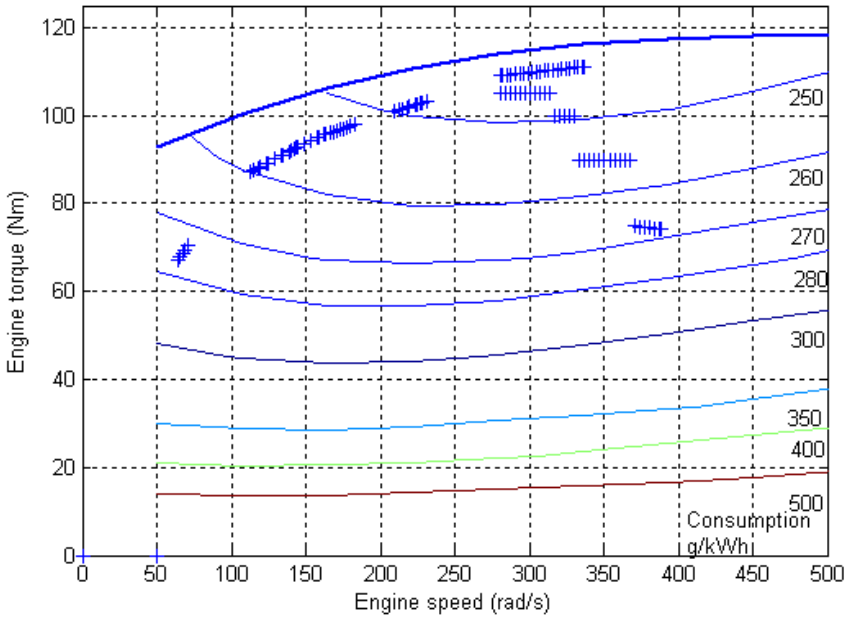

Fig 6.3 Engine operation points, NEDC cycle, dual epicyclic system

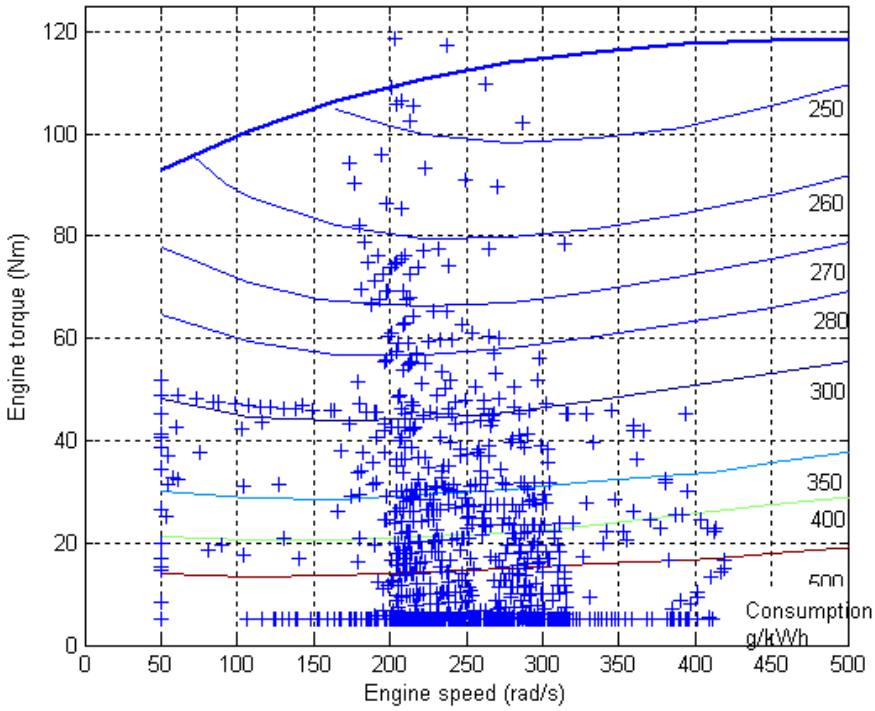

Fig 6.4 Engine operating points, FTP 75, traditional ICE vehicle

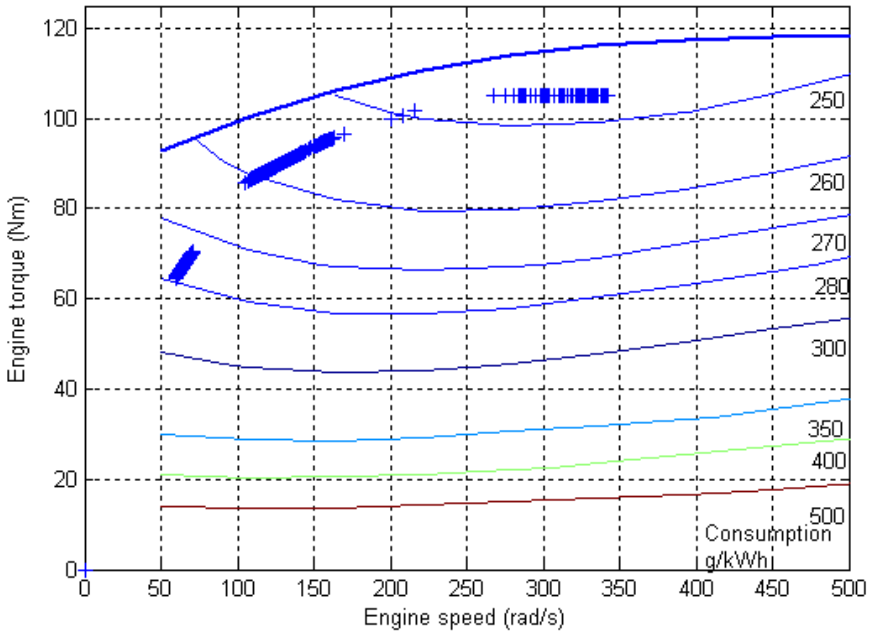

Fig 6.5 Engine operation points, FTP75 cycle, single epicyclic system

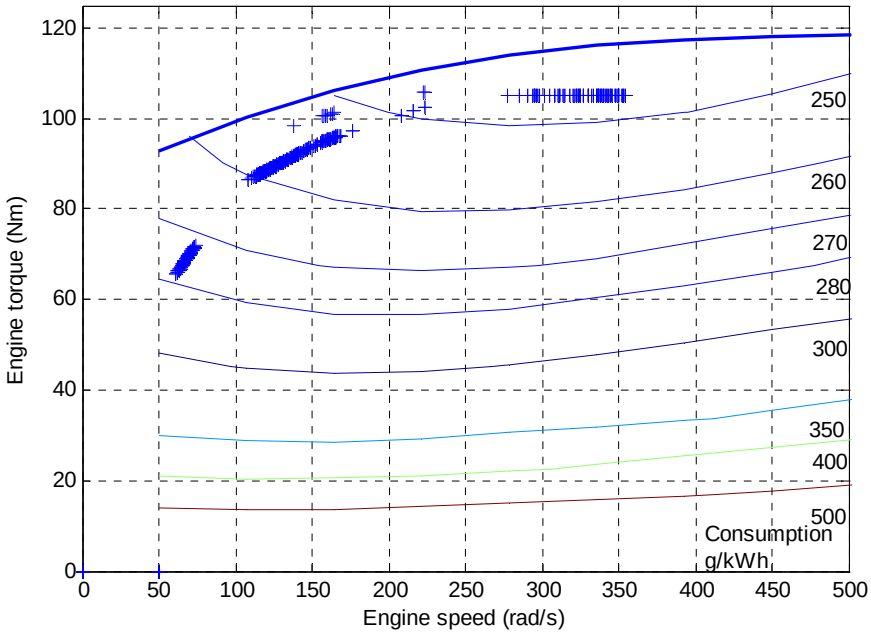

Fig 6.6 Engine operation points, FTP75 cycle, dual epicyclic system

Further insight into the detailed behavior of the single and dual epicyclic gearboxes can be seen in the time history plots in Fig 6.7 and Fig 6.8 for the NEDC cycle and Fig 6.9 and Fig 6.10 for the USA FTP-75 cycle. The power utilization of the IC engine and two motor generator units, MG1 and MG2 are plotted along with the vehicle speed profile specified in each of these driving cycles.

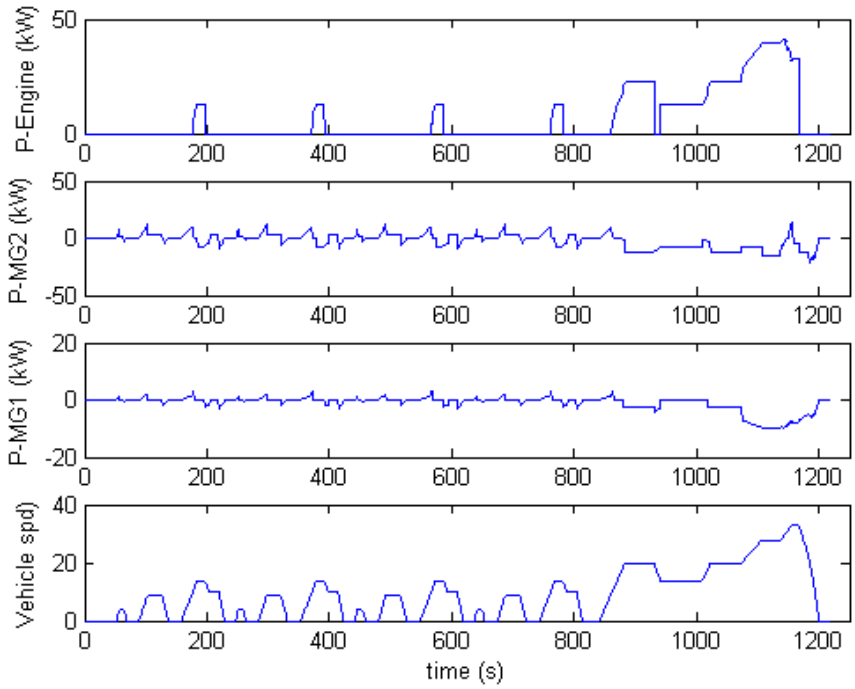

Fig 6.7 Power flows in the HEV with the single epicyclic gearbox over NEDC driving cycle

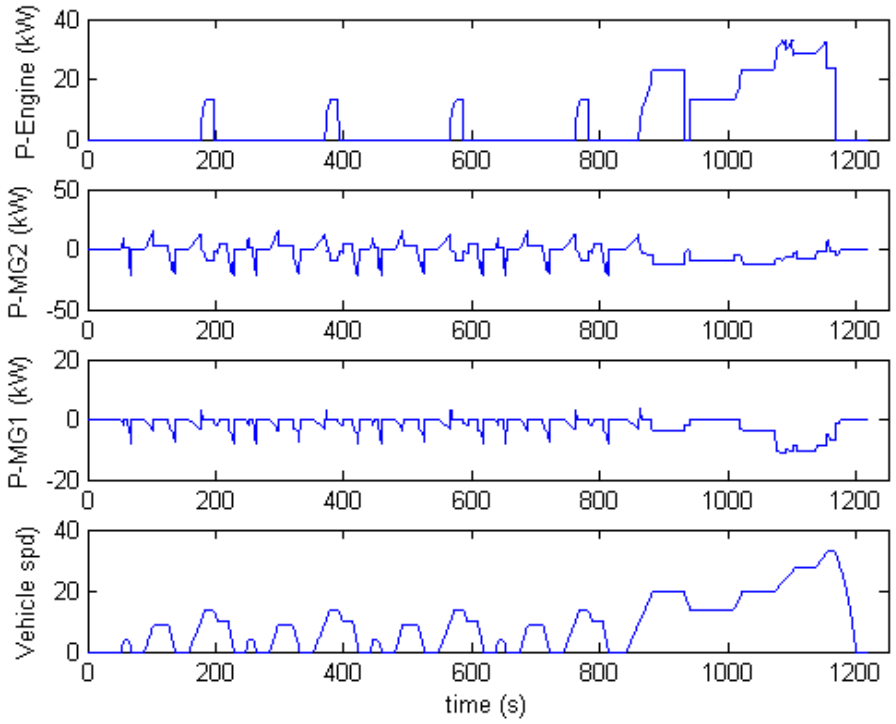

Fig 6.8 Power flows in the HEV with the dual epicyclic gearbox over NEDC driving cycle

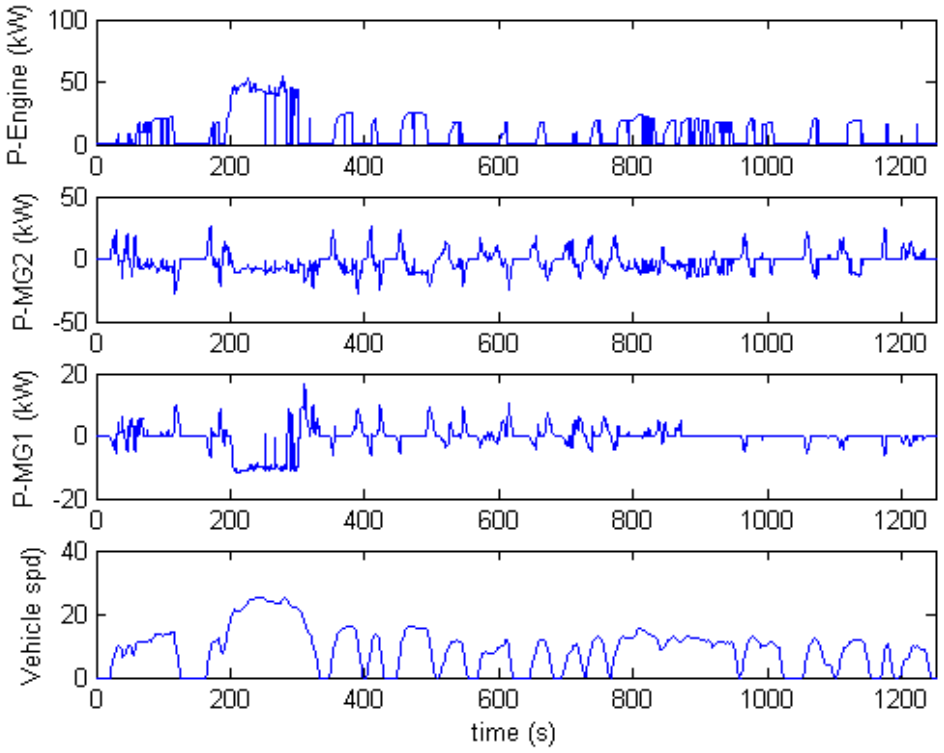

Fig 6.9 Power flows in the HEV with the dual epicyclic gearbox over FTP-75driving cycle

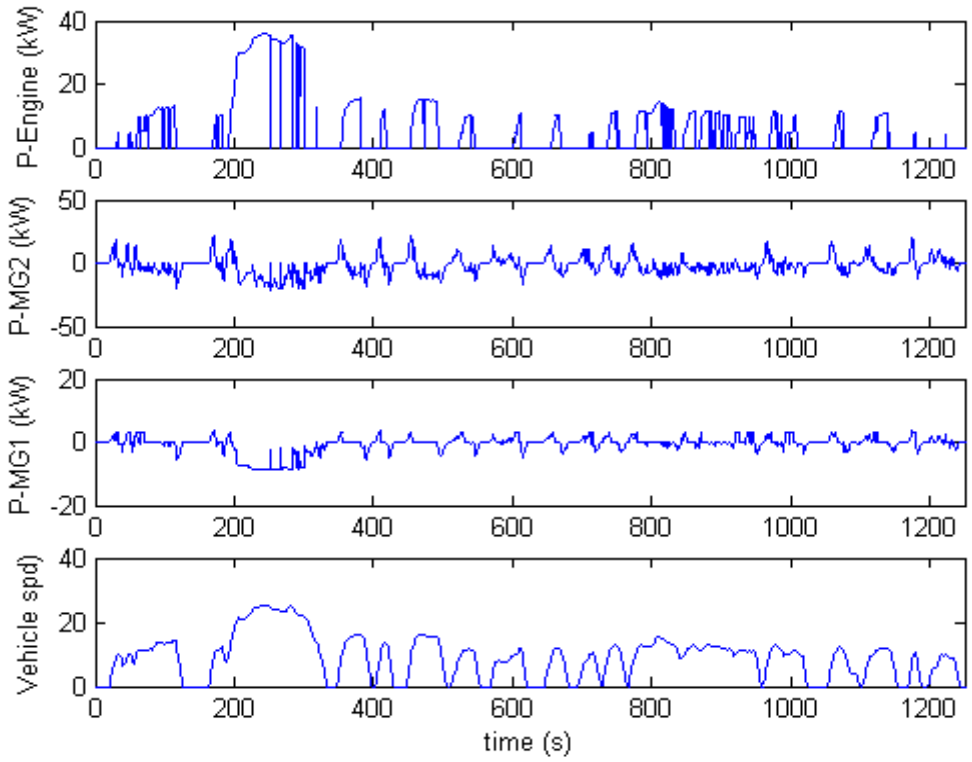

Fig 6.10 Power flows in the HEV with the dual epicyclic gearbox over the FTP-75driving cycle

The results in Figs 6.7 to 6.10 also highlight the substantial differences between the European and USA standard driving cycles; the European version contains a much greater number of stationary and constant speed running events, whereas the USA version is almost continually changing speed in its version of an urban cycle. This reflects a fundamental difficulty within the vehicle industry when it has to try and make fair comparisons of competing driveline technologies regarding their energy consumption – what actually constitutes a representative driving pattern over which to make comparisons? The answer is likely to vary across the three major global automotive markets – Europe, USA and the Far East.

But the acceptance of a so-called standard cycle also raises another potential problem – that in the quest for the best headline figures, the driveline and particularly its controller is actually optimised around the specific cycle. This can lead to engineering developments based more around the standard than around a drivable, efficient vehicle across a wider range of operating conditions.

Battery SOC plays an important role in the research of HEV performance and all energy management strategies need to take the SOC into consideration. For example, keeping the SOC at the end of driving cycles the same as the beginning

of the cycle is the goal of some strategies. In this research, the SOC is kept in a reasonable range, from 0.5 to 0.75. Fig 6.11 and Fig 6.12 show example of the change of SOC over the two cycles.

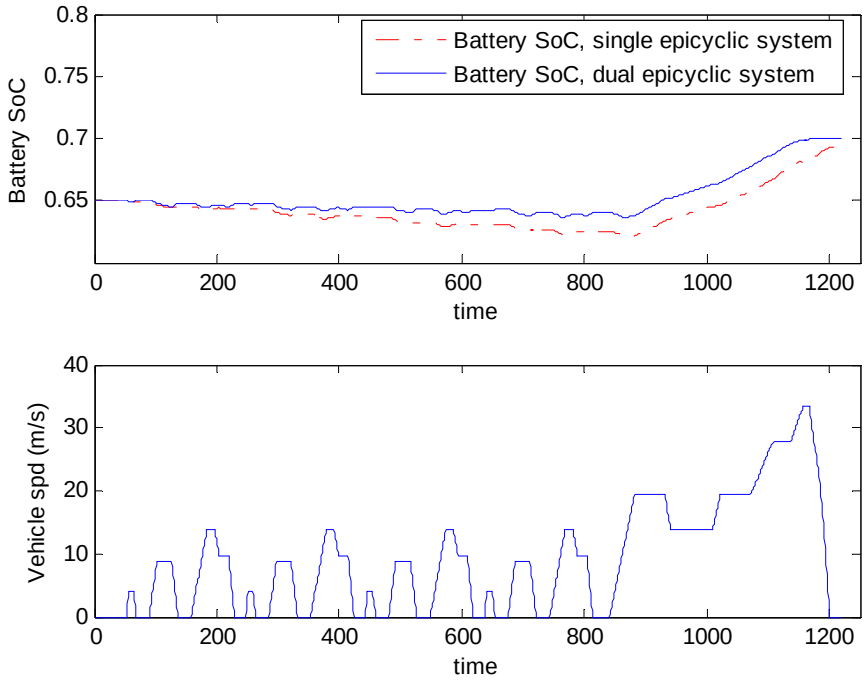

Fig 6.11 Battery SOC over the NEDC5 cycle

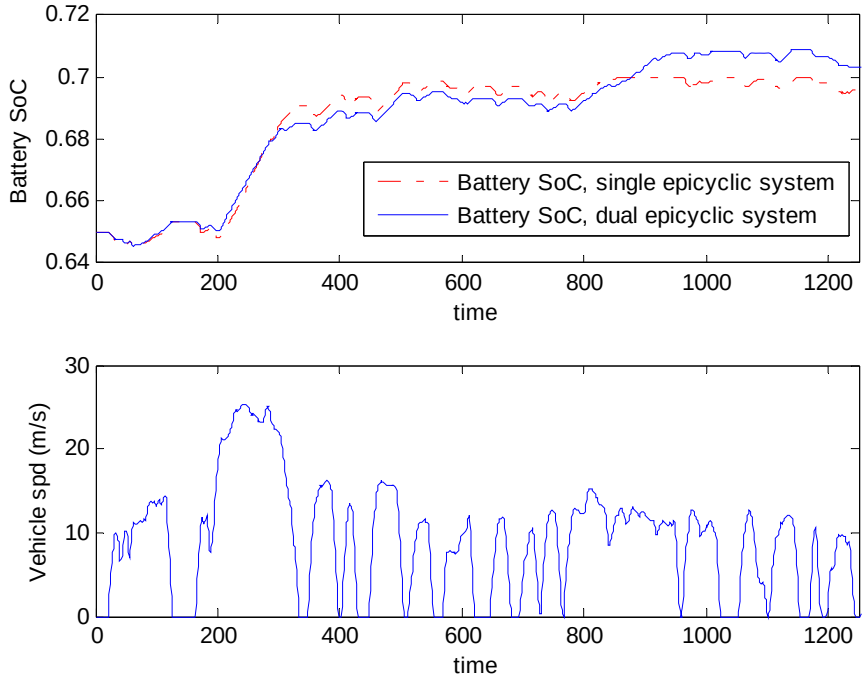

Fig 6.12 Battery SOC over the FTP-75 cycle

6.3.3 Mode selection analysis

For HEVs with single and twin epicyclic transmission, the selection of driving mode during NECD and FTP-75 cycle is shown in Fig 6.13 and Fig 6.14 respectively. The main difference is that for twin epicyclic transmission, one more mode: high efficiency mode is selected. The percentage of time spent in each mode selected is shown in Fig 6.15 and Fig 6.16. For HEV with twin epicyclic transmission, during NEDC cycle, the percentage of time spent in the high efficiency mode is 1.7%, while during FTP-75 cycle, this figure is 3.7%. This goes some to explaining why the improvement of fuel consumption over NEDC cycle is lower than the improvement over FTP-75 cycle (Table 6.1).

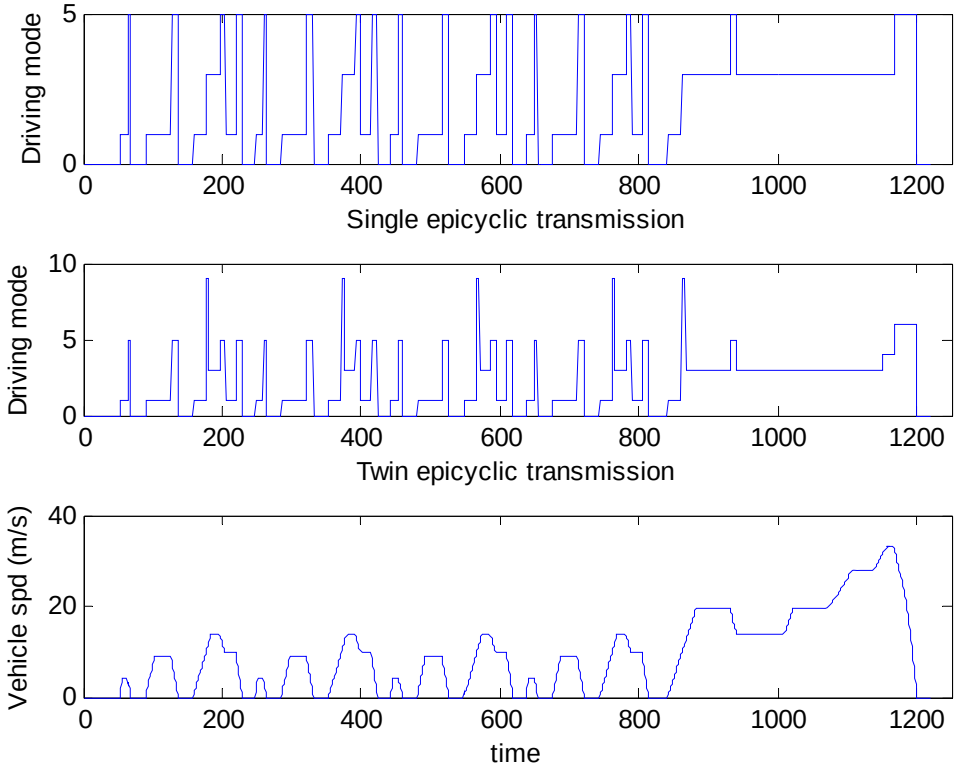

Fig 6.13 Mode selection, Europe NEDC cycle

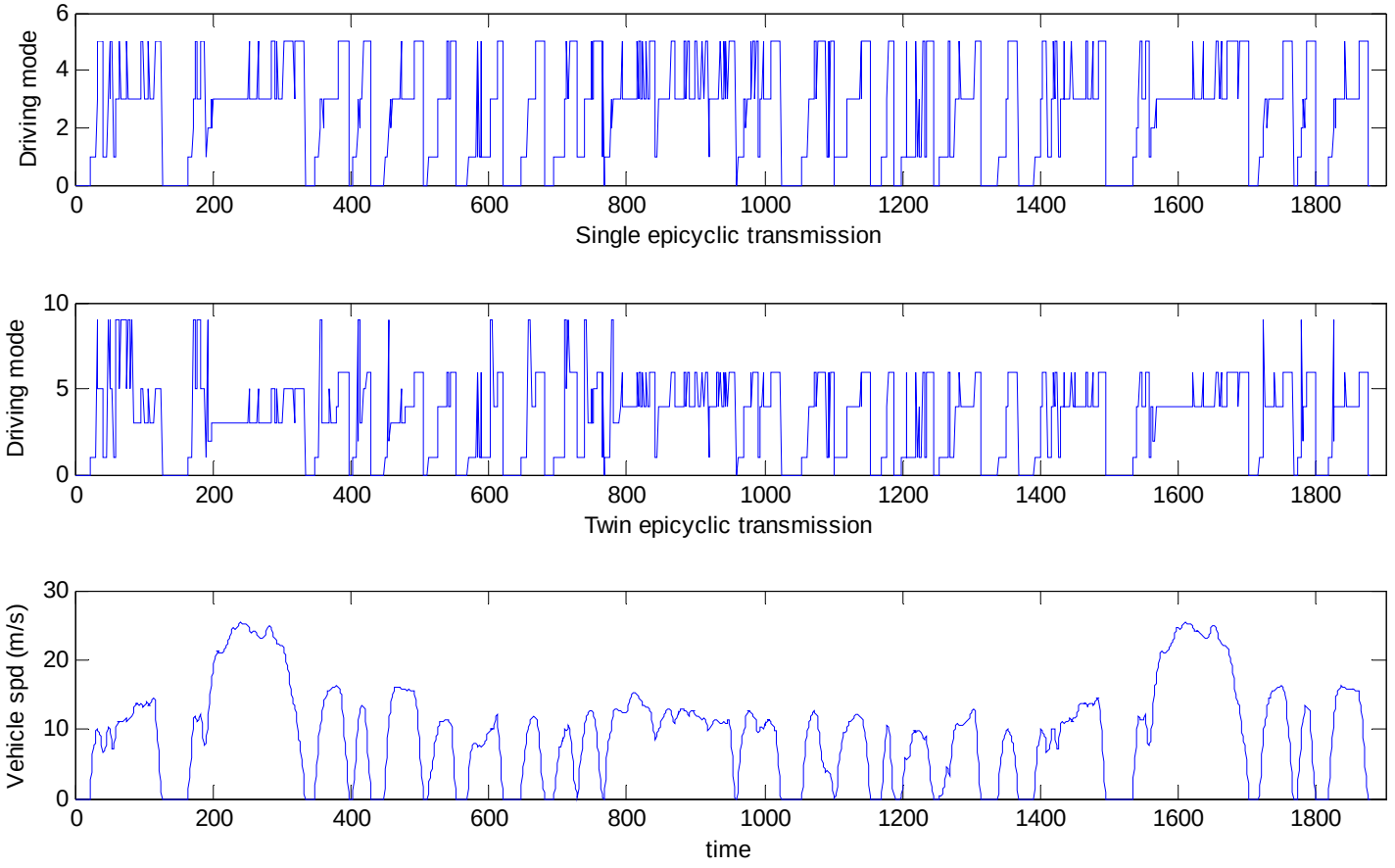

Fig 6.14 Mode selection, USA FTP-75 cycle

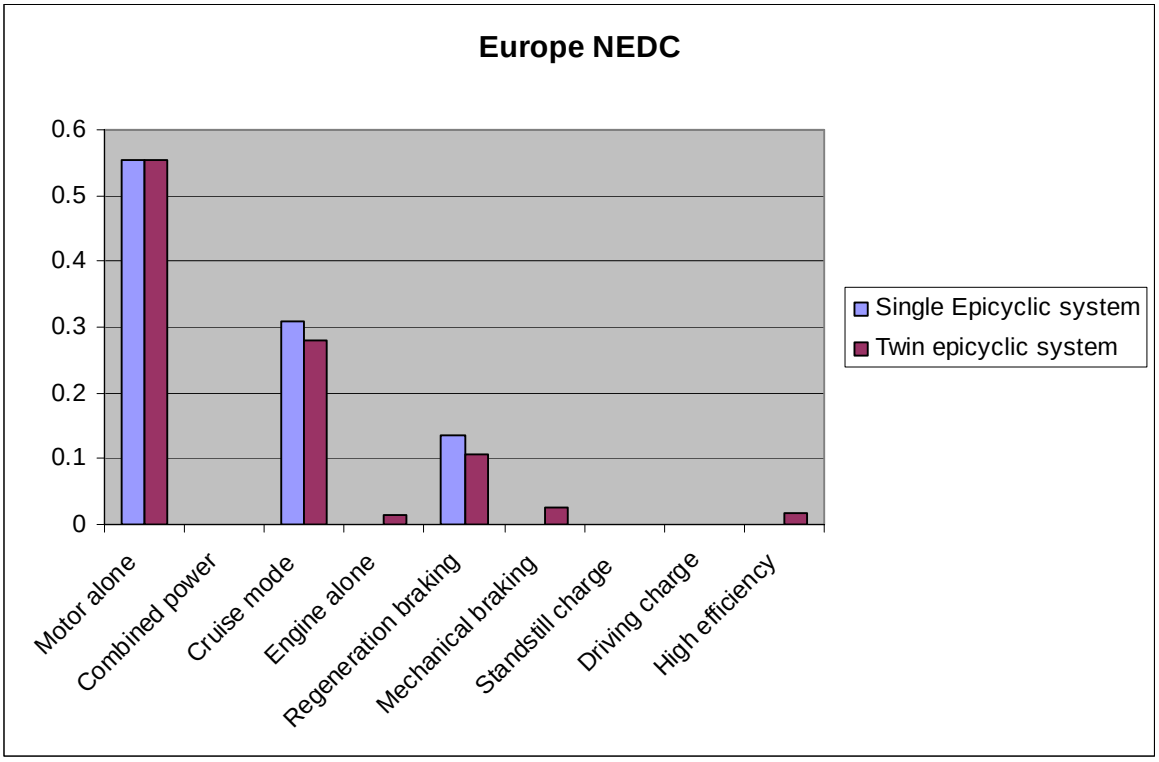

Fig 6.15 Relative amount of time spent in each mode, NEDC cycle

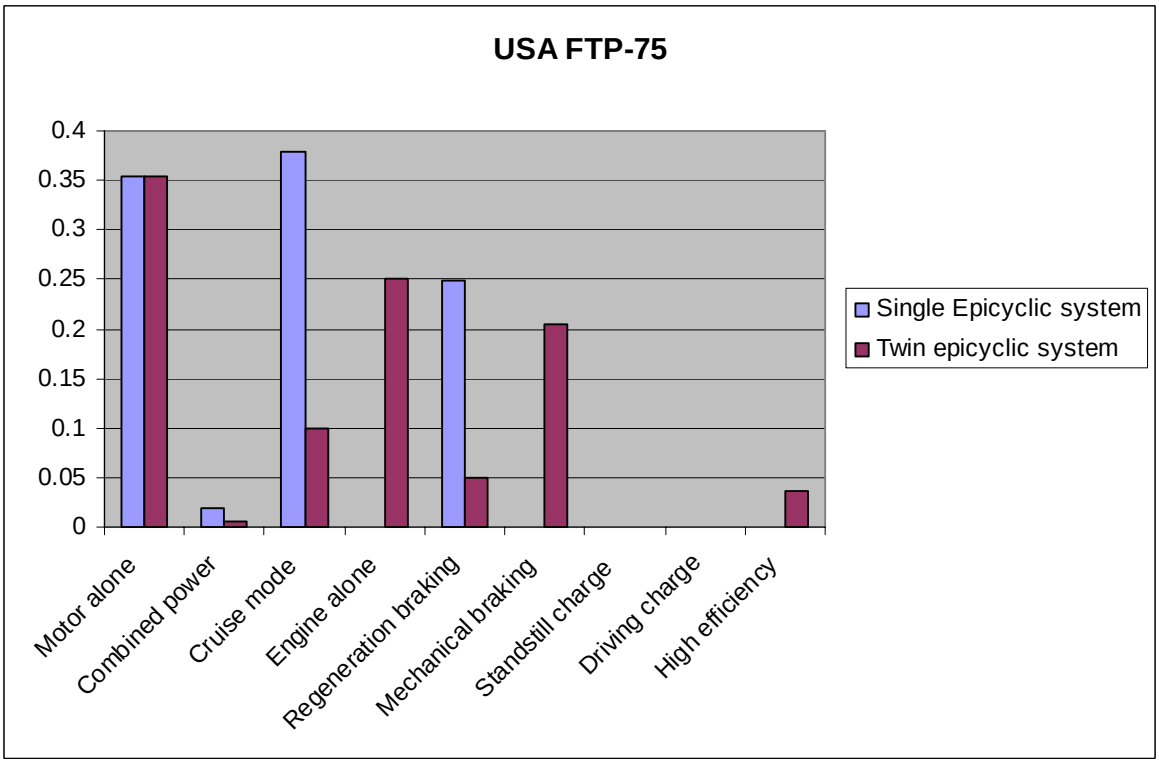

Fig 6.16 Relative amount of time spent in each mode, FTP-75 cycle

6.3.4 Motor and generator operation points

For the HEV with the single epicyclic transmission, the operation points of MG1 and MG2 over NEDC cycle are shown in Fig 6.17 and Fig 6.19. For the HEV with the twin epicyclic transmission, the operation points of MG1 and MG2 over NEDC cycle are shown in Fig 6.18 and Fig 6.20.

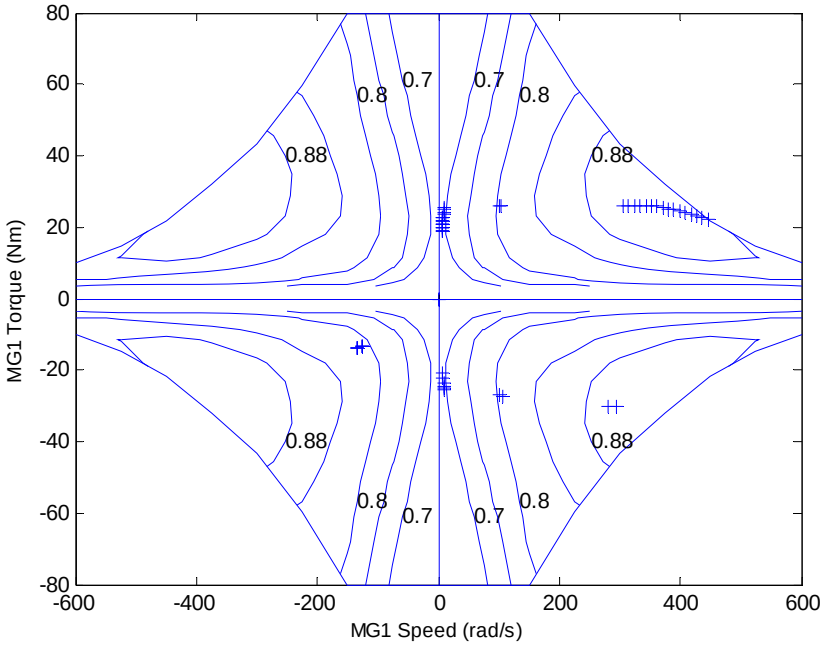

Fig 6.17 Operation of MG1, single epicyclic system, NEDC cycle

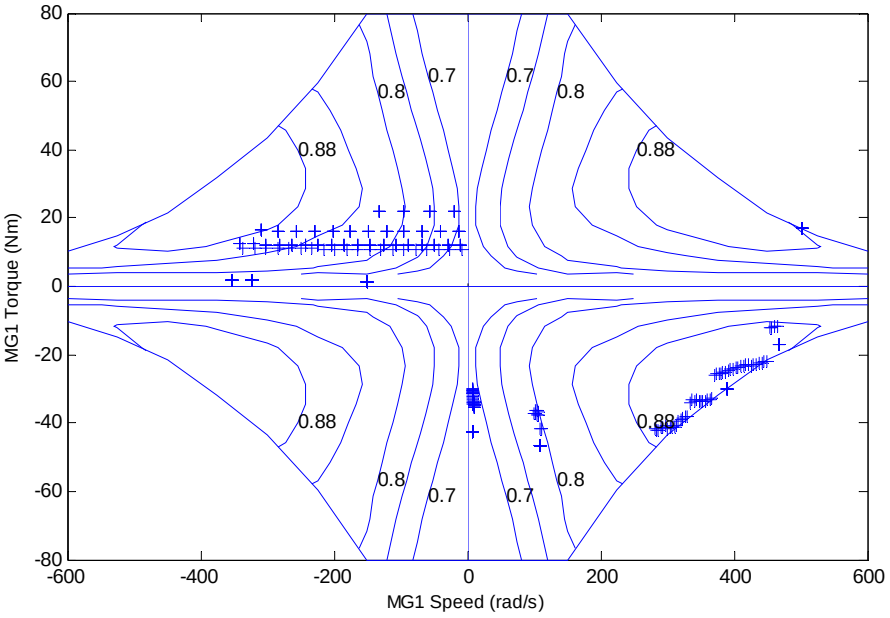

Fig 6.18 Operation of MG1, twin epicyclic system, NEDC cycle

For both MG1 and MG2, the control strategies were designed that the motor/generators work within the maximum torque curve. If one of the calculation points suggests that one of the electric machines is overspeed or overload, the controller will change the speed and/or torque of the engine to make sure every element is working in the correct operation range.

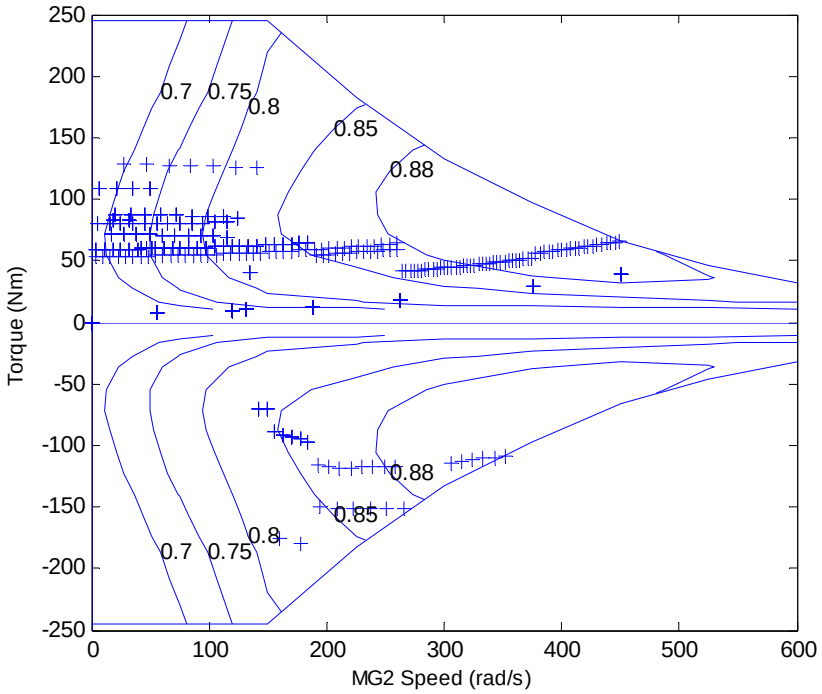

Fig 6.19 Operation of MG2, single epicyclic system, NEDC cycle

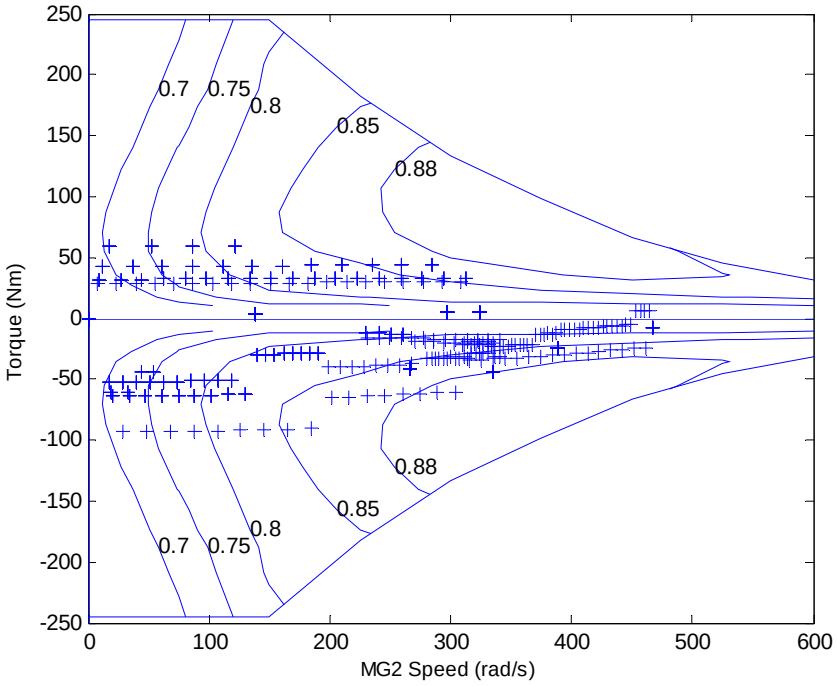

Fig 6.20 Operation of MG2, twin epicyclic system, NEDC cycle

6.4 Vehicle performance

6.4.1 Top speed

For conventional IC engined vehicle, the top speed that can be reached on level road with a given transmission ratio can be found by intersecting the curve of the available power at the wheels with that of the required power on level road (Genta and Morello 2008). The available power for gears I, II, III, IV and V are calculated as: for the given gear ratio, assume the engine always works on the 'engine speed-maximum engine torque' curve.

$$P_a = \eta_t P_e = \eta_t \omega_{eng} \times T_{eng\_\max} \quad (6.2)$$

$$P_n = (F_{rr} + F_{ad}) \times V \quad (6.3)$$

where:

P_a is the available power;

P_n is the required power;

$T_{eng\_\max}$ is the engine's miximum torque

F_{rr} is the rolling resistance force;

F_{ad} is the aerodynamic drag;

η_t is the efficiency of the whole powertrain;

The vehicle speed under each gear is

$$V = \frac{\omega_{eng}}{i_{gear} \times i_{differential}} \times r \quad (6.4)$$

r is the radius of the tire;

i_{gear} is the transmission ratio of each gear;

$i_{differential}$ is the transmission ratio of the differential.

The power required and the available power for each gear ratio are shown in Fig 6.21. For the IC engined vehicle the top speed is 54.5 m/s (196.2km/h).

For full hybrid vehicles, if the engine is not downsized, the vehicle is almost retain to have better overall performance compared with a conventional vehicle (Chan 2007). As far as the top speed is concerned, because the power split device is actually a CVT, it can change the transmission ratio to achieve the highest top

speed, as shown in Fig 6.22. the top speed for the HEV with a E_CVT is 58.6 m/s (210.9 km/h).

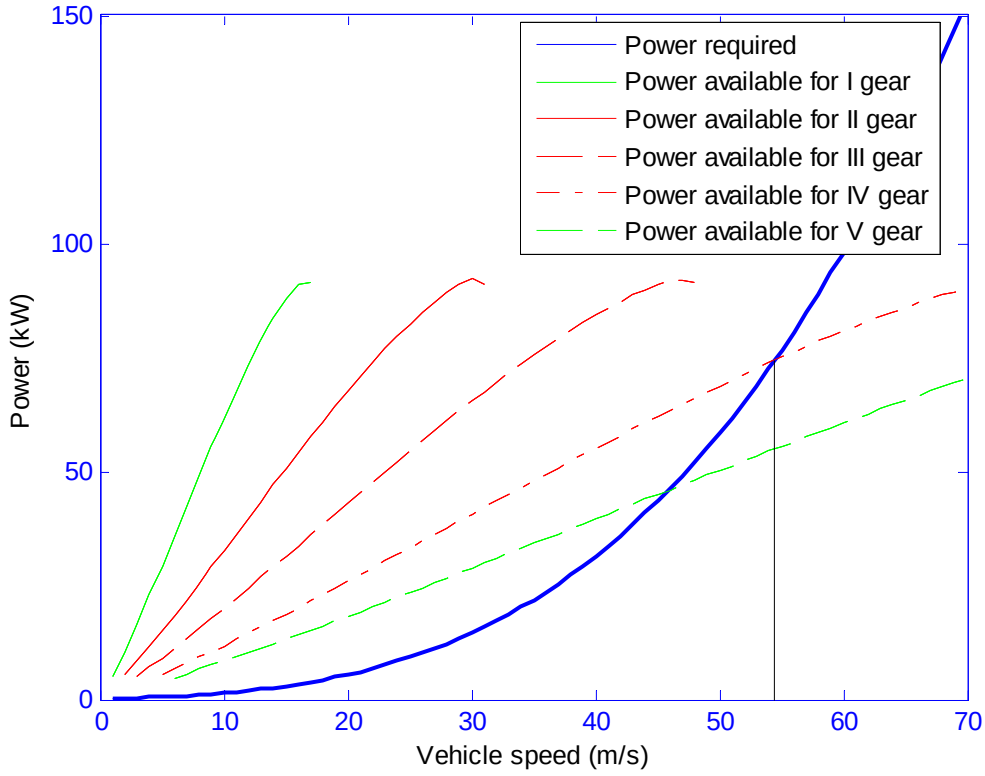

Fig 6.21 Top speed for the conventional vehicle (55.92m/s)

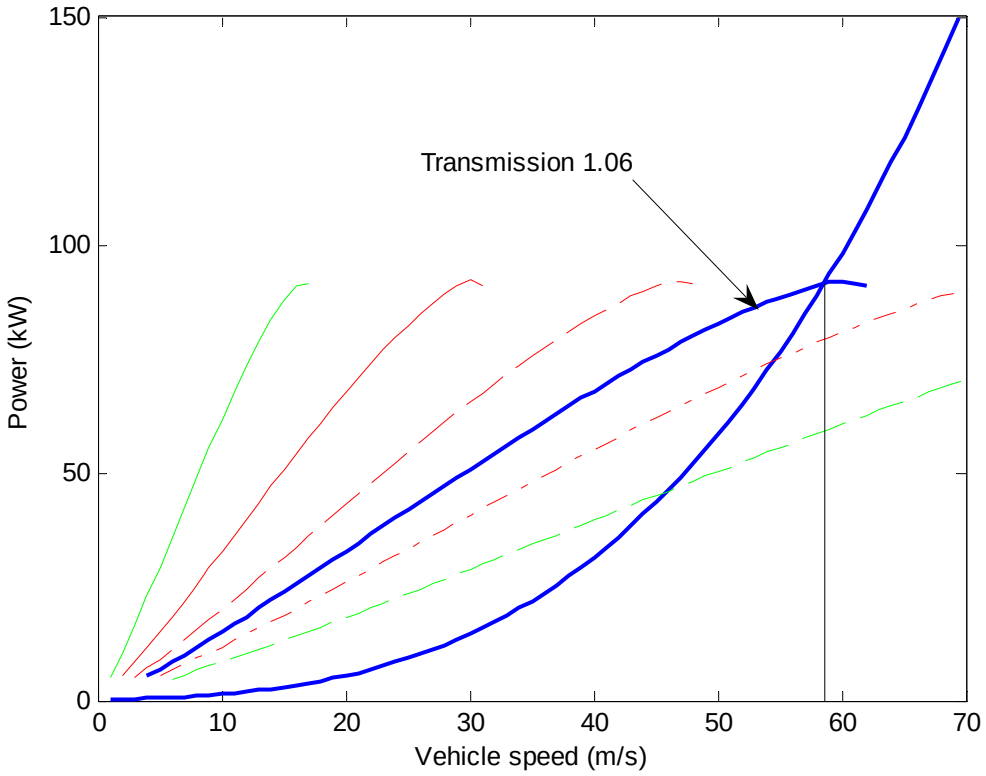

Fig 6.22 Top speed for a HEV with a CVT

In practice, for a full HEV it is normal design practice to downsize the IC engine. The challenge for the controller design is then to maximize the time spent by the engine toward its optimum efficiency region by controlling the power flows to and from the battery. However, this should not compromise overall performance and drivability compared to the equivalent IC engine vehicle. So the controller exploits the continuously variable transmission ratio to address this compromise.

6.4.2 Acceleration

The maximum acceleration a vehicle is capable of at various speeds is (Genta and Morello 2008):

$$\left(\frac{dV}{dt}\right)_{\max} = \frac{\eta_t P_e - P_n}{m_e V} = \frac{\eta_t P_e - (F_{rr} + F_{ad})V}{m_e (V+1)} \qquad (6.5)$$

where

m_e is the equivalent mass of the vehicle;

P_e is the engine power;

P_n is the required power.

The plot of maximum acceleration versus vehicle speed of the tradition IC engined vehicle with a five speed gear box is shown in Fig 6.23. The minimum time need to accelerate from speed V_1 to V_2 can be calculated by integrating Eq. (6.6), but usually numerical integration is performed.

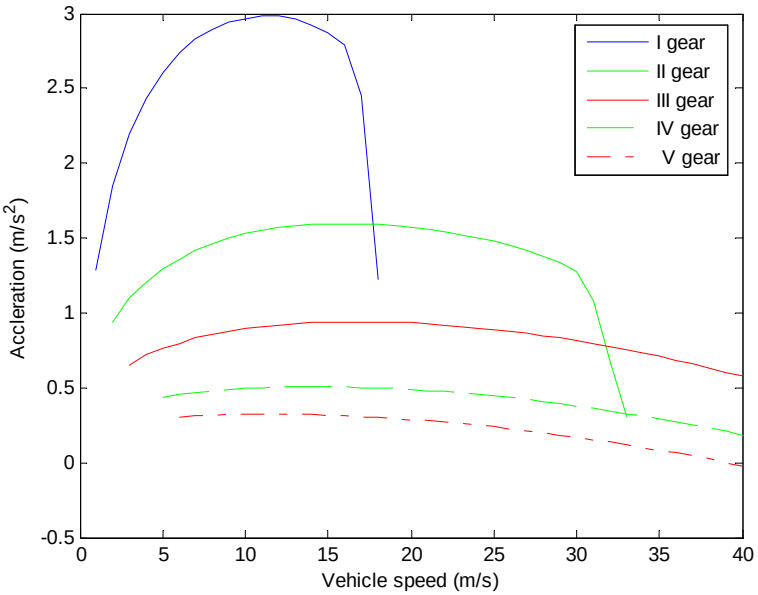

Fig 6.23 Maximum acceleration versus vehicle speed

A graphical interpretation of the integration is shown in Fig 6.24, which plots (1/acceleration) vs. vehicle speed. The area under the curve 1/a is the minimum time required for the acceleration.

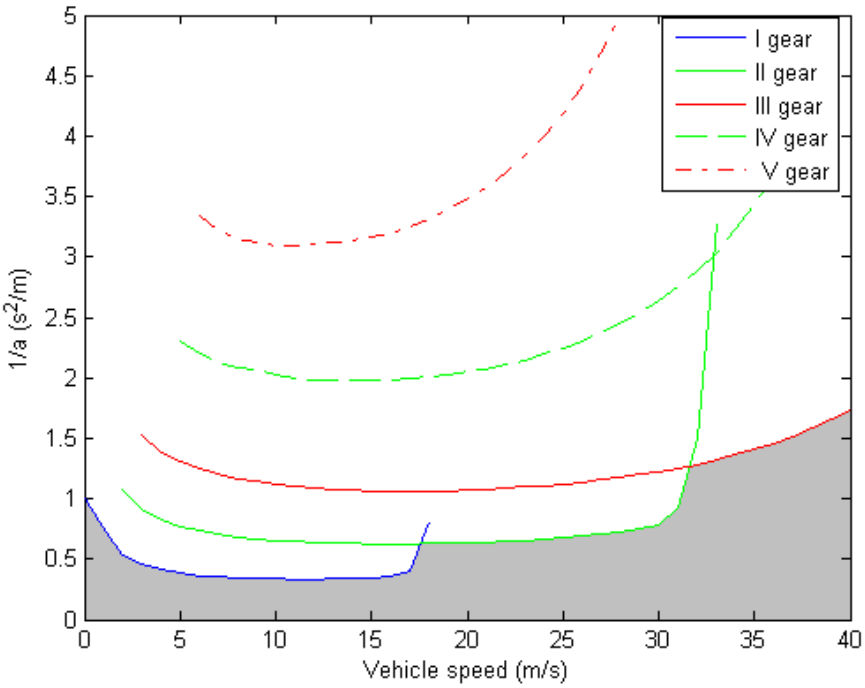

Fig 6.24 1/a versus vehicle speed

The minimum time of acceleration for a HEV with a PST (power split transmission) is shown in Fig 6.25. The dark area is the time to speed for a HEV with a CVT.

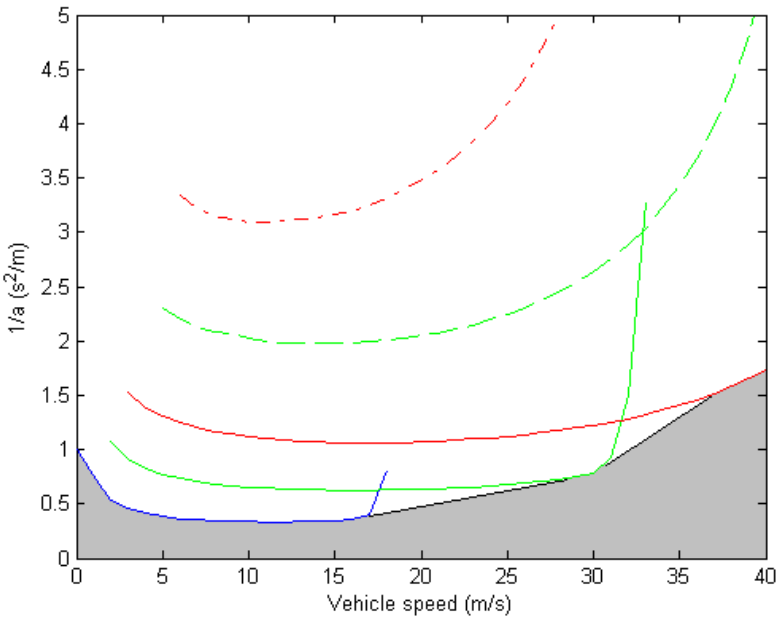

Fig 6.25 1/a versus vehicle speed.

The time-speed curve, as shown in Fig 6.26 can be obtained by integrating the dark area in Fig 6.24 and Fig 6.25. From Fig 6.26, it shows that the time to accelerate from 0 to 100 km/h (27.78 m/s) for a vehicle with a geared transmission and a HEV with a PST is 12.3 s and 14.4 s, respectively.

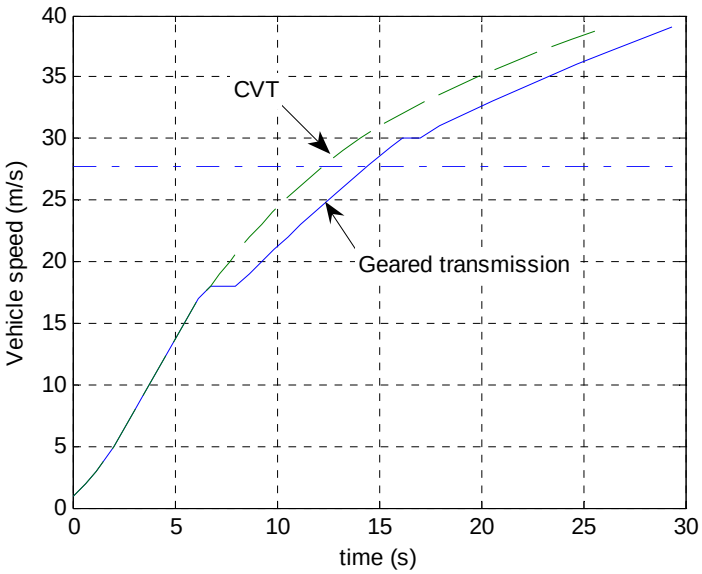

Fig 6.26 Speed versus time curve

6.4.3 Driving aggressiveness

A study at the Argonne laboratory demonstrated that HEVs have a higher fuel consumption sensitivity to aggressive driving (Sharer, Leydier et al. 2007). They define more aggressive driving to mean more use of periods of higher accelerations that indicated in the typical driving cycles. In this study, the sensitivity of the two HEV models to driving aggressiveness was calculated and the results are shown below.

The FTP 75 driving cycle is used as a baseline driving input for the comparisons. Then, a simple multiplier factor of 0.8. 0.9, 1.1 and 1.2 was imposed to get cycles that represent different driving aggressiveness. The bigger the factor , the more aggressive the driving cycle becomes since the speeds and hence accelerations are simply increased. Factor 0.8 means the cycle is less aggressive than the baseline cycle and factor 1.2 means the cycle is more aggressive than the baseline cycle, as shown in Fig 6.27.

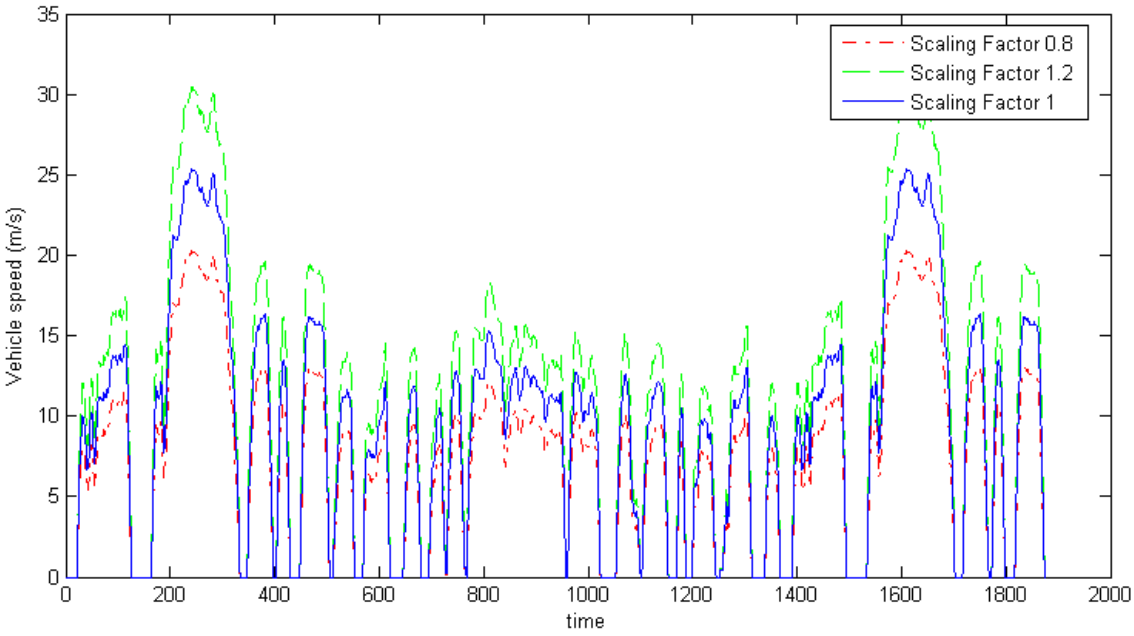

Fig 6.27 Driving cycles with different driving aggressiveness

The simulation result is shown is Table 6.3.

Table 6.3 Fuel consumptions with different driving aggressiveness

Scaling Factor	Traditional ICE		Single epicyclic system		Dual epicyclic system	
	Overall Fuel consumption	Normalized Fuel consumption	Overall Fuel consumption	Normalized Fuel consumption	Overall Fuel consumption	Normalized Fuel consumption
0.8	3.39	0.93	3.07	0.84	2.64	0.73
0.9	3.50	0.96	3.03	0.83	2.37	0.65
1	3.64	1	3.02	0.83	2.36	0.65
1.1	3.79	1.04	3.57	0.98	2.64	0.72
1.2	3.97	1.09	4.42	1.21	3.22	0.88

*Note: all the normalized fuel consumptions are normalized to 3.64, which is the overall fuel consumption of the traditional ICE with scaling factor 1.

First, the overall benefits of the twin epicyclic over the single epicyclic and the traditional ICE are shown to occur consistently over all limited range of driving aggressiveness tested here. Then, the same results are plotted in Fig 6.28 showing the trend of the fuel consumption figures normalized to the traditional ICE at a scaling factor of 1. These curves provide information on how sensitive each system is to driving aggressiveness as indicated by the slope of the lines. The ICE case is shown to be rather insensitive; the twin epicyclic is somewhat less

sensitive than the single epicyclic as the driving aggressiveness increases above 1. this again relates to the greater flexibility of managing the power flows between the mechanical and electrical paths.

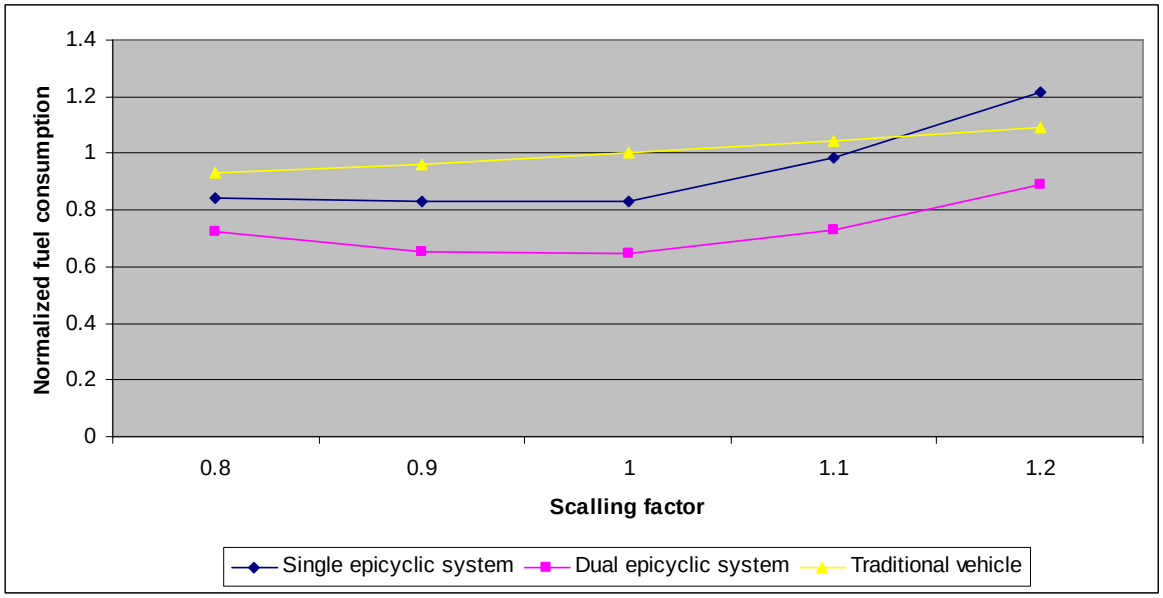

Fig 6.28 Sensitivity to driving aggressiveness – fuel consumption normalized to the baseline ICE condition

6.5 Concluding remarks

- The four branch, dual epicyclic gearbox arrangement offers a significant performance benefit over the three branch, single epicyclic arrangement; fuel economy improvements of 7 and 20% were shown over the two main European and USA driving cycles.
- The performance benefits arise from the greater flexibility of control over the torques, speeds and power flows through the two motor generator units available with the dual epicyclic scheme.
- For a HEV with a PST, which provides the benefits of a CVT gearbox, if the engine is not downsized, the HEV will have better drivability, namely higher top speed and shorter acceleration time.
- In practice, the normal design approach for a HEV is to downsize the engine, and improve overall fuel consumption, whilst exploiting the transmission and controller properties to obtain similar performance to the equivalent ICE vehicle.

- The four branch system is slightly less sensitive to increased driving aggressiveness than the 3 branch system, because it can control the power flows better according to different driving conditions.
- In practice, further benefits are probably available; first, the dual arrangement has two nodal positions at which zero electrical power circulates and these can be designed to occur at convenient speeds, e.g. in the UK, 30 mile/h in urban driving and 70 mile/h motorway cruising. Second, with the dual arrangement it is possible to downsize the motor generator units to retain the same driveability but with reduced weght and cost.
- Although the results presented here have been based on relatively simple vehicle models, it is likely that the promising results for the twin epicyclic transmission could be further improved using more sophisticated optimisation strategies for the control system.

7 Electric vehicle with transmission system

7.1 Introduction

The work on transmission performance for HEVs is extended in this chapter to investigate the potential role of transmission design for EVs.

As observed in the introduction in Chapter 1, global interest in EVs has grown at a dramatic rate particularly over the current decade. Many of the major OEMs, e.g. GM, Nissan, Renault will shortly be marketing commercial versions of EVs. In the UK, the government has been very active in trying to promote the EV industry as part of its Low Carbon Vehicle (LCV) Technology programmes.

This has resulted in many companies becoming involved in development of EVs – sometimes for niche markets – in order to establish early leadership of the developing technology.

Despite this high worldwide level of interest in EVs some aspects of the vehicle technology have received little attention. The transmission design is one such area and perhaps it is understandable that the majority of research attention has to date focused on the more obvious topics of batteries, motors and power electronics.

The aim of this chapter is to investigate whether there are any potential efficiency or performance benefits for using geared transmissions for EVs. Predicted results are compared for a typical EV without a gearbox, with a CVT and with a conventional stepped gearbox. As for the HEV results, predictions are made over the standard driving cycles.

One of the critical features in this study is the usage of the electric motor in its region of high efficiency. Consequently, two motors were modeled in this work in order to understand the sensitively of the results to the assumptions about motor efficiency maps. These motors will be referred to as a theoretical motor derived from generic equations and a practical motor which is effectively a look-up map from the manufacturers data.

7.2 Electric vehicle modeling

7.2.1 Vehicle modeling

The modelling of the electric vehicle performance is also done using the QSS Toolkit (Guzzella and Amstutz 2005). This is a quasistatic simulation package based on a collection of Simulink blocks and the appropriate parameter files that can be run in any Matlab/Simulink environment. The vehicle model itself is straightforward and is shown in Fig 7.1; it is a conventional plug-in type EV with the addition of a gearbox in the power train.

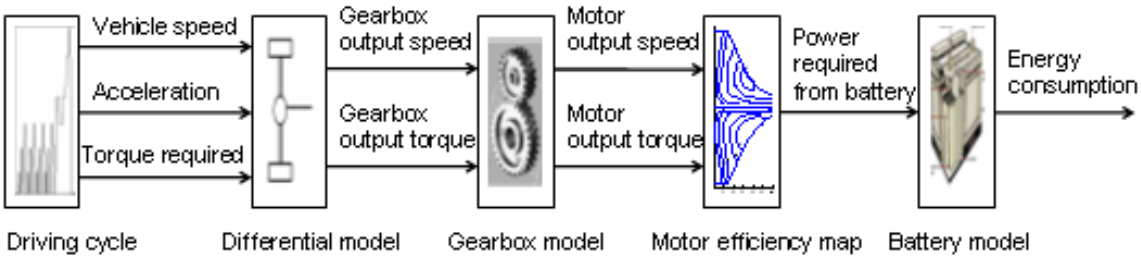

Fig 7.1 Block diagram of EV model

Two types of motors were used in this research: a generic motor and a practical motor. The generic motor characteristics are intended to represent a typical generic motor of 40 kW. They were taken from Larminie's book (Larminie and Lowry 2003) who presents a Matlab script to generate a set of generic motor properties based on assumptions about the losses within the motor.

The data of the practical motor were given by UQM (www.uqm.com 2009), an American company that develops and manufactures high-performance, power-dense and energy-efficient electric motors**,** generators and related power electronics. This motor was selected as being representative of a current, off-the-shelf motor suitable for electric vehicle application.

The input to the model is one of the standard driving cycles – the NEDC cycle and USA FTP 75 are used extensively in this work – and the solution procedure is based on stepping through the driving cycle at typically one second steps, calculating the equilibrium condition and then collecting all the data for plotting at the end of the cycle. The modelling assumptions are kept very simple in this initial work, so that no account is included of losses in the gearbox. Thus, the focus of attention is on the motor efficiency map and the major issue of whether it is

possible to improve overall energy usage by operating at or near to the best efficiency points.

7.2.2 Method of selecting motor operation point

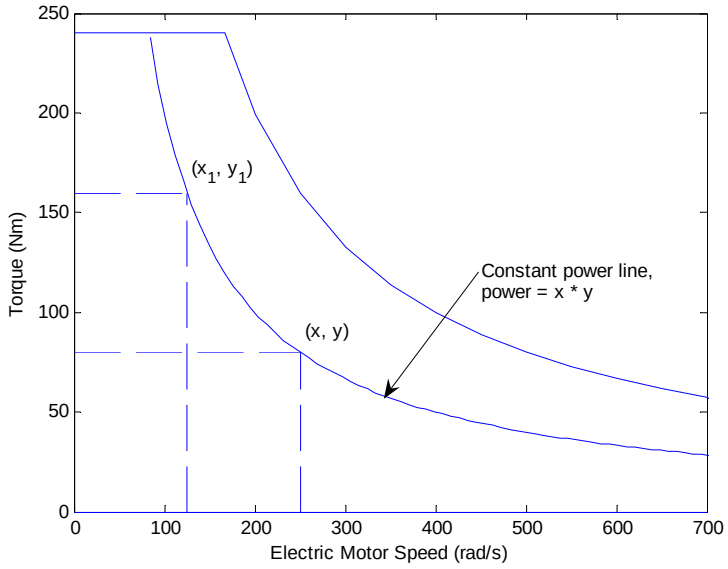

Fig 7.2 Schematic diagram of selecting motor operation point

The schematic diagram of selecting motor operation point is shown in Fig 7.2.

For a generic motor, the efficiency of each point is calculated as follows.

For any given point (x, y),

$$Power_{output} = x * y \quad (7.1)$$

$$Power_{input} = Power_{output} + kc * y^2 + ki * x + kw * x^3 + ConL \quad (7.2)$$

$$\eta(x, y) = \frac{Power_{output}}{Power_{input}} = \frac{x * y}{x * y + kc * y^2 + ki * x + kw * x^3 + ConL} \quad (7.3)$$

where $kc * y^2$, $ki * x$, $kw * x^3$ and $ConL$ are copper losses, Iron losses, windage losses and constant motor losses respectively. In this study, kc, k, kw and $ConL$ are 0.2, 0.008, 0.00001 and 400 respectively.

Let (x_1, y_1) represent any point along the constant power line on which $power = x * y$,

$$x_1 * y_1 = x * y \qquad (7.4)$$

$$eta(x_1, y_1) = \frac{x_1 * y_1}{x_1 * y_1 + kc * {y_1}^2 + ki * x_1 + kw * {x_1}^3 + ConL} \qquad (7.5)$$

For Equation (7.5), replace y_1 with $\frac{x * y}{x_1}$, we can obtain

$$eta(x_1, y_1) = \frac{power * x_1^2}{kw * {x_1}^5 + ki * x_1^3 + (power + ConL)x_1^2 + kc * {power}^2} \qquad (7.6)$$

Once the expression of efficiency for any point along the constant power line is given, Matlab can be used to search for the most efficient point.

For the practical motor, the efficiency of each point is obtained via interpolation of data given by the motor manufacturer, so effectively it is input as a look-up table and Matlab is used to interpolate between the data points to find a specific operating condition.

7.3 Results with a generic motor

The vehicle parameters for the EV with the generic motor are summarised in Table 7.1; they are intended to be representative of a typical generic vehicle rather than any specific design. The motor rated power is 40 kw, and the total vehicle mass is set to be 950 kg.

Table 7.1 Vehicle parameter data

Parameter, units	Value
Total vehicle mass, kg	950
Wheel diameter, m	0.5
Aerodynamic drag coefficient	0.22
Frontal area, m^2	2
Rolling resistance coefficient	0.008
Motor maximum torque, Nm	240
Motor maximum speed, rad/s	800
Motor power, kW	40
Final drive ratio	3.5

7.3.1 EV with single transmission ratio

The first results shown in Fig 7.3 refer to the baseline condition of the vehicle with no gearbox. Each point on the map of motor torque vs. speed is the solution at a single point during the NEDC cycle; the cycle defines inputs from t = 0 s to t = 1220 s. The top half of the figure refers to conditions in which the motor is delivering power and the bottom half to conditions in which the motor acts as a generator and regenerates power which is fed back to the battery.

The efficiency lines in the top half are defined as (input power required/output power delivered); the efficiency lines in the lower half are defined as (power regenerated/input power) From 0 to 166.7 rad/s the maximum torque that the motor can deliver is 240 Nm, and after this point the maximum power line is shown in Fig 7.3.

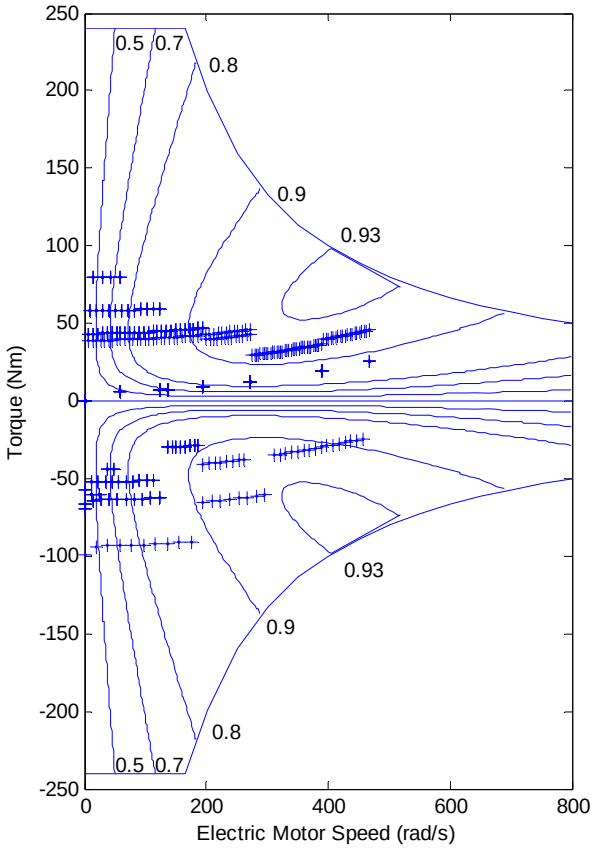

Fig 7.3 Motor operation points with no gearbox

In this case, the maximum power line is actually the line for rated power, which is 40 kW. On each point of that line,

$$power = torque \times speed = 40kW \qquad (7.7)$$

This means that if it is run at this power, its temperature will settle down to a safe level. Because it is fairly large and heavy, it takes some time to heat up to a dangerous value. So if in any case more power is needed, it can be run in excess of 40 kW, as long as this is controlled less than about 1 minute. This is extremely useful for a electric vehicle as peak power may only needed for a short period of time, such as when accelerating (Larminie and Lowry 2003).

7.3.2 EV with continuously variable gearing

The next results assume that the gearbox is infinitely variable so that any ratio can be selected; in fact upper and lower limits are applied so that the ratio can be any value between 4 and 0.6. The calculation procedure is effectively a simplified optimisation strategy. At any point in the drive cycle, the torque and speed demanded of the motor are first calculated; then, for this power requirement a search routine is used with the motor map to find the point of maximum efficiency and the appropriate gear ratio selected so that the motor can operate at this point and still deliver the necessary torque and speed to the driving wheels.

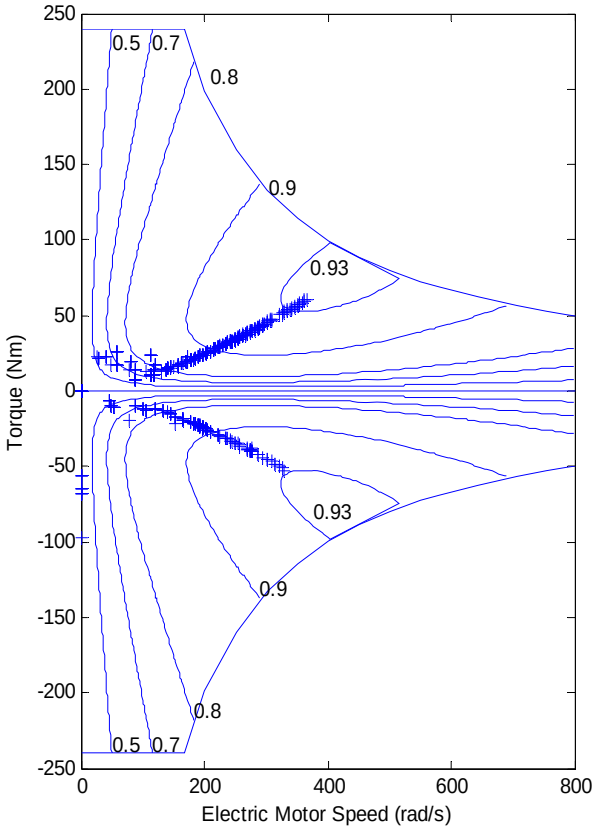

Fig 7.4 Motor operation points with continuously variable gear

It is further assumed that the gearbox response would be fast enough to follow these changing requirements. Thus, the results shown in Fig 7.4 effectively describe the optimisation of the motor usage over the selected NEDC drive cycle. It is clear from Fig 7.4 that the results follow the nominal line of maximum efficiency of the motor. The gear ratios selected by the algorithm to achieve this are shown in Fig 7.5.

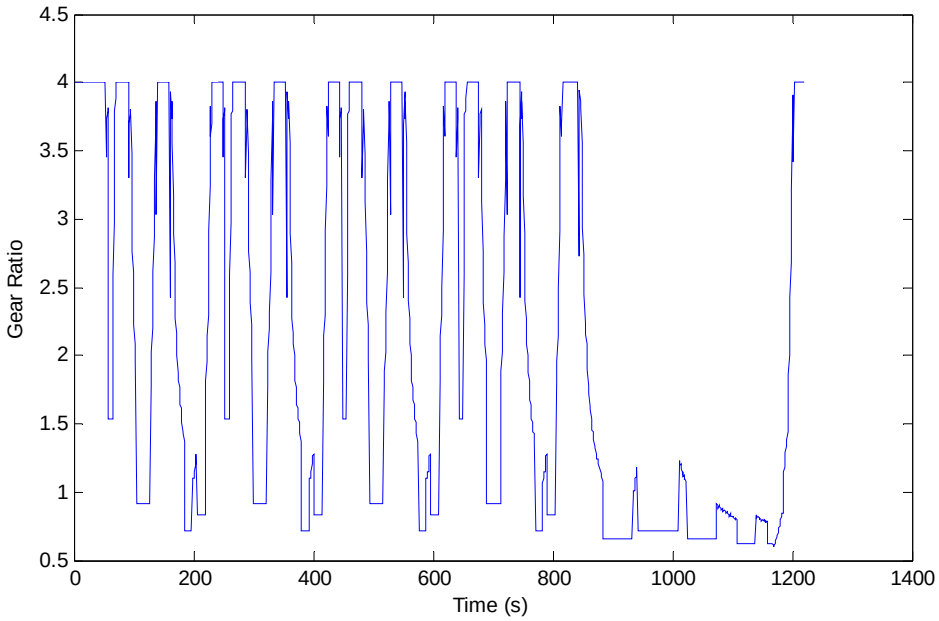

Fig 7.5 Gear ratios selected by optimisation strategy

7.3.3 EV with a multispeed gearbox

The results shown in Fig 7.6 refer to the case in which it is assumed that a four speed gearbox is fitted in the transmission. The ratios are selected in a rather subjective fashion after inspection of Fig. 4, and are 2.5, 1.5, 1 and 0.8; in practice, the gear ratio selection would be done automatically rather than manually as with a conventional IC engine car. Here, a simplistic gear selection strategy is used:

i) For constant speed running the highest gear (lowest numerical ratio) is selected

ii) When accelerating, the ratio is based simply on speed – such that the above ratios are selected for the speed ranges 0-100, 100-200, 200-300 and 300-800 rad/s.

It is not suggested that this is in any way optimal, but this approach is chosen to understand the sensitivity of the energy usage predictions to practical design issues.

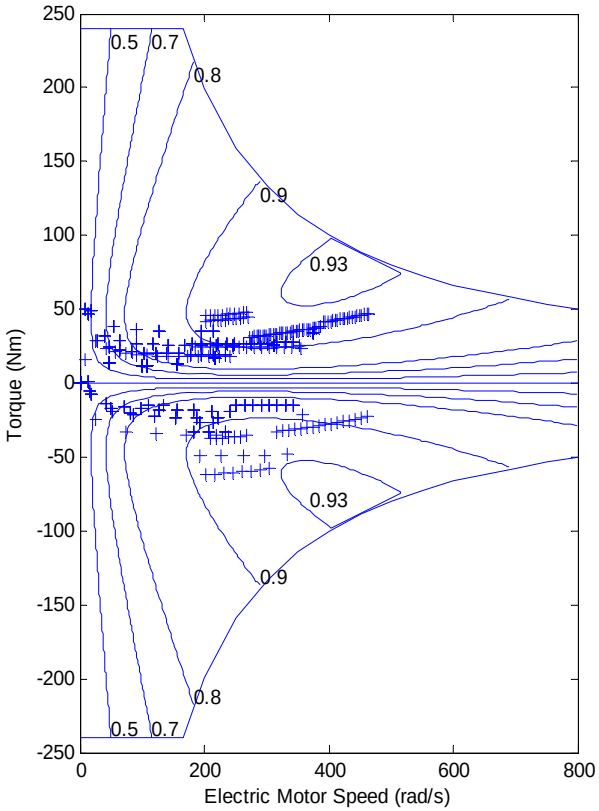

Fig 7.6 Motor operation points with four gear ratios

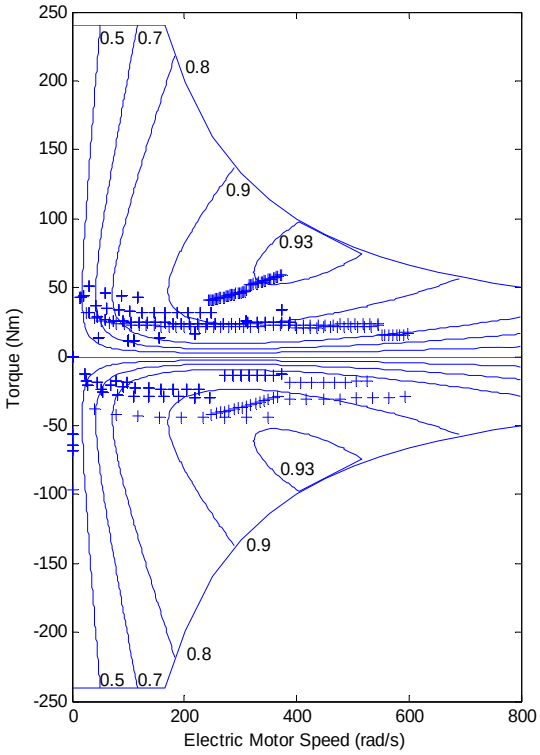

Fig 7.7 Motor operation points with two gear ratios

The results are then repeated for two other gearboxes:

i) 3 speed with ratios of 2, 1 and 0.8

ii) 2 speed with ratios of 2 and 0.8 for the speed ranges 0-300 and 300-800 rad/s

The motor operation points for the 2 gear system are shown in Fig 7.7.

The results are summarized in Table 7.2 showing the relative energy consumptions for the different geared systems over the NEDC cycle. The improvements resulting from fitting an additional gearbox are actually rather modest over the NEDC cycle. The percentage improvements would, in practice, be immediately cancelled out by the additional efficiency losses in the gearbox itself, which have initially been ignored in this work.

One of the potential advantages of a geared transmission relates to possible improvements in drivability. For example, the 0 to 100 km/h acceleration time of the fixed gear vehicle is 18.3 s, whereas with just 2 gears, this time is reduced to 12.4 s. The top speed of 183 km/h of course remains unchanged.

Table 7.2 Efficiency improvements for different gearboxes over the NEDC cycle

	Energy consumption per 100km (kWh/100km)	Improvement %
no gear	8.33	-
CVT	7.89	5.28
4 speed	7.96	4.45
3 speed	8.01	3.76
2 speed	8.10	2.71

This raises the possibility that one of the advantages of a simple geared system would be to downsize the motor, but still retain the same drivability characteristics. Whether this is a practical proposition will depend largely on the specific vehicle application, and the detailed properties of the motor selected relative to the critical vehicle properties of mass, rolling resistance and aerodynamic drag. For example, although the NEDC is widely used as a standard driving cycle, the peak power demanded from the motor is only 21.9 kW. In practice, the peak power of the

motor would have to be around double this value in order to provide a sufficiently high level of acceleration to meet customer demands.

7.3.4 Effect of drive cycle

One of the fundamental problems now facing the automotive industry in their quest to develop energy efficient vehicles is a methodology which enables robust comparisons of competing designs. The approach adopted to date has largely depended on standard driving cycles. This is defensible from a scientific point of view because vehicle designs are then compared under like-for-like input conditions. But one of the major issues is then what exactly constitutes typical driving cycles which somehow represent normal everyday driving? Inevitably, this has led to the development of many so-called standard driving cycles – and these to some extent do reflect different driving patterns in the three major world markets: Europe, USA and Far East.

Some idea of this problem is highlighted in Table 7.3, in which the EV results are repeated for six different driving cycles. These results are somewhat more promising. Over four of the six cycles, the improvement using continuously variable gearing is between 9.6 and 12.4%. Even though some of these efficiency gains would be lost through the losses in the transmission, there are still some worthwhile gains to be exploited. Of course, these would also be set against the additional cost, weight and complexity of the transmission system. However, small efficiency gains of this order would be seriously considered in IC engined vehicles – as part of the relentless quest for any efficiency gains possible. Hence, it is likely that as electric vehicles become more common, companies will be searching for all potential ways of improving efficiency.

The two most representative driving cycles are the Europe NEDC and the USA FTP-75; the Europe City and USA City 1 are actually only subsets of these longer cycles and the Japan cycles are rather short and simple. The results for the USA FTP-75 are rather promising; this cycle has less constant speed running and include more acceleration cycles up to the 40 to 50 km/h region. So the effect of the continuously variable gearbox over these conditions is to offer a greater improvement.

Table 7.3 Comparisons of improvements in energy consumption over 6 different driving cycles

Driving cycle	No gearbox	4 speed gearbox		Continuously variable gearbox	
	Energy consumption (kWh/100km)	Energy consumption (kWh/100km)	Improvement %	Energy consumption (kWh/100km)	Improvement %
Europe NEDC	8.33	7.96	4.5	7.89	5.3
Europe City	6.87	6.22	9.7	6.12	11.0
USA FTP-75	8.45	7.77	8.0	7.53	10.9
USA City I	9.06	8.43	7.0	8.19	9.6
Japan 11 mode	6.93	6.61	4.6	6.55	5.4
Japan 10 mode	7.20	6.41	11.0	6.31	12.4

7.4 Results with the practical motor

The vehicle parameters for the practical motor are summarised in Table 7.4. Compared with the parameters used for the previous motor, the vehicle is heavier and has bigger drag coefficient. This is because the data for the motor is from a 75 kW motor, which should be used on a larger vehicle. This does not affect the usefulness of the results, because the primary objective is to investigate the potential benefits of different transmissions in a typical EV application.

Table 7.4 Vehicle parameter data for the model with UQM motor

Parameter, units	Value
Total vehicle mass, kg	1200
Wheel diameter, m	0.5
Aerodynamic drag coefficient	0.3
Frontal area, m^2	2
Rolling resistance coefficient	0.008
Motor maximum torque, Nm	240
Motor maximum speed, rad/s	750
Motor power – continuous , kW	45
Motor power – maximum, kW	75

7.4.1 Results from simulations over the NEDC cycle

- **No gearbox**

The first set of results were all carried out using the NEDC driving cycle; this is remain the most commonly used driving profile used in Europe, although as observed previously considerable controversy surrounds the idea of what are claimed to be 'standard' driving cycles. The NEDC cycle and the resulting torque demand or this vehicle are shown in Fig 7.8.

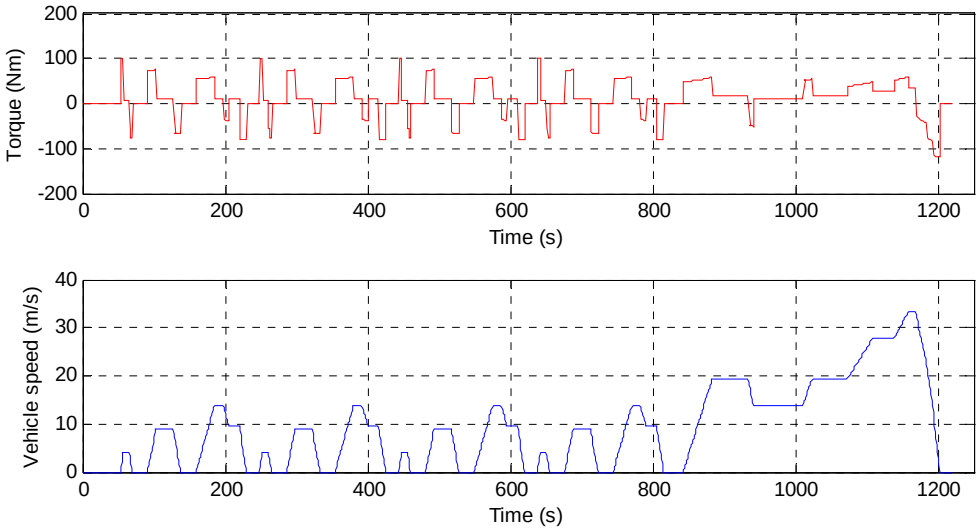

Fig 7.8 NEDC cycle – vehicle speed profile and required torque at the differential

The first phase of the NEDC cycle comprises four repeats of a 'city' phase, in which there are significant periods of low speed constant running. The second phase is intended to represent 'urban' driving and consists again of substantial periods of constant speed running, this time at higher speeds. The required torque figures at the input to the differential – assuming that the reduction gear would be incorporated here – emphasise the low torque requirement whenever the vehicle is running at constant speed.

For the conventional arrangement in which there is no gearbox, the choice of single reduction, final drive ratio is important; it is a compromise between acceleration performance – or more generally the whole feeling of drivability – and overall energy usage. Several final drive ratios were tested over the NEDC cycle and the results are shown in Table 7.5. The ratio of 3.5 was selected on the basis

of a fairly subjective judgement of minimising energy consumption whilst retaining reasonable acceleration capability

Table 7.5 Energy consumption over the NEDC cycle for different final drive ratios

Final drive ratio	Energy consumption per 100km (kWh/100km)
3	14.26
3.5	14.43
4	15.60
5	16.11

The motor operation points with no gearbox are shown in Fig 7.9.

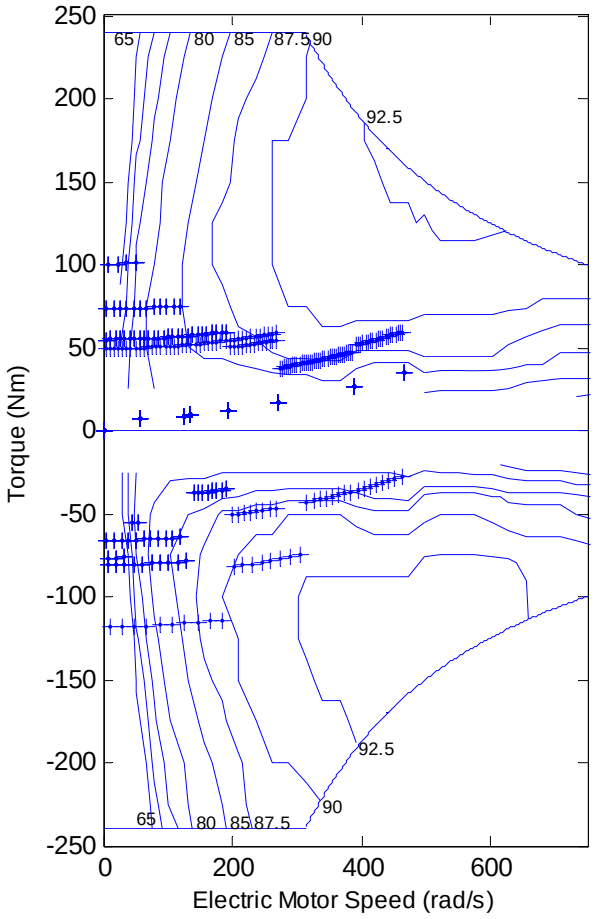

Fig 7.9 Motor operation points with no gearbox – NEDC cycle

Each point is the result of an individual calculation at 1s intervals. However, some care must be used when interpreting this graph because in the constant speed running conditions, the required tractive motor torque is constant – and so many points lie exactly on top of each other. Hence, the seven points of low torque

– below 25Nm – are actually much more significant than might appear, because each point actually represents several seconds of constant speed running; the exact data can be extracted from Fig 7.8. But these points are important in overall energy calculations because they all lie in a region of very low motor efficiency.

Of course, the overall effects on the total energy losses are a combination of the facts that although the motor efficiency is low, so too is the absolute value of torque delivered – hence the overall effect may not be as significant as it may first appear.

- **Continuously variable gearbox**

The NEDC cycle is then repeated assuming a continuously variable gearbox is fitted in the transmission, and the motor operation points are shown in Fig 7.10. These are simplified, idealised calculations ignoring at this stage any efficiency losses in the transmission itself.

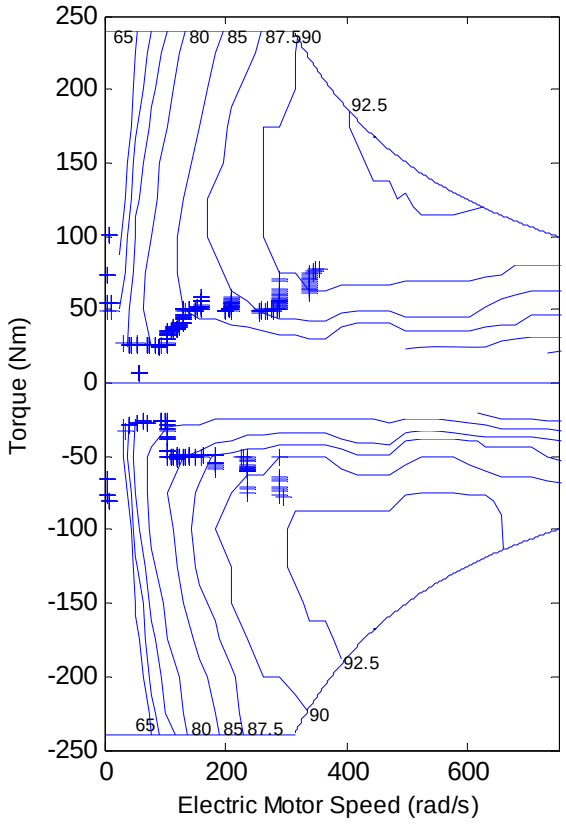

Fig 7.10 Motor operation points with a continuously variable gearbox – NEDC cycle

The calculations are based on the following procedure: for each torque demand sample the gear ratio is calculated which results in the motor torque and speed being optimised in terms of the motor operating efficiency. The calculation requires some interpolation of the motor data points which are shown as joined-up curves in Fig 7.10.

Thus, the overall approach is effectively a simple optimisation procedure, and the results in Fig 7.10 show how the points now congregate in the optimum motor efficiency region.

In practice, the gear ratio selection is a compromise between acceleration capability – more generally referred to as drivability – and energy usage or fuel consumption. This is, of course, the case for all vehicles, irrespective of their power source. Hence, two further sets of results to highlight the sensitivity of the gear ratio selection are shown in Fig 7.11 and Fig 7.12.

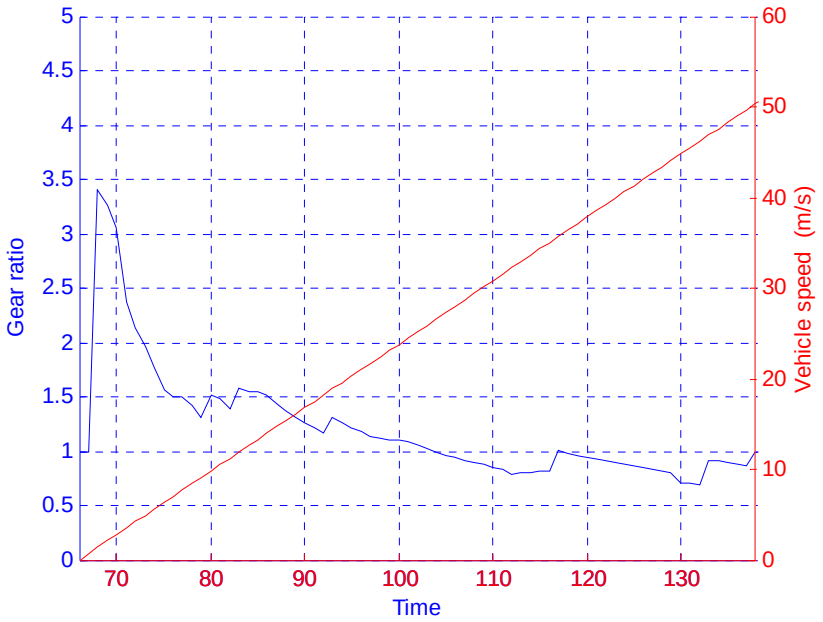

Fig 7.11 Gear ratio selection for maximum motor efficiency for a constant acceleration of 0.7 m/s^2

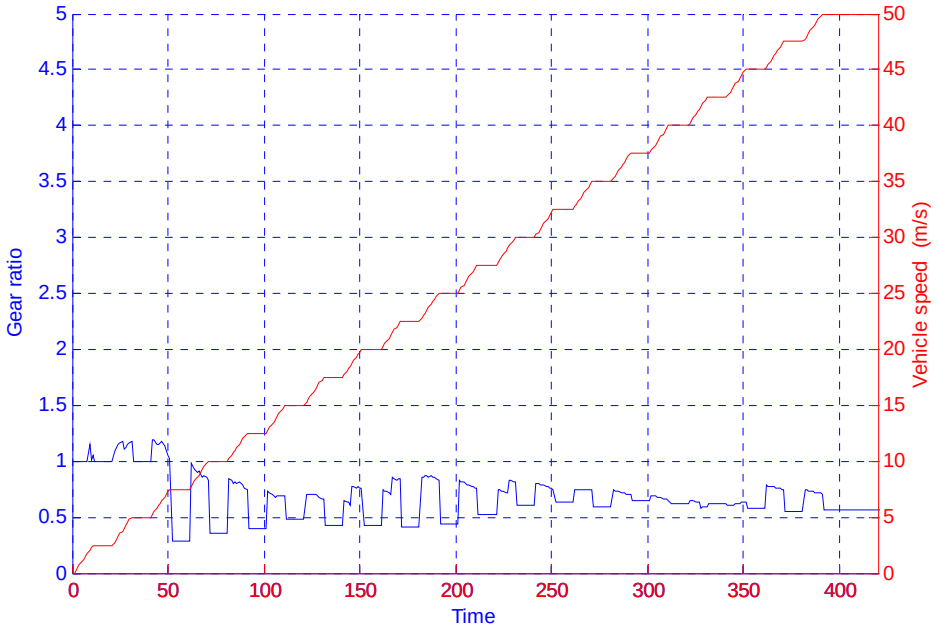

Fig 7.12 Gear ratio selection for maximum motor efficiency for increasing values of constant running speed

In Fig 7.11 the vehicle is assumed to start from rest and accelerate at a constant value of 0.7 m/s^2 up to its maximum speed. In Fig 7.12, the vehicle effectively does the same thing except that it also now includes a period of constant running at each increment of 2.5 m/s. At first sight the values for selected gear ratio are not as smooth as might be expected as the speed changes – but this is simply a result of the interpolation required on the motor torque/speed/efficiency map.

However, two important trends are highlighted; firstly, when accelerating, the selected gear ratio is nearly always around one – or higher at the lower speeds, and secondly, for the vast majority of the constant speed conditions the gear ratio is around the 0.5 figure. The implication is that for the NEDC cycle, a simple transmission which just has two ratios may offer a combination of mechanical simplicity and significant energy improvement.

This idea is then tested by plotting out a probability distribution for the gear ratios selected by the continuously variable gearbox strategy during the NEDC cycle (Fig 7.13). Each bar in Fig 7.13 represents a bandwidth of 0.4 of the gear

ratio distribution. These results suggest that a gearbox based on just two ratios of around 0.6 and 1 may offer benefits.

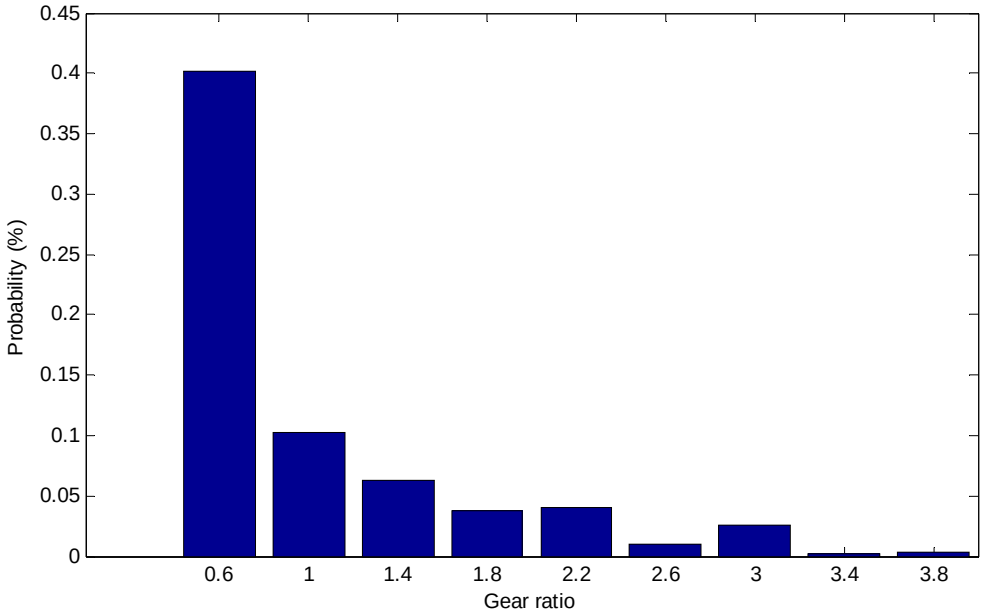

Fig 7.13 Gear ratio selection shown as a probability distribution over the NEDC cycle assuming a continuously variable gearbox

- **Four speed gearbox**

First however, the results are repeated assuming a rather conventional four speed gearbox with ratios of 0.5, 0.8, 1 and 1.5 is fitted. Again, it can be seen in Fig 7.14 that this results that motor operation points fairly well clustered around the optimum motor efficiency region.

The overall energy consumption results over the total NEDC cycle are compared with those for the continuously variable gearbox in the top row of Table 7.6. The improvements over the no gearbox case are 18.7% for the CVT and 11.4% for the four speed gearbox. These are clearly very significant improvements, even allowing for the mechanical efficiencies of the gearbox in practice.

Table 7.6 Comparisons of improvements in energy consumption over 6 different driving cycles

Driving cycle	No gearbox	Continuously variable gearbox		4 speed gearbox		2 speed gearbox (no acc: 0.5; acc: 1)	
	Energy consumption (kWh/100km)	Energy consumption (kWh/100km)	Improvement %	Energy consumption (kWh/100km)	Improvement %	Energy consumption (kWh/100km)	Improvement %
Europe NEDC	14.4	11.7	18.7	12.8	11.4	13.1	9.2
Europe City	9.7	8.5	12.3	9.3	3.7	9.7	0
USA FTP-75	13.2	10.7	19.2	12.3	6.8	12.6	4.1
USA City I	14.8	12.0	19.0	13.6	8.6	14.0	5.7
Japan 11 mode	10.4	9.3	10.6	9.7	6.8	9.9	5.4
Japan 10 mode	9.4	8.8	5.8	9.1	2.6	9.4	0

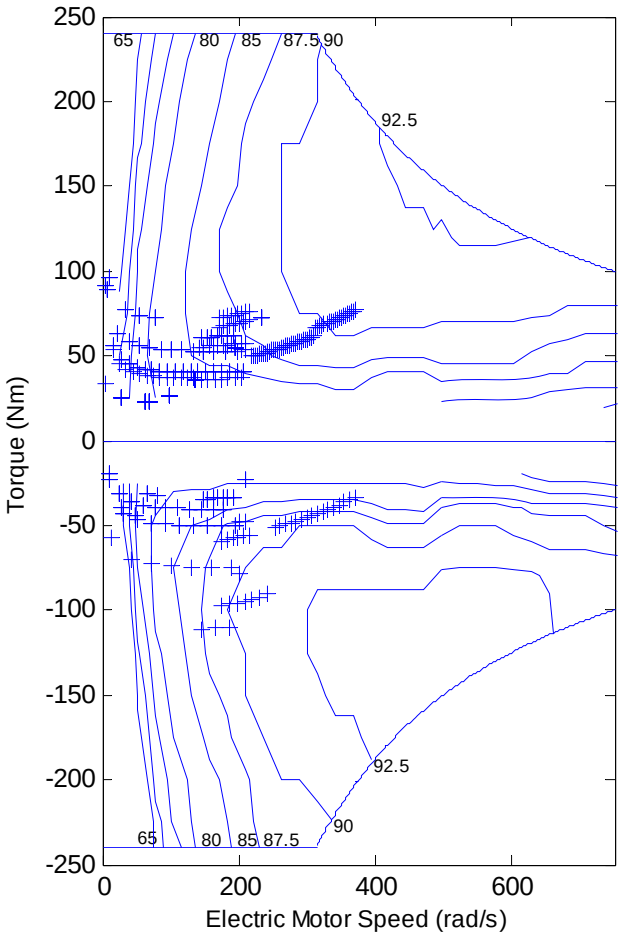

Fig 7.14 Motor operation points with a 4 speed gearbox – NEDC cycle

- **Two speed gearbox**

Next, the results are repeated for a two speed gearbox with ratios of 0.5 and 1. A very simple gear selection strategy is now used; for constant speed running the value of 0.5 is used and for all other conditions a value of 1 is selected.

The results in Fig 7.15 suggest that this approach leads to results similar to those obtained for the four speed case. And the results in Table 7.6 confirm this observation; the overall improvement for the two speed case is 9.2% compared with the 11.2% figure obtained for the four speed case and 18.7% for the CVT.

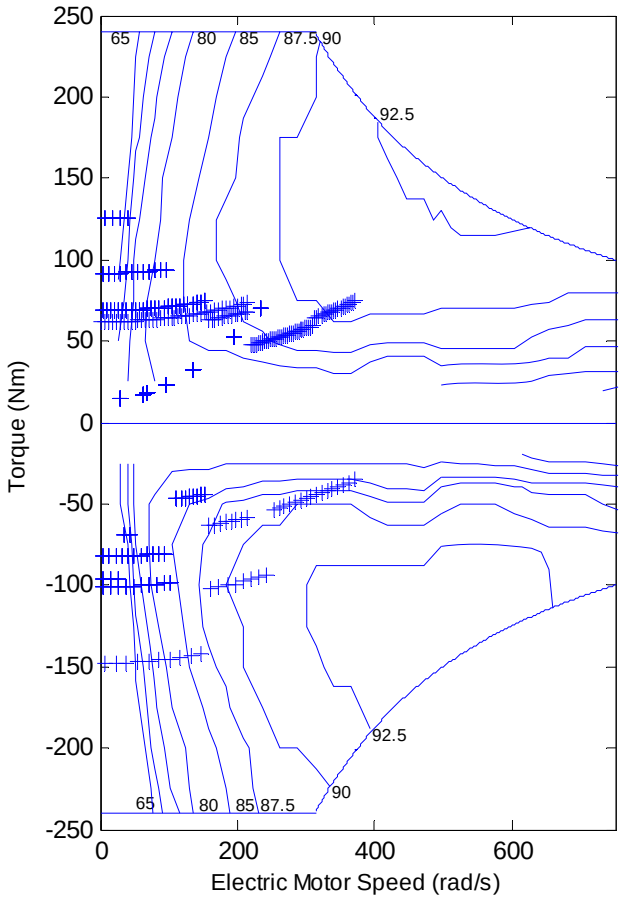

Fig 7.15 Motor operation points with a 2 speed gearbox – NEDC cycle

7.4.2 Simulation results for the USA FTP-75 cycle

- **No gearbox**

The USA FTP-75 driving cycle along with the required torque values for the vehicle data used in this study are shown in Fig 7.16. Although this is similar in length to the NEDC cycle, a major difference is apparent – it involves hardly any

constant speed running. The consequences of this are twofold; the improvement offered by the CVT remains substantial at 19.2%, but the improvements offered by the two and four speed gearbox cases are significantly less than for the NEDC conditions.

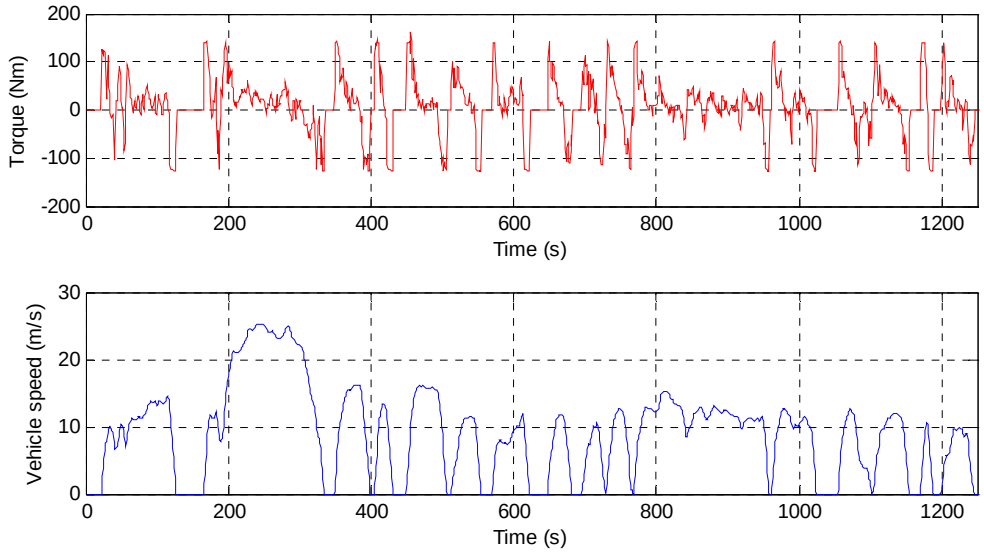

Fig 7.16 USA FTP-75 cycle – vehicle speed profile and required torque at the differential

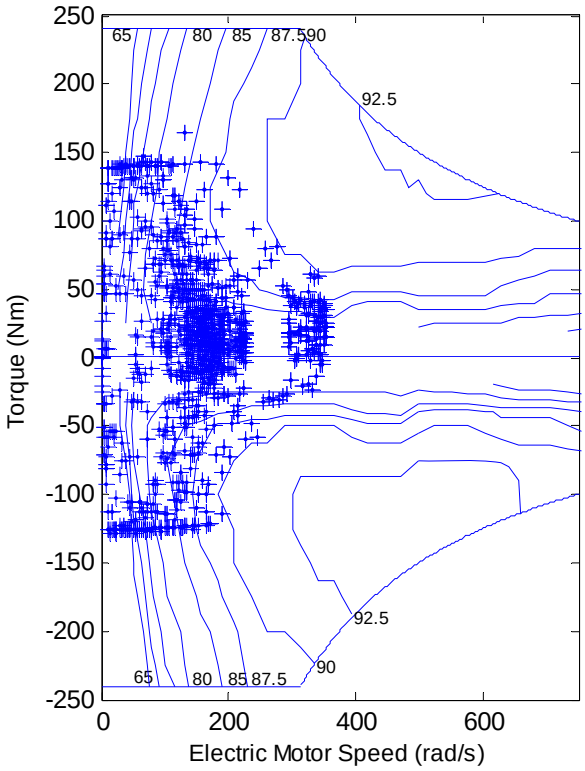

Fig 7.17 Motor operation points with no gearbox – USA FTP-75 cycle

These differences are seen more clearly, for example, in Fig 7.17 which plots the motor operation points with no gearbox. Because the required acceleration in the USA FTP-75 is continuously changing, the motor operation points are much more widely spread than those for the equivalent NEDC results in Fig 7.9.

- **CVT gearbox**

The results using the CVT arrangement are shown in Fig 7.18 and as before, it is clear how the simple optimisation strategy works in congregating the points around the optimum motor efficiency region.

Finally, in Fig 7.19, the probability distribution of gear ratios for the USA FTP-75 is plotted using a similar scale to the previous one (Fig 7.13) for the NEDC cycle. The spread of gear ratio usage throughout the cycle is shown to be significantly greater than that for the NEDC cycle.

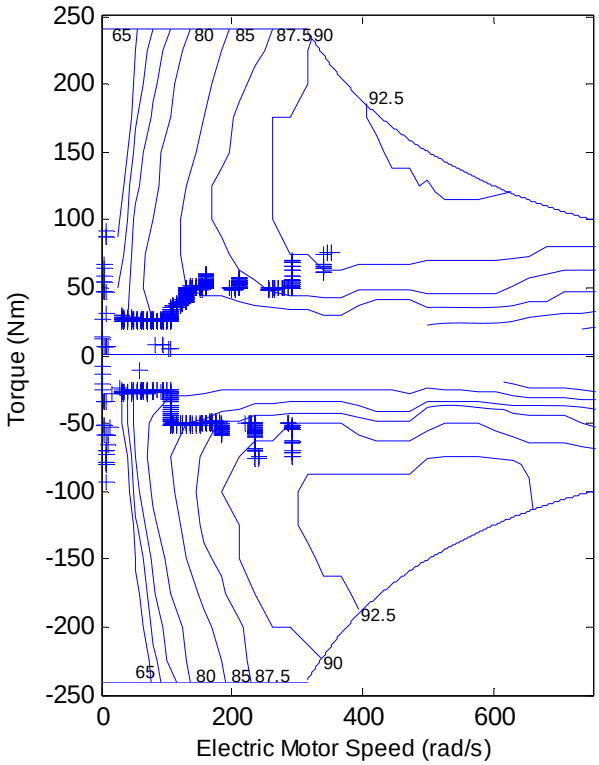

Fig 7.18 Motor operation points with a CVT – USA FTP-75 cycle

Overall, these results highlight one of the concerns facing the industry involved in low carbon vehicle technology. Whilst it is perfectly reasonable form a scientific viewpoint to compare competing schemes over a standard driving cycle so the vehicle powertrains are subjected to exactly the same requirements, it is also a

matter for debate as to what constitutes a reasonable and representative driving cycle. And a further complication is that the answer to this question is likely to be substantially different in different markets around the world. There are obvious difference between transportation systems and road infrastructures across the three major automotive markets – in Europe, USA and Far East. And already it can be observed that different 'standard' driving cycles have been recognized in these markets.

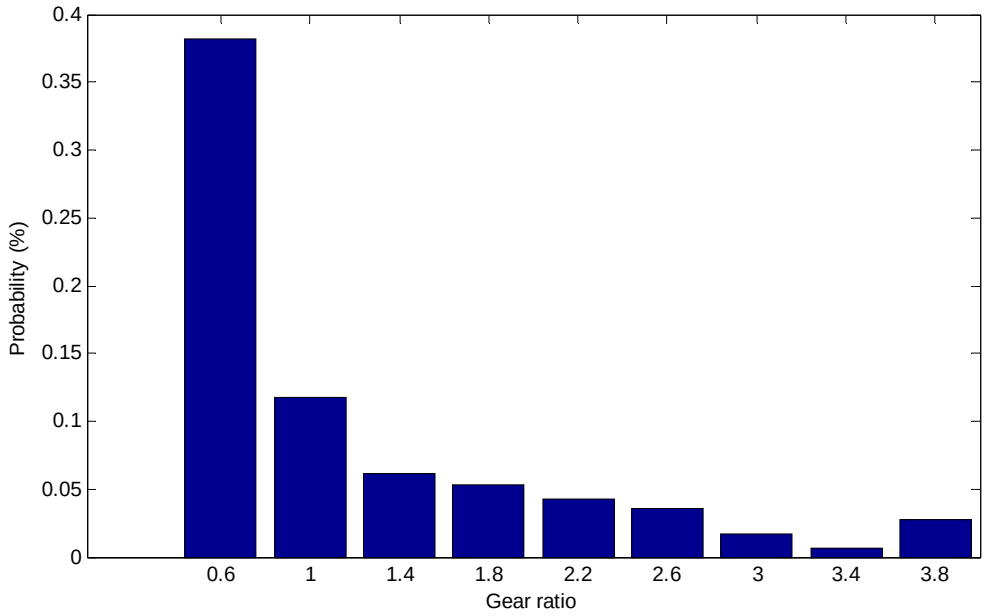

Fig 7.19 Gear ratio selection shown as a probability distribution over the USA FTP75 cycle assuming a continuously variable gearbox

7.4.3 Effect of driving cycle

The sensitivity of these results to different driving cycles is summarised in Table 7.6 using those cycles which are available in the QSS software. The results are rather variable: the CVT arrangement nearly always results in significant improvements – but the results for the two and four speed cases are not as promising.

The results highlight a major issue which is relevant to all the work on comparisons of alternative propulsion systems – the energy usage results are highly sensitive to the driving cycle used. This conclusion emphasises the need for extreme caution in interpreting claimed improvements with competing systems for energy efficient vehicles.

For the results calculated here, the NEDC and USA FTP-75 cycles are probably the two most representative cycles involving a combination of city and urban driving over a substantial period. The Europe City and USA City are actually subsets of these cycles and the Japanese cycles are very short and simple.

7.4.4 Comparison of the results from two motors

The results of energy consumption for the vehicle with a generic motor are shown in Table 7.3. The results of energy consumption for the vehicle with a practical motor are shown in Table 7.6. The next stage is to analyze the difference between the two motors.

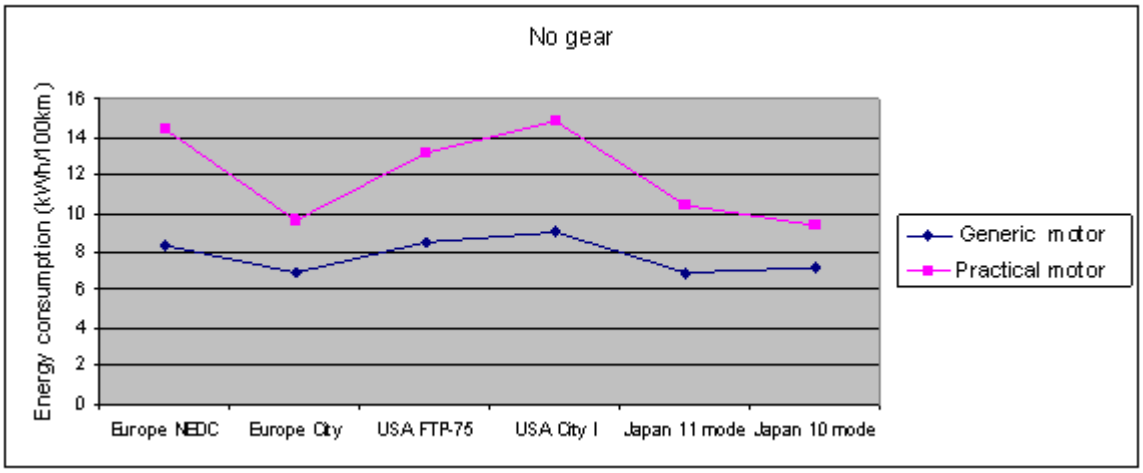

Fig 7.20 Comparison of energy consumption

Fig 7.20 shows the energy consumption for the two motors over 6 driving cycles. The vehicle with the practical motor has higher energy consumption than the vehicle with the practical motor. This is simply because some of the vehicle parameters are different (Table 7.1 and Table 7.4). But the trends over driving cycles are the same – USA City I is the highest and Europe City is the lowest.

It is obvious that, for both the generic motor and the practical motor, the vehicle with a CVT has higher improvement than the vehicle with a 4 speed gear box, which is shown in Fig 7.21 and Fig 7.22. This is because with a CVT, more freedom of selecting the highest efficiency operation point is available.

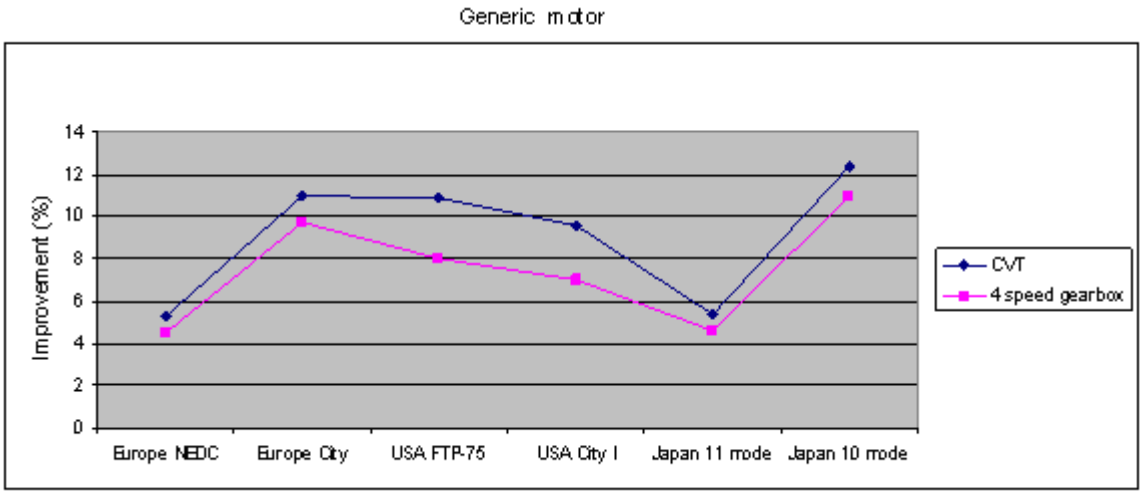

Fig 7.21 Comparison of the generic motor with a CVT and a 4 speed gearbox

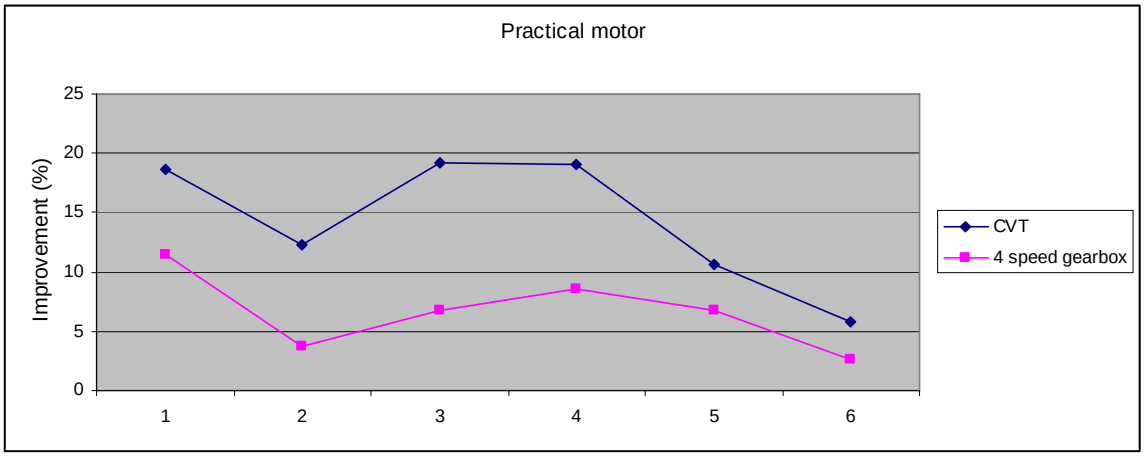

Fig 7.22 Comparison of the practical motor with a CVT and a 4 speed gearbox

The average improvement over 6 driving cycles for vehicles with different combination of a transmission and a motor is shown in Table 7.7. The average improvement of for vehicles with the two motors ranges from 6.7% to 14.3%.

Table 7.7 The average improvement over 6 cycles

	CVT	4 speed gearbox
Generic motor	9.1%	7.5%
Practical motor	14.3%	6.7%

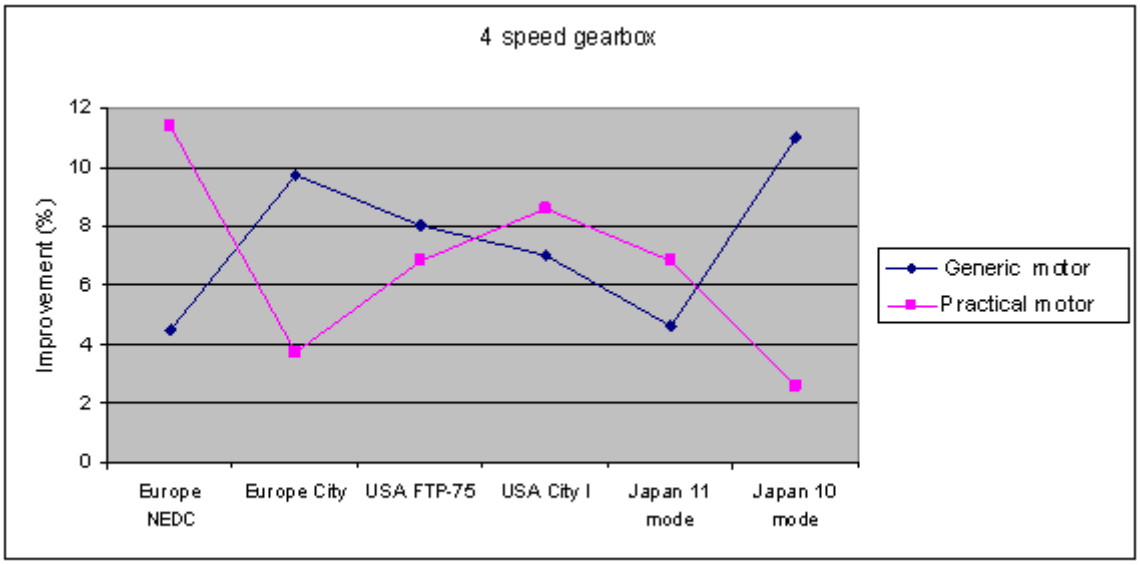

Fig 7.23 Improvement with a 4 speed gear box

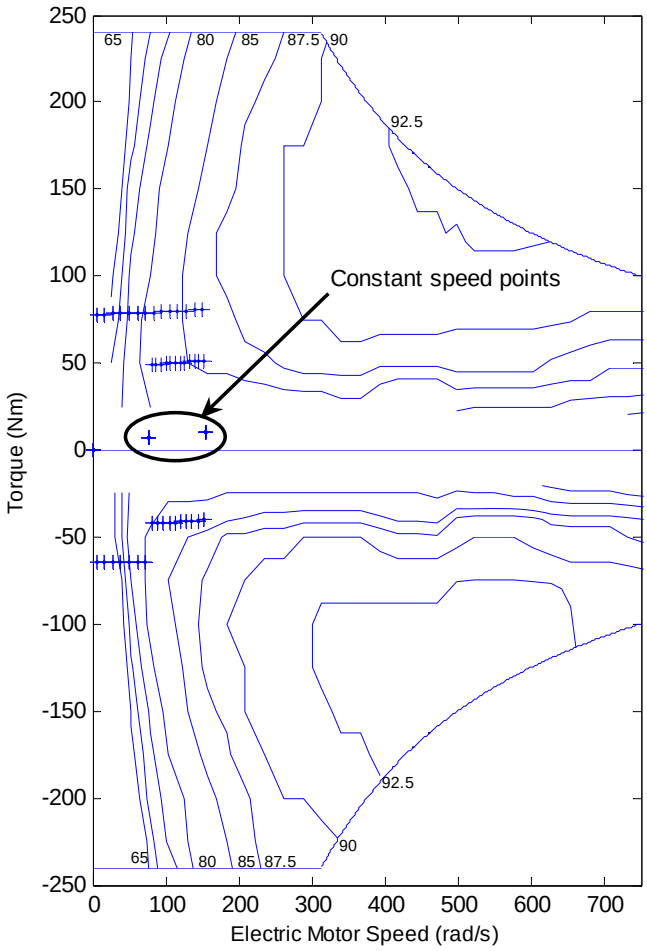

Fig 7.24 Motor operation points with no gearbox – Japan 10 mode

Fig 7.23 shows the improvement with a 4 speed gearbox with different motors. From this it can be seen that the vehicle with the practical motor over the Japan 10 mode has the lowest improvement. This is because for the practical motor, at the areas where speed or torque is near zero, data for the motor efficiency are not available. In these areas, the efficiency is all set to be 0.5. For some operation points where the required power (speed times torque) is too low, it is possible that along the constant power line, all 4 operation points with the 4 gear ratios falls into that area. So there is no improvement as a result of moving the operation points. Among the 6 driving cycles, the Japan 10 mode has the lowest maximum constant speed (40km/h). All of its constant speed points fall into the constant efficiency area, as shown in Fig 7.24. This leads to the result that the vehicle with the practical motor and a 4 speed gearbox has the lowest improvement over the Japan 10 mode cycle.

Fig 7.25 shows the improvement with a CVT over the fixed single gear ratio case. In this case, there is a slight trend to suggest that the practical motor offers greater advantages compared with the generic motor assumptions.

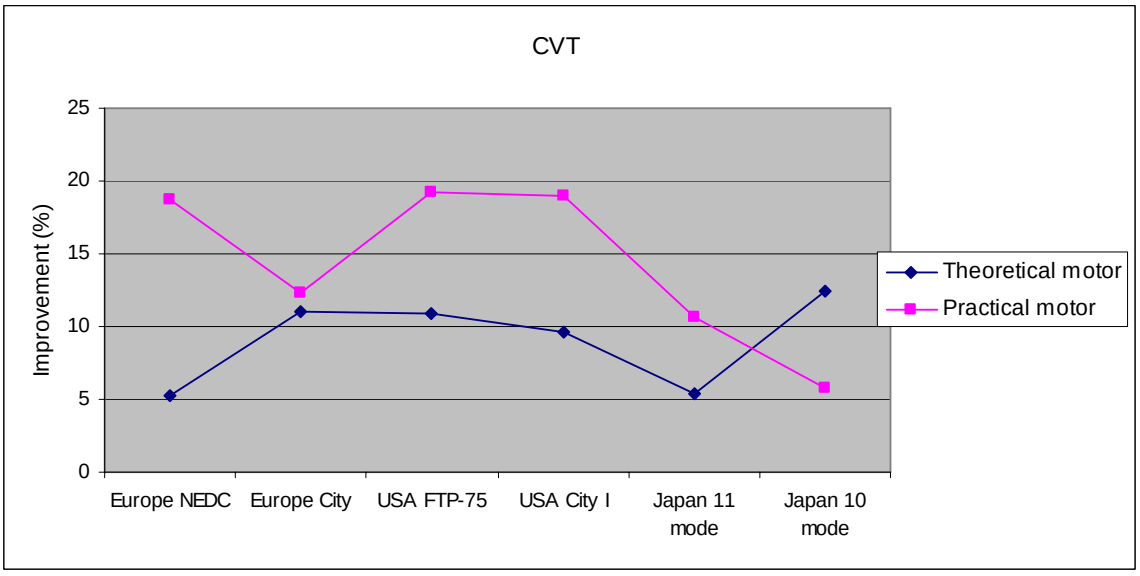

Fig 7.25 Improvement with a CVT

7.5 Effect of drivability

The consumer acceptance of alternative powertrains depends on much more than just the headline economy figure and society's reaction to the feeling of contributing to the green economy. Vehicles still need to be pleasurable, convenient and satisfying to drive. Many of these aspects of driving dynamics are

captured under the title of ‘drivability’. Attempts have been made to quantify aspects of drivability and to a limited extent this has proved possible by defining new metrics. However, the interesting but elusive feature of drivability is that much of the assessment is based on qualitative judgements and the subjective impressions of the driver.

One of the challenges facing the industry is temptation to optimise their design around achieving a top result in the driving cycle test – thus resulting in leading headline figures for fuel economy and carbon dioxide usage. Overall, this is clearly not a desirable situation – when the nature of the test procedure actually drives the engineering development of the vehicle. It also raises another major area for research into energy efficient vehicles – referred to as ‘drivability’. This term is used to cover an extensive range of vehicle properties which result in the drivers’ satisfaction levels with the car. The future work could focus the drivability of electric vehicles with different transmissions.

7.6 Concluding remarks

There are several promising outcomes form this work listed below; these must be interpreted in the context of the modeling approach used. The analysis has been kept at a very simple level in order to gain an initial understanding of whether the introduction of a geared transmission into an electric drivetrain offers any potential. The next step could be to develop a more rigorous model of the vehicle and powertrain system to confirm the initial promising predictions.

Several conclusions may be drawn, some more positive than others:

- For the vehicle with a generic motor, using the NEDC cycle the efficiency improvement assuming a continuously variable gearbox is fitted is only 5.3% for the typical generic vehicle used. In practice, the losses in the transmission would counteract these gains, so the net result would be zero.
- However, using the USA FTP-75 cycle which has a different balance between accelerating and constant speed running, the gain is predicted as 10.9% - a much more promising figure even accounting for transmission losses.

- For the vehicle with a practical motor, the use of a continuously variable gearbox in an electric drivetrain offers substantial improvements over the conventional arrangement of a single reduction gear; over the NEDC and USA FTP-75 cycles the improvements are 18.7% and 19.2 % respectively.
- Using a simple two speed gearbox offers a worthwhile performance improvement of around 9.2% over the NEDC cycle, but a much smaller gain with the USA FTP-75 cycle which involves much less constant speed running.
- Other potential benefits of a transmission system may be in overall drivability and the potential to downsize the motor somewhat whilst retaining acceleration capability for the limited times that maximum acceleration is required.
- Overall, this simplified modeling suggests that the idea of using a geared transmission in an electric vehicle is worthy of further research using a more sophisticated driveline model and attempting to quantify both efficiency gains and drivability improvements.

8 Conclusions and future work

8.1 Summary and conclusions

Overall, the thesis has shown that there are worthwhile performance advantages available through improved transmission designs for both HEVs and EVs. For example, this thesis has shown that the novel twin epicyclic gearbox for hybrid electric vehicles has some performance advantages over the single epicyclic gearbox which has been used successfully, for example, in the Toyota Prius. An HEV with a twin epicyclic gearbox was predicted to have lower fuel consumption than a HEV with a single epicyclic gearbox whilst retaining good drivability. In addition, research in this thesis has shown that an EV with a stepped or variable transmission can result in significant improvements in overall performance compared with an EV without a transmission.

The research work has resulted in several papers published at international conferences and these are referenced within this conclusion section.

In Chapter 2, previous work on HEVs, EVs, transmission designs and control strategies are reviewed. With the rise of awareness of sustainable development, interest in HEVs and EVs has increased rapidly over recent years. As an important part of the powertrain, transmissions for HEVs have been an area of rapidly changing technology, whilst transmissions for EVs have received surprisingly little attention. The performance of a HEV is heavily dependent on its control strategy. Three generic types are likely to have a future in the short to medium term: rule based, which is at the heart of most practical and prototype systems; equivalent energy methods and dynamic programming, which are mostly used in simulation and are useful in informing rule based system design (Crolla, Ren et al. 2008).

In Chapter 3, the twin epicyclic transmission, together with its counterpart – the single epicyclic transmission is analyzed in detail. The matrix method is chosen in this research to analyze the epicyclic transmissions. The speeds and the torques for each component in the twin and single epicyclic gearbox are analyzed and the relationships of MG1 and MG2 with the engine and the output shaft are given. A software package to analyse epicyclic transmissions, especially transmissions for

hybrid vehicles is developed and examples of using the software are given (Ren, Crolla et al. 2007a).

The behaviors of the single and twin epicyclic transmissions are compared in Chapter 4. A simple vehicle model is developed and two driving conditions are included: constant speed running and constant acceleration at 0.8 m/s^2. The different torque and power splits for the single and twin epicyclic transmissions are compared. The results confirm the limitations of the single epicyclic gearbox which has a fixed ratio of torque to the wheel vs. torque to the generator. In contrast, for the twin epicyclic gearbox, this ratio can be changed. So for the twin epicyclic gearbox, less percentage of engine power is transmitted via electrical path, which means less energy is wasted. Also, there is one node point for the single epicyclic gearbox, while there are two node points for the twin epicyclic gearbox. The control strategy can be tuned to exploit these points of higher transmission efficiency. Finally, the powers of electric machines (MG1 and MG2) for the twin epicyclic gearbox shown to be smaller than those for the single epicyclic gearbox. This provides a possibility of downsizing the electric machines and reducing the overall system cost and complexity (Ren and Crolla 2007b).

In Chapter 5, three vehicle models have been developed; a conventional IC engine vehicle with a manual gear box, an HEV with a single epicyclic gearbox, and an HEV with a twin epicyclic gearbox (Ren, Crolla et al. 2007c). The models were derived using a combination of the QSS toolbox together with additional Matlab/Simulink blocks. In this approach, it was convenient to use the QSS software for some of the straightforward subsystems such as the IC engine and battery, whereas new Simulink blocks were written for more specialized subsystems such as the epicyclic gearboxes.

For the hybrid electric vehicle models, a total of eight driving modes were identified. In addition, for the HEV model with the twin epicyclic gearbox, one more mode was added to make a good use of the additional node point. Rule based control strategies were derived for both the single and dual epicyclic gearbox cases. For the modelling of the motor generator units, it was found that the QSS software experienced difficulties at very low torques, so a new Simulink S function approach was proposed to overcome this problem.

Comparisons of HEVs fitted with single and dual epicyclic transmissions were described in Chapter 6. Vehicle models built in Chapter 5 were run over 6 different driving cycles. For the fuel consumption, the twin epicyclic gearbox arrangement offers significant performance benefits over the three branch, single epicyclic arrangement; fuel economy improvements between 7 to 20% were shown over the two main European and USA driving cycles. The increased performance benefits during the USA FTP-75 cycle are thought to be due mainly to the increased use of the twin epicyclic high efficiency mode (mode 9). The performance benefits arise from the greater flexibility of control over the torques, speeds and power flows through the two motor generator units available with the dual epicyclic scheme (Ren, Crolla et al. 2009a; Ren, Crolla et al. 2009b).

In terms of overall vehicle performance, if the engine is not downsized, HEVs have better performance, namely higher top speed and shorter acceleration time. HEVs have higher energy consumption sensitivity to aggressive driving compared to the traditional ICE vehicles. And the HEV with the twin epicyclic system was shown to be less sensitive to driving aggressiveness than the single epicyclic system. This was shown to occur because it can control the power flows according to different driving conditions.

In practice, further benefits are available; first, the dual arrangement has two nodal positions at which zero electrical power circulates and these can be designed to occur at convenient speeds, e.g. in the UK, 30 mile/h in urban driving and 70 mile/h motorway cruising. Second, with the dual arrangement it is possible to downsize the motor generator units to retain the same driveability but with reduced weght and cost. Further research work is suggested to explore these benefits along with optimsation strategies for the control system.

In Chapter 7, electric vehicles without a gearbox, with a continuously variable transmission (CVT) and with a 4 speed gearbox were modeled. Two types of motors were used in the models: a generic motor and a practical motor. This approach of repeating the results with two motors was pursued to investigate how sensitive the predicted results using a gearbox are to the detailed motor efficiency map, because the motor efficiency map is a crucial element of the assumptions used. For vehicle models with different motors, simulations of energy consumption

were carried out over 6 typical driving cycles and the results were compared and analyzed (Ren, Crolla et al. 2009b).

The analysis was intentionally kept at a simple level in order to gain an initial understanding of whether the introduction of a geared transmission into an electric drivetrain offers any potential. The next step would be to develop a more rigorous model of the vehicle and powertrain system to confirm the initial predictions.

For the vehicle with the assumption of a generic motor, using the NEDC cycle the efficiency improvement assuming a continuously variable gearbox is fitted is only 5.3% for the typical generic vehicle used. In practice, the losses in the transmission would counteract these gains, so the net result would be zero. However, using the USA FTP-75 cycle which has a different balance between accelerating and constant speed running, the gain is predicted as 10.9% - a much more promising figure even accounting for transmission losses.

For the vehicle with the data from a practical motor, the use of a continuously variable gearbox in an electric drivetrain offers substantial improvements over the conventional arrangement of a single reduction gear; over the NEDC and USA FTP-75 cycles the improvements are 18.7% and 19.2% respectively. Using a simple two speed gearbox offers a worthwhile performance improvement of around 9.2% over the NEDC cycle, but a much smaller gain with the USA FTP-75 cycle which involves much less constant speed running (Ren, Crolla et al. 2009c).

Overall, the novel aspects of the work are: the analysis and modelling the twin epicyclic gearbox; the analysis and modelling of the twin epicyclic system in a vehicle and a comparison of the results with single epicyclic system; and the anlysis and modelling of EVs with and without a transmission system of varying levels of complexity. The conclusions of the research have met the original aim and objectives. The overall performance benefits of equipping HEVs and EVs with different transmissions has been predicted to offer significant benefits in energy consumption over typical driving cycles.

8.2 Future work

The future work could focus on other potential benefits of a transmission system, for instance, the drivability of an HEV and an EV with different transmissionlayout. Examples of the subjective terms used to assess drivability are; idle conditions,

launch feel, ‘throttle’ response and feel, cruise stability, tip-in, tip-out, shunt oscillations, brake feel and brake blending with regeneration etc. There is clearly a future research opportunity to investigate whether there are robust relationships between measurable vehicle properties and the subjective assessments of drivers, and also the effect of different transmissions on the drivability.

Another potential benefit of transmission systems for HEVs and EVs which could be investigated is whether it is possible to downsize the motor while retaining acceleration capability for the limited times that maximum acceleration is required. The simplified modeling in this research suggests that the idea of using a geared transmission in an electric vehicle will improve the fuel consumption. In the future work, a more sophisticated driveline model, for example, taking into consideration the driveline dynamics including, for example, the reaction time of the motor/generator, could be built up, and the research could focuse on attempting to quantify both efficiency gains and drivability improvements.

References

Ahn, K., S. W. Cha, et al. (2007). Three Types of Simulation Algorithms for Evaluating the HEV Fuel Efficiency. SAE Paper 2007-01-1771.

Argonne (2007). Power Systems Analysis Toolkit (PSAT), Argonne National Laboratory. 2007.

Arsie, I., M. Graziosi, et al. (2004). Optimization of Supervisory Strategy for Parallel hybrid Vehicle with Provisional Load Estimate. AVEC'04.

Ayers, C. W., J. S. Hsu, et al. (2004). Evaluation of 2004 Toyata Prius hybrid electric drive system interim report, Oak Ridge National Laboratory.

Babik, B. (2006). Advanced Technology and Energy Strategies, General Motors.

Baumann, B. M., G. Washington, et al. (2000). "Mechatronic design and control of hybrid electric vehicles." IEEE/ASME Trans. Mechatronics 5(1): 58-72.

Benford, H. and M. Leising (1981). "The Lever Analogy: A New Tool in Transmission Analysis." Society of Automotive Engineers.

Cacciatori, E., B. Bonnet, et al. (2005a). Regenerative braking strategies for a parallel hybrid powertrain with a torque-controlled IVT. Powertrain and Fluid Systems Conference, Texas.

Cacciatori, E., B. Bonnet, et al. (2005b). Launch and drivability performance enhancement for a parallel hybrid vehicle with a torque-controlled IVT. Powertrain and Fluid Systems Conference, Texas.

Chan, C. C. (2007). "The State of the Art of Electric, Hybrid, and Fuel Cell Vehicles." Proc IEEE 95(4): 704-718.

Chan, C. C. and K. T. Chau (2001). Modern electric vehicle technology, Oxford University Press.

Chau, K. T. and C. C. Chan (2007). "Emerging energy efficient technologies for hybrid electric vehicles." Proc IEEE 95(4): 821-835.

Chau, K. T. and Y. S. Wong (2002). "Overview of power management in hybrid electric vehicles." Energy Conversion Management 43: 1953-1968.

Cho, B. and N. D. Vaughan (2006b). "Dynamic Simulation Model of a Hybrid Powertrain and Controller Using Co-Simulation- Part II: Control Strategy." International Journal of Automotive Technology 7: 785-793.

Cho, S., K. Ahn, et al. (2006a). "Efficiency of the planetary gear hybrid powertrain." J Automobile Engineering 220 Part D: 1445-1454.

Cole, A. C. and D. Amann (2009). Unravelling and resolving hybrid electric vehicle design conflicts. Low-carbon vehicles 2009, London, Institute of Mechanical Engineers.

Corey, C. A. (2003). Epicyclic Gear Train Solution Techniques with Application to Tandem Bicycling, Virginia Polytechnic Institute.

Crolla, D. A., Q. Ren, et al. (2008). Controller design for hybrid vehicles - State of the art review. IEEE Vehicle Power and Propulsion Conference (VPPC), Harbin, China.

Delprat, S., T. M. Guerra, et al. (2001). Optimal control of a parallel powertrain: from global optimization to real time control strategy. 18th International Electric Vehicle Symposium, Berlin, Germany.

Delprat, S., T. M. Lauber, et al. (2004). "Control of a parallel hybrid powertrain; optimal control." IEEE Trans on Vehicular Technology 53: 872-881.

Ehsani, M., Y. Gao, et al. (2004). Modern electric, hybrid electric and fuel cell vehicles. Florida, CRC Press.
Ehsani, M., Y. Gao, et al. (2007). "Hybrid Electric Vehicles: Architecture and Motor Drives." Proceeding of the IEEE 95(4).
ExxonMobil (2007). New Outlook for Energy: A View to 2030. Texas, ExxonMobil.
Friedman, D. (2003). A New Road: the technology and potential of hybrid vehicles. UCS publications, The Union of Concerned Scientists Report.
Gao, D. W., C. Mi, et al. (2007). "Modeling and Simulation of Electric and Hybrid Vehicles." Proc IEEE 95(4).
Gelb, G. H., N. A. Richardson, et al. (1971). "Electromechanical Transmission for Hybrid Vehicle Power Trains - Design and Dynamometer Testing (TRW Systems Group)." SAE Paper 710235.
Genta, G. and L. Morello (2008). The Automotive Chassis Volume2: System Design, Springer.
Gonder, J., T. Markel, et al. (2007). Using GPS Travel Data to Assess the Real World Driving Energy Use of Plug-In hybrid Electric Vehicles (PHEVs). Washington, Transportation Research Board,86th Annual Meeting.
Grewe, T. M., B. M. Conlon, et al. (2007). Defining the General Motors 2 mode hybrid transmission. SAE Paper 2007-01-0273.
Guzzella, L. and A. Amstutz (2005). "The QSS Toolbox Manual."
Guzzella, L. and A. Sciarretta (2007). Vehicle propulsion systems introduction to modeling and optimization. Berlin, Springer.
Hirsch, R. L., R. Bezdek, et al. (2005). Peaking of World Oil Production: Impacts, Mitigation & Risk Management.
Hofman, T., M. Steinbuch, et al. (2007a). "Rule-based energy management strategies for hybrid vehicles." Int. J. Electric and Hybrid Vehicles 1(8): 71-94.
Hofman, T., M. Steinbuch, et al. (2007b). Rule-Based Equivalent Fuel Consumption Minimization Strategies for Hybrid Vehicles. 17th IFAC World Congress.
Honeywill, T. (2009). "Electricis get teeth." Automotive Engineer(June 2009): 41.
Hung, Y. H., J. F. Tsai, et al. (2007). On-line Suboptimal Control Strategies for a Power-assist hybrid Electric Vehicle. SAE Technical Paper 2007-01-0275.
Husain, I. (2003). Electric and hybrid vehicles; design fundamentals., CRC Press.
IME (2009). Brochure for Integrating Technologies for Low Carbon. Integrating Technologies for Low Carbon, Norfolk, Institution of Mechanical Engineers.
Inoue, T., M. Kusada, et al. (2000). Improvement of a highly efficient hybrid vehicle and integrating super low emissions. SAE Paper 2000-01-2930.
IPIECA (2004). Transportation and climate change: opportunities, challenges and long-term strategies. AN IPECA workshop, Baltimore, USA.
Ippolito, L., V. Loia, et al. (2003). "Extended Fuzzy C-Means and Genetic Algorithms to Optimize Power Flow Management in Hybrid Electric Vehicles." Fuzzy Optimization and Decision Making 2: 359-374.
Kheir, N. A., M. A. Salam, et al. (2004). "Emissions and Fuel Economy Trade-Off for Hybrid Vehicles Using Fuzzy Logic." Mathematics and Computers in Simulation 66: 155-172.
Kim, D.-H., J. M. Kim , et al. (2007). "Optimal brake torque distribution for a four-wheel drive hybrid electric vehicle stability enhancement." Proc. IMechE, Part D: J Automobile Engineering vol. 221: 1357-1366.
Koot, M., J. T. B. A. Kessels, et al. (2005). "Energy Management Strategies for Vehicular Electric Power Systems." IEEE Transactions on Vehicular Technology 54(3).

Larminie, J. and J. Lowry (2003). Electric vehicle technology explained. West Sussex, England, J. Wiley.
Lin, C.-C., Z. Filipi, et al. (2004). "Modelling and Control of a medium-duty hybrid electric truck. Heavy Vehicle Systems." Int. J. of Vehicle Design 11(3/4): 349-370.
Lin, C.-C., Z. Filipi, et al. (2001a). Integrated, Feed-Forward Hybrid Electric Vehicle Simulation in Simulink and its Use for power Management Studies. SAE Paper No. 2001-01-1334.
Lin, C.-C., J.-M. Kang, et al. (2001b). Energy management strategy for parallel hybrid truck. Proc American Control Conf, Arlington.
Lin, C.-C., J.-M. Kang, et al. (2003). Energy Management Strategy for a Parallel Hybrid Electric Truck. Proc American Control Conf, Arlington.
Lin, C.-C., M.-J. Kim, et al. (2006). "System-Level Model and Stochastic Optimal Control for a PEM Fuel Cell Hybrid Vehicle." Trans ASME, Journal of Dynamic Systems, Measurement, and Control 128.
Manzie, C., H. Watson, et al. (2007). "Fuel Economy Improvements for Urban Driving: Hybrid vs. Intelligent Vehicles." Transportation Research Part C 15: 1-16.
Markel, T., A. Brooker, et al. (2002). "ADVISOR: A systems analysis tool for advanced vehicle modelling." J Power Sources 110(2): 255-266.
Mashadi, B. and A. M. Emadi (2009). Dual-mode power split system for hybrid vehicles. IEEE Transactions on Mechatronics.
Mi, C., Y. Zhang, et al. (2003). "Dynamic Modeling and Simulation of Hybrid Electric Vehicles."
Miller, J. M. (2004). Propulsion systems for hybrid vehicles. Stevenage, Herts, UK, Institution of Electrical Engineers.
Miller, J. M. (2006). "Hybrid Electric Vehicle Propulsion System Architectures of the e-CVT Type." IEEE Transactions on Power Electronics 21: 756-767.
Miller, J. M. and J. N. J. Miller (2005). "Comparative Assessment of Hybrid Vehicle Power Split Transmissions."
Moeller, F. (2005). Automotive vehicle transmmission systems. USA.
Moeller, F. (2006). Power combining single regime transmissions for automotive vehicles. IMechE Integrated Powertrain and Driveline Systems Conference, London.
Montazeri-Gh, M., A. Poursamad, et al. (2006). "Application of genetic algorithm for optimization of control strategy in parallel hybrid electric vehicles." Journal of the Franklin Institute 343: 420-435.
Musardo, C., G. Rizzoni, et al. (2005). A-ECMS: An Adaptive Algorithm for Hybrid Electic Vehicle Energy Management. 44th IEEE Conference on Decision and Control and the European Control Conference, Seville, Spain.
Nitz, L. (2006a). General Motors innovative hybrid and two mode hybrid systems. FISITA 2006 Conf, Yokohama, Japan.
Nitz, L., A. Truckenbrodt, et al. (2006b). "The new two mode hybrid system for the global cooperation. 27th International Vienna Motor Symposium." Reihe 12(622).
Oh, K., J. Min, et al. (2007). "Optimization of Control Strategy for a single-shaft parallel Hybrid Electric Vehicle." Proc. IMechE, Part D: J Automobile Engineering 221.
Paganelli, G., G. Ercole, et al. (2001). "General Supervisory Control Policy for the Energy Optimization of Charge-Sustaining Hybrid Electric Vehicles." JSAE Review 22: 511-518.
Paganelli, G., T. M. Guerra, et al. (2000b). "Simulation and assessment of power control strategies for a parallel hybrid car." J Automobile Engineering 214(7): 705-717.

Perez, L. V., G. R. Bossio, et al. (2006a). "Optimisation of power management in a hybrid electric vehicle using dynamic programming." Maths and Computing in Simulation 173: 244-254.
Perez, L. V., G. R. Bossio, et al. (2006b). "Supervisory Control of an HEV Using an Inventory Control Approach." Latin American Applied Research 36.
Perez, L. V. and A. Pilotta (2007). "Optimal power split in a hybrid electric vehicle using direct transcription of an optimal control problem." Mathematics and Computers in Simulation.
Pisu, P. and G. Rizzoni (2007). "A Comparative Study of Supervisory Control Strategies for Hybrid Electric Vehicle." IEEE Transactions on Control Systems Technology 15(3).
Pu, J. and C. Yin (2007). "Optimal control of fuel economy in parallel hybrid electric vehicles." Proc IMechE, , Part D; Journal of Automobile Engineering 221(1097-1106).
Raghavan, M., N. Bucknor, et al. (2006). THE DESIGN OF ADVANCED TRANSMISSIONS. FISITA 2006.
Raghavan, M., N. Bucknor, et al. (2007). The algebraic design of transmissions and EVTs. SAE Paper 2007-01-1458.
Rajagopalan, A., W. G., et al. (2003). Development of Fuzzy Logic and Neural Network control and advanced emissions modelling for parallel hybrid vehicles, NREL Report SR-540-32919.
Randall, B. P. M. (2009). Electric cars - are they really 'green'? Low-carbon vehicles 2009, London, Institution of Mechanical Engineers.
Ren, Q. and D. A. Crolla (2007b). Analysis of a continuously variable transmission based on a twin epicyclic power split device. SAE 2007 Congress.
Ren, Q., D. A. Crolla, et al. (2009a). Effect of transmission design on Electric Vehicle (EV) performance. IEEE Vehicle Power and Propulsion Conference (VPPC), Dearborn, USA.
Ren, Q., D. A. Crolla, et al. (2009b). Performance comparisons of single and dual epicyclic power split transmissions for hybrid electric vehicles. EAEC 2009 Congress, Bratislava, Slovak Republic.
Ren, Q., D. A. Crolla, et al. (2009c). Effect of geared transmissions on electric vehicle drivetrains. ASME Design Engineering Technical Conference, San Diego, USA.
Ren, Q., D. A. Crolla, et al. (2007a). Power split transmissions for hybrid electric vehicles. EAEC 2007 Congress, Budapest.
Ren, Q., D. A. Crolla, et al. (2007c). Power management and control strategies for a hybrid vehicle with a dual mode power split transmission. Fifth IFAC Symposium on Advances in Automotive Control, California.
Rizzoni, G. (2000). Vp-Sim: a Unified Approach to Energy and Power Flow Modeling Simulation and Analysis of Hybrid Vehicles. Future Car Congress, April 2000, Session: HEV Modeling, Crystal City, VA, USA.
Rizzoni, G., L. Guzzella, et al. (1999). "Unified Modelling of Hybrid-Electric Vehicle Drivetrains." IEEE/ ASME Trans. Mechatronics 4(3): 246-257.
Salman, M., N. J. Schouten, et al. (2000). Control strategies for parallel hybrid vehicles. Proc. American. Control Conf.
Schultz, M. (2006). "Set values for a power split hybrid electric vehicle through numerical optimisation." Int J Alternative Propulsion 1(12): 6-61.
Schulz, M. (2004). "Circulating mechnaical power in a power-split hybrid electric vehicle transmission." ImechE 218: 1419-1425.

Sciarretta, A., M. Back, et al. (2004). "Optimal control of parallel hybrid electric vehicles." IEEE Trans. Control Systems Technology 12(2): 352-363.
Scordia, J., M. Besbois-Renaudin, et al. (2005). "Global optimization of energy management laws in hybrid vehicles using Dynamic Programming." Int. J. Veh. Design 39(4): 349-367.
Shabashevich, A., D. Saucedo, et al. (2007). Consumer Ready Plug-in Hybrid Electric Vehicle.
Sharer, P., R. Leydier, et al. (2007). Impact of Drive Cycle Aggressiveness and Speed on HEVs Fuel Consumption Sensitivity,, Argonne National Laboratory.
Stobart, R. and R. Chen (2009). Duty Cycles, Standardisation and Validation of Low Carbon Power Systems. Low Carbon Vehicle Power Systems?Delivering Next Generation Power seminar, MIRA Ltd.
Suzuki, M., S. Yamaguchi, et al. (2007). Fuel Economy Improvement Strategy for Light Duty Hybrid Truck based on Fuel Consumption Computational Model Using Neural Network. 17th IFAC World Congress.
Tian, L. and L. Lu (1997). "Matrix system for automatic vehicle transmission design." Journal of Mechanical Design 119: 333-337.
Van, M. J., G. Maggetto, et al. (2006). "Which energy source for road transport in the future? A comparison of battery, hybrid and fuel cell vehicles." Energy Conversion and Management 47: 2748-2760.
Vaughan, N. (2008). HEV systems overview, an intorduction to hybrid electric vehicles, Hybrid electric vehcle short course programme, Cranfield University.
Wang, L. (2005). Hybrid Electric Vehicle Design Based on A Multi-Objective Optimization Evolutionary Algorithm, Walter J. Karplus Summer Research Report.
Wei, X., L. Guzzella, et al. (2007). "Model-Based fuel Optimal Control of Hybrid Electric Vehicle Using Variable Structure Control Systems." Trans ASME, Journal of Dynamic Systems, Measurement and Control 129(13).
Westbrook, M. H. (2001). The electric and hybrid electric car. Warrendale, Pa.London, UK, Society of Automotive Engineers,The Institution of Electrical Engineers.
Williams, G. (2007). Function gjelim. http://www.dyu-.edu.tw/~lhuang/class/adv_lin_algebra/mfile/Gjelim.m.
Wipke, K. B., M. R. Cuddy, et al. (1999). "ADVISOR 2.1 A user-friendly advanced powertrain simulation using a forward/backward approach." IEEE Trans Vehicular Tech 48(6): 1751-7-1761.
Won, J.-S. and R. Langari (2002). "Fuzzy torque distribution control for a parallel hybrid vehicle." Expert Systems 18(1).
www.uqm.com (2009). PoqwePhase 75 Traction System, UQM Technologies. 2009.
Zhang, Y., H. Lin, et al. (2006). "Performance modelling and optimization of a novel multi mode hybrid powertrain." Trans. ASME, J. Mech. Design 128(1): 79-89.
Zhu, Y., Y. Chen, et al. (2006). "Otimisation design of an energy management strategy for hybrid vehicles." Int J Alternative Propulsion 1(12): 47-62.

Appendix

Appendix 1 Matlab function of 'Gauss-Jordan elimination'

```
function Y=gjelim(P)
%GJELIM
%Gauss-Jordan elimination.
%Options: rational number format
%        count of operations
%        all steps
%Calling format: gjelim(A)

%Can use given tolerance of 1e-20
%or change to own tolerance
%MATLAB computes to about 16 decimal digits

%Copyright Gareth Williams, Stetson University
%gwilliam@stetson.edu, http://www.stetson.edu/~gwilliam
%Accompanies "Linear Algebra with Applications" by Gareth Williams

%Initial values
adds=0;totadds=0;mults=0;totmults=0;swaps=0;totswaps=0;
ops=[0];

%hold off
%default graphics window mode
tol=1e-20;
[n,m]=size(P);
format compact

disp(' ')
h=input('Rational numbers? y/n: ','s');
q=input('Count of operations? y/n: ','s');
g=input('All steps? y/n: ','s');

disp(' ')
disp('initial matrix')
if h=='y'
  disp(rats(P))
 else
  disp(P)
end

if g=='y';
 disp('[press Enter at each step to continue]')
 disp(' ')
```

```
 pause
end

%find a pivot
j=1;
for i=1:n,
 if j <= m
  found=0;
  if abs(P(i, j)) <= tol %end is in line 101
    while (found == 0) %over 2 spaces since 1st part of
                    % if-else-end, lines 99,101
%search for a leading one and interchange rows if necessary
     for s=i:n,
      if (abs(P(s, j)) > tol)
              if  (found == 0)
        found=1;
        if s~=i
         for r=j:m,
          temp=P(i, r);
          P(i, r)=P(s, r);
          P(s, r) = temp;
         end
         swaps = m-j+1;
         totswaps = totswaps + swaps;
         if g=='y'; %allsteps
          disp('swap rows')
          if h=='y'
            disp(rats(P))
           else
            disp(P)
          end
          if q=='y'
           disp('element swaps:')
           disp(swaps)
          end
          disp('--------------------')
          pause
         end %allsteps
        end
       end
      end
     end

     if (found==0)
      if (j <= m)
       j = j + 1;
      end
     end

     if j>m
```

```
      found=1;
     end
    end  %of while loop, line 52
    if  j > m
     found = 0;
    end
   else
    found = 1;
  end  %starts line 51

%normalize leading element in row changing the rest of the row accordingly
  if found == 1
   k=i;
   if (P(k, j) ~= 1)
    if (abs(P(k, j)) > tol)
     y = P(i, j);
     for l=j:m,
      P(k, l) = P(k, l)/y ;
     end
     mults = m-j;
     totmults = totmults + mults;
     if g=='y'; %allsteps
      disp('normalize')
      if h=='y'
        disp(rats(P))
       else
        disp(P)
      end
      if q=='y'
       disp('multiplications:')
       disp(mults)
      end
      disp('--------------------')
      pause
     end %allsteps
    end
   end
   for r=1:n,
    if (abs(P(r, j)) >tol)
     if (r ~= i)
      z=P(r, j);
      for c=j:m,
       P(r, c)=P(r, c) - z * P(i, c);
      end
      adds = m-j;
      mults = m-j;
      totadds = totadds + adds;
      totmults = totmults + mults;
      if g=='y'; %allsteps
       disp('create zero')
```

```
      if h=='y'
        disp(rats(P))
       else
        disp(P)
      end
      if q=='y'
       disp('additions, multiplications:')
       ops=[adds mults];
       disp(ops)
      end
      disp('--------------------')
      pause
     end %allsteps
    end
   end
  end
 end

 j = j + 1;

 end
end %end i loop

%print out final matrix
disp('-reduced echelon form-')

if h=='y'
   disp(rats(P))
else
   disp(P)
end

if q=='y'
 disp('Total additions, multiplications, element-swaps:')
 ops=[totadds totmults totswaps];
 disp(ops)
 disp('--------------------')
end
Y=P;
disp(' ')
format loose
```

Appendix 2 Matlab programme to get speed coefficient matrix and to get the rotation speed relationships for the single epicyclic gearbox

```
%%% to get speed coefficient matrix for the single epicyclic gearbox
a1=-0.8;
 a2=3.25;

A(1,1)=1;
A(1,5)=-1;

A(2,1)=1;
A(2,8)=-1;

A(3,2)=1;
A(3,7)=-1;

A(4,2)=1;
A(4,9)=-1;

A(5,3)=1;
A(5,10)=-1;

A(6,4)=1;
A(6,6)=-1;

A(7,3)=1;
A(7,4)=-a1;
A(7,5)=a1-1;

A(8,6)=1;
A(8,7)=-a2;
A(8,8)=a2-1;

%%% using gjelim to get the rotation speed relationships for the single epicyclic gearbox
B(:,1:8)=A(:,3:10);
B(:,9:10)=A(:,1:2);
D=gjelim(B)
```

Appendix 3 Speed coefficient matrix A_n for the single epicyclic gearbox

		Column									
		1	2	3	4	5	6	7	8	9	10
Row	1	1	0	0	0	-1	0	0	0	0	0
	2	1	0	0	0	0	0	0	-1	0	0
	3	0	1	0	0	0	0	-1	0	0	0
	4	0	1	0	0	0	0	0	0	-1	0
	5	0	0	1	0	0	0	0	0	0	-1
	6	0	0	0	1	0	-1	0	0	0	0
	7	0	0	1	0.8	-1.8	0	0	0	0	0
	8	0	0	0	0	0	1	-3.25	2.25	0	0

Appendix 4 Relationship of rotation speed for the single epicyclic gearbox

						MG2 speed	MG1 speed	Engine torque	Output speed
n3	n4	n5	n6	n7	n8	n9	n10	n1	n2
1	0	0	0	0	0	0	0	-18/5	13/5
0	1	0	0	0	0	0	0	45/20	-65/20
0	0	1	0	0	0	0	0	-1	0
0	0	0	1	0	0	0	0	45/20	-65/20
0	0	0	0	1	0	0	0	0	-1
0	0	0	0	0	1	0	0	-1	0
0	0	0	0	0	0	1	0	0	-1
0	0	0	0	0	0	0	1	-18/5	13/5

Appendix 5 Matlab program to plot MG1 and MG2 speed vs. transmission ratio for the single epicyclic gearbox

```
global a1
global a3

a1=-0.8;
a3=-0.8;

coeffi_matrix_A2_0503;

w_e=1;
 A(17,1)=1;
 A(17,19)=w_e;

  for i=1:35

A(18,18)=1;
A(18,19)=w_e/(i/10);

D=my_gjelim1(A);
DD(:,i)=D(:,19);
E(i)=i/10;
 end


plot(E,DD(15,:));
%xlim([0.4 2.5]);text(E(20),DD(15,20),'\leftarrow MG2', 'HorizontalAlignment','left')

hold on; plot(E,DD(16,:),'-.') ;xlim([0 3.5]);ylim([-1,3]);
legend('MG2','MG1');
bsr1 = interp1(DD(16,:), E, 0); %boundary speed ratio 1
bsr2 = interp1(DD(15,:), E, 0);  % boundary speed ratio 2

plot( linspace(bsr1,bsr1,81), -1:0.05:3, '--r');
plot( linspace(bsr2,bsr2,81), -1:0.05:3, '--r');
plot( 0:0.05:3.5,linspace(0,0,71), '--r');

xlabel('Transmission Ratio')
ylabel('Speed of MG1 and MG2')
title('4 branch system')

%text(E(20),DD(16,20),'\leftarrow MG1', 'HorizontalAlignment','left')
hold on;
y=0;
plot(y);xlim([0 3.5]);ylim([-1,3]);

 grid on;
```

Appendix 6 Matlab programme to get torque coefficient matrix and to get torque relationships for the single epicyclic gearbox

```
%%% to get torque coefficient matrix for the single epicyclic gearbox
a1=-0.8;
a2=3.25;

eta=0.985;
t=0;

T(1,1)=1;
T(1,5)=1;
T(1,8)=1;

T(2,2)=1;
T(2,7)=1;
T(2,9)=1;


T(3,3)=1;
T(3,10)=1;


T(4,4)=1;
T(4,6)=1;

T(5,3)=a1*(eta^t);
T(5,4)=1;

T(6,3)=1;
T(6,4)=1;
T(6,5)=1;

T(7,6)=a2*(eta^t)
T(7,7)=1;

T(8,6)=1;
T(8,7)=1;
T(8,8)=1;

%%% using gjelim to get the torque relationships for the single epicyclic gearbox

T1(:,1:8) = T(:,3:10);
T1(:,9:10) = T(:,1:2);
H=gjelim(T1);
```

Appendix 7 Torque coefficient matrix AT for the single epicyclic gearbox

		Column									
		1	2	3	4	5	6	7	8	9	10
Row	1	1	0	0	0	-1	0	0	0	0	0
	2	1	0	0	0	0	0	0	-1	0	0
	3	0	1	0	0	0	0	-1	0	0	0
	4	0	1	0	0	0	0	0	0	-1	0
	5	0	0	1	0	0	0	0	0	0	-1
	6	0	0	0	1	0	-1	0	0	0	0
	7	0	0	1	0.8	-1.8	0	0	0	0	0
	8	0	0	0	0	0	1	-3.25	2.25	0	0

Appendix 8 Relationship of torque for the single epicyclic system

						MG2 torque	MG1 torque	Engine torque	Output torque
T3	T4	T5	T6	T7	T8	T9	T10	T1	T2
1	0	0	0	0	0	0	0	0	-5/18
0	1	0	0	0	0	0	0	0	-2/9
0	0	1	0	0	0	0	0	0	1/2
0	0	0	1	0	0	0	0	0	2/9
0	0	0	0	1	0	0	0	0	-13/18
0	0	0	0	0	1	0	0	0	1/2
0	0	0	0	0	0	1	0	1	13/18
0	0	0	0	0	0	0	1	0	5/18

Appendix 9 Matlab programme to get speed coefficient matrix and to get speed relationships for the twin epicyclic gearbox

```
%%% to get torque coefficient matrix for the twin epicyclic gearbox
a1=-0.8;  a3=-0.8;
a2=2-1/a1;
a4=2-1/a3;

A(1,1)=1;
A(1,5)=-1;
A(2,1)=1;
A(2,8)=-1;

A(3,2)=1;
A(3,7)=-1;
A(4,2)=1;
A(4,11)=-1;
A(5,2)=1;
A(5,14)=-1;

A(6,3)=1;
A(6,9)=-1;
A(7,3)=1;
A(7,16)=-1;

A(8,4)=1;
A(8,6)=-1;
A(9,10)=1;
A(9,12)=-1;
A(10, 13)=1;
A(10, 15)=-1;

A(11,3)=1;
A(11,4)=-a1;
A(11,5)=a1-1;

A(12,6)=1;
A(12,7)=-a2;
A(12,8)=a2-1;
A(13,9)=1;
A(13,10)=-a3;
A(13,11)=a3-1;

A(14,12)=1;
A(14,13)=-a4;
A(14,14)=a4-1;
%%% using gjelim to get the speed relationships for the twin epicyclic gearbox
A1(:,1:14)=A(:,3:16);
A1(:,15:16)=A(:,1:2);
D=gjelim2(A1);
```

Appendix 10 Speed coefficient matrix A_n for the twin epicyclic gearbox

		Column															
		1	2	3	4	5	6	7	8	9	10	11	12	13	14	15	16
Row	1	1	0	0	0	-1	0	0	0	0	0	0	0	0	0	0	0
	2	1	0	0	0	0	0	0	-1	0	0	0	0	0	0	0	0
	3	0	1	0	0	0	0	-1	0	0	0	0	0	0	0	0	0
	4	0	1	0	0	0	0	0	0	0	0	-1	0	0	0	0	0
	5	0	1	0	0	0	0	0	0	0	0	0	0	0	-1	0	0
	6	0	0	1	0	0	0	0	0	-1	0	0	0	0	0	0	0
	7	0	0	1	0	0	0	0	0	0	0	0	0	0	0	0	-1
	8	0	0	0	1	0	-1	0	0	0	0	0	0	0	0	0	0
	9	0	0	0	0	0	0	0	0	0	1	0	-1	0	0	0	0
	10	0	0	0	0	0	0	0	0	0	0	0	0	1	0	-1	0
	11	0	0	1	0.8	-1.8	0	0	0	0	0	0	0	0	0	0	0
	12	0	0	0	0	0	1	-3.25	2.25	0	0	0	0	0	0	0	0
	13	0	0	0	0	0	0	0	0	1	0.8	-1.8	0	0	0	0	0
	14	0	0	0	0	0	0	0	0	0	0	0	1	-3.25	2.25	0	0

Appendix 11 Relationship of rotation speed for the twin epicyclic system

												MG2 speed	MG1 speed	Engine torque	Output speed
n3	n4	n5	n6	n7	n8	n9	n10	n11	n12	n13	n14	n15	n16	n1	n2
1	0	0	0	0	0	0	0	0	0	0	0	0	0	-18/5	13/5
0	1	0	0	0	0	0	0	0	0	0	0	0	0	9/4	-13/4
0	0	1	0	0	0	0	0	0	0	0	0	0	0	-1	0
0	0	0	1	0	0	0	0	0	0	0	0	0	0	9/4	-13/4
0	0	0	0	1	0	0	0	0	0	0	0	0	0	0	-1
0	0	0	0	0	1	0	0	0	0	0	0	0	0	-1	0
0	0	0	0	0	0	1	0	0	0	0	0	0	0	-18/5	13/5
0	0	0	0	0	0	0	1	0	0	0	0	0	0	3	-4
0	0	0	0	0	0	0	0	1	0	0	0	0	0	0	-1
0	0	0	0	0	0	0	0	0	1	0	0	0	0	9/2	-11/2
0	0	0	0	0	0	0	0	0	0	1	0	0	0	18/13	-31/13
0	0	0	0	0	0	0	0	0	0	0	1	0	0	0	-1
0	0	0	0	0	0	0	0	0	0	0	0	1	0	18/13	-31/13
0	0	0	0	0	0	0	0	0	0	0	0	0	1	-18/5	13/5

Appendix 12 Matlab program to plot MG1 and MG2 speed vs. transmission ratio for the twin epicyclic gearbox

```
% clear;
global a1
global a2
a1=-0.8;
a2=3.25;
w_e=1;

coeffi_matrix_A_priux1;

 for i=1:35

A(10,2)=1;
A(10,11)=w_e/(i/10);


D=gjelim2(A);
DD(:,i)=D(:,11);
E(i)=i/10;
 end

 subplot(2,1,1);
 plot(E,DD(9,:)); xlim([0, 3.5]);ylim([-1,3]);

hold on; plot(E,DD(10,:),'-.' );xlim([0, 3.5]);ylim([-1,3]);
legend('MG2','MG1')
grid on;

xlabel('Transmission Ratio')
ylabel('Speed of MG1 and MG2')
title('3 branch system');

bsr = interp1(DD(10,:), E, 0); %boundary speed ratio for prius


plot( linspace(bsr,bsr,81), -1:0.05:3, '--r');

plot( 0:0.05:3.5,linspace(0,0,71), '--r');
```

Appendix 13 Matlab programme to get torque coefficient matrix and to get torque relationships for the twin epicyclic gearbox

```
%%% to get torque coefficient matrix for the twin epicyclic gearbox
a1=-0.8;  a3=-0.8;
 eta=0.985; t=0;
a2=2-1/a1; a4=2-1/a3;

T(1,1)=1; T(1,5)=1; T(1,8)=1;

T(2,2)=1; T(2,7)=1;
T(2,11)=1; T(2,14)=1;

T(3,3)=1; T(3,9)=1;
T(3,16)=1;

T(4,4)=1; T(4,6)=1;

T(5,10)=1; T(5,12)=1;

T(6,13)=1; T(6,15)=1;

T(7,3)=1; T(7,4)=1; T(7,5)=1;

T(8,3)=a1*(eta^t); T(8,4)=1;

T(9,6)=1; T(9,7)=1; T(9,8)=1;

T(10, 6)=a2*(eta^t);
T(10, 7)=1;

T(11,9)=1;
T(11,10)=1;
T(11,11)=1;

T(12,9)=a3*(eta^t);
T(12,10)=1;

T(13,12)=1;
T(13,13)=1;
T(13,14)=1;

T(14,12)=a4*(eta^t);
T(14,13)=1;

%%% using gjelim to get the torque relationships for the twin epicyclic gearbox

T1(:,1:14)=T(:,3:16);
T1(:,15:16)=T(:,1:2);
H=gjelim2(T1);
```

Appendix 14 Torque coefficient matrix AT for the twin epicyclic gearbox

		Column															
		1	2	3	4	5	6	7	8	9	10	11	12	13	14	15	16
Row	1	1	0	0	0	1	0	0	1	0	0	0	0	0	0	0	0
	2	0	1	0	0	0	0	1	0	0	0	1	0	0	1	0	0
	3	0	0	1	0	0	0	0	0	1	0	0	0	0	0	0	1
	4	0	0	0	1	0	1	0	0	0	0	0	0	0	0	0	0
	5	0	0	0	0	0	0	0	0	0	1	0	1	0	0	0	0
	6	0	0	0	0	0	0	0	0	0	0	0	0	1	0	1	0
	7	0	0	1	1	1	0	0	0	0	0	0	0	0	0	0	0
	8	0	0	-0.8	1	0	0	0	0	0	0	0	0	0	0	0	0
	9	0	0	0	0	0	1	1	1	0	0	0	0	0	0	0	0
	10	0	0	0	0	0	3.25	1	0	0	0	0	0	0	0	0	0
	11	0	0	0	0	0	0	0	0	1	1	1	0	0	0	0	0
	12	0	0	0	0	0	0	0	0	-0.8	1	0	0	0	0	0	0
	13	0	0	0	0	0	0	0	0	0	0	0	1	1	1	0	0
	14	0	0	0	0	0	0	0	0	0	0	0	3.25	1	0	0	0

Appendix 15 Relationship of torque for the twin epicyclic system

												MG2 torque	MG1 torque	Engine torque	Output torque
T3	T4	T5	T6	T7	T8	T9	T10	T11	T12	T13	T14	T15	T16	T1	T2
1	0	0	0	0	0	0	0	0	0	0	0	0	0	-5/18	0
0	1	0	0	0	0	0	0	0	0	0	0	0	0	-2/9	0
0	0	1	0	0	0	0	0	0	0	0	0	0	0	1/2	0
0	0	0	1	0	0	0	0	0	0	0	0	0	0	2/9	0
0	0	0	0	1	0	0	0	0	0	0	0	0	0	-13/18	0
0	0	0	0	0	1	0	0	0	0	0	0	0	0	1/2	0
0	0	0	0	0	0	1	0	0	0	0	0	0	0	-65/324	-5/18
0	0	0	0	0	0	0	1	0	0	0	0	0	0	-13/81	-2/9
0	0	0	0	0	0	0	0	1	0	0	0	0	0	13/36	1/2
0	0	0	0	0	0	0	0	0	1	0	0	0	0	13/81	2/9
0	0	0	0	0	0	0	0	0	0	1	0	0	0	-169/324	-13/18
0	0	0	0	0	0	0	0	0	0	0	1	0	0	13/36	1/2
0	0	0	0	0	0	0	0	0	0	0	0	1	0	169/324	13/18
0	0	0	0	0	0	0	0	0	0	0	0	0	1	155/324	5/18

Appendix 16 Matlab program to compare the single epicyclic gearbox and the twin epicyclic gearbox

```
%2006/10/18
clear
global w_dl  %rotation speed
global m_dl   %torque
global w_e
global m_e

acc=0.8; % m/s2
for i=1:65
    t=0.5*(i-1);
    v=10+acc*t; %m/s
     v_mph(i)=v*2.2286; %mph  1m/s=1/0.28 km/h
     v_vehicle(i)=v;
%%%%%%%%%%%%%%%%%%%%%%%%%%%%%%%%%%%%%%%%%%%%%%%%%%%%%%%%%%%%%%%%%%%%%%%%%%%%%%%%%%%%%%%%%%%%%%%%%%%%%%%%%%%%%%%%%%%%%%%%%%%
%calculate output speed of the transmission at certain vehicle speed
    %wheel radius r=0.3045 [m]
r=0.292;
% first step is to calculate the road load during cruise
m=1257;  %kg

   Ft=98.33+0.4103*(v^2)+acc*m;  %N
%  Ft=98.33+0.4103*(v^2);  %N, no acceleration

Pt=Ft*v/1000;      %[Kw]
% torque on the wheel [Nm]
m_t=Ft*r;
% rotation speed of the wheel n_wheel=v/(2*pi*r*60)  [rotaion per sec]
%n_wheel=v/(2*pi*r)
w_wheel=v/r;

%rotation speed before diff, the ratio of the diff is set to be 3.95.
%n_dl is rotation speed of output shaft [rotation per sec]
%w_dl is angular speed of output shaft [rad/s]
g_fd=3.95;

type=1;  %% type=1: twin epicyclic system; type=2: single epicyclicsystem
            switch type
```

```
            case 1     %% Nexxtdrive
          w_dl=-w_wheel*g_fd;  %%%%speed of engine is positive, w_dl is negative
          dri_shaft_speed(i)=w_dl*9.548; %rpm
            case 2     %% Prius
              w_dl=w_wheel*g_fd;  %%%%speed of engine is positive, w_dl is negative
              dri_shaft_speed(i)=w_dl*9.548; %rpm
          end

%torque before differential m_dl [Nm].
eta_diff=0.82;

          switch type
            case 1
          m_dl=m_t/(eta_diff*g_fd);

            case 2
          m_dl=-m_t/(eta_diff*g_fd);
          end
%%%P_dl=m_dl*w_dl/1000  %%%P_dl is negative, means it takes power out
 engine_radps =[ 10 30 70 104.7200  157.0800  209.4400  261.8000  314.1600  366.5200  418.8800 460 512];
  engine_torque=[ 10 15 35 45 60 70 80 85 90 95 100 115 ];

  engine_power=engine_radps.*engine_torque;
  w_e=interp1(engine_power, engine_radps, Pt*1000);
 m_e=interp1( engine_radps, engine_torque, w_e);
                if Pt>512*115/1000
              w_e=512;
              m_e=115;
            elseif Pt<104.72*45/1000
              w_e=104.72;
              m_e=45;
            end

switch type
   case 1
% % twin epicyclic gearbox
 global a1
      global a3
      global a5
```

```
        a1=-0.8;
        a3=-0.8;
          %%%from the power demand, decide how fast you would like the ICE to spin
 % rpm=[1000 1500 2000 2500 3000 3500 4000];
  %engine_radps=rpm*0.10472;
    coeffi_matrix_A2_0503;
     D=my_gjelim1(A);
      DD(:,i)=D(:,19);

      i_nexxt(i)=D(1,19)/D(18,19);

      %%%%torque
       global eta
       global t

%        eta=0.985;
 eta=1;
       t=0;
       coeffi_matrix_T;
        G=my_gjelim1(T);

         % 3 , 4, 5
       T1=T;
       if G(3,19)*(D(3,19)-D(5,19))<0
          T1(8,3)=a1*(eta^1);

       elseif G(3,19)*(D(3,19)-D(5,19))>0
          T1(8,3)=a1*(eta^(-1));

       else
          T1(8,3)=a1*(eta^0);
       end

       % 6, 7 , 8
       if G(6,19)*(D(6,19)-D(8,19))<0
          T1(10, 6)=a2*(eta^1);

       elseif G(6,19)*(D(6,19)-D(8,19))>0
          T1(10, 6)=a2*(eta^(-1))   ;
```

```
else
   T1(10, 6)=a2*(eta^0)  ;
end

      % 9, 10, 11
if G(9,19)*(D(9,19)-D(11,19))<0
   T1(12,9)=a3*(eta^1);
elseif G(9,19)*(D(9,19)-D(11,19))>0
   T1(12,9)=a3*(eta^(-1))      ;
else
   T1(12,9)=a3*(eta^0)  ;
end

% 12, 13, 14
if G(12,19)*(D(12,19)-D(14,19))<0
   T1(14,12)=a4*(eta^1);
elseif G(12,19)*(D(12,19)-D(14,19))>0
   T1(14,12)=a4*(eta^(-1))    ;
 else
   T1(14,12)=a4*(eta^0) ;
end

%% so the coefficient matrix for torque is T1
 H=my_gjelim1(T1);
 HH(:,i)=H(:,19);
 torq_split(1,i)=-H(2,19)/H(16,19);
 P(:,i)=D(:,19).*H(:,19)/1000  ; %kW
power_split(1,i)=P(2,i)/P(1,i);
  power_e(1,i)=P(1,i);
   power_dl(1,i)=P(2,i);
 power_mg1_nexxt(1,i)=P(16,i);
  power_mg2_nexxt(1,i)=P(15,i);
  power_total(1,i) = power_e(1,i)+power_dl(1,i)+power_mg1_nexxt(1,i)+power_mg2_nexxt(1,i);
%     elec_power(i)=P(15,i)+P(16,i);
%     elec_verse_engine_power(i)=elec_power(i)/P(1,i);
 if P(15,i)>0
  if P(16,i)>0
     P_elec_req(i)= P(15,i)+  P(16,i);
  else
      P_elec_req(i)= P(15,i)+  P(16,i)*0.855;
```

```
            end
          else
              if P(16,i)>0
              P_elec_req(i)= P(15,i)*0.855+  P(16,i);
              else
                P_elec_req(i)= P(15,i)*0.855+  P(16,i)*0.855;
              end
          end
%%%%%%%%%%%%%%%%%%%%%%%%%%%%%%%%%%%%%%%%%%%%%%%%%%%%%%%%%%%
    case 2
 %single epicyclic gearbox
 global a1
global a2
a1=-0.8;    %-24/30;
a2=3.25 ;   %%78/24;

coeffi_matrix_A_priux1;
D=my_gjelim1(A);
   i_prius(i)=D(2,11)/D(1,11);

global eta1
global eta2
global t

%eta1=0.985;
% eta2=0.985;
 eta1=1;
 eta2=1;
t=0;

coeffi_matrix_T_prius;
G=my_gjelim1(T);

T1=T;
if G(3,11)*(D(3,11)-D(5,11))<0
    t1=1;
        T1(5,3)=a1*(eta1^1);

    elseif G(3,11)*(D(3,11)-D(5,11))>0
        t1=-1;
```

```
        T1(5,3)=a1*(eta1^(-1));

    else
        T1(5,3)=a1*(eta1^0);
        t1=0;
 end
%

   % 6, 7 , 8
if G(6,11)*(D(6,11)-D(8,11))<0
    t2=1;
    T1(7, 6)=a2*(eta2^1);

elseif G(6,11)*(D(6,11)-D(8,11))>0
    t2=-1;
    T1(7, 6)=a2*(eta2^(-1))  ;

    else
        T1(7, 6)=a2*(eta2^0)  ;
        t2=0;
end

H=my_gjelim1(T1);

torq_split(1,i)=H(7,11)/H(3,11);
P(:,i)=D(:,11).*H(:,11)/1000 ;
 power_split(1,i)=P(7,i)/P(3,i);

 power_e(1,i)=P(1,i);
          power_dl(1,i)=P(2,i);
   power_mg1_prius(1,i)=P(10,i);
         power_mg2_prius(1,i)=P(9,i);
         power_total(1,i) = power_e(1,i)+power_dl(1,i)+power_mg1_prius(1,i)+power_mg2_prius(1,i);

  elec_power(i)=P(9,i)+P(10,i);
  power_elec(i)=P(10,i)/P(1,i);
  %         elec_verse_engine_power(i)=elec_power(i)/P(1,i);
  v_vehicle(i)=v;
        if P(9,i)>0
              if P(10,i)>0
```

```
                P_elec_req(i)= P(9,i)+  P(10,i);
            else
                P_elec_req(i)= P(9,i)+  P(10,i)*0.855;
            end
        else
            if P(10,i)>0
                P_elec_req(i)= P(9,i)*0.855+  P(10,i);
            else
                P_elec_req(i)= P(9,i)*0.855+  P(10,i)*0.855;
            end
        end
elec_verse_engine_power(i)=P_elec_req(i)/P(1,i);
end
end   % end of first for
% plot (v_vehicle, power_mg1)

switch type
   case 1
       n=2;
% subplot(n,1,1); plot(v_vehicle,P(15,:));title('4 Branch System, MG2'); xlabel('vehicle speed, m/s');ylabel('power,kW');xlim([10 35]);ylim([-4 -1]);grid on ;
% subplot(n,1,2);  plot(v_vehicle,P(16,:));title('4 Branch System, MG1');xlabel('vehicle speed, m/s');ylabel('power,kW');xlim([10 35]);ylim([-1 8]);grid on ;

 plot(v_vehicle,power_total);grid on ;

% subplot (2,1,1); plot(v_vehicle,torq_split); title('4 Branch System, torque split');xlabel('vehicle speed, m/s');ylabel('Torque to Wheel/to MG2');xlim([10 35]);grid on ;
% % subplot (2,1,2); plot(v_vehicle,power_split); title('power split');xlabel('vehicle speed, m/s');ylabel('power split, power to wheel vs power to MG2');xlim([10 35]);grid on ;
%
% subplot (2,1,2); plot(v_vehicle,power_elec); title('4 Branch System, power split');xlabel('vehicle speed, m/s');ylabel('Power of MG2/power of engine');xlim([10 35]);grid on ;
% power_elec_4= power_elec;
   case 2

 n=2;
% subplot(n,1,1); plot(v_vehicle, P(9,:));title('3 Branch System, MG2');xlabel('vehicle speed, m/s');ylabel('power,kW');xlim([10 35]);grid on ;
%  subplot(n,1,2);  plot(v_vehicle,P(10,:));title('3 Branch System MG1');xlabel('vehicle speed, m/s');ylabel('power,kW');xlim([10 35]);grid on ;
plot(v_vehicle,power_total);grid on ;
```

```
% plot(v_vehicle,elec_power); title('3 Branch System, total electrical power');xlabel('vehicle speed, m/s');ylabel('Power of M/G1+power of M/G2,kW');


% subplot (2,1,1); plot(v_vehicle,torq_split); title('3 Branch System, torque split');xlabel('vehicle speed, m/s');ylabel('Torque to Wheel/to MG2');ylim([2.4 2.77]);xlim([10 35]);grid on ;

% %  subplot (2,1,2); plot(v_vehicle,power_split); title('power through mechanical way');xlabel('vehicle speed, m/s');ylabel('power split, power to wheel vs power to M/G2');

%

% subplot (2,1,2); plot(v_vehicle,power_elec); title('3 Branch System, power split');xlabel('vehicle speed, m/s');ylabel('Power of MG2/power of engine');xlim([10 35]);grid on ;

% power_elec_3= power_elec;

end
```

Appendix 17 Matlab program for the controller for the HEV with the single epicyclic gearbox

```
function dx=control_logic3(Acc,T_e1, w_e1,Spd, T_dl, w_dl, dw_dl, SoD)
% Acc=u(1);
% T_e=u(2);
% Spd=u(3);
% T_req=u(4);
% SoD=u(5);
global w_EG_row
global T_EG_max
w_EG_upper =5500/9.549;
eng_best_w=[ 0   50 100   157.08   246.1     261.81   366.53   418.89];
eng_best_trq = [0 60 80 90 100 100 95 93];
w_mg2_row =[0  75         150        225        300        375        450        525        600];
T_mg2_max = [245 245 245 182 133 98 66.5 45.5 31.5];
w_mg1_row =[0  75         150        225        300        375        450        525        600];
T_mg1_max = [80 80 80 59.429 43.429 32 21.714 14.857 10.286];

w_eng_min=50;

eff = 0.95;
Tm_lim=300;
SoD_high =0.7;
SoD_low = 0.5;
if Spd > 0
   if T_dl >0
      if Spd >9.8 %35 * 0.28 = 9.8 m/s, 1 km/h=0.28m/s  Mi: 35mph
         if  T_dl  < T_e1
            if SoD < SoD_high
               if SoD >= SoD_low
                  mode = 3;
               else
               mode  = 8;
               end
            else mode  = 4;
            end
         else
            if SoD > SoD_low
               mode  = 2;
            else mode = 4;
            end
         end
      else
         if SoD > SoD_low
            if T_dl <= Tm_lim
               mode  = 1;
            else mode = 2;
            end
         else mode  = 4;
         end
      end
   else

      if SoD < SoD_high
         mode  =5;
      else
         mode  = 6;
      end
   end
```

```
else
   if SoD > SoD_low
      mode  = 0;   %%%%%%% stationary

   else mode  = 7;
   end
end

% 1='moter_alone'
% 2='combined_power'
% 3= 'CVT';
% 4= 'engine_alone'
% 5='regenerate '
% 6='Mech_brake'
% 7=  'stand_charge'
% 8=  'driving charge'

switch mode
case 1   % motor alone

              w_e = 0;
              dw_e = 0;
              T_e = 0;

             [w_mg1,w_mg2,T_mg1,T_mg2] = prius(w_e,w_dl, T_e,-T_dl);

            if w_mg1 ==0
               dw_mg1 =0;
            else
               dw_mg1 =w_mg1/w_dl * dw_dl;
            end

             if w_mg2 ==0
                 dw_mg2 =0;
             else
                 dw_mg2 =w_mg2/w_dl * dw_dl;
             end

 case 2  %2= combined power'

                 w_e = w_e1;
                       dw_e = (w_e / w_dl) * dw_dl;
                 T_e = T_e1;
                 [w_mg1,w_mg2,T_mg1,T_mg2] = prius(w_e,w_dl, T_e,-T_dl);

                  j=1;
          while    abs(T_mg2) >  interp1(w_mg2_row, T_mg2_max, abs(w_mg2)) | abs(T_mg1)
          >interp1(w_mg1_row, T_mg1_max, abs(w_mg1));
             T_e = T_e -5*j;
             j=j+1;
             [w_mg1, w_mg2, T_mg1,T_mg2] = prius(w_e,w_dl, T_e,-T_dl);
               end

             if w_mg1 ==0
                 dw_mg1 =0;
             else
                 dw_mg1 =w_mg1/w_dl * dw_dl;
             end

             if w_mg2 ==0
```

```
        dw_mg2 =0;
    else
       dw_mg2 =w_mg2/w_dl * dw_dl;
    end


case  3  %cruise mode

       w_e = w_e1;
      dw_e = (w_e / w_dl) * dw_dl;
      T_e = T_e1;
       [w_mg1,w_mg2,T_mg1,T_mg2] = prius(w_e,w_dl, T_e,-T_dl);

        j=1;
    while    abs(T_mg2) >  interp1(w_mg2_row, T_mg2_max, abs(w_mg2)) | abs(T_mg1)
  >interp1(w_mg1_row, T_mg1_max, abs(w_mg1));
    T_e = T_e -5*j;
    j=j+1;
    [w_mg1, w_mg2, T_mg1,T_mg2] = prius(w_e,w_dl, T_e,-T_dl);
      end

   if w_mg1 ==0
      dw_mg1 =0;
   else
      dw_mg1 =w_mg1/w_dl * dw_dl;
   end

    if w_mg2 ==0
        dw_mg2 =0;
    else
        dw_mg2 =w_mg2/w_dl * dw_dl;
    end

case 4  %4= 'engine alone'

     w_e = 13/18 * w_dl;
     dw_e = 13/18 * dw_dl;
     T_e = 18/13 *T_dl;

     w_mg2 = 0;
    dw_mg2 = 0;
    T_mg2 = 0 ;

     w_mg1 = 0 ;
    T_mg1 =0;
    dw_mg1 = 0;

    w_CE_row = [50   107.14          164.29   221.43   278.57   335.71   392.86   450       507.14
            564.29   621.43   678.57   735.71   792.86   850];

    T_CE_max = [46.449    50.201   53.136   55.356   56.962   58.058   58.744   59.124   59.283
            59.219   58.897   58.279   57.329   56.01     54.286]*2;


    if T_e>interp1( w_CE_row, T_CE_max, w_e)
       T_e = interp1( w_CE_row, T_CE_max, w_e)-5;
       w_mg2 = w_dl;
       T_mg2 = T_dl - T_e  ;
    end
```

```
case 5        %5= 'regenerative brake, battery not full'
              w_e = 0;
              dw_e = 0;
              T_e = 0;


              [w_mg1,w_mg2,T_mg1,T_mg2] = prius(w_e,w_dl, T_e,-T_dl);
                 T_mg2 = sign(T_mg2) *min(abs(T_mg2), interp1(w_mg2_row, T_mg2_max, abs(w_mg2))) ;
               T_mg1 = sign(T_mg1) *min(abs(T_mg1), interp1(w_mg1_row, T_mg1_max, abs(w_mg1))) ;


              if w_mg1 ==0
                  dw_mg1 =0;
             else
                  dw_mg1 =w_mg1/w_dl * dw_dl;
             end

              if w_mg2 ==0
                  dw_mg2 =0;
              else
                  dw_mg2 =w_mg2/w_dl * dw_dl;
              end




case 6         %6= 'Mech_brake'

             w_e = 0;
              dw_e = 0;
              T_e = 0;

              w_mg2 = w_dl;
              dw_mg2 = dw_dl;
              T_mg2 = 0;

              w_mg1 = -2.6 * w_dl;
              T_mg1 = 0;
              dw_mg1=0;

case 7  %7= 'stand_charge'

             w_e = 100;  % 1 rad/s = 9.548 rpm
              dw_e = 0;
              T_e = 90;

              w_mg2 = 0;
              dw_mg2 = 0;
              T_mg2 = 0;

              w_mg1 = -3.6 * w_e;
              T_mg1 = 0.28 * T_e;
              dw_mg1=0;


case 8   %  'driving charge
```

```
            w_e = w_e1 ;
            dw_e = dw_dl;
            T_CE_max = [46.449    50.201   53.136   55.356   56.962   58.058   58.744   59.124   59.283
                   59.219   58.897   58.279   57.329   56.01    54.286];
            w_CE_max =[50         107.14   164.29   221.43   278.57   335.71   392.86   450      507.14
                   564.29   621.43   678.57   735.71   792.86   850];

            T_e = interp1(w_CE_max, T_CE_max * 2, w_e)-10;

           [w_mg1,w_mg2,T_mg1,T_mg2] = prius(w_e,w_dl, T_e,-T_dl);

%%%%%%%%% to check overload and overspeed for MG2
             j=1;
            while    abs(T_mg2) >  interp1(w_mg2_row, T_mg2_max, abs(w_mg2)) | abs(T_mg1)
          >interp1(w_mg1_row, T_mg1_max, abs(w_mg1));
            T_e = T_e -5*j;
            j=j+1;
            [w_mg1, w_mg2, T_mg1,T_mg2, P_total] = prius(w_e, -w_dl, T_e, T_dl);
              End
%%%%%%%%%%%%%%%%%%%%%%%%%%%%%%%%

           if w_mg1 ==0
              dw_mg1 =0;
          else
              dw_mg1 =w_mg1/w_dl * dw_dl;
          end

            if w_mg2 ==0
                dw_mg2 =0;
            else
                dw_mg2 =w_mg2/w_dl * dw_dl;
            end


 otherwise
    error(['Unhandled mode ']);
end

dx=[w_mg2, dw_mg2, T_mg2, w_mg1,dw_mg1, T_mg1,w_e, dw_e, T_e, mode];
```

Appendix 18 Matlab program for the controller for the HEV with the twin epicyclic gearbox

```
function dx=control_logic_nexxt_optimized(Acc,T_e1, w_e1,Spd, T_dl, w_dl, dw_dl, SoD)
% Acc=u(1);
% T_e=u(2);
% Spd=u(3);
% T_req=u(4);
% SoD=u(5);
global w_EG_row
global T_EG_max
w_EG_upper =5500/9.549;
eng_best_w=[ 0   50 100   157.08   246.1     261.81   366.53   418.89];
eng_best_trq1 = [0 60 85 95 105 105 105 103];
eng_best_trq = [0 60 80 90 100 100 95 93];
w_mg2_row =[0  75         150       225       300       375       450       525       600];
T_mg2_max = [245 245 245 182 133 98 66.5 45.5 31.5];
w_mg1_row =[0  75         150       225       300       375       450       525       600];
T_mg1_max = [80 80 80 59.429 43.429 32 21.714 14.857 10.286];

% global eng_best_w
% global eng_best_trq
w_eng_min=50;

% w_e1 = w_e1*(rand+10)/10;
% T_e1 = T_e1*(rand+10)/10;


% global time1;
eff = 0.95;
Tm_lim=300;
SoD_high =0.7;
SoD_low = 0.5;
if Spd > 0
   if T_dl >=0
      if Spd >9.8 %35 * 0.28 = 9.8 m/s, 1 km/h=0.28m/s  Mi: 35mph
         if  T_dl  <T_e1
            if SoD < SoD_high
               if SoD > SoD_low
                  mode = 3;
               else
               mode  = 8;
               end
            else mode  = 4;
            end
         else
            if SoD > SoD_low
               mode  = 2;
            else mode = 4;
            end
         end
      else
         if SoD > SoD_low
            if T_dl <= Tm_lim
               mode  = 1;
            else mode = 2;
            end
         else mode  = 4;
         end
      end
```

```
    else

        if SoD < SoD_high
            mode  =5;
        else
            mode  = 6;
        end
    end
else
    if SoD > SoD_low
        mode  = 0;

    else mode  = 7;
    end
end


% 1='moter_alone'
% 2='combined_power'
% 3= 'CVT';
% 4= 'engine_alone'
% 5='reg'
% 6='Mech_brake'
% 7=  'stand_charge'
% 8=  'nutural'
% 9=' High efficiency mode'



switch mode
    case 1   % motor alone
     eeng_on = 0; % engine off

    w_e = 0;
    dw_e = 0;
    T_e = 0;

w_mg2 = 18/13 * w_dl;
dw_mg2 = 18/13 * dw_dl;
T_mg2 = 13/18 * T_dl;


w_mg1 = 0
T_mg1 = 0
dw_mg1 = 0
 P_total=0 ;
 P_electric=0;


    case 2  % combined power

        if w_dl>58 & w_dl<139.5  %%%%optimized mode
           mode=9;
            ratio=1.72;
            w_e = 240;
            dw_e=0;
            T_e=interp1(eng_best_w,eng_best_trq, w_e);

            w_mg2=0;
            dw_mg2=0;
```

```
          T_mg2=0;

          w_mg1=w_e *2.09;
          dw_mg1=dw_e*2.09;
          T_mg1 = -155/324 * T_e - 5/18 * T_dl ;
          P_total=0 ;
          P_electric=0;
       else

            w_e = w_e1;
            dw_e = (w_e / w_dl) * dw_dl;
            T_e = T_e1;
            [w_mg1, w_mg2, T_mg1,T_mg2, P_total,P_electric] = nexxt(w_e, -w_dl, T_e, T_dl);
            j=1;
            while    abs(T_mg2) >  interp1(w_mg2_row, T_mg2_max, abs(w_mg2)) | abs(T_mg1)
>interp1(w_mg1_row, T_mg1_max, abs(w_mg1));
          T_e = T_e -5*j;
          j=j+1;
          [w_mg1, w_mg2, T_mg1,T_mg2, P_total,P_electric] = nexxt(w_e, -w_dl, T_e, T_dl);
            end

        if w_mg1 ==0
          dw_mg1 =0;
        else
          dw_mg1 =w_mg1/w_dl * dw_dl;
        end

       if w_mg2 ==0
          dw_mg2 =0;
       else
          dw_mg2 =w_mg2/w_dl * dw_dl;
        end
  end


case  3  %3= 'CVT high mode'

       if w_dl>50 & w_dl<166.8  %%%%optimized mode
          mode=9;
          ratio=1.72;

          w_e = 200;
          dw_e=0;
          T_e=interp1(eng_best_w,eng_best_trq, w_e);

          w_mg2=0;
          dw_mg2=0;
          T_mg2=0;

          w_mg1=w_e *2.09;
          dw_mg1=0;
          T_dl=-T_dl;
          T_mg1 = -155/324 * T_e - 5/18 * T_dl ;

          %%% to check overload and over speed for mg1

          j=0;
          while abs(T_mg1)> interp1(w_mg1_row, T_mg1_max, abs(w_mg1))
             j=j+1;
             w_e=w_e-5*j;
```

```
            T_e=T_e-5*j;
            T_mg1 = -155/324 * T_e - 5/18 * T_dl ;
          end


          P_total=0 ;
          P_electric=0;
        else

           w_e = w_e1;
           dw_e = (w_e / w_dl) * dw_dl;
            T_e = T_e1;

          [w_mg1, w_mg2, T_mg1,T_mg2, P_total,P_electric] = nexxt(w_e, -w_dl, T_e, T_dl);
          j=1;
          while    abs(T_mg2) >  interp1(w_mg2_row, T_mg2_max, abs(w_mg2)) | abs(T_mg1)
>interp1(w_mg1_row, T_mg1_max, abs(w_mg1));
            T_e = T_e -5*j;
             w_e=w_e-5*j;
            j=j+1;
            [w_mg1, w_mg2, T_mg1,T_mg2, P_total,P_electric] = nexxt(w_e, -w_dl, T_e, T_dl);
          end

          if w_mg1 ==0
               dw_mg1 =0;
          else
            dw_mg1 =w_mg1/w_dl * dw_dl;
          end

          if w_mg2 ==0
            dw_mg2 =0;
          else
            dw_mg2 =w_mg2/w_dl * dw_dl;
          end
        end


case 4  %4= 'engine alone'

              w_e = 13/18*w_dl;
              dw_e = 13/18 * dw_dl;  %%% to be edited
              T_e = 18/13 * T_e1;

                 w_mg2 = 0;
              dw_mg2 = 0;
              T_mg2 = 0;

              w_mg1 =0;
              T_mg1 = 0;  % to be edited
              dw_mg1=0;

              w_CE_row = [50          107.14   164.29   221.43   278.57   335.71   392.86   450       507.14
                      564.29   621.43   678.57   735.71   792.86   850];
             T_CE_max = [46.449    50.201   53.136   55.356   56.962   58.058   58.744   59.124   59.283
                      59.219   58.897   58.279   57.329   56.01    54.286]*2;

              if T_e>interp1( w_CE_row, T_CE_max, w_e)
                 T_e = interp1( w_CE_row, T_CE_max, w_e)-5;
                 w_mg2 = w_dl;
                 T_mg2 = T_dl - T_e  ;
```

```
    end
    P_total = 0;
    P_electric = (w_mg1*T_mg1+w_mg2*T_mg2)/1000;

case 5 %5= 'regenerative brake, battery not full'

    w_e = 0;
    dw_e = 0;
    T_e = 0;


    [w_mg1,w_mg2,T_mg1,T_mg2] = prius(w_e,w_dl, T_e,-T_dl);
    T_mg2 = sign(T_mg2) *min(abs(T_mg2), interp1(w_mg2_row, T_mg2_max, abs(w_mg2))) ;
    T_mg1 = sign(T_mg1) *min(abs(T_mg1), interp1(w_mg1_row, T_mg1_max, abs(w_mg1))) ;


    if w_mg1 ==0
       dw_mg1 =0;
    else
       dw_mg1 =w_mg1/w_dl * dw_dl;
    end

    if w_mg2 ==0
       dw_mg2 =0;
    else
       dw_mg2 =w_mg2/w_dl * dw_dl;
    end

    P_total = 0;
    P_electric = (w_mg1*T_mg1+w_mg2*T_mg2)/1000;

case 6    %6= 'Mech_brake'

    w_e = 0;
    dw_e = 0;
    T_e = 0;

    w_mg2 = 0;
    dw_mg2 = 0;
    T_mg2 = 0;

    w_mg1 = 0;
    T_mg1 = 0;
    dw_mg1=0;
    P_total = 0;
     P_electric = (w_mg1*T_mg1+w_mg2*T_mg2)/1000;


case 7     %7= 'stand_charge'

    w_e = 100;     % 1 rad/s = 9.548 rpm
    dw_e = 0;
    T_e = 90;


    w_mg2 = -18/13 * w_e;
    dw_mg2 = -18/13 * dw_e;
    T_mg2 = 0.78* T_e;

    w_mg1 = 18/5 * w_e ;
```

```
        dw_mg1 = 18/5 * dw_e ;
        T_mg1 = 0.26* T_e;

        P_total = 0;
        P_electric = (w_mg1*T_mg1+w_mg2*T_mg2)/1000;


case 8   % 8= 'driving charge

            w_e =w_e1;
            dw_e = (w_e / w_dl) * dw_dl;
            T_CE_max = [46.449   50.201   53.136   55.356   56.962   58.058   58.744   59.124   59.283
                    59.219   58.897   58.279   57.329   56.01    54.286];
            w_CE_max =[50        107.14   164.29   221.43   278.57   335.71   392.86   450      507.14
                    564.29   621.43   678.57   735.71   792.86   850];

             T_e = interp1(w_CE_max, T_CE_max*2, w_e);
             [w_mg1, w_mg2, T_mg1,T_mg2, P_total,P_electric] = nexxt(w_e, -w_dl, T_e, T_dl);

             j=1;
             while   abs(T_mg2) >  interp1(w_mg2_row, T_mg2_max, abs(w_mg2))
                       | abs(T_mg1) >interp1(w_mg1_row, T_mg1_max, abs(w_mg1));
                                T_e = T_e -5*j;
                                j=j+1;
                                [w_mg1, w_mg2, T_mg1,T_mg2, P_total,P_electric] = nexxt(w_e, -w_dl, T_e,
                              T_dl);
             end

                      if w_mg1 ==0
                          dw_mg1 =0;
                      else
                          dw_mg1 =w_mg1/w_dl * dw_dl;
                      end

                     if w_mg2 ==0
                         dw_mg2 =0;
                     else
                       dw_mg2 =w_mg2/w_dl * dw_dl;
                     end

otherwise
   error(['Unhandled mode ']);
end

dx=[w_mg2, dw_mg2, T_mg2, w_mg1,dw_mg1, T_mg1,w_e, dw_e, T_e, mode,P_total ,P_electric];
```